

If not claimed within fourteen days please return to
Locked Bag 60
ADELAIDE MAIL CENTRE 5810

MINES and ENERGY
RESOURCES SOUTH
AUSTRALIA



Petroleum Division

Department of Mines and Energy Resources
PO Box 151
EASTWOOD, S.A. 5063
AUSTRALIA

SEDIMENTOLOGY OF THE OULDBURRA FORMATION
(EARLY CAMBRIAN), NORTHEASTERN OFFICER BASIN

JOHN N. DUNSTER
B.App. Sc. (Biology)
B.Sc. (Hons) (Geology)

Thesis submitted for the degree of

Master of Science

at the

Department of Geology and Geophysics

University of Adelaide

February 1987

VOLUME 1



5th January, 1987

This manuscript is a limited edition of a dissertation submitted for examination with the Adelaide University. At this date examination is not complete and examiners' recommendations are not included here. This manuscript may be used for your personal informational purposes. However, it is requested that you do not quote, copy, photograph or otherwise extract material from the manuscript without first consulting the author.

Thank you,

John Dunster

John N. Dunster.

ABSTRACT

The Ouldburra Formation (Early Cambrian) is a newly defined sequence of carbonates, mixed carbonate/siliciclastics and evaporites in the northeastern Officer Basin, northern South Australia. Deposition took place during the late stages of transgression and the subsequent regression of an epeiric sea with a flanking marine sabkha.

In the Manya area, deposition began with the precipitation of bottom nucleated halite in small isolated salinas on a peri-emergent siliciclastic sand flat. The transgression of the epeiric sea had extended throughout the Marla-Manya area by the Botoman Stage of the Cambrian. Archaeocyath/algal bioherms, stromatolitic and thrombolitic algal/mud mounds and thin ooid shoals developed offshore. The combination of very shallow conditions and a low degree of depositional slope produced a broad non-tidal nearshore zone in which algal mats were preserved and sedimentation was punctuated by storm events. The epeiric sea was flanked by a marine sabkha which contained displacive 'chicken-wire' anhydrite within the emergent sediment profile and was characterized by near-surface dolomitization, either by seepage reflux of sabkha derived brines or evaporative pumping of evolved marine water. Sedimentation is cyclic throughout much of the depositional history of the Formation. Shallowing-up cycles, typically 1-5 m thick, include a wide variety of lithologies and lithofacies and often terminate with exposure. More-pervasive subaerial exposure surfaces can be correlated over tens of kilometres. Carbonate sedimentation ended as sabkha 'red beds' prograded basinward, in some areas across exposed marine carbonates.

KEYWORDS (AESIS)

Archaeocyatha, Calcareous sediments, Cambrian, Evaporite minerals, Halite, Inland sea, Manya, Marla, Officer Basin, Red bed facies, Salt lakes, Sedimentary cycle, Sedimentary environments, Shallow water, Sulphate minerals.

CONTENTS

VOLUME 1 - TEXT

	PAGE NUMBER
ABSTRACT	(i)
KEYWORDS	(i)
LIST OF FIGURES AND TABLES	
CHAPTER 1 - INTRODUCTION	1
1.1 Description of Location	1
1.2 Tenure	3
1.3 Previous and Contemporaneous Work	3
1.3.1 Exploration history	3
1.3.2 Previous studies of the Ouldburra Formation	4
1.4 Methods of Study	4
1.4.1 Petrography	4
1.4.2 Insoluble residue studies	5
1.4.3 Isotope and trace element studies	5
1.4.4 Detailed sedimentological logs	6
1.5 Regional Geology	6
1.5.1 Archaean - Lower Proterozoic basement	6
1.5.2 Adelaidean lithostratigraphy	8
1.5.3 Cambrian to ?Lower Carboniferous lithostratigraphy	8
1.5.4 Permo-Carboniferous lithostratigraphy	11
1.5.5 Mesozoic lithostratigraphy	11
1.5.6 Cainozoic units	11
1.6 Tectonic History	12
1.7 Economic Potential	14
1.7.1 Base metal prospectivity	14
1.7.2 Petroleum prospectivity	16
CHAPTER 2 - STRATIGRAPHY OF THE OULDBURRA FORMATION	20
2.1 Definition of Type Section	20
2.1.1 Derivation	20
2.1.2 Lithostratigraphic definition	20
2.1.3 Type section	21
2.1.4 Synonymy	21
2.2 Distribution and possible correlatives	21
2.3 Thickness	27
2.4 Lithostratigraphic Relations	27
2.4.1 Relief Sandstone	27
2.4.2 Observatory Hill Formation	28
2.5 Biostratigraphy and age	29
2.6.1 Trilobita	31
2.6.2 Archaeocyatha	31
2.6.3 Biostratigraphic correlations	34

CHAPTER 3 - PRIMARY LITHOFACIES AND LITHOLOGIES	38
3.1 Carbonate Mudstones	39
3.1.1 Massive carbonate mudstone	39
3.1.2 Laminated and silty carbonate mudstone	40
3.1.3 Fenestral and stromatactic carbonate mudstone	43
3.1.4 ?Burrowed carbonate mudstone	46
3.2 Wackestones	47
3.2.1 Oncoid wackestone	47
3.2.2 Coated grain/ bioclastic wackestone	50
3.2.3 Intraclastic wackestone	50
3.2.4 Quartz feldspar wackestone	51
3.3 Packstones	51
3.3.1 Coated grain/bioclastic packstone	51
3.3.2 Intraclastic packstone	52
3.3.3 Quartz feldspar packstone	52
3.4 Grainstones	53
3.4.1 Coated grain/bioclastic grainstone	53
3.4.2 Intraclastic grainstone	54
3.4.3 Quartz feldspar grainstone	55
3.5 Floatstone/Rudstone	55
3.5.1 Plate breccia	58
3.6 Boundstones	58
3.6.1 Stromatolitic algal bindstone	59
3.6.2 Thrombolitic algal bindstone	62
3.6.3 Archaeocyath bafflestone/framestone	63
3.7 Clastics	63
3.7.1 Claystone	64
3.7.2 Siltstone	64
3.7.3 Quartz/feldspathic sandstone	67
3.7.4 Granule conglomerate	67
3.7.5 Sand/silt/mudstone sets	68
3.8 Evaporites	69
3.8.1 Halite	69
(a) Bedded halite	69
(b) Isolated hopppers	73
3.8.2 Gypsum/anhydrite	73
(a) Isolated crystals	76
(b) Macroscopic nodules	79
(c) 'Chicken-wire' anhydrite	80
CHAPTER 4 - SECONDARY LITHOLOGIES	82
4.1 Recrystallized Dolostone	82
4.2 Secondary Chert	82
4.3 Pressure Solution Textures	85
4.3.1 Stylobanded to stylolaminated carbonate mudstone	86
4.3.2 Stylonodular carbonate mudstone	89
4.3.3 Stylomottled carbonate mudstone	90
4.4 Solution Collapse Breccia	90

CHAPTER 5 - DIAGENETIC HISTORY	92
5.1 Carbonate Diagenesis	92
5.1.1 Cementation	92
5.1.2 Dolomitization	97
(a) Saddle dolomite	97
(b) Stratiform bedded dolostone	100
5.1.3 Dedolomitization	100
5.1.4 Petrogenesis of pressure solution textures	101
5.1.5 Emplacement of calcite veins	102
5.2 Evaporite Diagenesis	105
5.2.1 Paragenesis of sulphate evaporite nodules	106
5.2.2 Emplacement of gypsum/anhydrite veins	110
5.3 Collapse Brecciation	111
5.4 Authigenic Minerals and Syntaxial Overgrowths	113
5.4.1 Quartz overgrowth and authigenic quartz euhedra	113
5.4.2 Feldspar overgrowth	113
5.4.3 Authigenic glauconite	114
5.4.4 Native sulphur	114
5.5 Fracturing	115
5.6 Summary of Diagenesis	116
CHAPTER 6 - CYCLICITY OF SEDIMENTATION	120
6.1 Shallowing-upward Sedimentary Cycles	122
6.1.1 Halite/siliciclastic cycle	122
6.1.2 Halite/mixed carbonate/siliciclastic cycle	125
6.1.3 Archaeocyath/algal bioherm cycle	127
6.1.4 Algal bindstone cycle	130
6.1.5 Carbonate sabkha cycle	132
6.1.6 Mixed carbonate/siliciclastic sabkha cycle	134
6.2 'Markov Process' Analysis	136
6.3 Discussion	138
CHAPTER 7 - SEDIMENTATION MODEL	140
7.1 The Epeiric Sea and Flanking Sabkha Model	140
7.2 Palaeosetting	141
7.2.1 Australo-Antarctic palaeogeography	142
7.2.2 Local palaeogeography	145
7.3 Non-tidal Sedimentation	145
7.4 Storm Deposits	147
7.5 Hypersalinity	147
7.5.1 Preservation of cryptalgal mats	148
7.5.2 Paucity and reduced diversity of marine fauna	148
7.5.3 Widespread evaporite deposition	148
7.6 Emergence and Inundation	149
7.6.1 Correlations of shallowing-up cycles and transgressive 'kick-backs'	149
7.6.2 Correlation of subaerial exposure surfaces	151
7.7 Sabkha Dolomitization Models	154
CHAPTER 8 - HISTORY OF SEDIMENTATION	158
ACKNOWLEDGEMENTS	

REFERENCES

APPENDICES

- Appendix I Petrographic Classifications
- Appendix II Catalogue of Specimens
 - Index to thin sections
 - Index to polished slabs
- Appendix III Petrographic Descriptions

VOLUME 2 - SEDIMENTOLOGICAL LOGS

- Appendix IV Detailed Sedimentological Logs
 - Manya-1
 - Manya-2
 - Manya-3
 - Manya-6 (type section)
 - Marla-1, -1A, -1B
 - Marla-3
 - Marla-6
 - Marla-7
 - Middle Bore-1
 - Mt. Willoughby-1

LIST OF FIGURES AND TABLES

	PAGE NUMBER
<u>Chapter 1</u>	
Figure 1	2
Figure 2	7
Table 3	10
Figure 4	13
Table 5	15
Figure 6	17
Figure 7	19
<u>Chapter 2</u>	
Figure 8	22
Table 9	23
Table 10	24
Figure 11	26
Figure 12	(back pocket)
Table 13	30
Figure 14	32-33
Figure 15	35-36
Figure 16	37

Chapter 3

Figure 17	Laminated and silty carbonate mudstone.	41-42
Figure 18	Fenestral and stromatactitic carbonate mudstone.	44-45
Figure 19	Wackestones and grainstones.	48-49
Figure 20	Floatstone, rudstone and plate breccia.	56-57
Figure 21	Boundstones.	60-61
Figure 22	Clastics.	65-66
Figure 23	Bromine profile for halite from the <u>Manya-6</u> type section.	71
Figure 24	Halite.	74-75
Figure 25	Sulphate evaporites.	77-78

Chapter 4

Figure 26	Recrystallized dolostone.	83-84
Figure 27	Pressure solution textures.	87-88

Chapter 5

Figure 28	History of cementation of an ooid grainstone lens, thin section COM682, Marla-6, 679.33 m.	94
Figure 29	Grainstone diagenesis.	95-96
Figure 30	Schematic sketches of the most common occurrences of dolomite in the Ouldburra Formation.	98
Figure 31	Schematic diagram showing the petrogenesis of pressure solution textures from different precursor lithofacies.	103
Figure 32	Stylonodular texture overprinting an original planar laminated stromatolitic algal bindstone.	104
Figure 33	Diagenesis of sulphate evaporite nodules.	107-108
Figure 34	Paragenesis of sulphate nodules by alteration, replacement, solution and void filling processes.	109

Figure 35	Formation and diagenesis of solution collapse breccias.	112
Figure 36	Generalized overall paragenetic sequence for the Ouldburra Formation.	117

Chapter 6

Table 37	Number of complete sedimentary cycles in drillhole intersections based on empirical observation.	121
Figure 38	Typical halite/siliciclastic cycle.	123
Figure 39	Typical halite/mixed carbonate/siliciclastic cycle.	126
Figure 40	Idealized archaeocyath/algal bioherm cycle.	128
Figure 41	Idealized algal bindstone cycle.	131
Figure 42	Idealized carbonate sabkha cycle.	133
Figure 43	Typical mixed carbonate/siliciclastic sabkha cycle.	135
Table 44	Results of 'Markov process' analysis.	137

Chapter 7

Figure 45	Early Cambrian Australo-Antarctic palaeogeography.	143-144
Figure 46	Schematic palaeogeographic map of the eastern Officer Basin.	146
Figure 47	Drillhole correlation diagram, showing major regressions and transgressions.	152
Figure 48	Schematic diagrams showing various models of dolomitization.	155

Chapter 8

Figure 49	Regional sedimentation model for the Ouldburra Formation.	159
-----------	---	-----

Appendix I

- Figure 50 Carbonate classification.
Figure 51 Compositional classification of sandstones.

Appendix III

- Figure 52 Gypsum and anhydrite vein, thin section COM670, Marla-7, 364.50 m.
Figure 53 History of cementation of an ooid grainstone lens, thin section COM682, Marla-6, 679.33 m.
Figure 54 Cauliflower chert, thin section COM 750, Many-3, 537.20 m.
Figure 55 Cauliflower chert, SEM photo SEM750, Many-3, 537.20 m.
Figure 56 Energy dispersive SEM plot of core of cauliflower chert nodule, SEM750, Many-3, 537.20 m.
Figure 57 Partly silicified sulphate evaporite nodule, thin section COM768, Marla-6, 309.95 m.

CHAPTER 1

INTRODUCTION

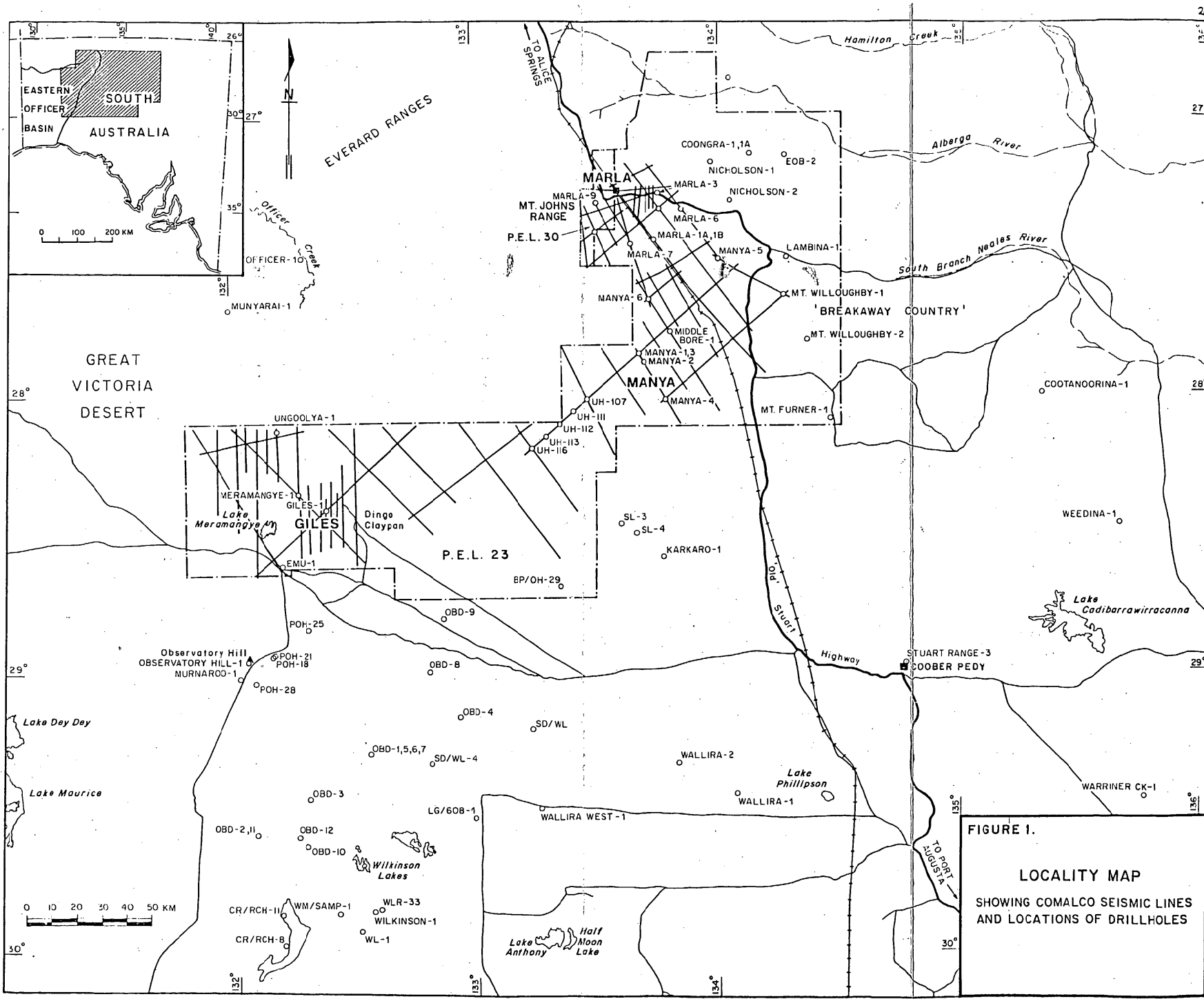
The Ouldburra Formation is a newly recognized unit of Early Cambrian carbonates, mixed carbonate siliciclastics and evaporites which has been intersected in a number of drillholes in the northeastern Officer Basin of South Australia. The Formation, as defined here-in, ranges from 143 m to over 1,200 m thick and is widespread in the sub-surface throughout the Marla-Manya area (Figure 1). This thesis presents a sedimentological history of the Ouldburra Formation and briefly describes the first significant palaeontological evidence for the age of the Formation.

1.1 Description of Location

The logistic centre is Marla, a road house and motel on the Stuart Highway 1,200 km north of Adelaide and 500 km south of Alice Springs. Marla is two kilometres from the rail siding of the same name on the main Tarcoola-Alice Springs line. Other access is confined to four wheel drive tracks, seismic and other survey lines.

The region has a Koppen type BWh arid desert climate. Maximum summer temperatures often exceed 45°C with high diurnal variation. During June and July, night-time minima fall below freezing point. The average annual rainfall is less than 150 mm p.a. with a mean annual evaporation around 3,500 mm.

The physiography of the region has been described by Krieg (1973), Pitt (1978) and Laut *et al.* (1977). The most significant contrasts are between the Everard and Mt Johns Ranges to the northwest, the 'Breakaway Country' to the east and the vegetated seif dunes of the Great Victoria Desert to the west.



Outcrop of Palaeozoic sediments is extremely sparse. The best examples occur in the Mt Johns Range and in the vicinity of Observatory Hill (Figure 1). Access is restricted, as both locations contain aboriginal 'sites of significance'. Silicified Palaeozoic carbonates also occur as surface float in the Giles to Dingo Claypan area. None of these exposures can be correlated with the Ouldburra Formation in the Marla-Manya area.

1.2 Tenure

Comalco Aluminium Limited (Comalco) holds Petroleum Exploration Licences (PEL) 23 and 30 (Figure 1) which cover the known distribution of the Ouldburra Formation in the Marla-Manya area.

1.3 Previous and Contemporaneous Work

1.3.1 Exploration History

The exploration history of the eastern Officer Basin is summarized in Kreis (1969), Pitt et al. (1980) and Robertson et al. (1980).

Interest in the Marla-Manya area began in 1980 when White and Youngs (1980) recognized the Observatory Hill Beds in the Marla area as a Cambrian terrestrial playa lake sequence containing pseudomorphs of trona. As part of its exploration for trona, Comalco Aluminium Limited began a programme of drilling and seismic reflection profiling. This data enabled Brewer, Henry and Weste (pers. comm., 1983) to differentiate between the alkali playa lake sequence in the Marla-Manya area (the Observatory Hill Beds, sensu Benbow, 1982) and an older, depositionally unrelated, sequence of Early Cambrian marine carbonates, mixed carbonate/siliciclastics and evaporites (the Ouldburra Formation).

Comalco shifted its exploration emphasis from trona to a petroleum search and expanded the regional seismic survey and stratigraphic drilling programme in PEL 23 and 30. To date, 2,100 km of seismic and 24 fully

cored drillholes have been completed. This sedimentological study of the Ouldburra Formation began in early 1985 in conjunction with work on source rock potential, maturation, porosity and permeability by other Comalco geologists.

1.3.2 Previous studies of the Ouldburra Formation

The only other sedimentological studies of the Ouldburra Formation were by Youngs (1980), who worked on the carbonates intersected in the South Australian Department of Mines and Energy (SADME) drillhole Marla-1A,B; and by Henry (pers. comm., 1984) who related the lithologies of Marla-1B to those intersected in two Comalco drillholes and postulated environments of deposition. Lydyard (1979) briefly described the petrography of carbonates intersected in Marla-1A,B, Manya-1 and five other drillholes from the eastern Officer Basin.

1.4 Methods of Study

This study is based on cores and wireline logs from seven fully cored and two spot cored drillholes in the Marla-Manya area and is augmented by regional seismic coverage and numerous shallow stratigraphic drillholes in PEL 23 and 30. In addition, outcrops at Observatory Hill and other exposures of possible Palaeozoic carbonates in the Marla to Emu area have been examined.

1.4.1 Petrography

Over 180 thin sections, showing the widest possible diversity of textures and lithologies, have been described. Appendix III contains those descriptions specifically referred to in the text.

The descriptions follow a modification of Dunham's (1962) carbonate classification by Embry and Klovan (1971) (Appendix I). Rocks containing more than 50 percent terrigenous material were classified using Swanson's

(1981) compositional classification. All particle and grain sizes are based on the scale of Wentworth (1922). The colour codes for hand specimen description are from the Geological Society of America Rock Colour Chart by Goddard *et al.* (1979) and refer to wet cut faces. The terminology for naming peloids, ooids and oncoids and aggregate grains follows the classification of Flugel (1982). The term 'dolostone' is used to distinguish the lithotype from 'dolomite' the mineral, and the terminology for dolomite crystal forms is from Friedman (1965) and Gregg and Sibley (1984).

Thin sections were prepared by AMDEL or Pontifex and Associates Pty Ltd. The carbonates have been stained with Alizarin Red-S; either directly in thin section; or the corresponding rock slice has been etched and stained. Potassium ferricyanide stain has been used to distinguish iron-rich carbonate phases. A limited number of X-ray diffraction analyses were undertaken to confirm the identity of various minerals. The prefix COM for specimen numbers refers to a thin section stored in the collection of Comalco Exploration, Glenside.

1.4.2 Insoluble residue studies

Over 50 samples of carbonates and mixed carbonate/siliciclastics from 6 drillholes have been dissolved in 10 percent acetic acid. The unconcentrated residues were examined initially under X40 magnification for microfossils and insoluble authigenic and detrital minerals.

1.4.3 Isotope and trace element studies

Isotope studies of carbonates from the northeastern Officer Basin (Lambert *et al.*, 1986) have been used as palaeoenvironmental indicators to distinguish marine from non-marine and to assist in the interpretation of diagenetic alteration. Some of these data; including $^{87}\text{Sr}/^{86}\text{Sr}$ ratios,

delta ^{13}C , and ^{34}S analyses were utilized in this study. A bromine profile was plotted for the bedded halite.

1.4.4 Detailed sedimentological logs

Cores from nine drillholes which intersected the Ouldburra Formation (totalling ca. 3,200 m) were logged at 1:50 scale to differentiate the various primary and secondary lithologies and to highlight diagnostic sedimentary structures. Logs were computer-drafted using modified AUSLOG software and reduced to A4 (Appendix IV). Cores are stored in the South Australian Department of Mines and Energy (SADME) Core Library, Glenside. The polished slabs referred to in the Catalogue of Specimens (Appendix II), are stored in the collection of Comalco Exploration, Glenside. Duplicate samples are kept in the SADME Core Library.

1.5 Regional Geology

The area described in this thesis is bordered by the Archaean to Lower Proterozoic crystalline basement of the Gawler Craton to the southeast and the Precambrian Musgrave-Mann Metamorphics to the north, and includes the Adelaidean to Devonian sediments of the eastern Officer Basin, the Permo-Carboniferous Arckaringa Basin and the Mesozoic Great Artesian Basin. Figure 2 summarizes the lithostratigraphy of the region.

1.5.1 Archaean-Lower Proterozoic basement

The oldest geological formations in the region are the Archaean-Lower Proterozoic basement in the Musgrave Block, the Gawler Craton and the small Ammaroodinna Inlier. Parker (1979) and Parker and Lemon (1982) revised the stratigraphy of the meta-sediments and recognized five major tectonic subdomains in the Gawler Craton. The Musgrave Block consists of Precambrian igneous, metamorphic and minor metasedimentary rocks. In the Western Australian portion of the

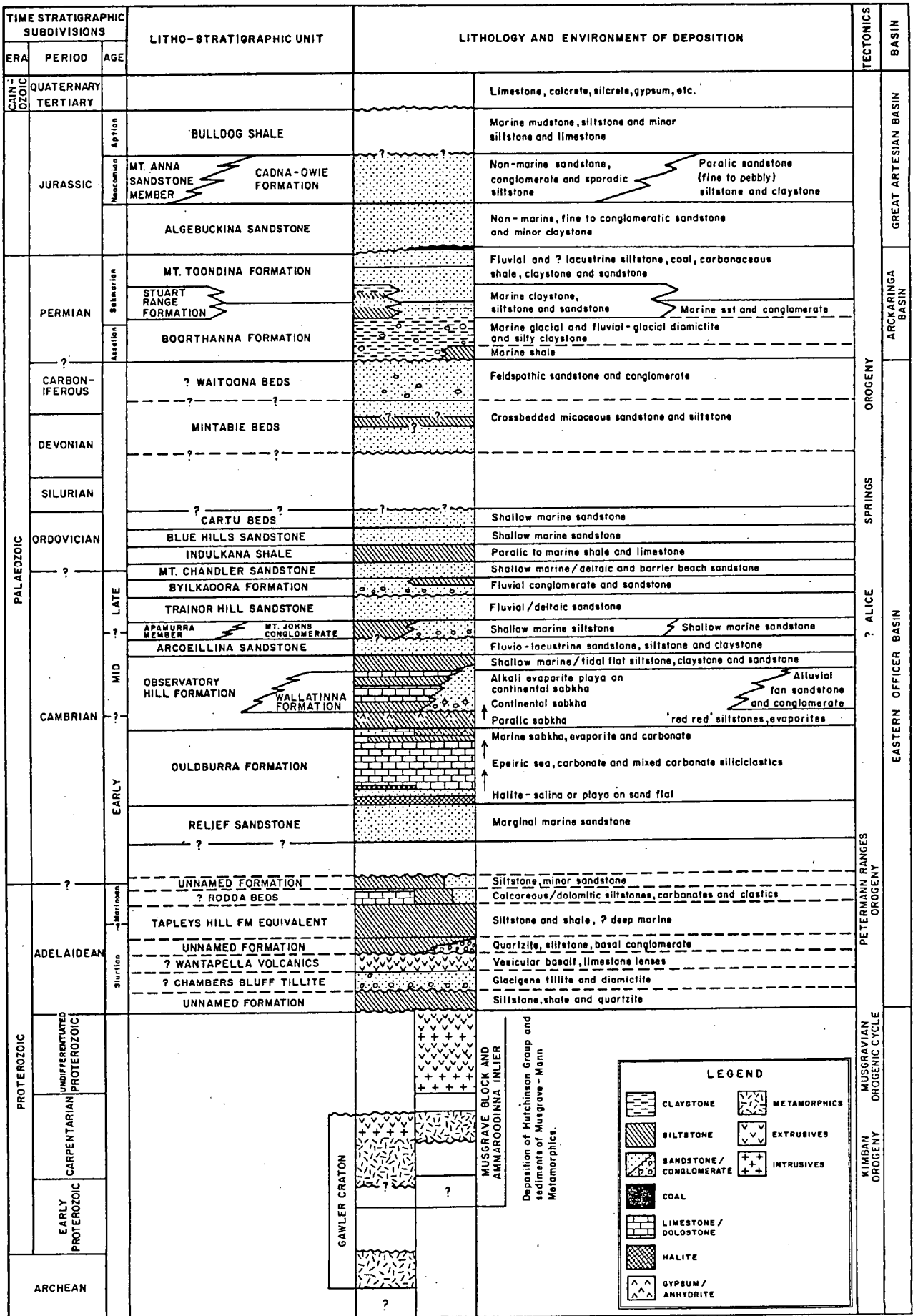


FIGURE 2: COMPOSITE STRATIGRAPHY OF THE NORTHEASTERN OFFICER BASIN. NOT TO SCALE. (after Benbow (1982); Hibburt (1984); Krieg (1973); and Pitt et al. (1980)).

Musgrave Block, the older basement rocks are mostly granulite, migmatite and granite. This nucleus is overlain by metasediments and metavolcanics (Jackson and van de Graaff, 1981). Moore and Goode (1978) describe similar middle Proterozoic metamorphics including felsic, mafic and quartz granulites; and calc-silicate rocks form the Musgrave Block in western South Australia. An isolated basement inlier, the Ammaroodinna Inlier, is exposed in one known locality in the Marla-Manya area and thus, is far removed from all other exposures of crystalline basement. Krieg (1972) described strongly foliated schists and gneisses of greenschist metamorphic facies. Ages of $1,096 \pm 20$ Ma (K/Ar) and $1,050 \pm 20$ Ma (Rb/Sr) have been obtained on a pegmatite from the inlier (Krieg, 1973).

1.5.2 Adelaidean lithostratigraphy

The Proterozoic sediments of the region were not originally considered to be part of the eastern Officer Basin (Krieg, 1969), however the currently favoured definition (Jackson and van de Graaff, 1981; Pitt *et al.*, 1980) includes sediments of Torrensian to Devonian age. Sporadic outcrops of folded Adelaidean sediments and minor volcanics have been reported from the northeastern Officer Basin. Krieg (1973) mapped a sequence in the Mt Johns area which he correlated with Marinoan and older formations in Adelaide Geosyncline. Depth to magnetic basement, seismic data and several drillhole intersections suggest that the Adelaidean section approaches two kilometres in thickness and locally includes glacials, basalt flows (Brewer, pers. comm., 1985), turbidites and deep marine facies.

1.5.3 Cambrian to ?Lower Carboniferous lithostratigraphy

The Cambrian lithostratigraphy of the northeastern Officer Basin was re-defined by Benbow (1982) and more recently by Brewer *et al.*

(1986). The ?Ordovician to ?Lower Carboniferous stratigraphy is less well understood and is known mainly from surface mapping by Krieg (1973). Table 3 summarizes the Cambrian to ?Lower Carboniferous lithostratigraphy of the Marla-Manya area including the Mt Johns Ranges outcrops.

Age	Stratigraphic Unit	Maximum Thickness (metres)	Lithology	Remarks
?Upper Devonian to ?Lower Carboniferous	Waioona Beds	183+	Outcrop: Friable, strongly kaolinized pebbly feldspathic sandstone and lens of polymict conglomerate with well rounded large pebbles. Subsurface: Friable feldspathic greywacke	Section penetrated in Continental Officer No. 1 stratigraphic well. Syntectonic deposit- ?Pertnajara Movement Boundaries unknown
	Mintable Beds	25+	Greyish-brown micaceous sandstone, arkosic and lithic; micaceous feldspathic siltstone. White kaolinitic opal-bearing sandstone at top	Large scale, arcuate and planar cross-bedding in lower sandstone units. Upper and lower boundaries unknown
?Unconformity-Chandleran Movement				
Lower to ?Middle Ordovician	Cartu Beds	600+	White medium to fine kaolinitic sandstone, green biotitic sandstone and siltstone, white and red shale, thin ferruginous bands	Upper boundary unknown
	Blue Hills Sandstone	1300	Red-brown weathering fine to medium sandstone with well sorted rounded grains, slightly kaolinized; gritty and pebbly bands	Rare, non-diagnostic organic trails
	Indulkana Shale	60	Red and green shale with rare thin limestone lens grading laterally to pale green, slightly calcareous siltstone and very fine sandstone	Thickest in Indulkana Range, thinning to southwest
	Mount Chandler Sandstone	100	Fine to medium well sorted sandstone with rounded grains; lower beds hard, white quartzitic; upper beds more reddish, slightly feldspathic. Some tabular-planar cross-bedding	Abundant <i>Scolithus</i> and <i>Diplocraterion</i> burrows
Local Disconformity				
?Mid to ?Upper Cambrian	Byilkaoora Formation	54	White cross-bedded kaolinitic sandstone, conglomeratic at base, minor siltstone at top	
	Trelnor Hill Sandstone	222	Cross-bedded well sorted medium to fine grained sandstone interbedded with red siltstone and claystone	
	Appamurra Member		Light red-brown dolomitic siltstone, sandstone, conglomeratic base	
	Mt Johns Conglomerate	78	Red polymict pebble to boulder conglomerate with sandy interbeds	
?Middle Cambrian	Arcoellinna Sandstone	182	Red-brown to white cross-bedded feldspathic micaceous and lithic sandstone with thin red-brown siltstone and claystone interbeds	
	Observatory Hill Formation	400	Red-brown calcareous claystone and siltstone, laminated red-brown to green grey micaceous calcareous siltstone and carbonate mudstones, alkali evaporite pseudomorphs, chaotically bedded 'red bed' siltstone and sandstone	
	Wallatina Formation	107	Thinly bedded coarse to granule arkose and interbedded red-brown to green siltstone	Interdigitates with Observatory Hill Formation
Lower Cambrian	Ouldurra Formation	1114	Mixed carbonate/siliciclastics limestone and dolostone, halite	See Section 2.1.2 this paper
	Relief Sandstone	79+	Pale red silica cemented feldspathic to quartzose sandstone ranging from fine to very coarse grained	See Section 2.5.1 this paper

TABLE 3: CAMBRIAN TO ?LOWER CARBONIFEROUS LITHOSTRATIGRAPHY, MARLA-MANYA AREA, (based on Benbow, 1982; Brewer *et al.*, 1986; and Krieg, 1973).

1.5.4 Permo-Carboniferous lithostratigraphy

The Permo-Carboniferous rocks of the region are assigned to the Arckaringa Basin (Moore, 1982) and have been discussed by Hibburt (1984), Townsend (1976), Townsend and Ludbrook (1975) and Wopfner et al. (1970). The stratigraphy consists of the marine glacials and fluvial-glacials of the Boorthanna Formation, overlain by marine shales and mudstones of the Stuart Range Formation, and the coal-bearing fluvatile and ?lacustrine Mt Toondina Formation. Seismic data and numerous shallow drillhole intersections in the Marla to Emu area have shown Permo-Carboniferous palaeo-channel sediments to be more widely distributed in the sub-surface than previously thought.

1.5.5 Mesozoic lithostratigraphy

The Mesozoic units in the region are, in ascending order, the Jurassic Algebuckina Sandstone (Wopfner et al., 1970), the Early Cretaceous (?Neocomian) Cadna-owie Formation (Wopfner et al., 1970), and the Aptian Bulldog Shale (Freitag, 1966). The Algebuckina Sandstone and the Cadna-owie sandstones and siltstones are thought to have been deposited in fluvatile and paralic environments respectively; the Bulldog Shale is dominantly marine.

1.5.6 Cainozoic units

The Tertiary to Holocene sequence consists of thin deposits of limestone, gravel, sand, silt, mud, shale, silcrete, calcrete and gypsum. Pitt (1976) and Krieg (1973) mapped these units in adjacent areas. The exposures are often calcified, silicified or ferruginised. Small deposits of opal are associated with the development of a late Tertiary duricrust in the vicinity of Ouldburra Hill and Sarda Bluff (Nichol, 1971).

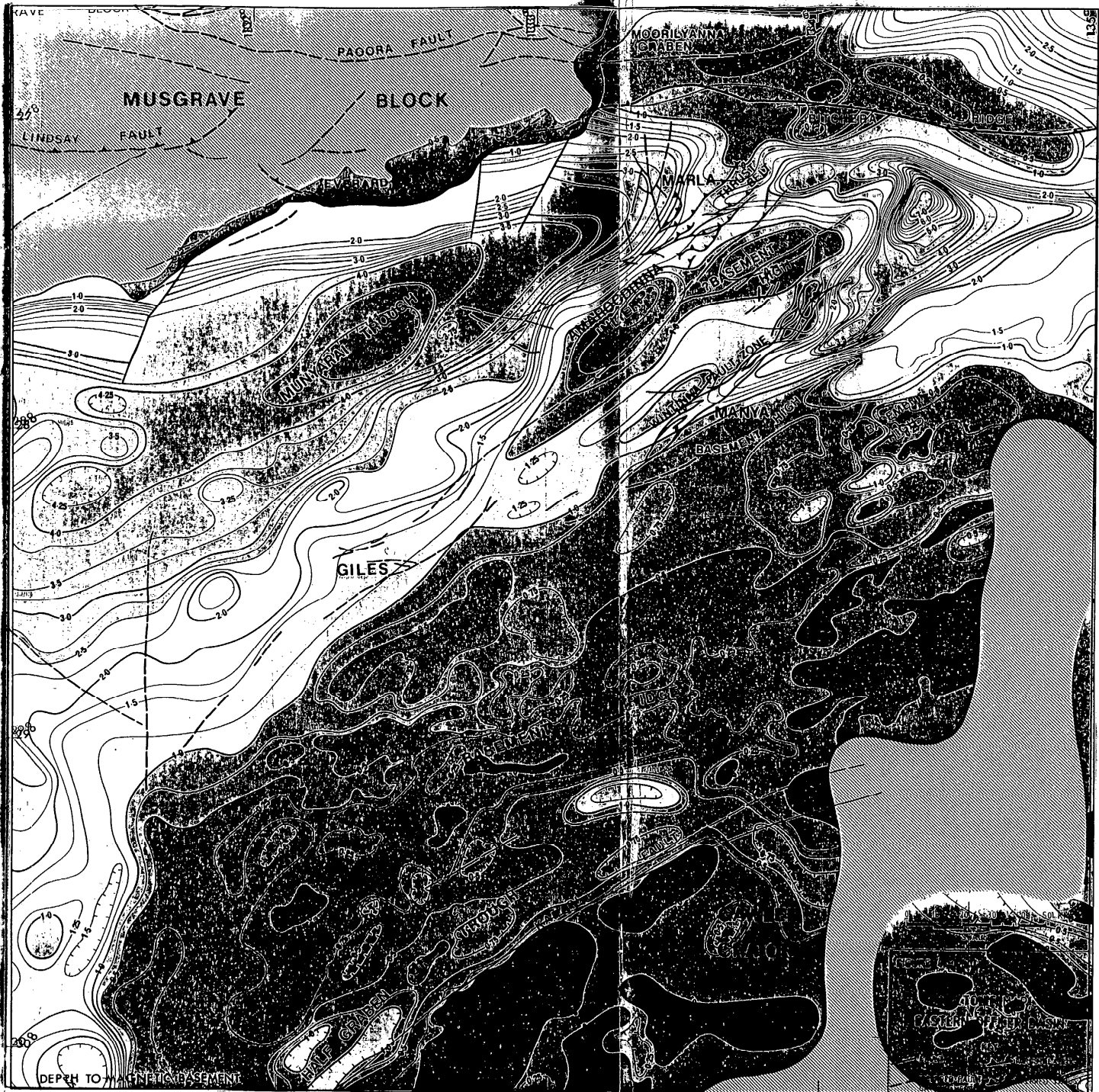
1.6 Tectonic History

The tectonic evolution of the eastern Officer Basin is poorly understood. Douth and Nicholas (1978), Milanovsky (1981) and Veevers et al. (1982) proposed Late Proterozoic aulacogen development as the precursor to Palaeozoic intracratonic development. Austin and Williams (1981) favoured tensional tectonism resulting from differential movements between two sub-continental blocks. Lambeck (1984) developed a mechanical model of intracratonic basin development based on crustal compression and isostatic adjustment.

Irrespective of the mechanism, subsidence in the eastern Officer Basin began in the Late Proterozoic and was accompanied by deposition of a thick sequence of Adelaidean sediments. This was terminated about 600 Ma by the Petermann Ranges (=Indulkian) Orogeny which folded and faulted the Adelaidean sediments in the northeastern margin of the basin. The orogeny was also accompanied by limited basaltic volcanism. Deformation appears to be more intense close to the Musgrave Block where Krieg (1973) mapped broad anticlines with up to 60° dips. Seismic data shows that the Adelaidean sediments are less deformed further into the basin.

A second sequence of events began in the Mid-Cambrian (Veevers et al., 1982) and culminated in the ?Devonian to Early Carboniferous Alice Springs Orogeny. The Musgrave Block was significantly uplifted and thrust over the northern boundary of the Munyarai Trough (Milton and Parker, 1973; Vozoff and Cull, 1981). This uplift was probably also responsible for the change from localized carbonate sedimentation to widespread clastic deposition in the eastern Officer Basin.

Late in this orogenic phase, a series of major northeast-southwest trending thrust faults were active in the Marla area (Figure 4).



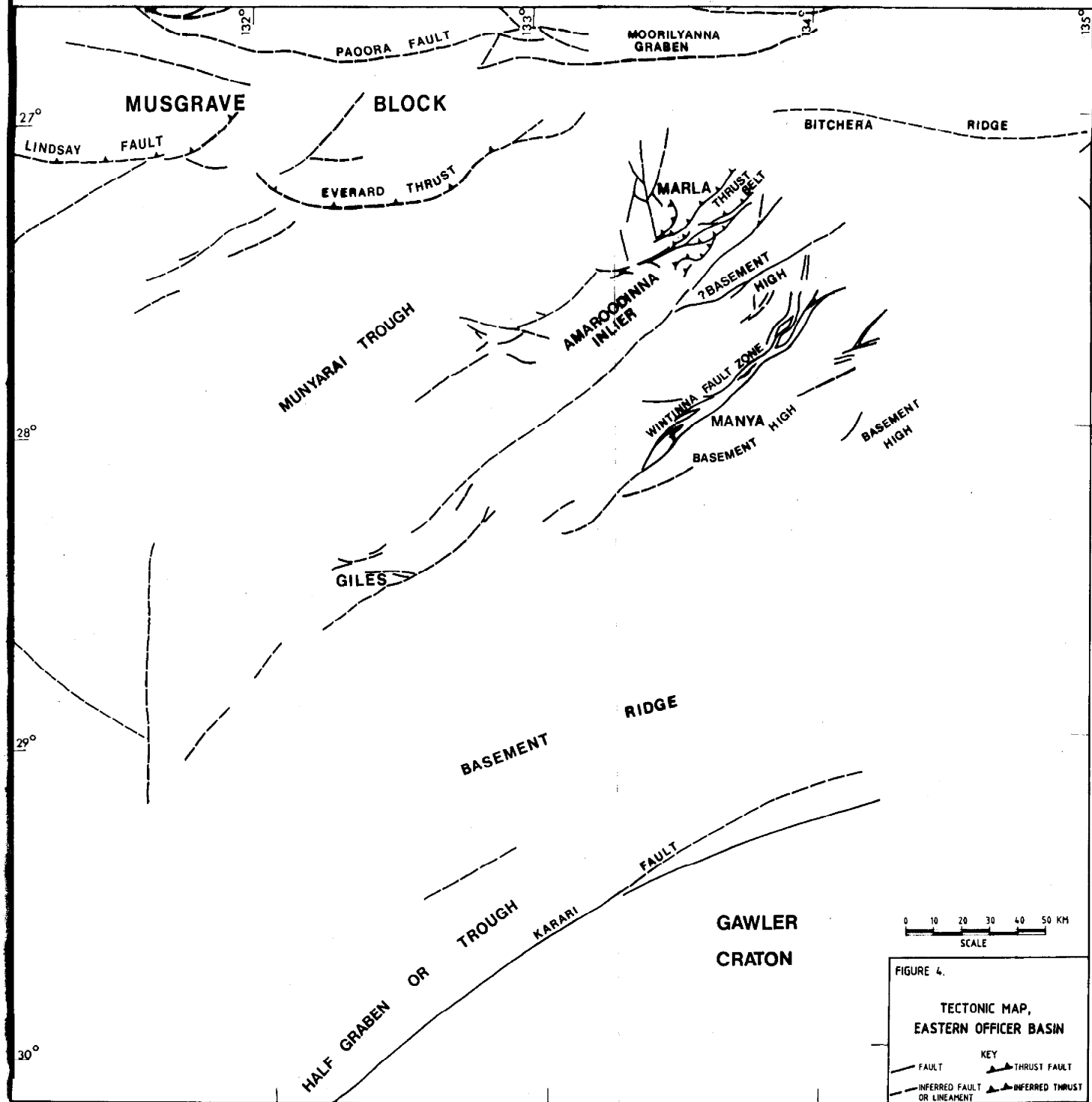


FIGURE 4.

TECTONIC MAP,
EASTERN OFFICER BASIN





Collectively, these faults have a horizontal displacement of at least 8 km. Several of the longest appear to have been reactivations of Precambrian extensional faults (Diekman, pers. comm., 1985).

The style of deformation differs in the vicinity of drillholes Manya-1, Manya-3 and Middle Bore-1, where the influence of lateral movements is made more obvious by the development of wide northeast-southwest trending fracture zones, wrench systems and horst structures (Diekman, pers. comm., 1985), which collectively make up the Wintinna Fault zone (Figure 4). There is evidence of vertical offset and a marked difference in thickness of both Adelaidean sediments and the Ouldburra Formation across the Wintinna Fault. This is interpreted as evidence of transcurrent movement with a lesser vertical component rather than growth faulting.

Flat lying Permian and younger sediments indicate that only gentle epeirogenic movements affected the eastern Officer Basin after the Alice Springs Orogeny.

1.7 Economic Potential

The Ouldburra Formation carbonates are potential hosts for Mississippi Valley type mineralization. Ore deposits known to be associated with intraformational pervasive subaerial exposure of carbonates (Bechstadt and Dohler-Hirner, 1983; Kyle, 1983) are also potential targets.

1.7.1 Base Metal Prospectivity

Continuous geochemical profiles of Cu, Pb and Zn have been plotted for all the major intersections of the Ouldburra Formation (data from Brewer, 1985). The stratigraphic location of significant concentrations are summarized below in Table 5. These sporadic anomalous intervals are apparently caused by sphalerite and pyrite, but are not regarded as being of economic significance. Disseminated pyrite occurs throughout various

DRILLHOLE	DEPTH (m)	ANOMALOUS METALS	MAXIMUM VALUE (ppm)
MANYA-3	200-206	Zn	200
	212-214	Cu	70
	228-230	Cu	65
		Zn	310
	244-246	Cu	75
		Zn	115
	324-326	Cu	120
		Zn	160
MANYA-6	906-908	Cu	440
		Zn	430
	934-936	Cu	60
		Zn	110
	1150-1152	Cu	70
		Zn	90
	1194-1196	Cu	220
		Zn	200
MARLA-1B	304	Pb	22
		Zn	120
	337	Pb	36
		Zn	80
	361-364	Pb	26
		Zn	65
MARLA-3	572-596	Pb	1600
		Zn	520
	614-628	Cu	420
MARLA-6	646-682	Pb	130
		Zn	690
MARLA-7	476-479	Pb	190
		Zn	300
	524-536	Pb	360
		Zn	8350
	540-542	Zn	240

TABLE 5: SUMMARY OF Cu,Pb,Zn ANOMALIES ABOVE THE 95 PERCENTILE FOR THE OULDBURRA FORMATION (data from Brewer, 1985).

lithologies ranging from sandstone to pressure solution textures, and is locally concentrated into millimetre scale irregular laminae and nodules. Sphalerite is most conspicuous where it is associated with replacement silicification in ooid grainstones and as void fill in the limited available secondary porosity in other carbonate facies. None of the examples of mineralization can be related to particular sedimentary facies or to subaerial exposure.

The drillhole Middle Bore-1 was targeted on coincident gravity and magnetic anomalies related to a fault which brought the Ouldburra Formation carbonates into contact with Precambrian pyroxene granulites. The hole intersected only minor mineralization.

1.7.2 Petroleum Prospectivity

The Ouldburra Formation contains source rocks, zones of porosity and permeability, and cap rocks suitable for the development of stratigraphic or structural hydrocarbon traps. Comalco Aluminium Limited is currently involved in hydrocarbon exploration in the Palaeozoic sediments of the eastern Officer Basin. To date, no wells have been targeted on plays in the Ouldburra Formation.

The source rock potential of the Ouldburra Formation can be demonstrated by locally significant levels of organic material. A collection of 170 samples from a variety of carbonate lithofacies in 6 drillholes have an average total organic carbon content (TOC) of 0.32 percent. The TOC of stromatolitic algal bindstones from the Ouldburra Formation ranges from 0.2 percent to 1.3 percent (Weste et al., 1984). McKirdy et al. (1984) reported 4.56 percent TOC from a stylocumulate at 127.12 m in drillhole Marla-1A. The average TOC content for carbonate rocks worldwide is 0.67 percent (Tissot and Welte, 1978). Known source rocks may have TOC contents as low as 0.3 to 0.5 percent (Palacas, 1983).

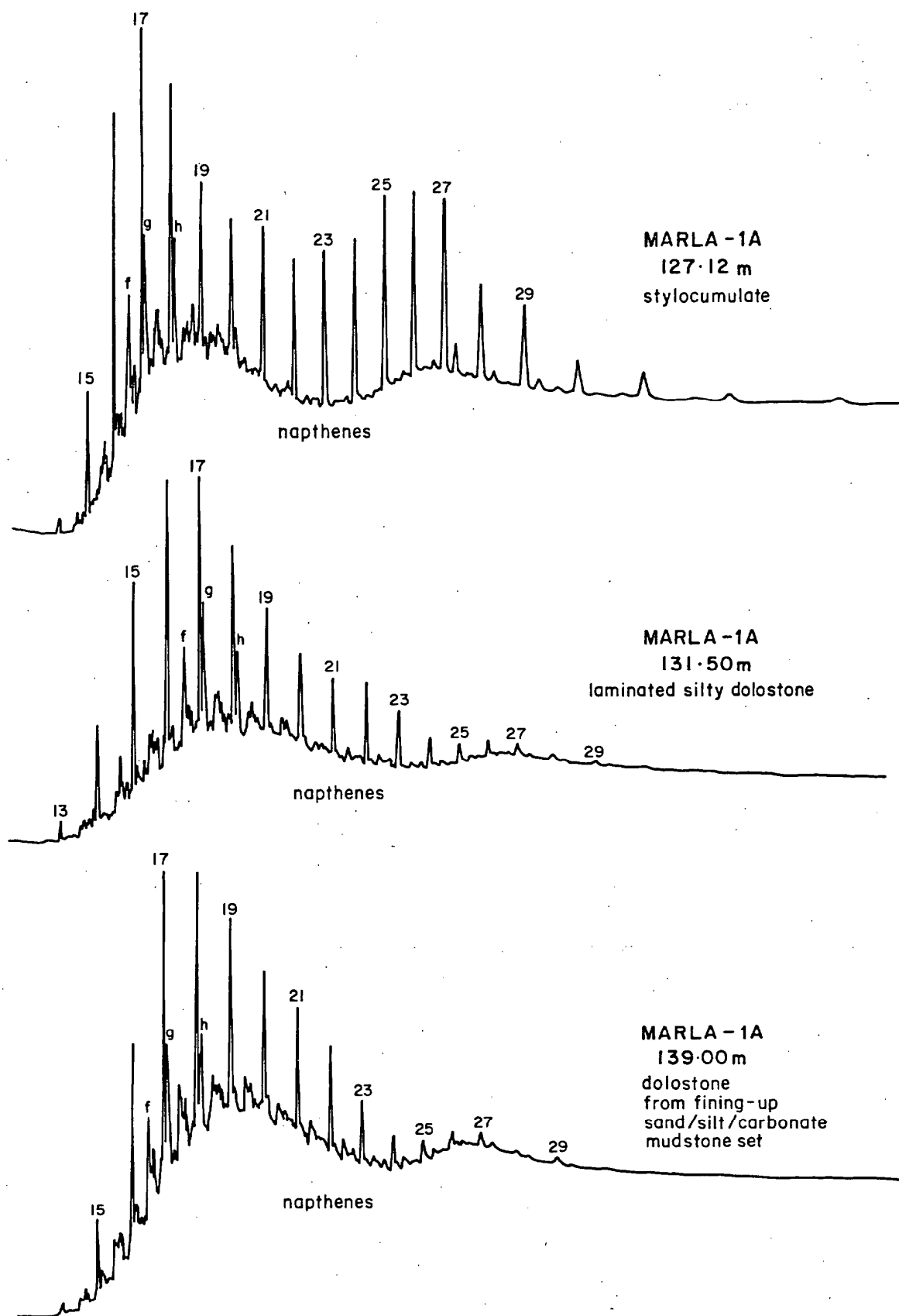


FIGURE 6: GAS CHROMATOGRAMS OF ALKANES FROM MARLA-1A
(after McKirdy IN Benbow, 1980).

f-h are the acyclic C_{18} - C_{20} regular isoprenoids, g = pristane, h = phytane

Rock-Eval pyrolysis indicates a maximum hydrogen index of 400 mg HC/g TOC from the Ouldburra carbonates. The analyses from Marla-1A, -1B show an n-alkane profile (Figure 6) and pristane to phytane ratio indicative of an algal source. Type III kerogen is dominant and is characterized by low atomic H/C ratios (0.67-0.69) and by a marked even or odd carbon-number preference in the C₁₂-C₂₀ range (Figure 7). Overall, these data indicate cyanobacterial action on a bluegreen algal precursor (McKirdy *et al.*, 1984).

The maturity of the organic matter in the Ouldburra Formation carbonates in the Marla-Manya area varies from gas prone to overmature (McKirdy, pers comm, 1986).

The Ouldburra Formation contains significant potential reservoirs in the form of leached carbonate zones associated with intraformational subaerial exposure and as pervasive zones of secondary dolomitization tens of metres thick. Up to 23 percent porosity and from 1,400 to 1,600 millidarcies permeability have been recorded from such sequences in the Manya-6 type section.

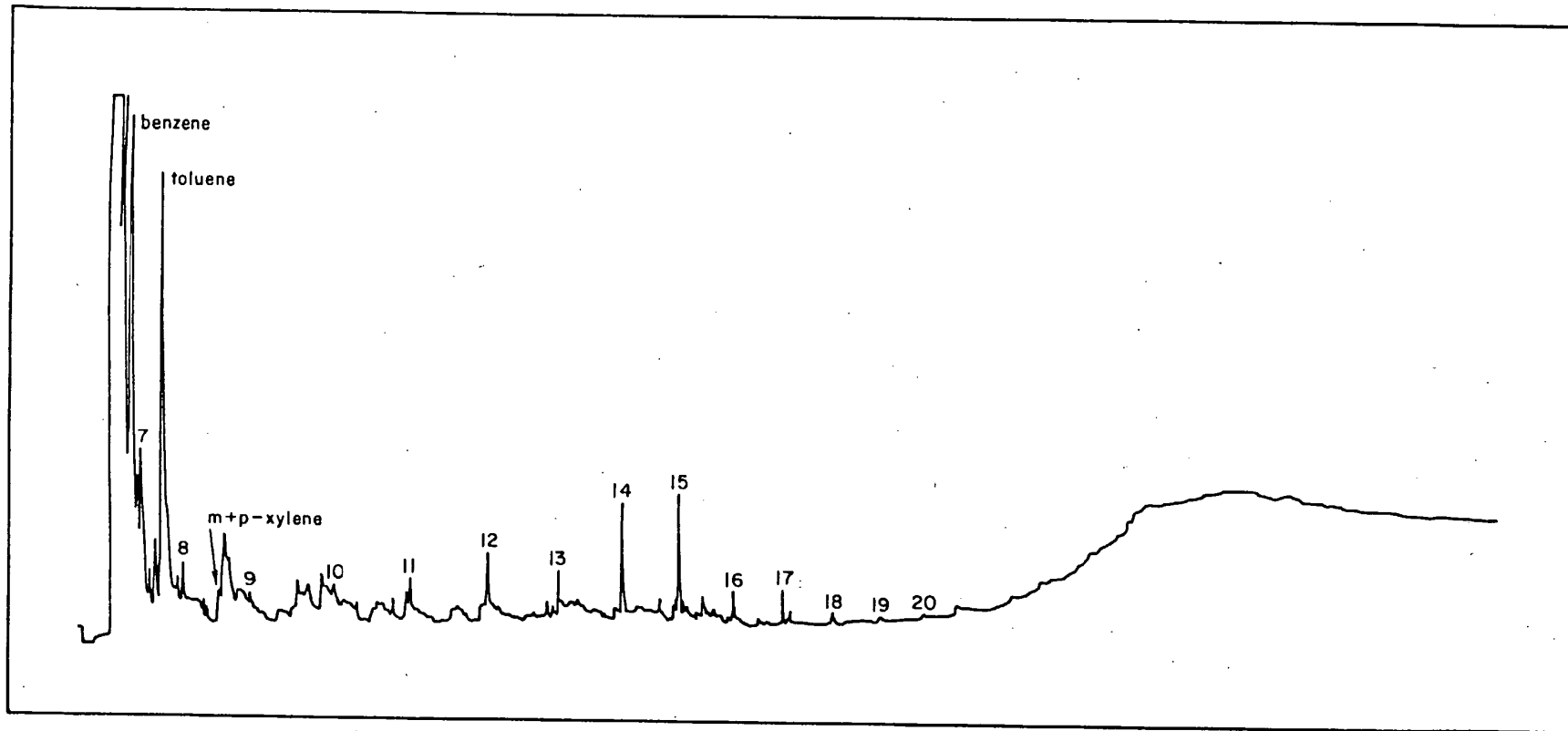


FIGURE 7: PYROLYSIS - GC TRACES OF TYPE III KEROGENS FROM MARLA-1A, 131-50.
Numbers refer to carbon number of n-alkene/n-alkane doublets (after McKirdy et al., 1984).

CHAPTER 2

STRATIGRAPHY OF THE OULDBURRA FORMATION

2.1 Definition of Type Section

Brewer et al. (1986) defined the non-marine Observatory Hill Formation to differentiate it from the older marine Ouldburra Formation. The Ouldburra Formation as strictly defined herein is known only in the Marla-Manyá area, although lithostratigraphic correlates are believed to be widespread to the east southeast and seismic stratigraphic correlates extend to the southwest.

2.1.1 Derivation

The Ouldburra Formation takes its name from Ouldburra Hill (Lat. 27° 31' 00" S, Long. 133° 55' 00" E approx.) on the Wintinna 1:250,000 topographic map.

2.1.2 Lithostratigraphic definition

The Ouldburra Formation consists of mixed carbonate/siliciclastics, marine carbonates and evaporites. Much of the Formation is characterized by the development of 1-5 m thick cycles. These include a wide variety of lithologies and lithofacies and occur over most of the known distribution of the Ouldburra Formation in the Marla-Manyá area. The base of the Formation is defined as the bottom of the lowermost carbonate unit, siltstone or halite bed, conformably overlying the Relief Sandstone. The upper boundary is taken as the top of the uppermost carbonate unit underlying the gypsiferous red beds of the Observatory Hill Formation. Both upper and lower contacts can easily be identified on downhole geophysical logs.

The top and bottom of the Ouldburra Formation, as intersected in several drillholes, correspond to time lines on seismic sections. These may, within the bounds of resolution, be traced throughout the Marla-Manya area. They correspond to important boundaries marked by changes in velocity and density to underlying and overlying formations, but do not necessarily reflect an homogenous lithological unit within this seismic interval.

2.1.3 Type section

A complete and conformable section of the Formation, intersected between 571.4 m and 1,685.6 m in the fully cored Comalco drillhole, Manya-6 (Lat. 27° 40' 08.0" S, Long. 133° 42' 59.7" E), is nominated as the type section (Figure 8). The core is stored at the South Australian Department of Mines and Energy Core Library, Glenside. The detailed sedimentological log is presented in Appendix IV.

2.1.4 Synonymy

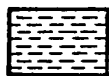
Prior to March 1985, the Ouldburra Formation has been informally referred to as the 'Wintinna Formation' by Comalco geologists.

Marine carbonates intersected in South Australian Department of Mines and Energy (SADME) drillholes Marla-1,-A,-B (Benbow, 1980) Mt Willoughby-1 (Thornton, 1971), and Manya-1 (Thornton, 1978) were correlated with the Observatory Hill Beds (Wopfner, 1969). These units are now assigned to the Ouldburra Formation.

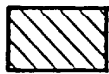
2.2 Distribution and possible correlatives

The Ouldburra Formation is not known to crop out; however, it has been intersected in numerous drillholes in the Marla-Manya area (Figure 11), and Comalco seismic data suggests that the Ouldburra Formation, as defined in this thesis, is widespread in the sub-surface throughout the area bordered by Lats. 27° 15' 00" S, 28° 07' 00" S and Longs. 133° 35' 00" E,

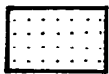
KEY TO FIGURE 8



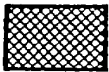
claystone



siltstone



sandstone



halite

134° 20' 00" E. This is an areal extent of 6,400 sq. km. Drillholes which intersected marine facies of the Ouldburra Formation are listed in Table 9.

COMPANY/ AUTHORITY	DRILLHOLE	DEPTH (m)
SADME	Manya-1	146.0-151.2
COMALCO	Manya-2	643.0-643.8 ✓ (TD 646.0 WCR)
COMALCO	Manya-3	174.0-812.9
COMALCO	Manya-6	571.4-1685.6
SADME	Marla-1,-1A,-1B	83.0-379.4
COMALCO	Marla-3	490.4-633.0
COMALCO	Marla-6	256.3-702.5
COMALCO	Marla-7	193.3-543.0
COMALCO	Middle Bore-1	160.0-371.8
SADME	Mt. Willoughby-1	623.6-639.7
COMALCO	UH107,-111,-112,-113,-116	

TABLE 9: INTERSECTIONS OF THE OULDBURRA FORMATION, MARLA-MANYA AREA.

Other possible lithostratigraphic correlates have been intersected in a number of other drillholes as shown in Table 10. These correlations have been suggested by Ambrose and Flint (1981), Hibburt (1984), Moore (1982) and Townsend (1976).

COMPANY/ AUTHORITY	DRILLHOLE	DEPTH (m)
SADME	Cootanoorina-1	891.54-948.23
SADME	Wallira West-1	314.9- <u>332.8</u> ? TD 358.8
KENNICOTT	Warriner Ck-1	283.0-411.0
PEXA	Weedina-1	726.0-1,624.0
SADME	Wilkinson-1	210.0- <u>710.0</u> 695.0 (695-710 ? Relief Sat)

TABLE 10: DRILLHOLE INTERSECTIONS OF POSSIBLE CORRELATES OF THE OULDBURRA FORMATION.

Within the conventionally accepted boundaries of the eastern Officer Basin (Flint and Parker, 1982; Pitt et al., 1980), the maximum possible distribution of the Ouldburra Formation is delimited by the 'Nurrai Ridge' to the west; the Musgrave Block to the north northeast; the Bitchera Ridge to the northeast, and the Gawler Craton to the southeast (Figures 4, 11).

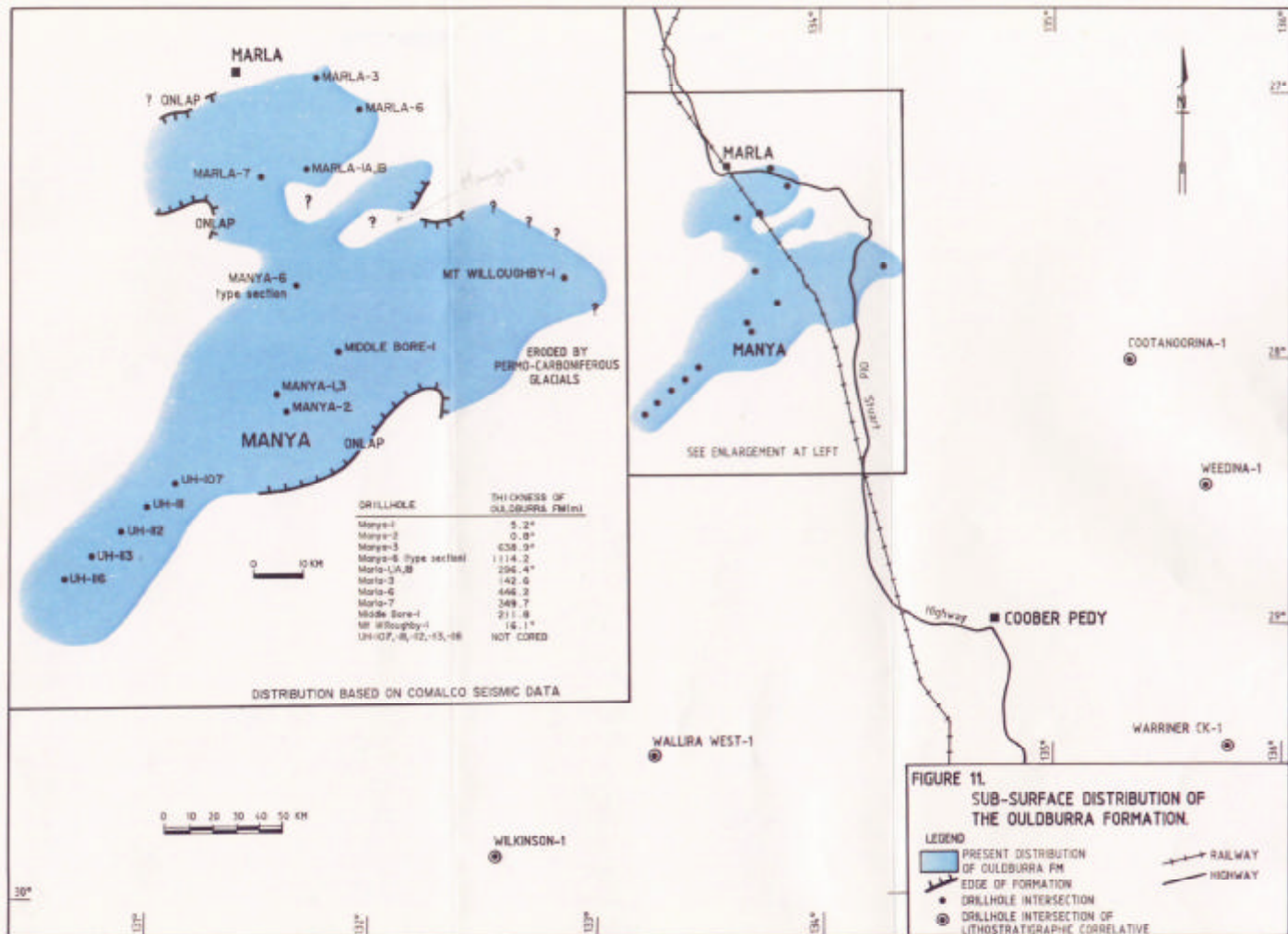
The Bitchera Ridge (Flint and Parker, 1982) is a gravity and aeromagnetic high to the northeast of Marla. The drillholes in this area (Nicholson-2 and Getty EOB-2) intersected only Permian and ?Adelaidean sediments. Limited very poor quality seismic data suggests onlap of Cambrian sediments and so this area is interpreted as a palaeo-high during the deposition of the Ouldburra Formation.

The 'Nurrai Ridge' is a north-south extension of the Musgrave Block prominent on both the Bouger gravity and total magnetic intensity maps. It is also believed to have been a palaeo-high during much of the Cambrian, separating the east and west Officer Basin, and forming a barrier to the western limit of Cambrian sedimentation (Anon., Phillips Australian Oil Company, 1984; Weste, pers. comm., 1984). Munyarai-1

and Officer-1 are the only open-file drillholes between the 'Nurrai Ridge' to the west, the Gawler Craton to the north, and the known occurrences of the Ouldburra Formation to the east. The stratigraphy in Munyarai-1 is interpreted as Devonian siltstones and claystones, and ?Cambrian sandstones, overlying Adelaidean sediments (Weste, pers. comm., 1984). Thus, it appears that the carbonates of the Ouldburra Formation are not present in the vicinity of Munyarai-1 although their deposition and subsequent erosion is also a possibility.

The southeastern limit of the Ouldburra carbonates in the Manya area can be fixed between drillholes Manya-2 and Manya-4. The former hole terminated in the top few metres of carbonates tentatively assigned to the Ouldburra Formation; while in the latter hole, the ?Observatory Hill Formation siltstones are underlain by a coarse grained sandstone which rests unconformably on Proterozoic gneiss. Seismic sections from this area show possible facies changes within the Ouldburra Formation as it on-laps basement. Further south, a number of shallow drillholes intersected Permo-Carboniferous and younger sediments on Archaean gneiss of the Gawler Craton (Figure 11). Seismic data shows onlap of the Cambrian sediments which suggests that this area was a palaeo-ridge separating the Cambrian sedimentation as evident in drillhole Wilkinson-1 from the Ouldburra Formation in the Manya area.

To the southwest of the Manya area, carbonates assigned to the Ouldburra Formation were intersected in a number of shallow drillholes (UH107, -111, -112, -113, and -116). In this area, the Ouldburra Formation is disconformably overlain by poorly consolidated Permo-Carboniferous sediments. Seismic data indicates that lateral equivalents of the Ouldburra are probably present further southwest. The lithological affinities of these correlates remains obscure.



Sub-Arckaringa Basin outliers intersected in Cootanoorina-1, Warriner Ck-1, and Weedina-1 were originally thought to be of Devonian age (Allchurch and Wopfner, 1973). However, Moore (1982) suggested a lithological correlation with the 'Early Cambrian marine Observatory Hill Beds' (ie. the Ouldburra Formation). It is not possible to make detailed lithological correlations between the Cootanoorina and Ouldburra type sections, and the relationship of the two units remains problematical.

2.3 Thickness

Isopachs of thickness (Figure 12) calculated from seismic data show that the thickest Ouldburra Formation occupies a northeast-southwest trending trough bordered to the southeast by the Wintinna Fault. The 1,114.2 m type section is situated within this trough. There is a marked difference in thickness across the fault. The Formation also thins considerably to the north as it on-laps basement. The drillhole Marla-3 intersected a complete basin-margin section only 142.6 m thick.

To the east, Permo-Carboniferous glaciation has removed a considerable thickness of the Formation. The Ouldburra also subcrops beneath Mesozoic sediments to the east of drillhole Marla-1.

2.4 Lithostratigraphic Relations

The Ouldburra Formation is underlain by the Relief Sandstone and overlain, sometimes disconformably, by the Observatory Hill Formation 'red beds'. The drillholes Manya-6 (type section) and Marla-3 penetrated all three formations in the Marla-Manya area.

2.4.1 Relief Sandstone

The Relief Sandstone in the Marla-Manya area consists of hard, pale red, silica cemented, feldspathic to quartzose sandstone. Grain size ranges from fine to very coarse, and sorting is moderate to poor. The unit is

characterized by stacked plane laminae, commonly defined by grain size variation. Small to medium scale planar cross-stratification is moderately common. An ephemeral fluvial sand plain, possibly incorporating some aeolian sand, has been suggested as an overall environment of deposition (Henry, pers. comm., 1984). Kendall (pers. comm., 1985) suggested that the upper part of the Formation intersected in Manya-6 consists of marginal coastal sands.

The drillholes Manya-6 and Marla-3 show a conformable contact between the Relief Sandstone and the overlying Ouldburra Formation. Sandstones in the basal section of the Manya-6 Ouldburra type section are compositionally similar to the Relief Sandstone but occur in association with claystones and commonly have a halite cement.

2.4.2 Observatory Hill Formation

The stratigraphy of the Observatory Hill Formation has been the subject of controversy for several years, and has recently been redefined by Brewer *et al.* (1986). The basal sequence of the Observatory Hill Formation is a chaotically bedded gypsiferous 'red bed' sequence of very fine grained sandstone, siltstone and claystone with minor coarser sandstone and conglomerate. In the Marla-Manya area, the base of the Observatory Hill Formation was probably paralic with alluvial fans introducing the coarser clastic sediments. The upper portion of the formation is believed to represent a continental sabkha which contained alkali playa lakes.

Seismic data shows that the contact between the Ouldburra Formation and the overlying Observatory Hill Formation 'red beds' is generally conformable in the Marla-Manya area. Core from the drillholes Manya-6, Marla-3 and Marla-7 shows an interdigitation of Ouldburra carbonates and interbeds lithologically more typical of the Observatory

Hill 'red-beds'. This interdigitation occurs over a 74 m interval in the Manya-6 type section.

Seismic profiles from the southeast of the Manya area show a locally disconformable relationship between the Ouldburra Formation and the Observatory Hill Formation. The drillhole Manya-2 intersected this contact. Carbonates tentatively assigned to the Ouldburra Formation are overlain by a basal conglomerate of an arenaceous facies of the Observatory Hill Formation. Core from drillhole Marla-6 also shows a disconformable contact between the two formations with some evidence of subaerial exposure and erosion of the upper Ouldburra carbonates before deposition of the overlying Observatory Hill 'red beds'.

2.5 Biostratigraphy and Age

Prior to this study, the only identified fossils from the Palaeozoic of the eastern Officer Basin were fragmentary trilobites from drillhole Marla-1 (Jago and Youngs, 1980); a possible Biconulites from outcrop (Gatehouse, 1976); and microfossils from drillholes Munyarai-1 (Harris, 1968) and Wilkinson-1 (Muir, 1979; Jackson and Muir, 1981, p87). The material from Munyarai-1 is Devonian (Harris, 1968; Gravestock, pers. comm., 1985); the remainder of the specimens were thought to be of Early Cambrian age.

This study has shown the Ouldburra Formation carbonates to be only sparsely fossiliferous and preservation is poor. However, trilobites, regular and irregular archaeocyaths, ?ostracods, hyolithids, sponge spicules and unidentified microfossils have been recognized (Table 13). These enable an Early Cambrian (late Atdabanian to early Botoman) age to be inferred. Further work is necessary to identify many of the specimens and will be the subject of a separate study. The trilobita and archaeocyatha are the most important groups in terms of biostratigraphic correlation.

<u>Drillhole</u>	<u>Manya-1</u>	<u>Manya-3</u>	<u>Manya-6</u>	<u>Marla-1A,8</u>	<u>Marla-3</u>	<u>Marla-6</u>	<u>Marla-7</u>	<u>Middle Bore-1</u>	<u>Mt. Willoughby-1</u>
Ouldburra Fm (m)	(146.0-151.2)	(174.0-812.9)	(571.4-1685.6)	(83.0-379.4)	(490.4-633.0)	(256.3-702.5)	(193.3-543.0)	(160.0-371.8)	(623.6-639.7)
Trilobita	present (Thornton,1978)	sporadic unidentified carapace fragments	<u>Wutingaspis</u> locally abundant carapace fragments	<u>?Redlichiidae</u> ¹ (Jago and Youngs,1980)				present	
Ostracoda		present	several species			several species			
Chitinozoa			?present						
Hyalolitha			present					?present	
Porifera		possible body fossils, isolated tetraxon and monaxon spicules	possible body fossils isolated tetraxon and monaxon spicules						
Archaeocyatha						locally abundant Irregular and Regular forms			
Algae		Stromatolites Thrombolites ?Oncoids	Stromatolites Thrombolites Oncoids	Stromatolites Thrombolites Oncoids	Stromatolites Thrombolites ?Oncoids	Stromatolites Thrombolites Oncoids <u>?Renalcis</u>	Stromatolites Thrombolites Oncoids	Stromatolites Oncoids	Stromatolites ?Thrombolites ?Oncoids
Microfossils		possible Acritarchs	possible Acritarchs						
Trace fossils		Burrows Tubes	Burrows ?Trails/Tracks	?Burrows Tubes	Burrows ?Tubes	Burrows Borings		?Burrows Tubes	

TABLE 13: SUMMARY OF PALAEOONTOLOGICAL DATA FOR THE OULDBURRA FORMATION

¹ Specimens P22981-3, stored in the collection of the South Australian Museum.

2.5.1 Trilobita

Trilobite carapace fragments have been recognized in core and thin section studies from Marla-1A,B (Jago and Youngs, 1980; Lydyard, 1979), Manya-1 (Thornton, 1978), Manya-3 and Manya-6. Jago and Youngs (1980) suggested that the fragmentary trilobites from Marla-1 have affinities with the genera Pararedlichia, Eoredlichia, Wutingaspis, Chaoaspis or a related genus of the Redlichiidae.

During this study, well preserved and locally abundant trilobites were recovered from stylomottled carbonate mudstones in the interval 967.80 m to 970.13 m in the Manya-6 type section. Specimens were identified by Jago (pers. comm., 1986) as Wutingaspis (Figure 14). An Early Cambrian age is inferred.

2.5.2 Archaeocyatha

Decimetre to metre scale layers of archaeocyath bafflestone/framestone were intersected between 399 m and 654 m in the drillhole Marla-6. Rare broken fragments occur in other lithofacies to the total depth of 702.50 m. Preservation is poor throughout because of pervasive secondary dolomitization. Individuals are only rarely preserved in growth orientation although their algal-bound debris probably constituted mounds (see Chapter 6.1.3).

Both Regulares and Irregulares have been identified from the least altered material (Gravestock, pers. comm., 1985). The largest Regulares visible in core are in excess of 7 cm in diameter, but their cup appears to be unusually broad and short, a morphological trait believed to be an adaption to greater current velocities (Balsam and Vogel, 1973). The majority of the Regulares (Figure 15b) have a maximum cup diameter between 1.0 and 1.5 cm and an overall length of 2.5 to 3.0 cm. The ratio

FIGURE 14: TRILOBITA

Cranidia of various trilobite specimens from drillhole Manya-6.

- a. 969.72 m, x3
- b. 967.70 m, x8
- c. 968.03 m, x5
- d. 969.72 m, x5
- e. 968.65 m, x5.



a



b



c



d



e

of intervallum width to cup diameter ranges from 0.12 to 0.17. Up to 30 complete parieties are visible in transverse sections. Both inner and outer walls are porous but pore ultrastructure is not sufficiently well preserved for detailed study.

Transverse sections of the Irregulares (Figure 15a) show the irregular pore arrangement in both walls and the porous and branching septae. Other diagnostic morphological features are obscured by dolomitization.

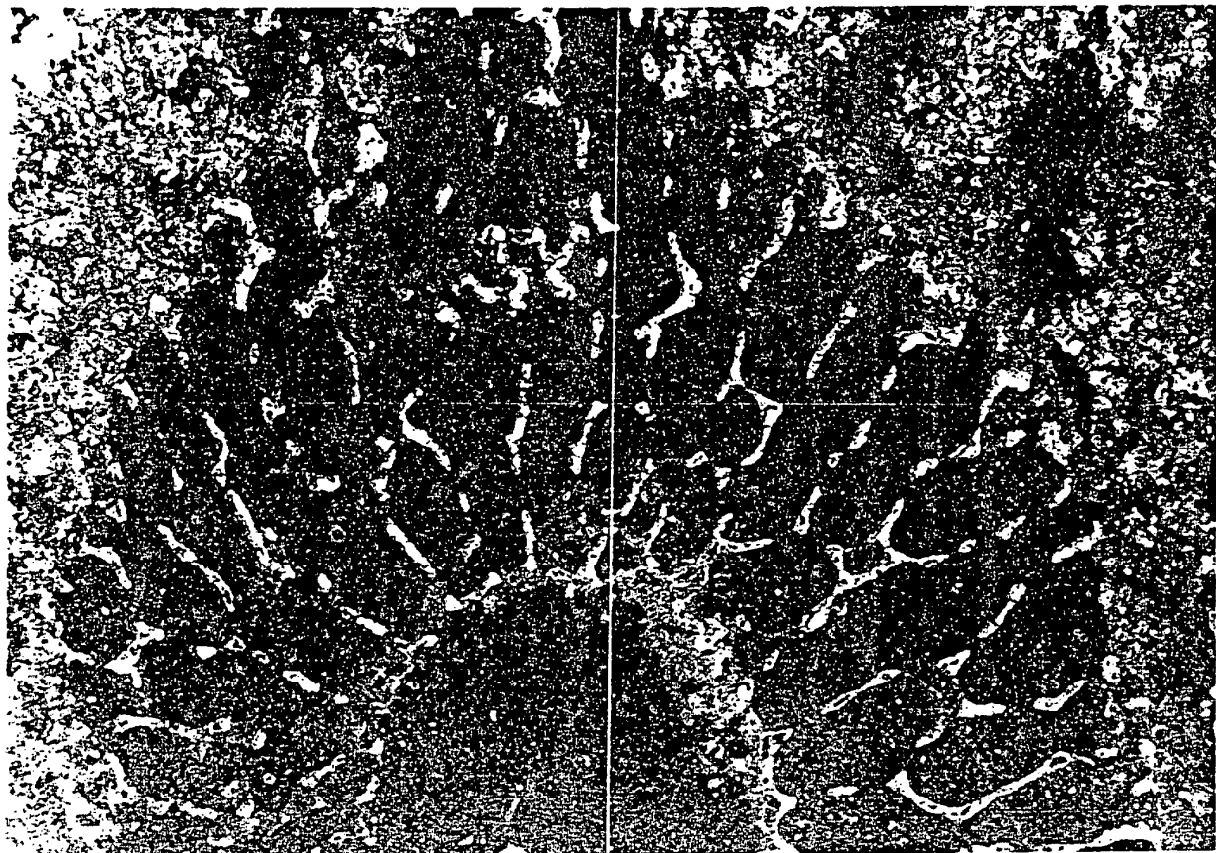
The presence of both Regulares and Irregulares indicates an Early Cambrian age (Gravestock, 1984; pers. comm., 1985).

2.5.3 Biostratigraphic correlations

A new biostratigraphic scale of stages for the Cambrian has recently been proposed by Spizharskiy et al. (1984) (Figure 16). The archaeocyaths and Wutingaspis from the Ouldburra Formation are assigned to Daily's (1956) faunal assemblage 3 which correlates with the Chuingchussu stage in China and the late Atdabanian to Early Botoman stages in the Soviet Union.

FIGURE 15: ARCHAEOCYATHA

- a. A partial transverse section of an Irregulares, showing irregular pore arrangement in both walls. COM 706, plane polarized light.
- b. A transverse section of a Regulares showing internal cement and porous walls and septae. COM 706, as above.



a

1mm



b

SERIES	SUPERSTAGE	STAGE	SOVIET UNION (Siberian platform and Kazakhstan region)		GREAT BRITAIN	SCANDINAVIA	NORTH AMERICA	CHINA	
			trilobites	archaeocyathids					
Lower Cambrian	Lenan	Toyonian	Anabaraspis splendens				Bonnia-Olenellus	Maoc- huang	Shantungaspis - Yaojiayuella
			Lermontovia grandis	Irinaecyathus grandiperforatus				Lungwan- gmiao	Redlichia nobilis; Redlichia mura- kamii - Hoffetella
			Bergeroniellus kotemensis	Botomocyathus zelenovi- Porocyathus squamosus					Tsanglangpu
		Bergeroniaspis ornata							
		Bergeroniellus asiaticus	Protolenid - Strenuellid		Proampyx linnarssoni	Nevadella			
		Bergeroniellus gurarii							
		Bergeroniellus micmaciformis- Erbilla							
		Botoman	Judomia - Uktaspis (Prouktaspis)		Fanscyathus lermentovae	Olenellid	Holmia kjerulfi group		
				Nochoroicyathus kokoulini					
			Pagetiellus anabarus	Porocyathus pinus					
			Fallotaspis	Leptocyathus polyseptus - Reticoscinus zegebarti					
			Proiallotaspis jakutensis						
		Tommo- tian		Dokidocyathus lenaicus	Non-trilobite	Schmidtellus mickwitzi		Meishucun	
				Dokidocyathus regularis					
			Aldanocyathus sunnaginicus						

FIGURE 16: BIOSTRATIGRAPHY OF THE LOWER CAMBRIAN FROM SPIZKHARSKIY ET AL. (1984).

CHAPTER 3

PRIMARY LITHOFACIES AND LITHOLOGIES

Detailed sedimentological descriptions and thin section studies of the Ouldburra Formation have enabled a number of characteristic lithologies and primary lithofacies to be defined. Each carbonate and mixed carbonate/siliciclastic lithofacies is distinguished by a dominant lithology or association of lithologies and includes diagnostic textures and sedimentary structures. The pure clastics and evaporites have been treated more simply and defined solely as lithologies.

The following primary lithofacies and lithologies have been recognized in the Ouldburra Formation and are used to standardize the description of core:-

Carbonate mudstones

Massive carbonate mudstone

Laminated and silty carbonate mudstone

Fenestral and stromatactitic carbonate mudstone

?Burrowed carbonate mudstone

Wackestones

Packstones

Grainstones

Floatstone/Rudstone

Boundstones

Stromatolitic algal bindstone

Thrombolitic algal bindstone

Archaeocyath bafflestone/framestone

Clastics

- Claystone
- Siltstone
- Quartz/feldspathic sandstone
- Granule conglomerate
- Sand/silt/mudstone sets

Evaporites

- Halite
- Gypsum/anhydrite

Environments of deposition (using the terminology of Flugel, 1982) have been postulated for each lithofacies. Whereas several individual lithofacies may be very good palaeo-environmental indicators, attempting to interpret sedimentary environments in isolation from underlying and overlying units obviously has limitations. Chapter 6 shows how the vertical arrangement of lithofacies can lead to a better understanding of the overall patterns of sedimentation.

3.1 Carbonate Mudstones

Carbonate mudstones are the most common lithology in the Ouldburra Formation. Four different lithofacies have been recognized:-

- i) massive carbonate mudstone,
- iv) laminated and silty carbonate mudstone,
- iii) fenestral and stromatactic carbonate mudstone,
- iv) ?burrowed carbonate mudstone.

3.1.1 Massive carbonate mudstone

Beds of grey carbonate mudstone lacking any macroscopic structures except local concentrations of irregular and columnar stylolites occur sporadically in the top of the Ouldburra Formation in the Marla-Manyra area. They are often interbedded with red siltstones, laminated mudstones and collapse breccias.

Generally, the carbonate mudstone consists of micrite with subordinate secondary dolomite phases. Examination of thin sections and insoluble residues reveals sporadic silt-sized detrital quartz and feldspar, disseminated clays, mica and opaque heavy minerals in a matrix of turbid very fine grained to microcrystalline subhedral to euhedral interlocking calcite crystals. These mudstones were probably deposited under low energy conditions with a limited clastic input. Such conditions could exist below wave base in a protected environment or in isolated shallow lagoons.

3.1.2 Laminated and silty carbonate mudstone

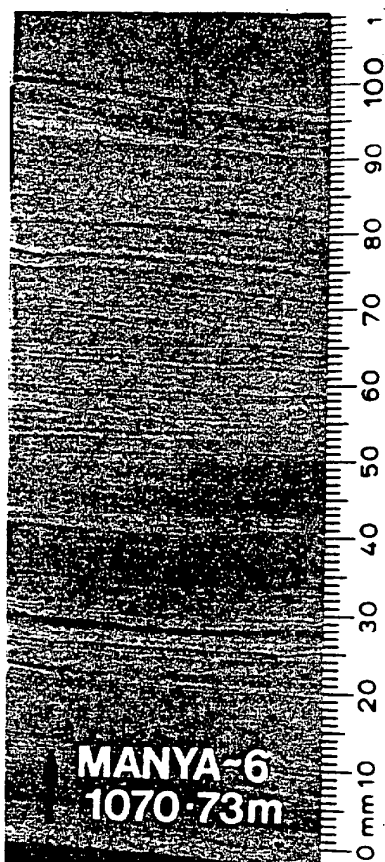
Laminated and silty carbonate mudstone is the dominant lithofacies in the Ouldburra Formation in the Marla-Manya area. The type section contains over 300 such beds, individually reaching a maximum thickness of six metres.

The laminations range from microlaminae to millimetre thickness and are visible in hand specimen as alternations of light and dark colour. In thin section, the difference is attributable to the local abundance of detrital quartz and feldspar silt, opaque heavy minerals (COM511) and clay (COM527, 653) or less commonly to crystalsize variation in the carbonates themselves (COM639).

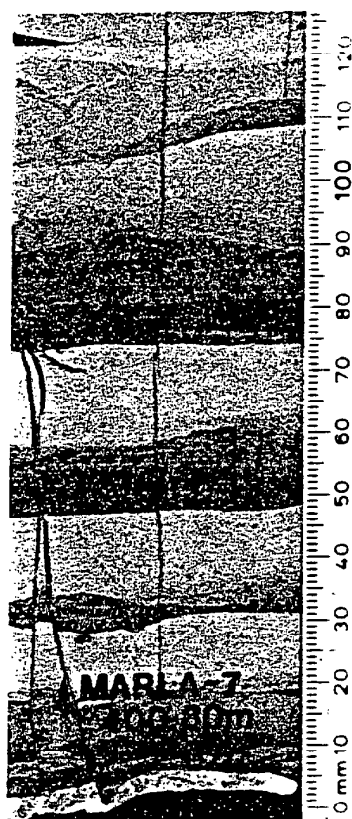
The most common examples occur as stacked couplets (Figure 17b). The basal unit is a silty carbonate mudstone containing graded detrital clastics. The cap is often a darker colour and is internally laminated in some instances. Similar couplets have been described as storm sets by Ball *et al.* (1963), Reineck and Singh (1972) and Brett (1983). Deposition is believed to occur from suspension clouds stirred up by spring tides or storms. In this process, the sediment-laden back-swash scours the bottom then deposits bed load silt. Settling of mud forms a laminated cap completing the storm couplet. These sediments form in shallow subtidal

FIGURE 17: LAMINATED AND SILTY CARBONATE MUDSTONE.

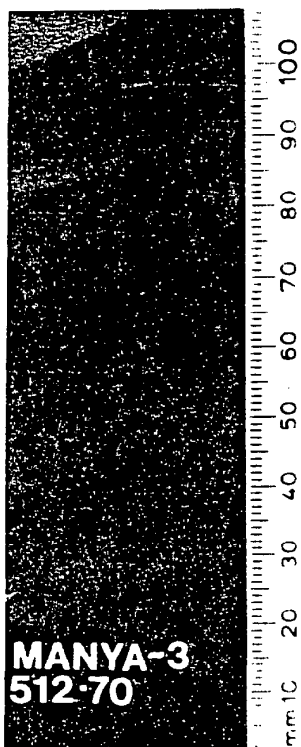
- a. Microlaminated carbonate mudstone, acid etched surface.
- b. Stacked sets of fining-up siltstone to carbonate mudstone couplets.
- c. Stacked sets of laminated and silty carbonate mudstone with abundant dewatering structures and small silty dykes.
- d. Thin section of single fining-up laminated and silty carbonate mudstone set (COM520).



a



b



c



d

settings under generally low energy conditions punctuated by high energy from storms (Brett, 1983; McCave, 1970). Many examples (Figure 17c) from the Ouldburra Formation show unequivocal evidence of exposure and desiccation; mudcracks, sheet cracks, and minor displacive gypsum nodules. These suggest that storm couplets similar to those described above were deposited as high as the supratidal zone. Exposure between flooding events led to the strong desiccation overprint.

Micro laminated examples (Figure 17a) are similar to those described by Budros and Briggs (1977) who inferred a quite, shallow subtidal to infratidal environment of deposition.

3.1.3 Fenestral and stromatactic carbonate mudstone

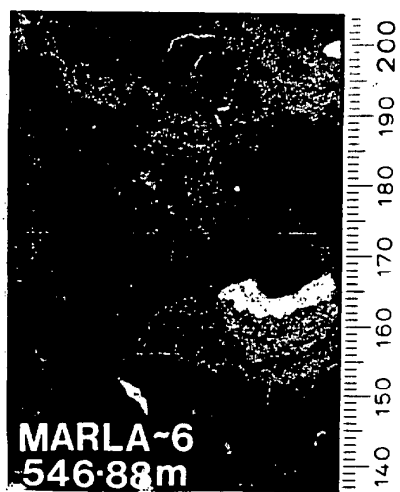
Fenestral and stromatactic textures occur in the marine carbonates of the Ouldburra Formation. The type section contains 11 beds, and Marla-6 intersected 38 beds over a 143 m interval. The beds range to a maximum thickness of three metres.

In hand specimen (Figure 18), this texture is typified by abundant centimetre scale irregularly shaped syngedimentary to post-sedimentary voids originally infilled with chemically deposited calcite spar and/or geopetal sediment (Flügel, 1982).

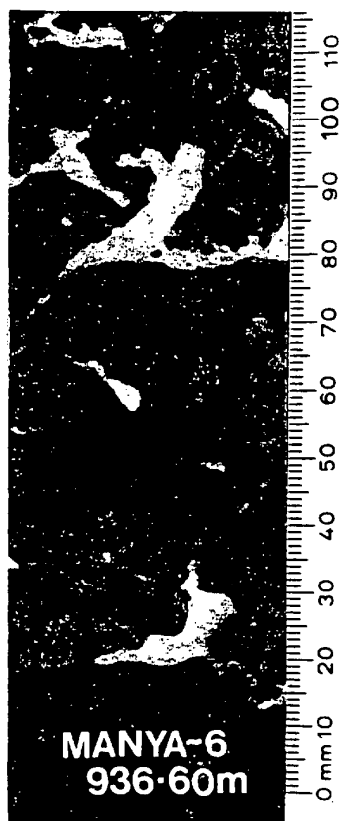
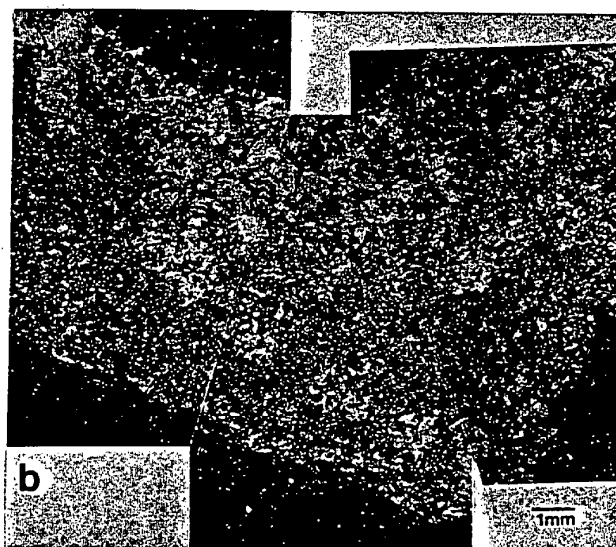
In thin section (COM732) (Figure 18b) the calcite cement in the top of the cavities is coarse to very coarsely crystalline ferroan spar with sixty degree interfacial angles. The darker coloured cement visible in hand specimen (Figure 18a) consists of fine to very fine crystals. It is also slightly less ferroan and contains sporadic heavy minerals, disseminated clays, and inclusions of the host mudstone. In other examples of stromatactis (COM733) (Figures 18c,d) the pale coloured cement is coarsely crystalline non-ferroan saddle dolomite with a thin layer of finely crystalline rhombs on the floor of the cavity.

FIGURE 18: FENESTRAL AND STROMATACTIC CARBONATE MUDSTONE.

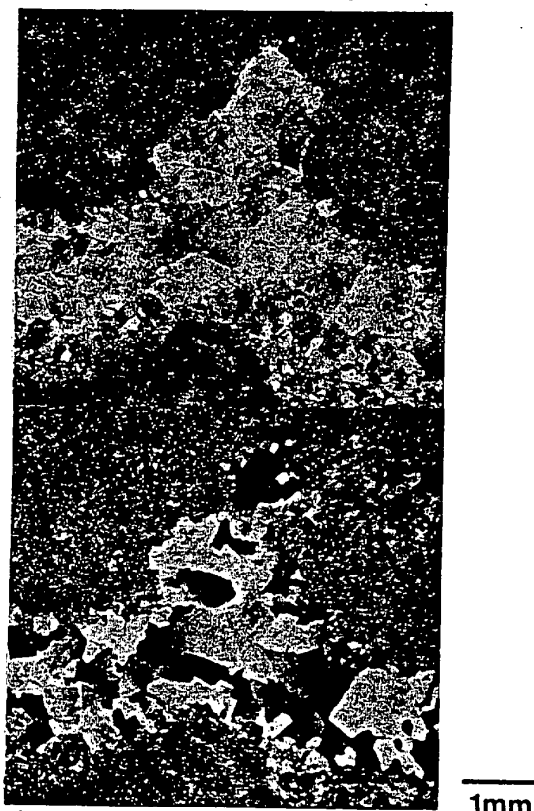
- a. Stromatactic and fenestral fabrics in mottled carbonate mudstone.
- b. Thin section of above showing sparry calcite cement grading down to turbid fine to very fine crystalline calcite (COM732, stained with Alizarin Red-S).
- c. A well developed stromatactic fabric consisting of large fenestrae with a characteristic flat base, irregular top and internal ?geopetal structure.
- d. Thin section of above showing coarsely crystalline saddle dolomite cavity fill (COM733, stained with Alizarin Red-S).



a



c



d

Flugel (1982) distinguishes between birdseyes, fenestrae and stromatactis. In this work, all fenestral and stromatactic textures which are not associated with burrows, algal bindstones or archaeocyath bafflestone/framestones are considered to constitute one lithofacies. In this sense they are synonymous with Folk's (1959) 'dismicrite', Fischer's (1964) 'loferites', and in agreement with the terminology of Shinn (1983a).

Explanation of the modes of origin of this texture include pressure solution in response to tensional stress (Logan, 1984; Logan and Semeniuk, 1976); subaerial solution (Semeniuk, 1971); differential compaction and gas or water escape (Shinn, 1968 ; Heckel, 1972); algal support of cavities (Wolf, 1965); sponge-constructed stromatactis (Bourque and Gignac, 1983); and the development of supratidal evaporites (Illing, 1959).

In spite of the uncertainty about the origin of fenestral and stromatactic fabrics, such textures are often used as palaeo-environmental indicators. The smaller, more regularly shaped forms ('birdseyes' sensu Flugel, 1982) occur preferentially in intertidal and supratidal environments (Flugel, 1982). The larger, irregular 'stromatactis' (sensu Wolf, 1965; Flugel, 1982) occur in shallow subtidal, intertidal (Flugel, 1982) and supratidal (Shinn, 1983a) environments.

3.1.4 Burrowed carbonate mudstone

The Ouldburra Formation intersected in Marla-3 contains numerous beds of leached dolomitic carbonate mudstone with characteristic open tubular vugs. Despite its poor preservation, this texture is used to define a separate carbonate mudstone lithofacies. It occurs in approximately 50 beds, each less than one metre thick.

The tubular vugs are less than 3.0 mm diameter and have a strong modal diameter of about 1.5 mm. Branching is moderately common but there appears to be no preferred orientation.

Shinn (1983a,b) described similar structures as 'pseudo-fenestrae' or 'pseudo-birdseyes' and illustrated examples from Ordovician and Cretaceous rocks. Recent supratidal muds deposited during Hurricane Donna in Florida Bay contain very similar structures (Shinn, 1983b). Shinn (1983a) interpreted these textures as being characteristic of peritidal deposits.

3.2 Wackestones

Various combinations of coated grain, bioclastic and lithoclastic wackestones are minor, but widespread, sedimentological components of the Ouldburra Formation. The wackestones have been grouped into four categories:-

- i) oncoïd wackestone
- ii) ooid peloid bioclastic wackestone
- iii) intraclastic wackestone
- iv) quartz feldspar wackestone.

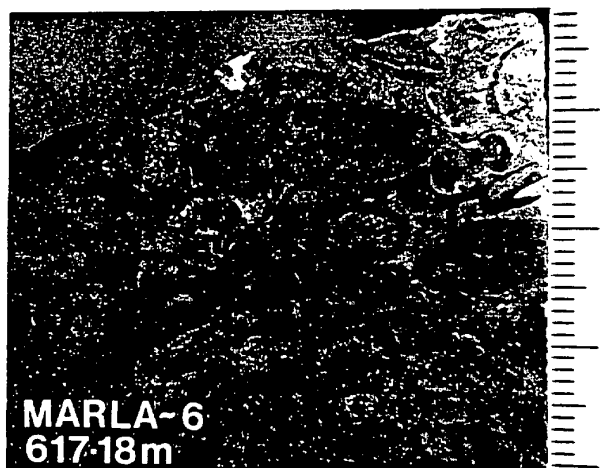
The original micritic matrix often exhibits patchy recrystallization to pseudo-spar, making it difficult to distinguish wackestones from grainstones in hand specimen.

3.2.1 Oncoïd wackestone

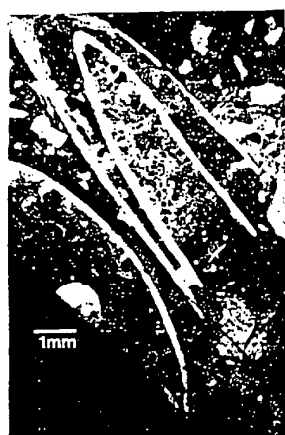
Beds of oncoïd wackestone (Figures 19a, b), up to 1.5 m thick, were intersected in all the Marla and Manya drillholes. They are often associated with domed stromatolitic or thrombolitic algal bindstones. The oncoïds are well rounded, up to 4.5 cm maximum diameter, with poorly preserved partially overlapping dark micritic laminae derived from ?algal coatings around a solid nucleus. Some examples from Marla-1B and Marla-6 core are vertically compressed with a maximum breadth to height ratio of about 4:1. The matrix of the wackestone is a micrite or dolomitic carbonate mudstone often with a relict peloidal texture.

FIGURE 19: WACKESTONES AND GRAINSTONES.

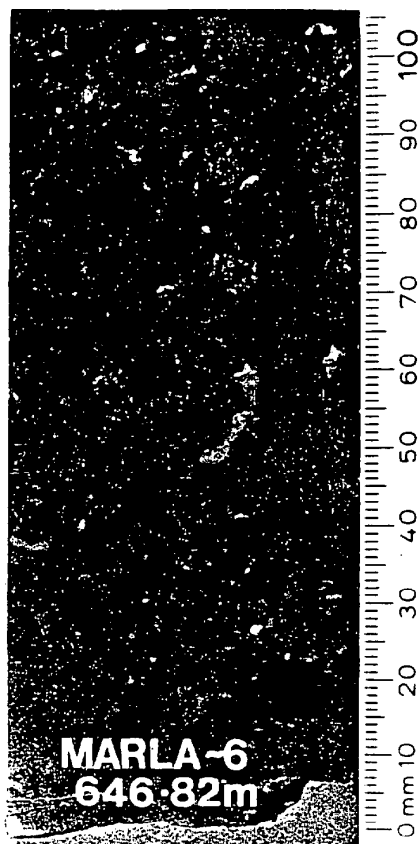
- a,b. Oncoid wackestones.
- c. Hyolithids in a thin bioclastic wackestone (COM627).
- d. Bioclastic peloid grainstone with abundant trilobite debris (COM648).



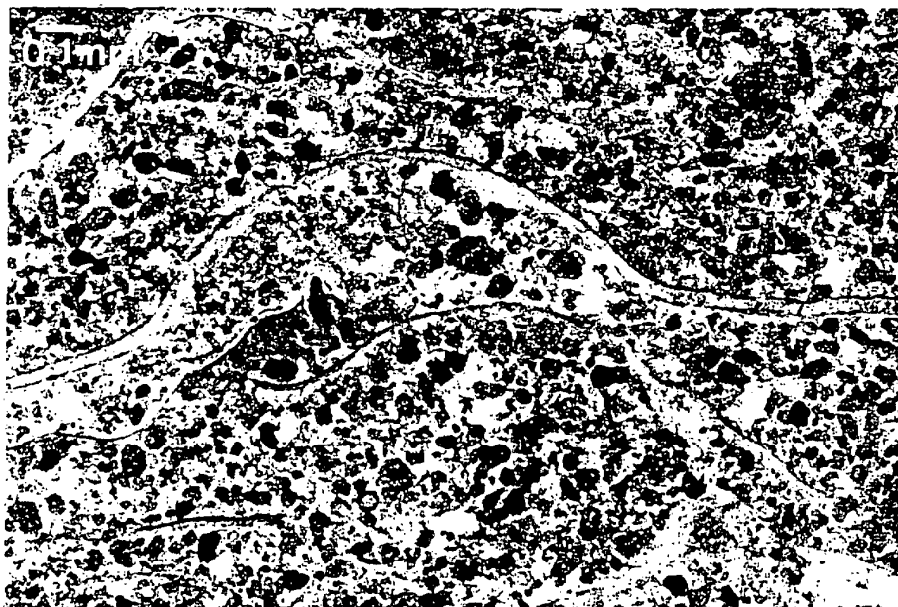
a



c



b



d

Centimetre scale algal oncoids have been reported from recent marine subtidal and lower intertidal zones with a sluggish current (Flügel, 1982); and from supratidal and high intertidal high energy shoals off Andros Island (Kendall, pers. comm., 1985). Similar ancient marine Girvanella -oncoids are taken to be indicative of low energy nearshore shallow water conditions.

3.2.2 Coated grain/bioclastic wackestone

Wackestone containing various proportions of ooids, peloids and bioclastic debris occurs sporadically throughout the carbonate section of the Ouldburra Formation. Wackestone beds in the type section range from several centimetres up to a maximum of several metres thick. They are generally gradational to packstone/grainstone textures. Relict ooid peloid wackestone occurs in drillholes Manya-3, Manya-6, Marla-1B and Marla-6. A quiet water shallow marine environment of deposition is postulated. Rare centimetre-scale 'hash' beds of bioclastic peloidal wackestone occur in most intersections of the Ouldburra carbonates. The bioclasts include hyolithid debris (COM627) (Figure 19c), trilobite fragments and microfossils. Flügel (1982) interpreted this texture as indicative of shallow waters with open circulation at, or just below, the wave base. The fossils certainly originated in shallow marine conditions but because of their occurrence in rare concentrated beds, they may be an allochthonous strand-line deposit.

3.2.3 Intraclastic wackestone

Relict intraclastic wackestone occurs in thin beds in most intersections of the Ouldburra Formation, including the Manya-6 type section. Examples from Marla-6 can easily be recognized in hand specimen despite being entirely dolomitized. In thin section (COM698), the intraclasts are visible as rounded ghosts varying in size from 6 mm to less than 1 mm. Less than 10 percent of the clasts exceed 2 mm across.

The intraclastic wackestone was probably deposited in a peri-emergent environment with the rounding of the carbonate mudstone clasts reflecting the degree of transport.

3.2.4 Quartz feldspar wackestone

Quartz feldspar wackestone (COM650) occurs in all Ouldburra Formation intersections. Beds generally grade to, or are interbedded with, massive carbonate mudstone (as terrigenous clasts decrease); through packstones to sandstones (as clasts increase); or to laminated silty carbonate mudstones. A complete spectrum of grainsizes, roundness and sphericity of detrital quartz and feldspar grains, basalt fragments and chert have been observed. The presence of high-energy derived grains in a carbonate mudstone is a textural inversion. This lithofacies indicates a predominantly quiet water marine carbonate environment with sporadic pulses of higher energy carrying in the detrital clastic grains.

3.3 Packstones

Beds of coated grain, peloid, intraclast or quartz feldspar packstone occur in all drillholes which intersected the Ouldburra Formation. Despite being widespread, packstones occur only sporadically with beds rarely exceeding 2 m thick. The beds are usually gradational to other lithofacies and they often grade internally from those dominated by one type of grain or particle to another.

3.3.1 Coated grain/bioclastic packstone

Thin beds and lenses of coated grain/bioclastic packstone occur in association with stromatolitic algal bindstone and archaeocyath bafflestone/framestone in drillholes Manya-6 and Marla-6. Ooids, coated aggragate grains, peloids and bioclastic debris occur together in a poorly preserved silty micritic matrix. These beds are interpreted as quiet water shallow marine deposits with an element of allochthonous input.

Exclusively peloidal packstone is rare. The high degree of sorting in this lithology may reflect a local faecal origin, but there is little evidence of burrowing or bioturbation of the surrounding sediments.

3.3.2 Intraclastic packstone

Intraclastic packstone occurs in beds up to 1.5 m thick throughout the lower part of the carbonate facies of the Ouldburra Formation. The carbonate mudstone intraclasts are subrounded to angular ranging in size from 1 mm to 4 mm; less than 10 percent of the clasts exceed 2 mm diameter. The larger clasts tend to be more angular and are rarely imbricated. Sporadic poorly defined centimetre scale interbeds of ooids and intraclasts and rare isolated oncoids occur within the thickest intraclastic packstones in Marla-6. The size and angularity of the intraclasts suggest brief periods of high energy close to the point of deposition.

3.3.3 Quartz feldspar packstone

Thin beds of quartz feldspar packstone occur throughout the Ouldburra Formation. This packstone texture is commonly gradational to sandstone or fining-up silty carbonate mudstone. An example from Manya-3 (COM528) shows a complete gradation from carbonate cemented feldspathic sandstone, through quartz feldspar packstone, to silty carbonate mudstone on a centimetre to decimetre scale. Compositionally, the detrital grains are mono- and polycrystalline quartz (up to 30 percent), microcline and K-feldspar (up to 30 percent), calcareous and dolomitic intraclasts (5 percent) and rare ?metamorphic rock fragments. The grains are poorly sorted, ranging in size from very coarse to very fine grained.

Where this texture occurs in a predominantly carbonate mudstone sequence, the detrital clasts were probably introduced during a pulse of

higher energy conditions (possibly aeolian). Examples gradational to sandstones reflect the introduction of micritic carbonate mudstone into a predominantly clastic environment.

3.4 Grainstones

Grainstones are uncommon in the Ouldburra Formation. This may be because they have been selectively dolomitized during diagenesis, however it seems more likely that their absence is a sedimentary phenomenon. Where grainstones do occur in the Ouldburra Formation, they are usually subordinate to, and gradational to, packstones as the cement/matrix grades to micrite. The grainstone and packstone textures may be intermixed on a scale of less than a centimetre and are difficult to differentiate in hand specimen. It is also difficult to distinguish poorly preserved primary cements from neomorphic microspar which is formed by the recrystallization of either pre-existing carbonate cement or a micritic matrix. Grainstone lithofacies are also subject to preferential silicification. This may pseudomorph existing carbonate cement textures or obliterate them entirely. The complex diagenetic history of the carbonate cements is discussed in Chapter 5.1.1. The following textures have been recognized in thin section studies:-

- i) coated grain/bioclastic grainstone
- ii) intraclastic grainstone
- iii) quartz feldspar grainstone.

3.4.1 Coated grain/bioclastic grainstone

Relict grainstone containing ooids, aggregate grains and bioclastic clasts occurs as centimetre to metre scale beds in most intersections of the Ouldburra Formation.

The best developed examples of ooid/aggregate grain grainstone were intersected in drillhole Manya-3 (COM747, COM749). Cross-bedded

units up to 8 m thick are believed to represent shallow marine shoals. Kennard (1981) described texturally similar dolomitized ooid grainstone from the Arrinthrunga Formation in the Georgina Basin. These units are up to 130 m thick, and were interpreted as a high energy shallow water shoal. The absence of such thick sequences from the Ouldburra Formation probably indicates generally quieter water conditions.

Other examples of ooid grainstones occur as centimetre scale lenses in stromatolitic algal bindstones (Marla-6) (COM682, 769), or within massive dolomitic sequences (Marla-1B). The lenticular nature and small scale of these examples suggests deposition in areas where wave action alternated with slack water. The complex history of cementation of these examples (see Section 5.1.1) shows exposure to both vadose and phreatic waters.

Thin beds of bioclastic grainstone (Figure 19d) (COM719, 720) occur in the Ouldburra carbonates in the Manya-6 type section and sporadically throughout other intersections of the Formation in the Marla-Manya area. They contain trilobite debris, microfossils, abundant peloids and in some cases, tubular trace fossils. The latter prone tubes contain internal geopetal sediment and marine cement. A shallow subtidal origin is inferred.

3.4.2 Intraclastic grainstone

Centimetre-scale beds of intraclastic grainstone are very rare in core from drillholes Manya-6 and Marla-6. Where present, they commonly also contain sporadic aggregate grains and rare ooids. Primary cement textures are generally not preserved because of dolomitization and recrystallization to neomorphic microspar. This grainstone was probably originally deposited in peri-emergent conditions with restricted circulation.

3.4.3 Quartz feldspar grainstone

Only very rare thin beds of quartz feldspar grainstone have been preserved in the Ouldburra Formation. They are usually gradational to packstones on a centimetre scale, or occur within essentially clastic sandstone sequences with local patches of calcite cement. The cements are generally coarsely crystalline subhedral turbid calcite, and it is not possible to distinguish any characteristic primary textures. The environment of deposition was probably submergent or regularly emergent with pulses of clastic input, possibly including some aeolian sand.

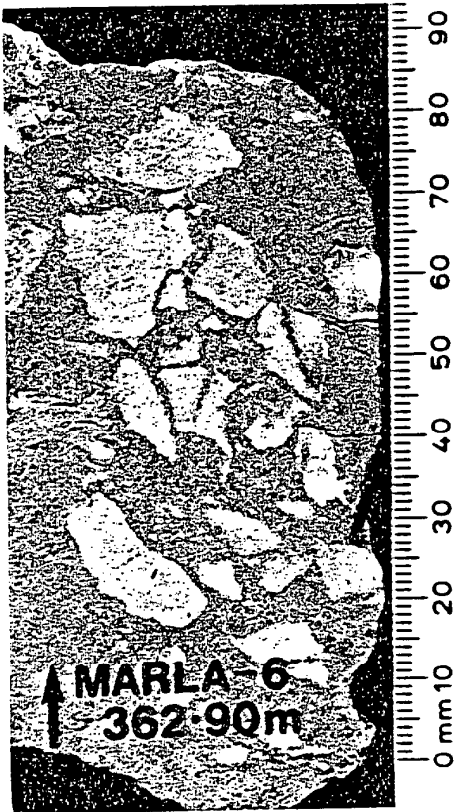
3.5 Floatstone/Rudstone

Embry and Klovan (1971) modified Dunham's (1962) original textural classification to recognize allochthonous limestones which contain particles exceeding 2 mm (granule sized or greater). Such rocks are 'floatstone' if matrix supported; 'rudstone' if particle supported. These terms are used only when the significant size of the detrital particles has been caused by erosion and redeposition (ie. excluding the possibility of 'oncoid rudstones' ; Flugel, 1982).

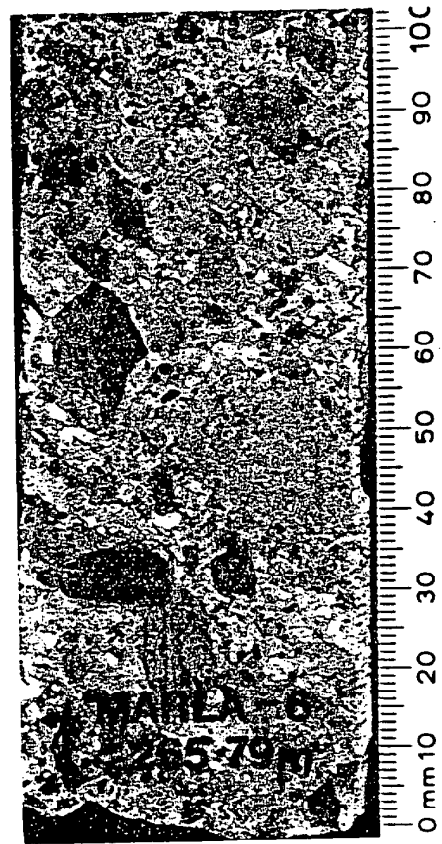
Depositional breccias with a floatstone/rudstone texture occur over a four metre interval in Marla-6 (Figure 20) and sporadically in the Manya-6 type section. The former example consists of angular clasts of weathered carbonate mudstones and banded cherts in a slightly to moderately calcareous brownish grey matrix/cement. In thin section (COM688), the matrix/cement consists of subhedral to euhedral sparry calcite crystals, averaging about 0.3 mm across. These incorporate scattered dolomite rhombs (to 0.05mm) and patches of chalcedonic silica. The matrix/cement and the bleached chert clasts contain small visible voids. Formation of this floatstone/rudstone is attributed to subaerial exposure of the Ouldburra Formation carbonates with development of siliceous and caliche-like crusts and then rapid marine transgression to work and redeposit this material (see Section 7.6.2).

FIGURE 20: FLOATSTONE, RUPTONE AND PLATE BRECCIA.

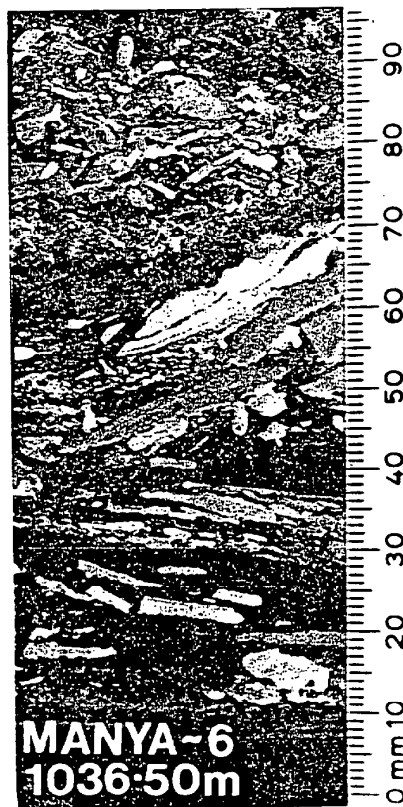
- a. Floatstone consisting of angular clasts of bleached chert in an altered carbonate matrix.
- b. Rudstone containing rounded to subrounded carbonate mudstone clasts.
- c. Plate breccia.



a



b



c

Other examples from Manya-6 may have been derived from submarine hard crusts, but are probably lag deposits in small channels.

3.5.1 Plate breccia

Edgewise to low angle imbricated plate breccia (Figure 20c) is an especially diagnostic form of floatstone or rudstone. Good examples occur sporadically throughout the Ouldburra carbonates as thin beds containing abundant angular flakes of carbonate mudstone in a carbonate mudstone or mixed carbonate/siliciclastic matrix. The flakes are often slightly curled, exhibiting internal microfracturing consistent with mudcracking and sheet cracking, and are composed of dolomite or horizontally laminated dolomite and dolomitic limestone. Rare examples appear to have a planar laminated algal cap.

Plate breccia is taken as an indicator of subaerial exposure, the curled plates having been formed essentially in situ as the sediment surface dried out. Minor transgression or storm surge then introduced the matrix material. Current velocity was sufficient to produce imbrication locally but insufficient to transport the larger plates (Sepkoski, 1982). Radke (1980) suggested that edgewise fabrics in plate breccias were a typical littoral feature. Sepkoski (1982) pointed out that such textures are uniquely abundant in Cambrian to Lower Ordovician shallow subtidal carbonate sediments where the in-fauna was restricted and/or bottom sediments were eroded to considerable depths.

3.6 Boundstones

Three distinct boundstone lithofacies have been recognized in the Ouldburra Formation carbonates. Two of these textures are attributable to sediment trapping and binding by algae or cyanobacteria to produce a cryptalgal fabric (sensu Aitken, 1967). The third type of boundstone is produced by sediment trapping around an algal encrusted archaeocyath framework. Using the original terminology of Aitken (1967) and the

classification of Embry and Klovan (1971) these textures are referred to as:

- i) stromatolitic algal bindstone
- ii) thrombolitic algal bindstone
- ii) archaeocyath bafflestone/framestone.

3.6.1 Stromatolitic algal bindstone

Thin layers of stromatolitic algal bindstone are a minor, but conspicuous, element in most of the Ouldburra Formation intersections. They reach thicknesses of up to eight metres in core from Marla-1, and are also well developed in Manya-6, Marla-3, Marla-6, Marla-7, and Middle Bore-1.

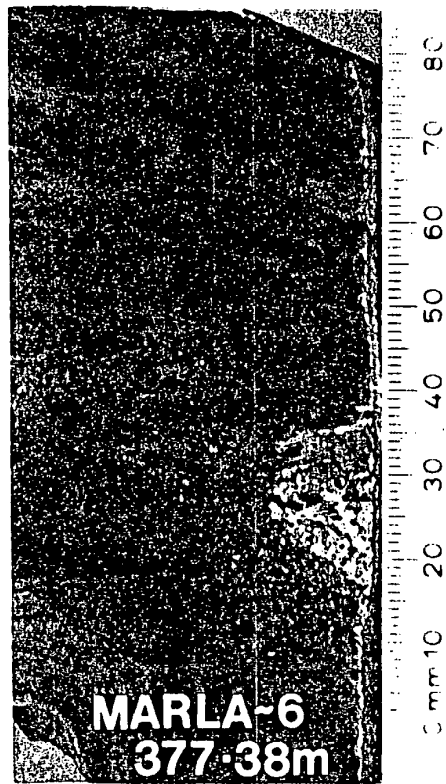
It is not possible to use a detailed morphological stromatolite classification when working with core. A simple distinction is made between obviously convex domed forms and flat laminated forms.

In hand specimen (Figure 21a), both forms consist of parallel to finely anastomosing dark brown to black draped laminae, interlaminated with thin sediment-rich layers. The cryptalgal texture is visible in thin section (COM651, 769 ; Figure 21d) as millimetre scale laminae of crenulated carbonaceous material and microcrystalline carbonate, alternately interlaminated with algal-bound silt to sand-sized clastic grains and carbonate intraclasts. Millimetre-scale open fenestrae are preserved sporadically. The cryptalgal lamination is finer and more regular in the smaller domed forms.

Modern analogues have been well documented in the literature (Kendall and Skipwith, 1968; Kinsman and Park, 1976; Logan et al., 1964; Park, 1972).

FIGURE 21: BOUNDSTONES.

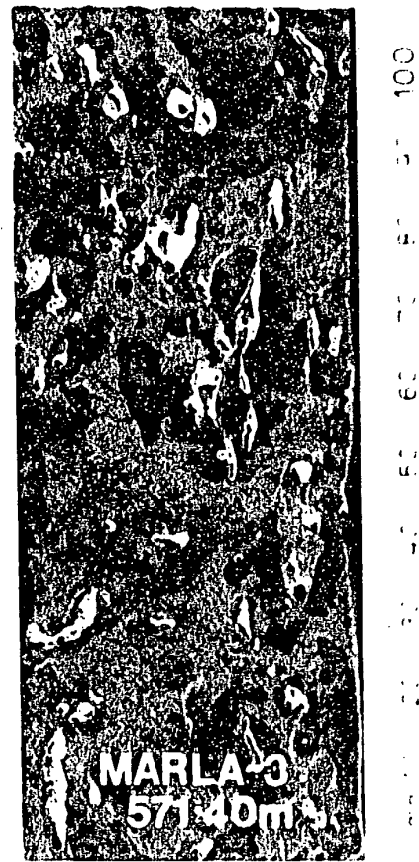
- a. Domed stromatolitic algal bindstone with ooid grainstone lens.
- b. Archaeocyath bafflestone/framestone showing internal cements and algae in cavities.
- c. Thrombolitic algal bindstone with possible burrows.
- d. Thin section of domed stromatolitic algal bindstone shown in Figure a (COM679).



a



b



c



d

Stromatolitic algal bindstone forms in conditions ranging from subtidal just below wavebase; through shallow subtidal, intertidal to supratidal; but is most common in the intertidal zone (Flügel, 1982). The domed forms predominate in the subtidal and lower intertidal zones (James, 1979). The high degree of laminae regularity in the domed forms may be related to areas of lower sediment supply (Haslett, 1975a). The effects of grazing gastropods in modern analogues suggest that ancient algal mats, not subject to such activities, were probably more widespread than they are today (Garret, 1970).

3.6.2 Thrombolitic algal bindstone

Layers of thrombolitic algal bindstone are present in cores from Marla-1, Marla-3, Marla-6, Marla-7, Manya-3 and Manya-6 where they form beds up to three metres thick.

The thrombolitic algal bindstone is a pale brown to grey carbonate that has a characteristic centimetre to millimetre scale clotted cryptalgal fabric (Figure 21c). In sporadic examples, the randomly mottled fabric grades to a crudely digitate texture defined by randomly oriented narrow columns ('walled columnar' stromatolite sensu Haslett, 1975a).

In thin section (COM633,707), the thrombolitic bindstone has a 'grumeleuse' texture defined by irregular patches of turbid microcrystalline to fine grained secondary dolomite intermixed with mottles of coarser grained calcite. Sporadic silt-sized detrital clastic grains occur throughout. Thin discontinuous anastomosing accumulations of ?carbonaceous material (possible relict algal laminae) are rarely preserved.

A thrombolitic texture is thought to result from sediment trapping and binding by the algae, with sediment accumulating in depressions between the algal knobs (Kennard, 1981). Oxidation leaves irregular fenestrae which are later infilled by clastic grains, sparry calcite or

geopetal sediments. Examples of thrombolitic algal bindstone from the Ouldburra carbonates generally have a finer grained and lower detrital clastic component than the stromatolitic forms. Similar textures have been described by Ahr (1971), Aitken (1967), Coniglio and James (1984), Haslett (1975a), Kennard (1981), and Read and Pfeil (1983). These have been interpreted as indicative of shallow subtidal platform settings. The reduced detrital clastic component may indicate that the thrombolitic forms favoured more protected conditions with a lower allochthonous input. Kennard (1981) and Radke (1980) suggested that the different distribution of thrombolitic and domed stromatolitic forms might also reflect differing salinities.

3.6.3 Archaeocyath bafflestone/framestone

Layers of archaeocyath bafflestone/framestone up to eight metres thick were cored in the drillhole Marla-6. The rock is a carbonate mudstone which contains abundant archaeocyaths; irregular fenestrae with internal marine cements; geopetal infill in cavities; and, locally, relict clumps of algae which bind the archaeocyaths and line cavities (Figure 21b). Individual archaeocyaths often have a sparry (drusy) calcite or coarsely crystalline dolomitic infill. Preferred growth orientation is detectable only locally and some of the archaeocyaths are broken. This may suggest some exposure to high energy conditions and the archaeocyath bafflestone/framestone probably formed, at and above the fairweather wavebase.

3.7 Clastics

The Ouldburra Formation contains numerous beds of clastics ranging from claystone to granule conglomerate. Clastic sequences dominate the basal portion of the Formation and occur sporadically throughout the upper carbonate dominated section in all intersections. Sandstone is the

most widespread siliciclastic lithology and silica, carbonate and evaporite cements have been recorded. Clastics also commonly occur as fining-up sand/silt/mudstone sets. These range from entirely clastic to those in which carbonate mudstone forms the matrix/cement and passes up through the triplet to constitute the overlying mudstone. The detrital clastics were derived from the Gawler Craton, Musgrave Block and basalts to the east of the Manya area.

3.7.1 Claystone

Soft blue grey and greenish grey claystone is common between 1550 and 1600 m in the Manya-6 type section where it occurs in association with bedded halite. It is finely laminated, with rare ripple cross-bedding, and ranges from entirely clastic to slightly dolomitic or calcareous. Some beds have finely disseminated interstitial halite and anhydrite needles. Well rounded (?aeolian) fine to medium grained quartz and feldspar grains occur rarely. Individual beds are usually less than 1 m thick and generally grade vertically to sand/silt/claystone sets. The claystone becomes fissile on drying and has deteriorated in core.

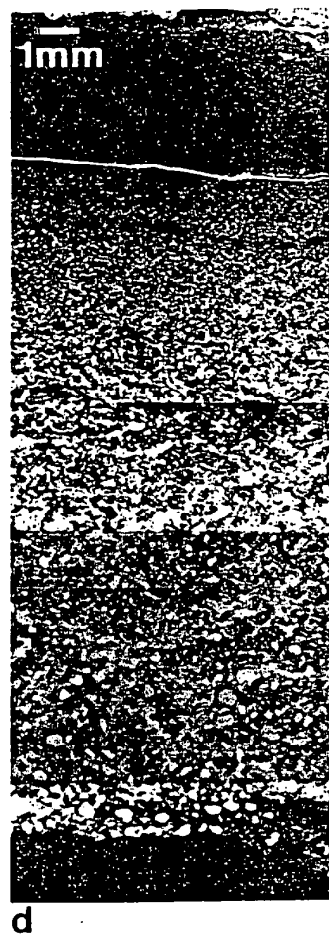
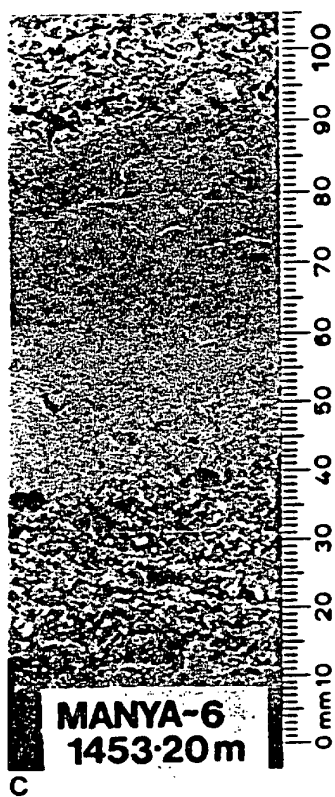
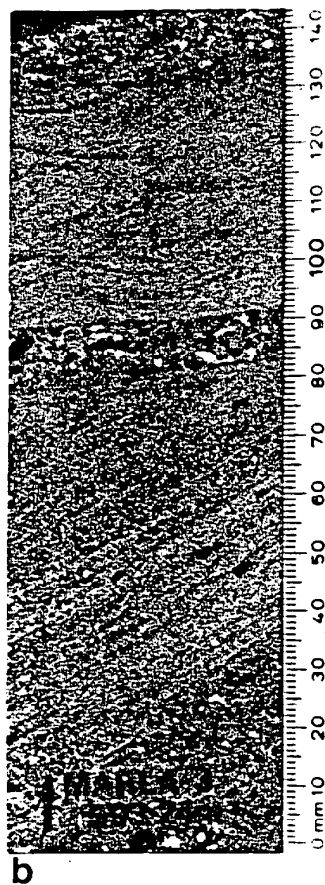
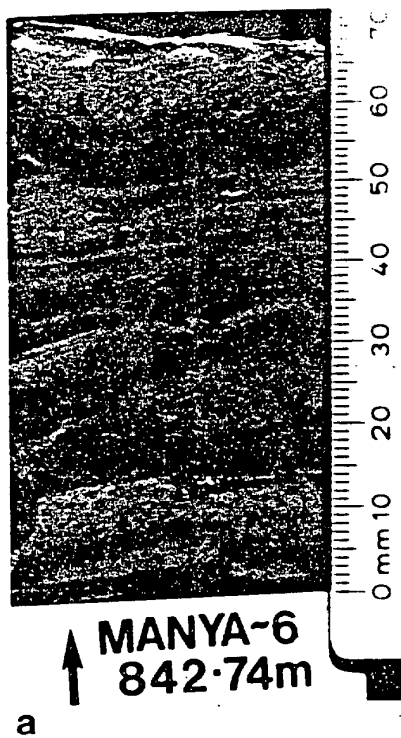
The association with the sand/silt/claystone sets and evaporites suggests that the claystone was deposited during periods of lower energy in a regularly emergent setting.

3.7.2 Siltstone

The upper Ouldburra Formation often contains 'red bed' siltstone (Figure 22a) sedimentologically more typical of the overlying Observatory Hill Formation in those instances where the two formations interdigitate. The type section contains red brown siltstone between 841 m and 849 m, and sporadic red thinly bedded siltstone from 1492 m to 1506 m. These correlate stratigraphically with similar units intersected in Marla-7. The siltstone has ubiquitous disturbed bedding often with thin discontinuous darker-coloured clay-rich laminae. It varies from entirely clastic to moderately calcareous or dolomitic and is sporadically micaceous. It also

FIGURE 22: CLASTICS.

- a. Interbedded 'red bed' siltstone and fine sandstone.
- b. Very fine grained to granular sandstone showing fining-up planar cross-stratification, horizontal planar lamination and thin beds, overlain by trough cross-laminated fine grained units.
- c. Fining-up sand/silt/claystone set.
- d. Thin section of a fining-up sand/silt/mudstone set (COM628).



hosts sulphate evaporites. The sedimentary associations of the 'red bed' siltstone are consistent with deposition on a sabkha.

3.7.3 Quartz/feldspathic sandstone

Beds of quartz/feldspathic sandstone occur sporadically throughout the Ouldburra Formation, but are most common at the base of the Formation as it grades into the underlying Relief Sandstone. Grain size ranges from fine to very coarse and a variety of different cements including silica, carbonate (COM681), halite (COM655) and anhydrite/gypsum (COM677) have been recognized in thin section studies. The type section contains numerous beds ranging in thickness from several centimetres to several metres. The thicker beds are usually massive but sporadic examples show small to medium scale planar cross-stratification. Ripped-up mudstone and claystone clasts are commonly observed near the base of these beds which are interpreted as having formed in channels cutting across peri-emergent flats (Henry, pers comm., 1984).

The drillhole Marla-3 also intersected abundant sandstone beds in the base of the Ouldburra Formation as it grades down to the Relief Sandstone. Some of these units show fining-upwards planar cross-stratification with angles of up to 25 degrees or small scale festoon cross-beds. They are frequently overlain by a thin laminar horizontal bedded sandstone unit, and in turn by ripple and flaser cross-bedded fine grained sandstone and siltstone (Figure 22b). These are interpreted as channel deposits with evidence of rapidly changing flow regimes.

3.7.4 Granule conglomerate

Quartz/feldspathic granule conglomerate is a rare lithology in the Ouldburra Formation. Conglomerate occurs at the base of fining-up sandstone sequences in the Manya-6 type section. Discrete thin beds of granule conglomerate and coarse sandstone occur between overlying laminated carbonate mudstone and underlying moderately calcareous

mudstone and siltstone in core from Marla-7. In thin section (COM676), they consist of a bimodal distribution of detrital granules to very fine grains of quartz, feldspar, basaltic rock fragments and detrital chlorite in a silty gypsiferous, dolomitic carbonate and clay matrix/cement. There is some evidence of reworking, so this lithology was possibly deposited during a brief period of increasing energy conditions.

3.7.5 Sand/silt/mudstone sets

Fining-up sand/silt/mudstone sets are a common feature of the Ouldburra Formation. The triplets average 5 to 10 cm thick, and are often stacked, forming sections several metres thick. Mixed carbonate/siliciclastic sets occur most frequently in the upper portion of the Formation. Lower in the type section, entirely clastic sand/silt/claystone sets (Figure 22c) are dominant. The cap often contains desiccation features and the triplet may host nodular evaporites.

In thin section (COM628) (Figure 22d), the matrix/cement of the sandstone and siltstone passes upward unchanged to constitute the overlying mudstone or claystone.

The basal sandstone is generally quartzose or feldspathic and poorly sorted with sporadic basaltic rock fragments, detrital chert and ripped-up clasts of the underlying mudstone. The better sorted units may show small scale planar, or rarely, herring-bone cross-stratification, varying from 8 to 20 degrees. The sandstone grades up to a siltstone which contains detrital mica in addition to the siliciclastics. The siltstone often shows small scale low angle planar, festoon or ripple cross-stratification. The mudstone cap is often dolomitic and only rarely laminated. Dewatering structures, mudcracks, pull-apart structures and possible burrows have been recorded.

Overall, the sand/silt/mudstone sets are similar to those from modern subtidal to intertidal mixed sand-mud flats (Reineck and Singh, 1980). The presence of desiccation features in some examples from the Ouldburra Formation indicates subaerial exposure.

3.8 Evaporites

Bedded evaporites including halite and gypsum/anhydrite have been recorded in several drillholes which intersected the Ouldburra Formation and a more widespread occurrence is suggested by extensive solution collapse brecciation seen in core from other intersections. Evaporites also occur as isolated crystals, and as nodules and pseudomorphs within other carbonate and mixed carbonate/siliciclastic facies of the Ouldburra Formation.

3.8.1 Halite

(a) Bedded Halite

The lower 402 m portion of the type section contains 78 halite beds (Figure 24d). Of these, 26 are greater than one metre thick ranging up to four metres. The halite varies in colour from translucent through various shades of grey to a dark reddish orange.

Bottom nucleation textures have been recognized in the Manya-6 bedded halite (Warren, pers. comm., 1984). Bottom nucleated halite crystals grow with a depressed face directed upward (tabular hoppers). If a cube grows uniformly, edges will advance more rapidly than faces, and corners more rapidly than edges. Thus, where cubes of halite are growing upwards in competition from the floor of the body of brine, those cubes that have edges and corners directed upwards will override those with cube faces directed upwards. This competitive growth will produce near-vertical elongate crystals (corner hoppers) with compromise boundaries between them and inclusions will be arranged so as to produce chevrons

that have their apices directed upwards (Dean and Schreiber, 1978). In areas of freshening of the overlying waters (implying shallow water) or occasional subaerial exposure, the uppermost surface is altered so that the crystal coigns are rounded or the chevrons truncated. The contact areas between adjacent crystals in the crust can be partially dissolved to form voids. Subsequent precipitation infills the cavities with clear halite (Shearman, 1978). In contrast, nucleation on the brine/air interface is believed to produce a hollow pyramidal hopper with its apex directed down (Raup, 1970; Southgate, 1982).

Trace element geochemistry can also be used to infer the environment of deposition of the bedded halite.

Bromine analysis of chloride evaporites is a useful technique for reconstructing palaeosalinities at the time of deposition and documenting diagenetic changes (Raup and Hite, 1978). Bromine occurs in solid solution as a replacement of chlorine in chloride minerals and the amount incorporated into the crystal phases of these minerals is dependant on the concentration of bromine in the parent solution. The partition coefficient of bromine is such that about 75 ppm would be expected in the first halite precipitated from seawater. Recrystallization or recycling by seawater will give values of about 7 to 10 ppm. Deposition from, or reworking by, non-marine water yields values as low as 3.5 to 5.0 ppm (Handford, 1981).

Figure 23 shows the bromine profile for the bedded halite in the lower Ouldburra Formation. Analyses were undertaken using XRF and a halite (rather than whole rock) standard. The values range from 12 ppm to 32 ppm with an average of 20 ppm and a standard deviation of 5 ppm. Although somewhat lower than the theoretical values for derivation from seawater, the results do preclude a non-marine origin of the bedded halite. The results do not vary significantly within any one bed and the

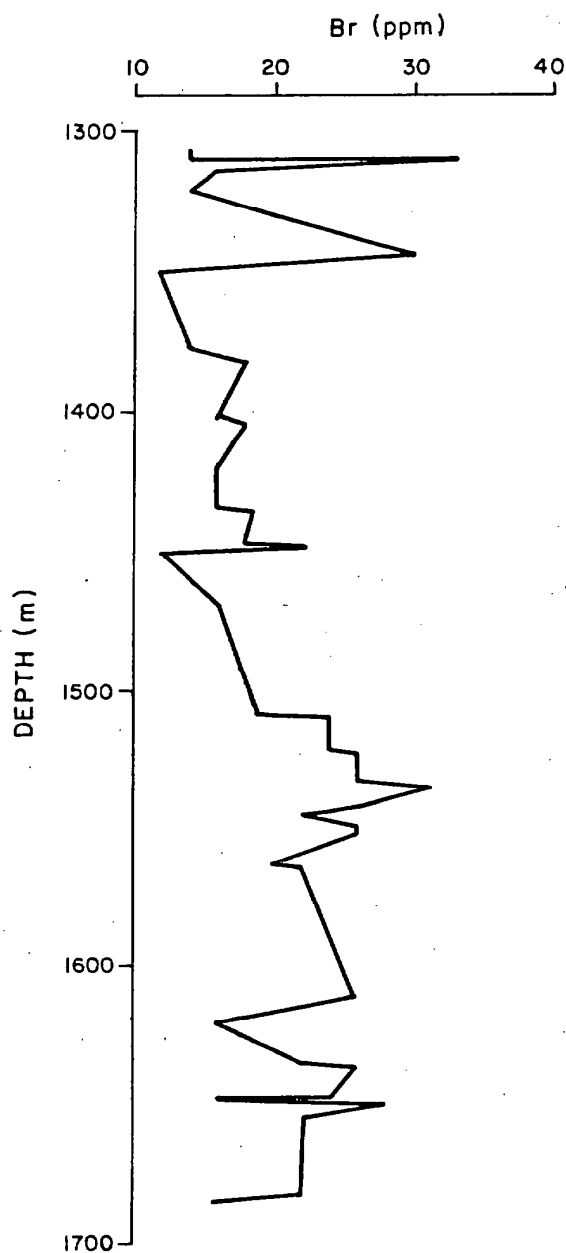


FIGURE 23: BROMINE PROFILE FOR BEDDED HALITE FROM THE
MANYA-6 TYPE SECTION.

overall profile is smooth in comparison with other examples figured by Raup and Hite (1978). With the exception of the variations at the top of profile, the bromine content of the halite ranges within ± 7 ppm of the mean. This indicates very little change in the salinity of the brine during deposition of hundreds of metres of interbedded siliciclastics, carbonates and halite. A closely balanced influx/evaporation/reflux system with a steady inflow of seawater and a corresponding reflux of bittern brines out of the basin is required to maintain such stability (Raup and Hite, 1978). The variations in the bromine concentration at the top of the bedded halite interval may indicate deposition in a series of disconnected or isolated salinas or may be attributed to diagenesis.

The strontium values over the halite interval range from <2 ppm to 90 ppm with an average of 30 ppm. These data are intermediate between the Sr concentrations from the upper part of Lower Cambrian salt beds of the southern Siberian Platform (average 9 ppm) and a variety of Permian to Recent halite deposits all of which average in excess of 45 ppm (Dean and Schreiber, 1978).

Lithium and total boron range from trace values to 14 ppm which is consistent with the normal ranges in marine derived halite (Dean and Schreiber, 1978). Potassium concentrations in the Ouldburra Formation halite range from 100 ppm to 2000 ppm with an average of 618 ppm; in general agreement with the average published range of 27-1,700 ppm (Dean and Schreiber, 1978).

Thus, the trace element geochemistry and the sedimentology suggest that the bedded halite in the Ouldburra Formation was precipitated as bottom nucleated crystals in small shallow salinas, probably from impounded marine waters.

(b) Isolated hoppers

In addition to the above described beds, displacive halite crystals up to 3.5 cm across occur sporadically within other lithofacies higher in the Ouldburra Formation.

Halite crystals which grow displacively in brine saturated mud may retain a solid euhedral cubic shape by simply physically displacing the surrounding matrix (Figure 24a). Alternatively, zoned inclusions of the enclosing mud may be incorporated within the halite crystal (Figure 24b). Since growth is more intensive on the edges and corners, skeletal crystals with hopper-like pyramidal hollows will form on each cube face resulting in cubic skeletal hoppers (Raup, 1970). Extreme skeletal development produces 'pagoda halite' (Southgate, 1982) (Figure 24c). All these textures are represented in core from Manya-6. Halite has not been preserved in core from the drillhole Manya-3, but well formed displacive halite hoppers have been pseudomorphed by sulphate evaporites. The pagoda halite form is preserved as dolomite ghosts in laminated and silty carbonate mudstones.

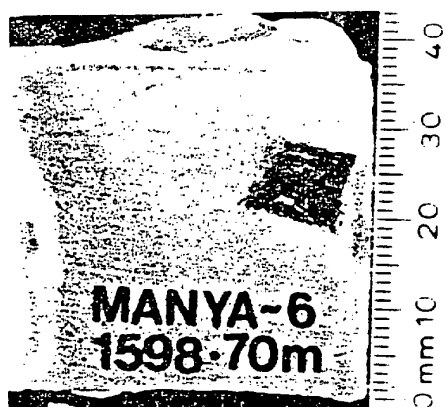
The formation of displacive halite requires a brine supersaturated host matrix and so many workers postulate that such halite can only form below subaerial mud flats of playas and sabkhat (plural of sabkha) (Warren, pers. comm., 1984).

3.8.2 Gypsum and anhydrite

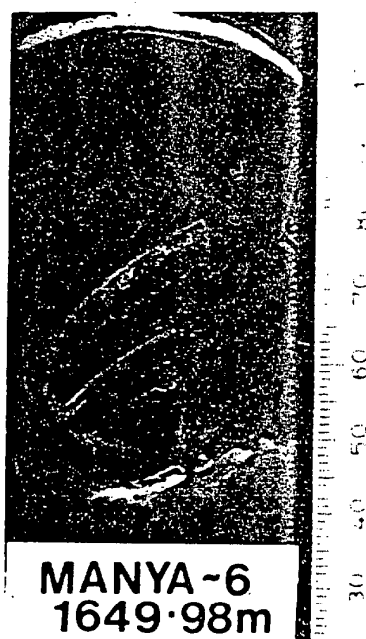
Beds, displacive nodules, isolated crystals and pseudomorphs of gypsum and/or anhydrite are ubiquitous features of the upper Ouldburra Formation. Subordinate barite and celestite also occur in association with the nodular anhydrite. Gypsum and anhydrite occur only rarely lower in

FIGURE 24: HALITE.

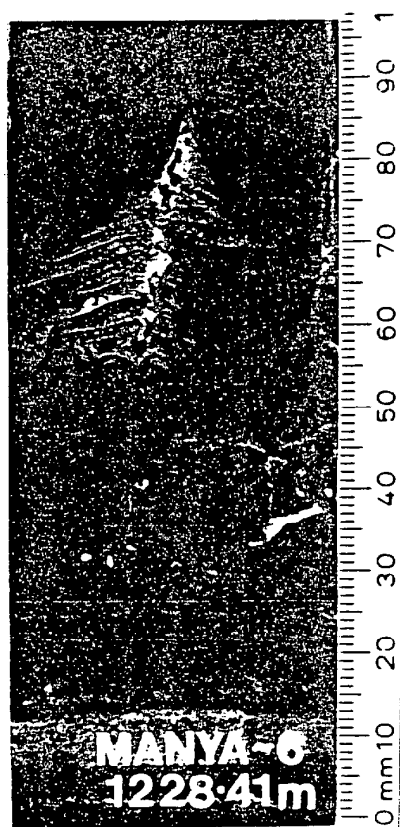
- a. Displacive halite hopper in fine grained sandstone.
- b. Skeletal halite hopper incorporating zones of host mudstone parallel to the crystal face.
- c. Pagoda halite.
- d. Bedded halite with thin mudstone stringers and abundant inclusions at the base of the bed.



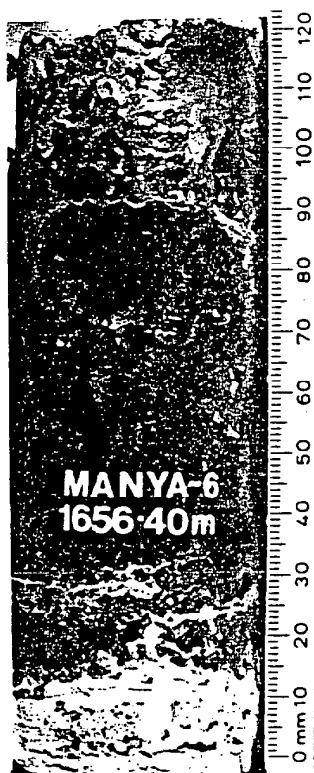
a



b



c



d

the Formation where they are associated with halite. Delta ^{34}S isotopes from calcium sulphate evaporites in the Ouldburra Formation are within the normal range of marine evaporites of this age (Lambert *et al.*, 1986).

The conversion of gypsum to anhydrite, and *vice versa*, and its significance in modern environments remains a point of some debate in the literature (Kinsman, 1969; Shearman, 1978; Shinn, 1983b; Warren and Kendall, 1985; West *et al.*, 1979). With the additional complication of the dehydration of gypsum to anhydrite during burial diagenesis, the interpretation and significance of original mineralogy in ancient examples remains doubtful. However, relict primary textures can often be identified in ancient sequences. Busson (1980), Guillemin (1980) and Warren and Kendall (1985) illustrate several examples. The following discussion briefly compares examples from the Ouldburra Formation with modern analogues to these characteristic textures.

(a) Isolated crystals

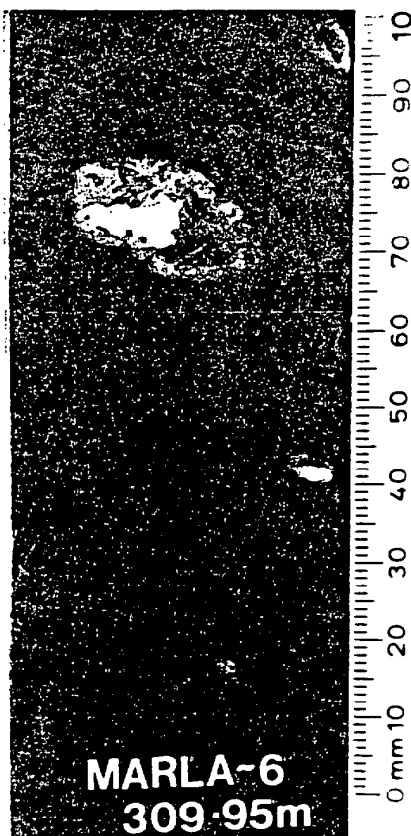
Isolated macroscopic gypsum/anhydrite crystals, and small clusters of crystals, occur sporadically throughout the carbonate mudstones and fine grained clastics of the Ouldburra Formation. The majority of the crystals are small swallow-tail twins and deformed discoidal hemipyramids. Individual crystals rarely exceed 1.0 cm in maximum dimension. Discoidal forms appear lensoidal to rhombohedral in cross section, with length to breadth ratios averaging about 4:1. Clumps of aggregate crystals are moderately common, but true rosettes are rare.

Anhydrite occurs as small lathes and needles throughout the mixed siliciclastic/carbonate mudstone sequence associated with the bedded halite in the base of the Ouldburra Formation.

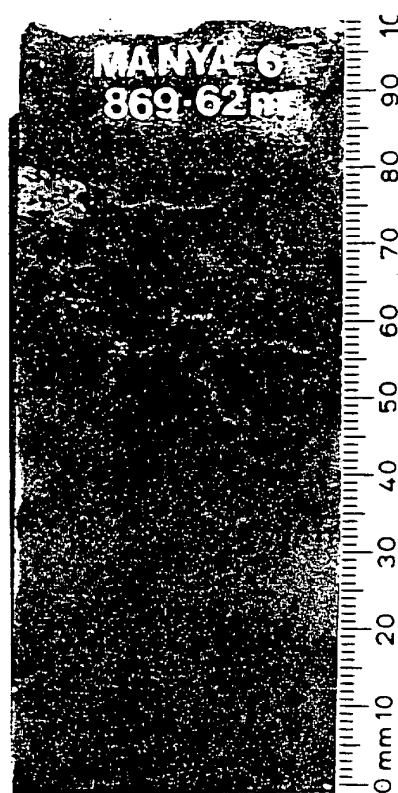
Elsewhere, gypsum, anhydrite and calcite pseudomorphs occur in small (<1.0 mm diameter) sub-spherical vugs. These are similar to the 'micro-patches' of Cussey (1980) and the 'pin-point' anhydrite of Longacre

FIGURE 25: SULPHATE EVAPORITES.

- a. Celestite nodules in a laminated and silty carbonate mudstone.
- b. 'Chicken-wire' anhydrite from the top of a metre thick bed.



a



b

(1980) and Shinn (1983b). It is also possible that the sulphate minerals are pseudomorphing original halite.

Recent studies of the morphology of isolated intrasediment gypsum crystals on a modern marine sabkha (Castens-Seidell, 1984) have shown crystal morphology varies with depositional conditions across the sabkha. Swallow-tail twins and discoidal hemipyramids similar to those in the Ouldburra sediments occur within the siliciclastic sediment of the mud flats surrounding an evaporite pan. They are of both vadose and phreatic origin (Castens-Seidell, 1984).

(b) Macroscopic nodules

Nodules of sulphate evaporites up to 5 cm across are common within the laminated carbonate mudstones of the Ouldburra Formation. The laminae of the host mudstone often curve around the nodules (Figure 25a); and the nodules are remarkably free of inclusions of the host lithology.

The nodules are comprised of gypsum, anhydrite, celestite or barite. The former two minerals occur as a felted mass of lathes or needles with the orientation of the crystals defining individual clumps within the nodules. The lathes may be crudely radially arranged to form a concentric zonation, or are decussate ('pile-of-bricks' texture). Celestite and barite commonly occur in association with nodular gypsum/anhydrite in modern coastal sabkhat (Kinsman, 1969; Schmidt, 1965). Celestite is most abundant in areas of intense dolomitization, being largely a byproduct of the replacement of aragonite by dolomite (Kinsman, 1969). Celestite and barite are the dominant sulphate minerals in nodules from drillhole Marla-6 (Figure 25a). Some of the celestite and barite is believed to be an early diagenetic replacement of anhydrite and occurs as interlocking subhedral to anhedral coarse grained crystals (COM768). The central portions of the replacing celestite or barite crystals may contain areas of relict anhydrite which are still in optical continuity under crossed

nicols. The sulphate evaporite nodules have a complex diagenetic history, often being silicified to produce 'cauliflower cherts' (see section 5.2.1).

Nodular sulphate evaporites are well documented in the literature as an early diagenetic product of sabkha environments. Shearman (1978) described the formation of nodular anhydrite on modern sabkhat where gypsum crystals are converted to, and pseudomorphed by, aggregates of anhydrite crystals in situ. The pseudomorphs grow displacively and penecontemporaneously with deposition of the surrounding sediment to eventually form nodules. These nodules are soft and putty-like and composed of loosely packed porous aggregates of tiny crystal lathes which form a divergent radiating fabric, or are decussate or sub-parallel. Subsurface and surface diagenetic nodular anhydrite is commonest in the middle supratidal zone of modern sabkhat; with the nodules increasing in size and number landward (Shearman, 1978; Shinn, 1983b).

By analogy, the porphyroblastic sulphate evaporite nodules in the Ouldburra Formation appear to have grown displacively, and in some instances retained an internal crystal orientation similar to examples from the middle supratidal region of modern sabkha environments.

(c) 'Chicken-wire' anhydrite

Beds of 'chicken-wire' and 'enterolithic' anhydrite have been intersected in several drillholes in the Ouldburra Formation in the Marla-Manya area. The type section contains 16 beds, several of which have retained the characteristic 'chicken-wire' texture (Figure 25b). The beds rarely exceed 1.0 m thick. Other ancient examples of 'chicken-wire' and 'enterolithic' textures have been well documented (Busson, 1980; Dean and Schreiber, 1978).

Thin section study of examples from Manya-6 (COM630) reveals that the anhydrite is composed of a felted mass of acicular crystals and lathes.

with an undulating preferential parallel orientation. This texture has been described as 'gneissic structure' by Guillevin (1980). On a larger scale, this orientation forms a series of horizontally oriented concentric zones several centimetres across.

Studies of modern analogues show that the 'chicken-wire' texture is generated in the sub-surface as growing gypsum/anhydrite nodules coalesce in layers parallel to bedding. The microscopic orientation of the crystal lathes changes from originally subparallel to bedding, to parallel to edges of the coalescing nodules (Shearman, 1978). Most sediment is displaced vertically as the gypsum/anhydrite nodules grow and coalesce. That sediment which remains forms thin stringers between the nodules and gives rise to the 'chicken-wire' texture. As growth of the nodules continues, the layer becomes contorted into the 'enterolithic' structure (Shearman, 1978).

Shinn (1983) describes the lateral and vertical variations of these textures on the Persian Gulf tidal flats. High intertidal to supratidal surficial gypsum grades laterally inland to buried contorted anhydrite. The lower part of this subsurface anhydrite zone contains the 'chicken-wire' texture. It grades upward into distorted layers of fine grained anhydrite (Shinn, 1983).

By analogy, the 'chicken-wire' anhydrite from the Ouldburra Formation probably formed within the sediment profile of a marine sabkha. This interpretation was also suggested by Warren (pers. comm., 1984) for examples from the type section.

However, as Warren and Kendall (1985) point out, the 'chicken-wire' anhydrite texture may also result from the diagenetic alteration of subaqueous gypsum and it is not possible to distinguish between this and sabkha anhydrite in the case of some individual beds in the Ouldburra Formation (Kendall, pers. comm., 1984).

CHAPTER 4

SECONDARY LITHOLOGIES

Diagenesis has produced a number of distinctive lithologies within the Ouldburra Formation carbonates. Recrystallized dolostone and secondary chert are often conspicuous elements of the upper portion of the Formation. Pressure solution textures and diagenetic solution collapse breccias occur in several drillhole intersections.

4.1 Recrystallized Dolostone

Pale brown and grey aphanitic to sucrosic recrystallized dolostone (Figure 26) is a prominent feature of the upper Ouldburra Formation, with some examples reaching tens of metres thick. It has formed as a diagenetic modification of former carbonates and the degree of recrystallization is often such that no relict texture is discernible. In thin section (COM 686), the dolostones contain sporadic scattered silt sized detrital quartz and feldspar grains and/or medium grained internally zoned euhedral dolomite rhombs in a turbid equigranular very fine grained to aphanitic ferroan dolomite groundmass. The origin of the replacement dolostone is discussed in Section 5.1.2.

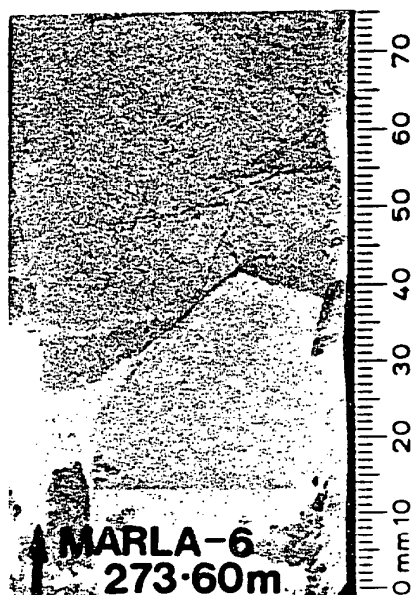
4.2 Secondary Chert

Secondary chert is a minor but conspicuous element of the Ouldburra Formation carbonates. It occurs as botryoidal nodules within host carbonate mudstones and less commonly as silicified limestone beds and thin crusts.

Nodular chert was first reported from the Ouldburra Formation carbonates intersected in the drillhole Mt Willoughby-1 (Thornton, 1971). It also occurs sporadically throughout the upper portion of the carbonate facies in all other intersections of the Ouldburra Formation. The largest examples reach 17 cm thick in core from drillhole Marla-3 and may, in

FIGURE 26: CRYSTALLIZED DOLOSTONE.

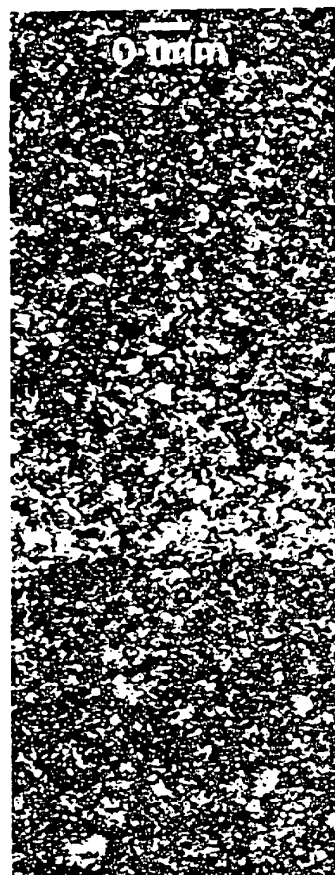
- a. Aphanitic dolostone, stained with potassium ferricyanide.
- b,c,d. Thin sections of replacement dolostone, showing a variety of crystalsizes and porosities (COM788, 779, 782).



a



b



c



d

fact, be lenses or bands rather than nodules. They show a complex arrangement of concentrically zoned chalcedonite, pseudo-fibrous spherulitic lutecite, quartzine and secondary calcite spar. Some examples contain concretionary pisoids suggesting a vadose diagenetic origin. Smaller examples (averaging from 0.5 cm to 2.0 cm) are present in all other intersections. These nodules, or 'cauliflower cherts' (Chowns and Elkins, 1974), consist predominantly of length-slow quartzine and chalcedonite and are believed to be after sulphate evaporites. Examples in homogenous carbonate mudstones are roughly circular in horizontal section and have a botryoidal upper surface. The nodules also have a conspicuous concentric internal zonation, indicating a complex diagenetic history, but often retaining an evaporite mineral at the core. Other, less symmetrical, examples are associated with small scale tepees and mudcracks (see Chapter 5.2.1).

Incipient and pervasive silicification of carbonate mudstones is also evident in core and thin section studies and was first recorded in core from drillhole Marla-1B by Benbow (1980). Beds up to several metres thick show varying degrees of silicification including isotropic opaline silica and colloform and radially fibrous chalcedonite. Different colour phases, from pale orange to blue grey, appear to parallel bedding at the edges of the zones of silicification, but may be concentric or independent of the primary fabric elsewhere. Well defined, thin beds and caliche-type crusts of chert are associated with pervasive subaerial exposure surfaces in the Ouldburra carbonates. These are more fully described in Section 7.6.2.

4.3 Pressure Solution Textures

Pressure solution overprints have been widely recognized in Palaeozoic carbonate rocks (Logan, 1984; Pfeil and Read, 1980; Radke, 1982; Simpson, 1985; Wanless, 1979, 1982), and have been artificially produced in modern marine sediments by Shinn and Robbin (1983). Cores

from drillholes Manya-6, and Manya-3 contain abundant stylolaminated, stylonodular and stylomottled textures in layers up to three metres thick. The textures often occur in association and grade from one to another.

The formation of these pressure solution textures remains a point of some debate in the literature and will be discussed more fully in Section 5.1.4.

4.3.1 Stylobanded to stylolaminated carbonate mudstone

These textures have been referred to as ribbon-rock (Brewer and Henry, pers. comm., 1984; Demicco, 1983; Pfeil and Read, 1980; Wanless, 1979); compressional-stress-response (CSR) laminates (Logan, 1984); and stylobanded to stylolaminated carbonate mudstones (Flügel, 1982).

In hand specimen, they exhibit a strongly developed layering with alternating thin beds or laminae of dark, internally stylolaminated dolomite and paler carbonate mudstone (Figure 27).

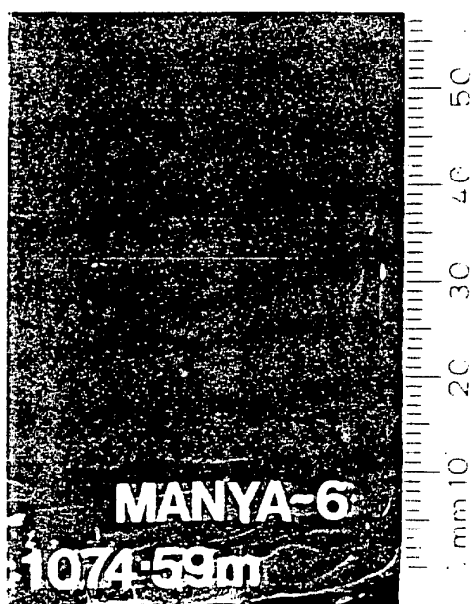
The stylolaminations are clearly visible in thin section (COM637). They are defined by local concentrations of up to 20 percent corroded to recrystallized fine grained to silt-sized detrital quartz and feldspar (stylocumulate; sensu Logan and Semeniuk, 1976) in a turbid ferroan dolomite groundmass containing abundant euhedral rhombs (reactate; sensu Logan and Semeniuk, 1976). The paler laminae and thin beds are slightly to moderately dolomitic calcite; generally micrite.

Shinn and Robbin (1983) used artificial compaction to produce banding and lamination very similar to these pressure dissolution textures as an enhancement of primary lamination in modern subtidal carbonate muds. Wanless (1979), however, suggested that stylolamination could be independent of the primary bedding structure.

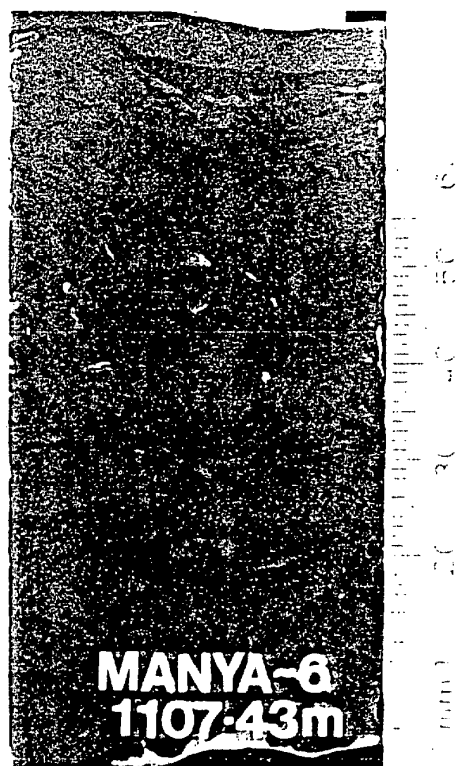
Examples from the Ouldburra Formation contain fragments of trilobites, peloids, microfossils and burrows which suggest a shallow

FIGURE 27: PRESSURE SOLUTION TEXTURES

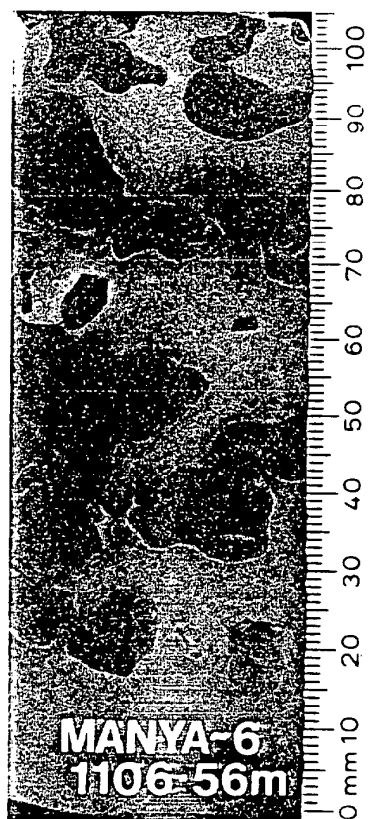
- a. Stylobanded to stylolaminated carbonate mudstone.
- b. Stylomottled carbonate mudstone.
- c. Stylonodular carbonate mudstone (ferroan dolomite stained with potassium ferricyanide).
- d. Thin section of stylonodular carbonate mudstone (COM640, stained with Alizarin Red-S).



a



b



c



d

marine origin. Pfeil and Read (1980) also interpreted similar stylolaminated textures as indicative of a low energy, shallow, subtidal setting below the wave base. However, stylolamination and stylobanding are diagenetic overprints and not all examples will necessarily be of subtidal origin.

4.3.2 Stylonodular carbonate mudstone

This texture has been described as 'tiger stripe' (Brewer and Henry, pers. comm., 1984); sedimentary boudinage, ball-and-flow, (Wilson and Jordan, 1983); compressional-stress-response nodular (Logan, 1984); and stylonodular (Flügel, 1982; Radke, 1982).

The stylonodular texture (Figure 27c) is characterised by isolated to interconnected, lenticular to rounded, boudin-like areas of slightly dolomitic calcite surrounded by laminated stylocumulate and reactate ferroan dolomite. In the examples from the Ouldburra Formation, the boudin-like nodules are generally paler in colour, approximately one centimetre in thickness and separated by varying amounts of the stylolaminated secondary material.

Thin section studies (COM516,640), show that the dark stylolitic material is recrystallized ferroan dolomite which contains abundant fine grained to silt sized detrital quartz and feldspar grains and clay concentrated in stylolaminae. The stylolaminae often encapsulate the nodules, or are rarely parallel to larger, more pervasive, macroscopic stylolites. The dolomite ranges from euhedral rhombs up to 0.1 mm across to equigranular microcrystalline. The paler nodules consist of microcrystalline to amorphous very slightly dolomitic calcite with highly disturbed internal laminae containing fine grained to silt sized detrital quartz, feldspar, calcite intraclasts and, less commonly, fossil fragments and peloids. Deformed peloid-filled burrows have also been identified in thin section. Sporadic nodules also contain microfractures with secondary sparry calcite infill.

The presence of sponge spicules and trilobite fossils suggests a shallow marine origin for at least some of the stylonodular carbonate mudstones from the Ouldburra Formation.

4.3.3 Stylomottled carbonate mudstone

Stylomottling (Flügel, 1982) or compressional-stress-response mottling (Logan, 1984) is alluded to less in the literature than the previous textures. It is characterized by isolated irregular shaped dark mottles which are scattered throughout a pale host carbonate mudstone. In the examples from the Ouldburra Formation, the mottles are tabular equant to irregularly shaped, one millimetre to three centimetres in size and composed of ferroan dolomite, detrital quartz, micas, clays, and iron-oxide along with calcareous grains in various stages of pressure dissolution or cataclastic granulation. Frequently, the mottles are isolated to interconnected, and randomly dispersed and oriented (Logan, 1984). They may, however, be localized around more pervasive pressure solution surfaces such as macroscopic irregular to columnar stylolites.

Incipient stylomottling (Figure 27b) occurs in a variety of host wackestones, packstones and otherwise massive carbonate mudstones in the Ouldburra Formation, often grading into other pressure solution textures. A single, original environment of deposition cannot be postulated; although a stylomottled unit in core from Manya-6 yielded the best preserved trilobite fossils yet found in the Ouldburra Formation.

4.4 Solution Collapse Breccia

Solution collapse brecciation is a common secondary texture in the Ouldburra Formation carbonates. Core from drillhole Manya-3 has extensive collapse brecciation presumably after the removal of bedded evaporites from lower in the sequence. In some examples, the evaporite has been remobilized as the matrix to the breccia and shows concentric

'flow' structures around the clasts. In other cases, the matrix is coarse non-ferroan calcite spar which may include diagenetic minerals or geopetal sediment (COM730,731). The formation of collapse breccia is discussed more fully in Chapter 5.3.

CHAPTER 5

DIAGENETIC HISTORY

The diagenetic history of the Ouldburra Formation carbonates and evaporites is extremely complex. The carbonates have undergone several generations of cementation, pervasive dolomitization, pressure solution, silicification and solution collapse. There is also some evidence of dedolomitization. Sulphate evaporite nodules show repeated chemical alteration and replacement by saddle dolomite and various forms of authigenic silica to produce 'cauliflower cherts'. Both the sulphate evaporites and the halite are locally remobilized as veins. Late stage calcite veining is also common locally.

To fully elucidate the multiple overprinting of these diagenetic effects is beyond the scope of this work. The following is a brief overview emphasizing those textures which may be used to infer an original environment of deposition or the setting of subsequent diagenetic overprints.

5.1 Carbonate Diagenesis

The Ouldburra Formation carbonate facies show extensive diagenetic alteration especially in the upper portion of the Formation where the effects of dolomitization are most pronounced. Elsewhere, pressure solution and cementation have largely obscured the original carbonate fabric.

5.1.1 Cementation

The extensive alteration of all but a few sporadic grainstones precludes the successful use of artificial staining (Evamy, 1969) in compilation of an overall 'cement stratigraphy' (Meyers, 1974). Mixtures of calcite, dolomite and silica occur as replacement cements in the

various grainstone lithofacies, in stromatactis cavities and as void fill in tubular fossils and archaeocyaths.

In addition to cementation, the ooid grainstones show a variety of diagenetic alterations; including, in order of increasing abundance:-

- i) pressure dissolution to form 'spastoliths',
- ii) ferruginization,
- iii) silicification,
- iv) micritization,
- v) recrystallization to neomorphic calcite spar,
- vi) dolomitization.

The interplay of these is such that the effects of up to four or more different processes can be observed in a single thin section (COM691, 699, 747, 749) (Figure 29). This intense diagenetic alteration has generally obliterated the original cement texture. However, in a few sporadic examples silica has pseudomorphed the ooids and the primary cement (see Wilson (1966) for criteria of replacement versus primary silica cements).

These examples (COM682) include multiple generations of meniscus (Figure 28c) and pendant (Figure 28d,1) vadose cements, followed by possible relict radial fibrous ferroan calcite cement (Figure 28e). This generation of cement may be interpreted as submarine (Kendall and Tucker, 1973) or vadose (Bechstadt, 1974). The stubby bladed spar (Figure 28f) and isopachous bladed calcite cements (COM769) suggest an active meteoric phreatic environment. Other examples of thick isopachous rinds (COM691; Figure 29 e,f) may have been precipitated in the active marine phreatic zone.

In comparison with other studies of Early Cambrian carbonate (cf. James and Klappa, 1983), the Ouldburra grainstones show a locally more complex cement stratigraphy and much more extensive diagenetic alteration. This may reflect more variable conditions during cementation and the subsequent further diagenesis of the Ouldburra Formation.

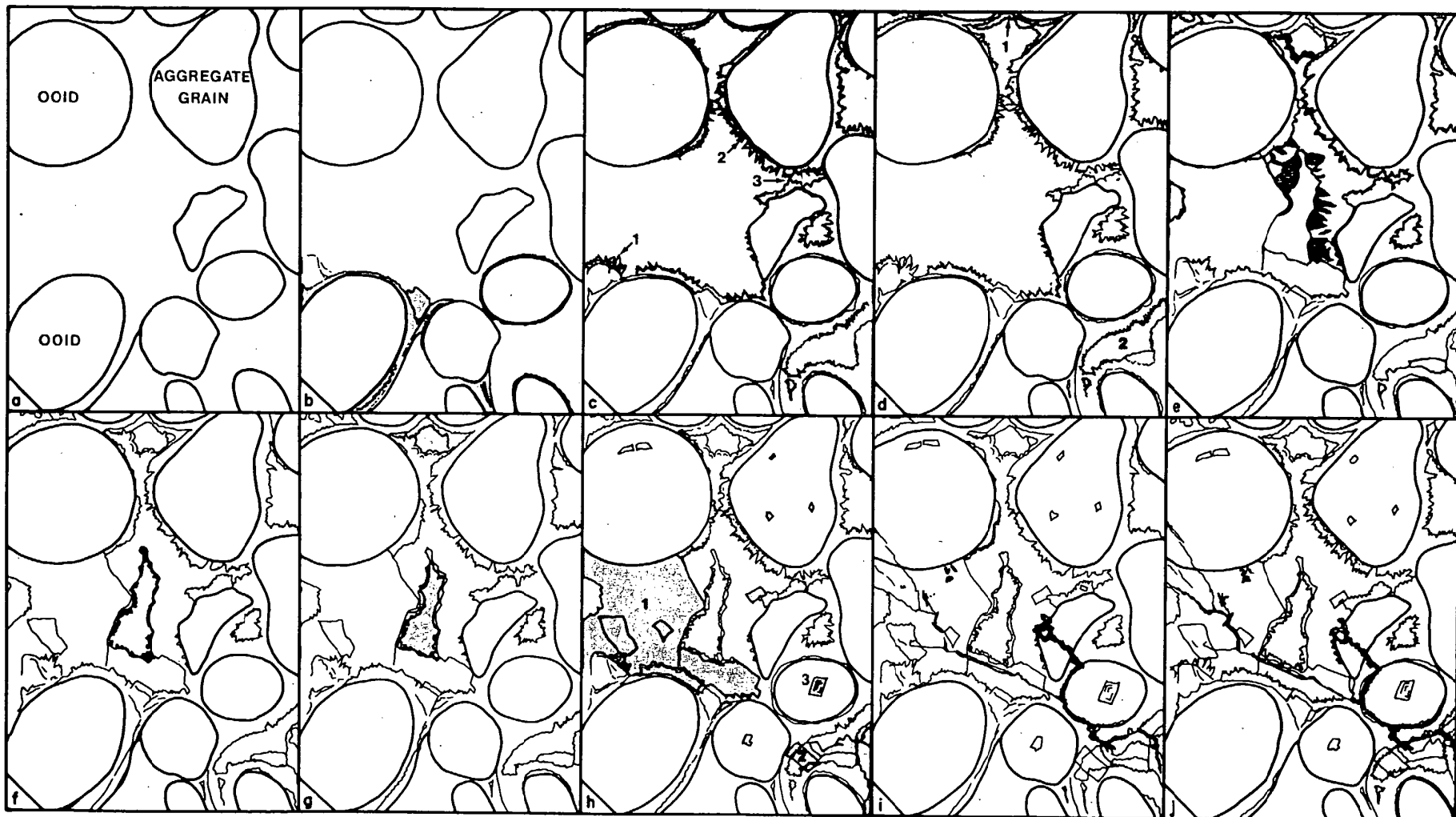
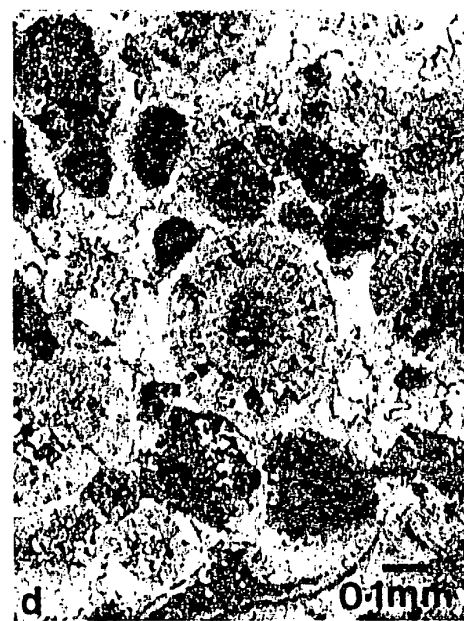
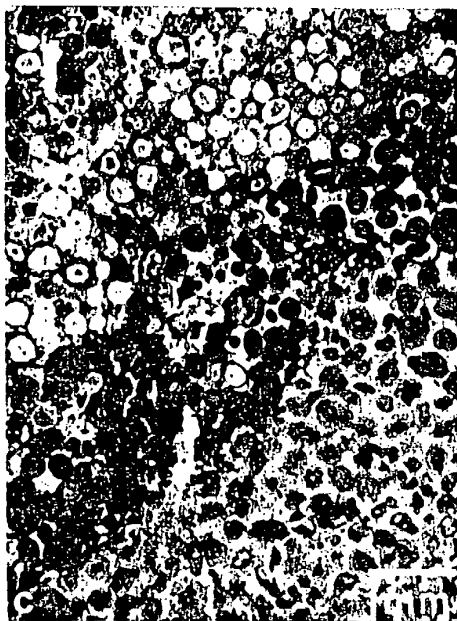
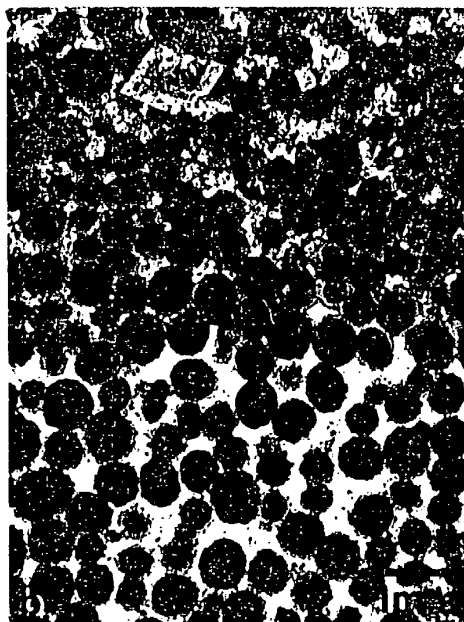
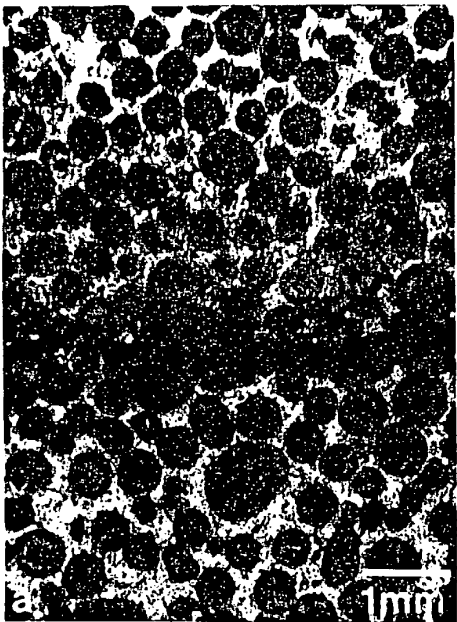


FIGURE 28: HISTORY OF CEMENTATION OF AN OOID GRAINSTONE LENS
THIN SECTION COM682, MARLA-6, 679-33m.

FIGURE 29: GRAINSTONE DIAGENESIS.

- a,b. Thin sections of an ooid grainstone showing recrystallization, stylolitization, preferential dolomitization of ooids, the formation of dolomite rhombs, silicification and ferruginization (COM749, stained with Alizarin Red-S).
- c. Thin section showing stylolitization, ferruginization and dolomitized ooids (COM747, stained with Alizarin Red-S).
- d. Thin section of an ooid bioclastic peloid grainstone showing recrystallization to pseudospar independent of original syntaxial overgrowth on the ooids (COM635, unstained thin section).
- e,f. Micritized, dolomitized and silicified ooid grainstone showing isopachous rinds of fibrous cement and final cavity fill with crystal size increasing toward the centre of the cavity (COM691, plane polarized light and crossed nicols).



5.1.2 Dolomitization

Ouldburra Formation carbonates have undergone ubiquitous dolomitization to form dolostones. These range from pervasive massive dolomitized zones tens of metres thick to thin crusts finely interlaminated with silty limestone. Dolomite also occurs in pressure solution textures, as void fill, as a replacement of sulphate evaporites, and in association with coarse calcite spar in late stage veins and in the matrix of solution collapse breccias. These occurrences are shown schematically in Figure 30.

The dolomite in the Ouldburra Formation occurs in three main petrographic forms (sensu Friedman, 1965). The first is an aphanitic to very finely crystalline equant xenotopic habit which has formed as replacement of pre-existing carbonate textures (Gregg and Sibley, 1984). This has a stratiform occurrence, ranging from massive zones tens of metres thick to fine laminae. The second form of dolomite consists of euhedral to subhedral idiotopic to hypidiotopic (Friedman, 1965) ferroan dolomite rhombs. These occur as isolated crystals or small crystal aggregates (porphyrotopic texture) within a wide variety of calcareous lithofacies. They are also the prominent crystal habits associated with pressure solution textures. The third petrographic form is coarsely crystalline saddle dolomite which ranges from idiotopic to xenotopic.

(a) Saddle dolomite

Saddle (or baroque) dolomite is a variety of dolomite that has a warped crystal lattice. This is manifest as curved crystal faces, curved cleavage, and sweeping undulose extinction (Radke and Mathis, 1980). The crystals are generally turbid distorted rhombohedra, often with an internal zoning of inclusions parallel to the crystal faces.

Saddle dolomite occurs as a replacement mineral or void filling cement throughout a variety of carbonate lithofacies in the Ouldburra Formation. These occurrences are:-

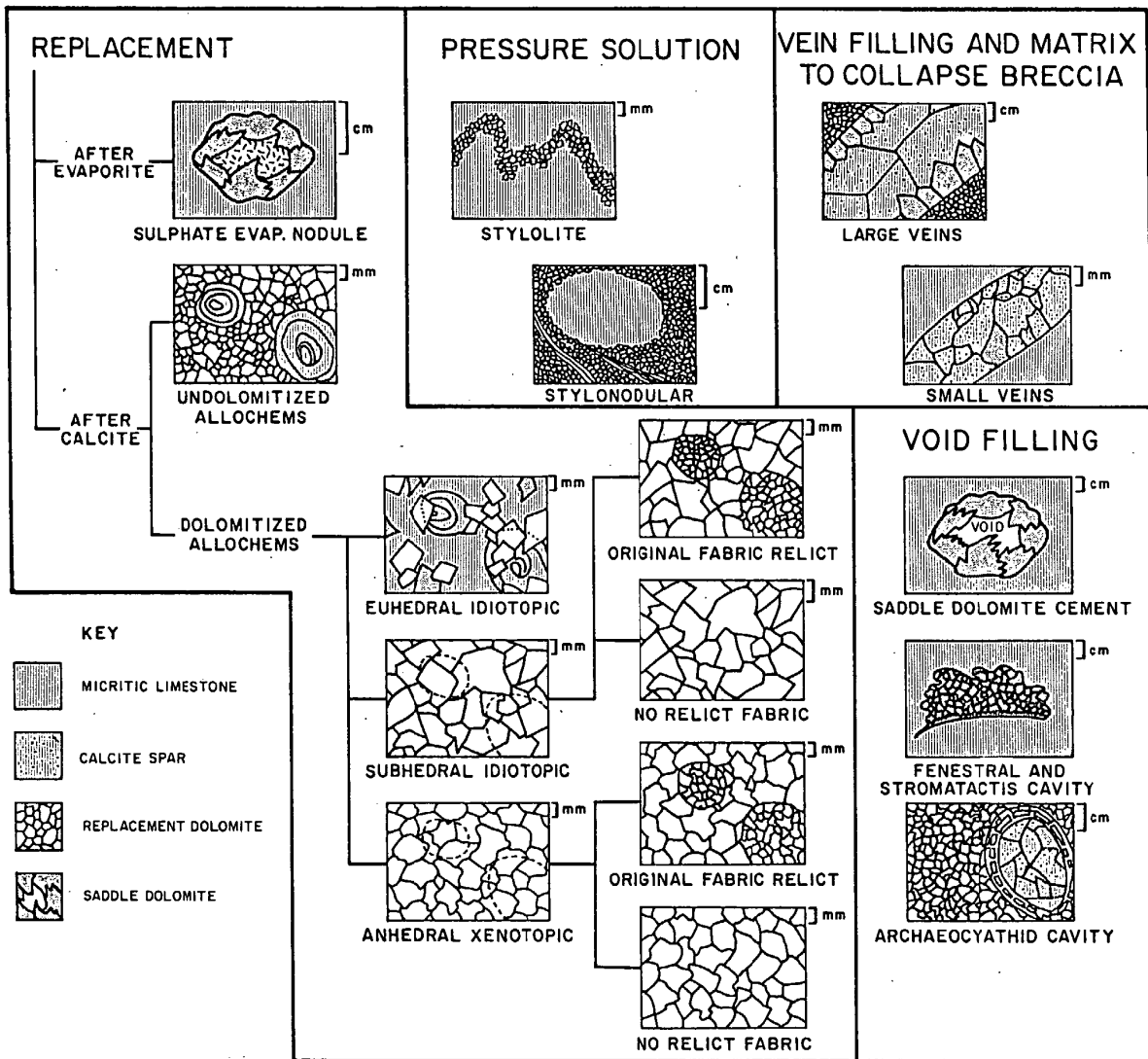


FIGURE 30: SCHEMATIC SKETCHES OF THE MOST COMMON OCCURRENCES OF DOLOMITE IN THE OULDBURRA FORMATION (PARTLY AFTER GREGG AND SIBLEY, 1984; AND MATTES AND MOUNTJOY, 1980).

- i) with coarse calcite spar as late stage vein infill,
- ii) with coarse calcite spar and remobilized sulphate evaporites in the matrix/cement of solution collapse breccia,
- iii) with replacement silica and calcite spar as infill to archaeocyaths,
- iv) as irregular patches in grumeleuse fine grained dolomite and micrite in thrombolitic algal bindstone,
- v) as cavity fill in fenestral and stromatactitic carbonate mudstone (COM733),
- vi) with coarse calcite spar in irregular patches in diagenetically altered peloid intraclastic packstone/grainstone,
- vii) as part of a concentric zonation of replacement minerals in cauliflower cherts (COM739).

The formation of saddle dolomite appears to have been an enduring phase of mid to late diagenesis in the Ouldburra Formation carbonates. Late stage calcite spar replaces the saddle dolomite in some examples. Elsewhere, saddle dolomite hosts inclusions of euhedral calcite crystals. The idiomorphic faces of saddle dolomite rhombs are juxtaposed with secondary silica textures in cauliflower cherts; but in areas of intraformational pervasive subaerial exposure, saddle dolomite appears to have undergone preferential silicification in comparison with adjacent calcite spar.

The occurrence of saddle dolomite has been interpreted as indicating original hypersaline carbonate deposition (Friedman and Radke, 1979), or the presence of original organic matter or sulphate evaporites. It has also been suggested as a geothermal indicator of temperatures of 60° - 150°C (Gregg, 1983; Radke and Mathis, 1980). However, recent work by Pluim (1984) has demonstrated that saddle dolomite can form as a relatively early, shallow diagenetic event. Laboratory studies have shown that sulphate reduction reactions are not necessary for the formation of

saddle dolomite (Gregg, 1983). In view of these findings, the presence of saddle dolomite alone cannot be used as indicator of thermal maturity or to infer the presence of original sulphate evaporites in the Ouldburra Formation carbonates.

(b) Stratiform bedded dolostone

Stratiform bedded replacement dolostone occurs throughout the Ouldburra Formation carbonates as metre thick pervasive zones ranging down to millimetre scale laminae and thin beds. It is generally massive, although sedimentary structures and original calcareous textures are sometimes relict by variation in the crystalsize of the replacement dolomite. The dolomite ranges from aphanitic to a xenotopic finely crystalline habit. Coarser euhedral ferroan dolomite rhombs commonly occur within a more finely crystalline matrix.

Where stratiform dolostone is intercalated with calcareous marine carbonates, the upper contact of the dolostone is commonly sharper than the lower boundary. Lithic fragments of dolostone are present in plate breccias and other lithofacies with a calcareous matrix. Such features were interpreted by Schmidt *et al.* (1980) to indicate that at least some dolomitization preceded further deposition of marine carbonates.

The stratiform dolostones are an important reservoir facies in the Ouldburra Formation. Their possible origins are discussed in more detail in Chapter 7.7.

5.1.3 Dedolomitization

Two types of dedolomitization texture are present in the Ouldburra Formation carbonates. The first type represents the replacement of isolated dolomite rhombs by equicrystalline mosaics of anhedral calcite (Evamy, 1967). Such dedolomitization textures are generally related to surface diagenesis (Chafetz, 1972). The presence of sulphate ions derived

from the evaporation of interstitial brines is believed to have assisted dedolomitization (Flügel, 1982).

The second and more abundant type of dedolomitization texture formed as saddle dolomite is pseudomorphed by secondary sparry calcite. Similar replacement was described by Moore (1971) and Radke (1982). The replacement calcite is non-ferroan and pseudomorphs the curved crystal faces and internal zones of inclusions typical of saddle dolomite. This replacement is believed to be a late stage diagenetic event.

5.1.4 Petrogenesis of pressure solution textures

Pressure solution textures, including thin sutured stylolites and a range of stylolaminated to stylonodular textures, are common diagenetic features of the Ouldburra Formation carbonates.

Thin sutured stylolites can be considered ubiquitous in Palaeozoic carbonate rocks (Longman, 1981), including those of the Ouldburra Formation. The majority of the stylolites in the Ouldburra carbonates are horizontal, or at a low angle to bedding; although well developed vertical columnar stylolites occur sporadically (eg. Marla-6, 408.5 m). The largest and thickest stylolites are high amplitude columnar forms in carbonate mudstones. They commonly have in excess of 15 mm of reactate and stylocumulate in the 'peaks and troughs' of the stylolite. The irregular stylolites are most common as parallel or anastomosing sets in mixed carbonate/siliciclastic lithofacies. Horsetail and low amplitude irregular stylolites are generally associated with grainstones.

The morphology of the stylolites is commonly a reflection of the carbonate fabric (Buxton and Sibley, 1981) and the degree of pressure solution. Stylolites are believed to have been formed at several tens to hundreds of metres depth of burial by dissolution associated with either subsurface brine migration or decarboxylation (Longman, 1981).

The stylolaminated, stylobanded, stylonodular and stylomottled textures in the Ouldburra Formation are described in Section 4.3. These examples show that an original alteration between carbonate mudstone and grainstone is commonly enhanced by pressure solution to produce a stylonodular texture (Figures 31, 32). In other cases, the pressure solution textures exaggerate original non-stratiform inhomogeneities such as burrows and dewatering structures (Figure 31).

The petrogenesis of similar pressure solution textures was discussed by Logan (1984), Logan and Semenuik (1976) and Radke (1982). A complex interplay of compaction, pressure dissolution and shear fracture results in dolomitization and recrystallization to produce characteristic textures. Radke (1982) and Wilson and Jordan (1983) stressed the importance of inhomogeneity in the original sediment as a necessary precursor to the formation of these pressure solution textures.

The pressure solution of carbonates results in the loss of large volumes of calcareous sediment and provides effective permeability barriers. It also concentrates organic matter to provide locally high TOC values (total organic carbon content).

5.1.5 Emplacement of calcite veins

Most intersections of the upper portion of the Ouldburra Formation contain calcite veins and veinlets. Individual veins rarely exceed 5 cm thick. They are displacive and in sharp contact with the host wall rock. Calcite veins are most common in core from the drillholes Manya-3 and Middle Bore-1 where they are associated with solution collapse and faulting respectively.

Examples from Manya-3 crosscut one another. They precede the development of stylonodular pressure solution textures (COM516) and both precede and postdate thin sutured stylolites. The vein fill consists of

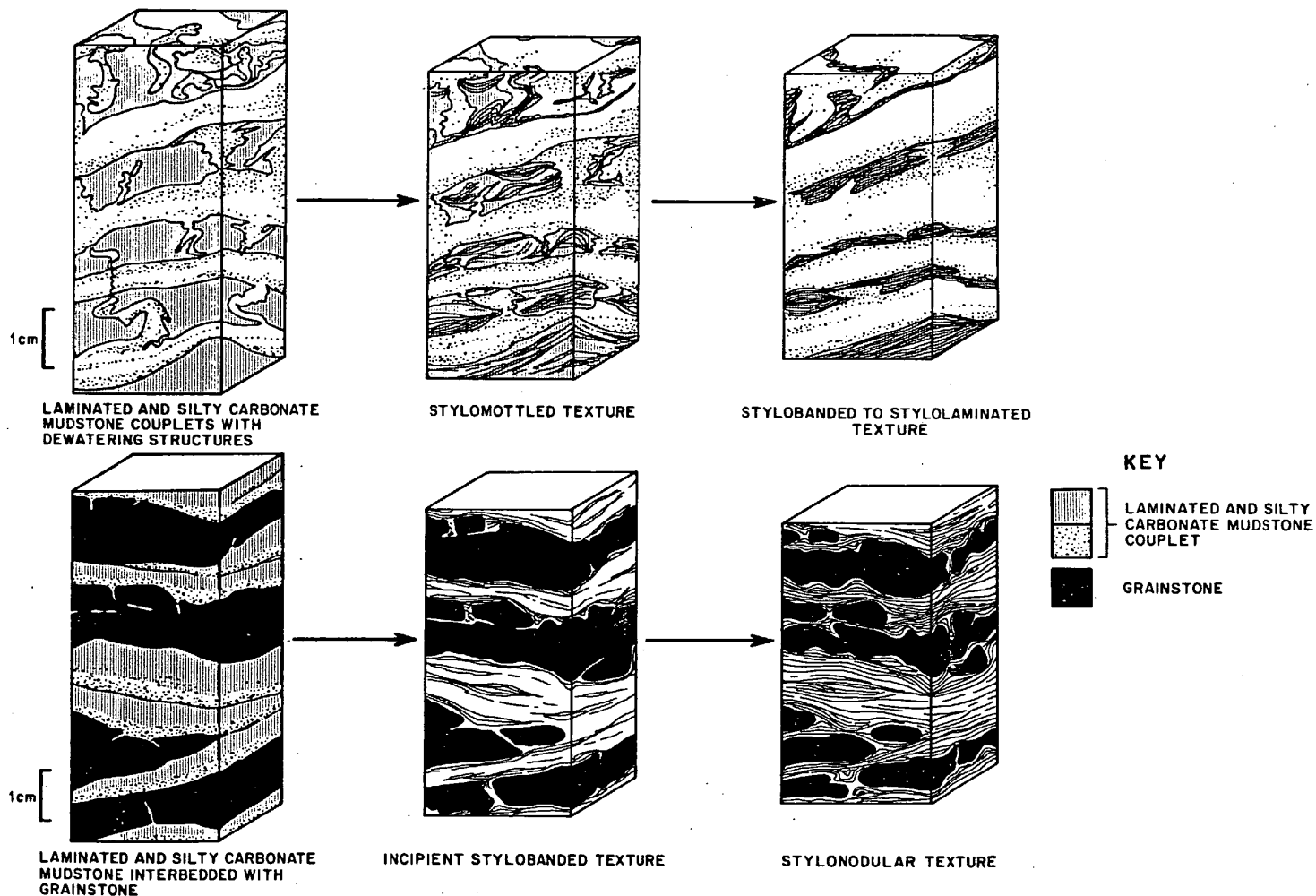
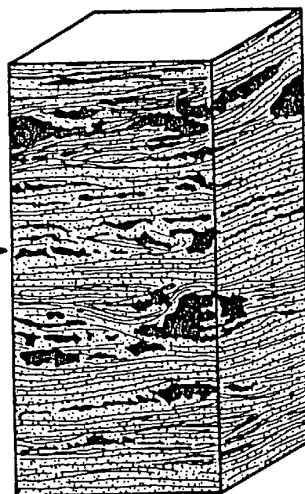


FIGURE 31: SCHEMATIC DIAGRAM SHOWING PETROGENESIS OF PRESSURE SOLUTION TEXTURES FROM DIFFERENT PRECURSOR LITHOFACIES.



PLANAR LAMINATED
STROMATOLITIC ALGAL
BINDSTONE



INCIPIENT PRESSURE
SOLUTION



STYLONODULAR TEXTURE

=



KEY



LAMINATED MICRITIC
ALGAL BINDSTONE



GRAINSTONE

FIGURE 32: STYLONODULAR TEXTURE OVERPRINTING AN ORIGINAL PLANAR LAMINATED STROMATOLITIC ALGAL BINDSTONE.

coarsely crystalline subhedral to anhedral non-ferroan calcite spar with subordinate saddle dolomite, rare siliceous replacements, and rare fluorite, pyrite and native sulphur.

The calcite veining is more intense in the Ouldburra Formation carbonates from Middle Bore-1. The veins occur in an echelon arrangement and as an irregular crosscutting network, related to local tectonic faulting. Some of the larger examples contain millimetre and centimetre scale open voids, others contain minor sulphide mineralization. The thickest veins have an outer zone of scalenohedral dolomite crystals arranged perpendicular to the vein with extremely coarse equant calcite spar in the centre of the vein.

The Manya-6 type section contains only sporadic thin high angle calcite veins. They are generally restricted to packstone and grainstone lithofacies. Subordinate saddle dolomite, rare pyrite, fluorite and native sulphur occur in association with the coarsely crystalline calcite spar vein fill. These examples postdate the sutured stylolites.

Other intersections of the Ouldburra Formation show that, in the absence of faulting or solution collapse, the emplacement of calcite veins was a late stage diagenetic effect associated with deep burial.

5.2 Evaporite Diagenesis

The sulphate evaporites from the Ouldburra Formation have a complex late diagenetic history which includes alteration, remobilization and replacement. Isolated nodules of gypsum/anhydrite have been replaced by barite, saddle dolomite, calcite and various forms of authigenic silica. The sulphate evaporites are commonly remobilized as the matrix of collapse breccias. These examples show a similar diagenetic history to that of the nodules but are only rarely replaced by silica. Abundant and widespread late diagenetic sulphate veins are the most conspicuous evidence of evaporite diagenesis.

In contrast, the bedded halite shows little evidence of diagenetic alteration other than local remobilization into veins by rheological processes.

5.2.1 Paragenesis of sulphate evaporite nodules

The upper Ouldburra Formation carbonate mudstones commonly host millimetre to centimetre scale sulphate evaporite nodules. These nodules show alteration from gypsum/anhydrite to barite (COM768), or celestite (SEM750); or may be replaced by calcite (COM530) or saddle dolomite (COM739). They have, almost invariably, undergone some degree of silicification to produce the so-called 'cauliflower cherts' (Chowns and Elkins, 1974) (Figures 33,34). Similar paragenesis has been proposed for other examples of Palaeozoic (Radke, 1982; Siedlecka, 1972) and Proterozoic (Siedlecka, 1976; Walker *et al.*, 1977) evaporite nodules in host carbonate mudstones.

Chalcedonite, megaquartz, pseudo-fibrous length-slow lutecite and quartzine are the main forms of authigenic silica in cauliflower cherts from the Ouldburra Formation (Figure 33). Lutecite spherulites (COM673, 740, 766) and spherulitic chalcedonite are the most common first generation replacement textures. Concretionary colloform rinds ('overlays' *sensu* Wilson, 1966) of chalcedonite are usually encrusted on another form of quartz or a saddle dolomite substrate (COM739 Figure 33c). This texture is believed to have formed as infill to solution voids (Radke, 1982), although there is some evidence from the Ouldburra Formation and elsewhere (Maleev, 1972), that continued growth may be displacive. Chalcedonite also commonly occurs in association with lutecite as a replacement texture (COM673). Alternating zones of lutecite and chalcedonite may indicate fluctuating salinities during their precipitation (Folk and Pittman, 1971). Megaquartz occurs as both a

FIGURE 33: DIAGENESIS OF SULPHATE EVAPORITE NODULES.

a. Cauliflower chert with an evaporite core,

1. spherulitic to pseudofibrous lutecite
2. anhydrite

(COM673, plane polarized light and crossed nicols).

b. Cauliflower chert showing:-

1. dolomite rhomb
2. calcite spar
3. pseudofibrous lutecite

(COM750, crossed nicols).

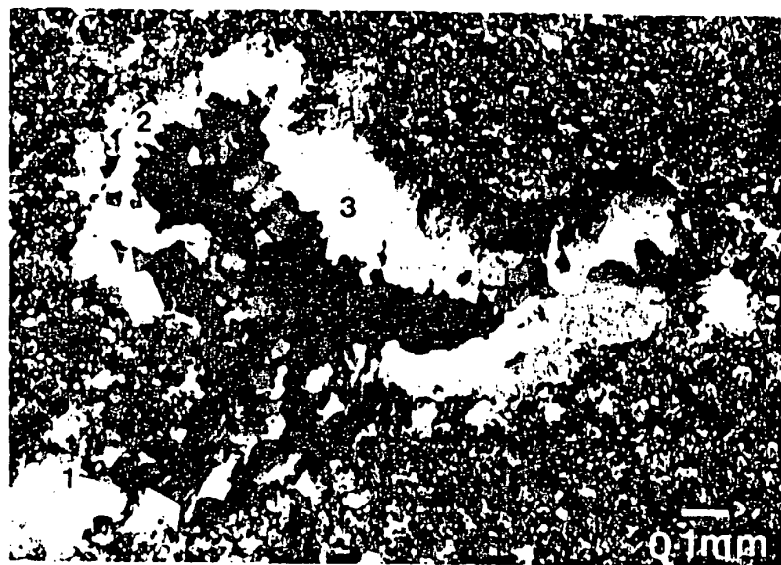
c. Sulphate evaporite nodule with zones of silicification.

1. saddle dolomite
2. calcite spar
3. microlaminated chalcedonite
4. quartzine with inclusions of finely crystalline calcite, barite and extremely small euhedral quartz crystals.

(COM739, stained with Alizarin Red-S, plane polarized light).



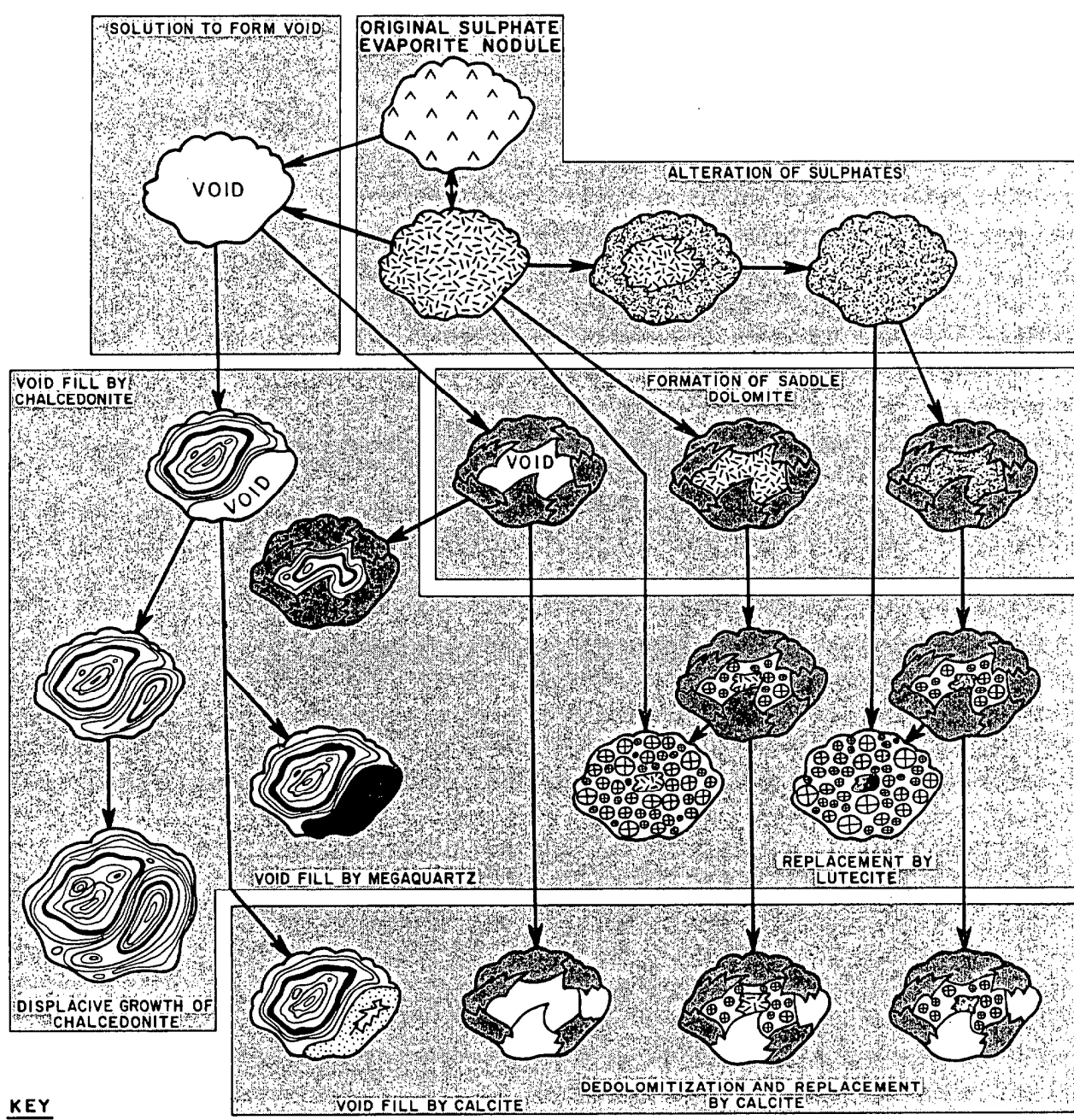
a



b



c



KEY

		VOID	Fluid filled void
SULPHATE		Gypsum	
		Anhydrite	
		Barite or celestite	
SILICA		Lutecite and/or quartzine	
		Chalcedonite	
		Megaquartz	
CARBONATE		Replacement calcite spar	
		Dog-tooth calcite spar	
		Saddle dolomite	

FIGURE 34:
PARAGENESIS OF SULPHATE NODULES BY
ALTERATION, REPLACEMENT, SOLUTION
AND VOID FILLING PROCESSES
 (partly after Radke, 1982).

replacement texture and as void fill. In the latter case, it is invariably the last stage cavity fill and can occur in association with the least soluble evaporites such as celestite.

In some of the nodules, silicification has possibly pseudomorphed the original decussate and felted texture of original anhydrite lathes, with individual crystals being replaced by lutecite (COM768). In other examples, anhydrite lathes remain poikilotopically enclosed in megaquartz or chalcedonite (COM530).

5.2.2 Emplacement of gypsum/anhydrite veins

Gypsum/anhydrite veins are ubiquitous throughout the upper Ouldburra Formation and are most abundant where the Ouldburra Formation interdigitates with the overlying Observatory Hill Formation. The veins range up to 15 cm thick but average approximately 3 cm thick. Overall, they show no preferred orientation with respect to bedding, although the largest veins are invariably conformable. The vein contacts are sharp with only minor millimetre scale brecciation of the wall rock. Anastomosis of veins is common but multiple generation veining is only of local significance.

The majority of the veins consist of equant tabular gypsum crystals arranged perpendicular to the vein boundaries or fibrous gypsum with individual bundles of fibres perpendicular to the vein. Rare anhydrite needles occur dispersed throughout the fibrous fabric. Some veins (COM670) show multi-layering defined by differences in gypsum and anhydrite crystal morphology.

The gypsum/anhydrite veins precede and postdate the thin sutured stylolites. The emplacement of the veins is believed to have been a relatively late stage diagenetic event associated with subsurface brine migration through rocks under tensional stress. The gypsum to anhydrite conversion results from burial dehydration.

5.3 Collapse Brecciation

Collapse brecciation occurs in decimetre scale zones throughout most intersections of the Ouldburra Formation carbonates. It is most extensive in core from Manya-3 where zones of collapse commonly range up to several metres thick. Collapse brecciation is believed to result from the remobilization or dissolution of interbedded evaporites from lower in the sequence. Similar examples are described by Blount and Moore (1969) and Middleton (1961). The Manya-3 drillhole is situated close to the Wintinna Fault zone and this could have provided a conduit for deep fluid migration during much of the late diagenetic history of the Ouldburra Formation.

Several possible scenarios, as shown schematically in Figure 35, explain the different forms of collapse breccia observed in the Ouldburra Formation. In some instances, the evaporite removal has been very early, which enabled plastic deformation of relatively unconsolidated overlying sediments. More commonly, however, the overlying carbonates are subject to mechanical fracture and/or chemical dissolution. Remobilized evaporite may be introduced as a matrix to the resulting breccia. In these cases, the zone of brecciation has a sharply defined lower boundary, usually corresponding to the base of an original evaporite bed. The evaporite matrix often shows a crude flow texture around the host carbonate mudstone clasts. The clasts are essentially in situ, and almost invariably angular. Examples of this texture occur in core from Manya-3. In other cases, complete dissolution of the original evaporite leads to the development of calcite, saddle dolomite and/or silica replacements and void fill. In some examples, the clasts are generally in situ, but are accompanied by geopetal vadose sediment. In other examples, the clasts of host carbonate mudstone have obviously been rotated and moved about within the cavity (COM731). Rare fluorite, pyrite and celestite occur in

association with both remobilized evaporite matrix and carbonate cements in collapse breccias.

5.4 Authigenic Minerals and Syntaxial Overgrowths

Thin section and insoluble residue studies of the Ouldburra Formation have identified syntaxial overgrowths of quartz and feldspar, authigenic quartz euhedra, possible bioepigenetic sulphur and possible authigenic glauconite.

5.4.1 Quartz overgrowth and authigenic quartz euhedra

Syntaxial overgrowth on quartz grains is very common throughout the Ouldburra Formation. The overgrowths range from thin rims of optically continuous quartz on detrital grains to the development of an authigenic euhedral crystal form. Some examples of the latter are nucleated on detrital grains, ooid nuclei, or possible siliceous sponge spicules (COM 748), while other examples may have been associated with dissolution of sulphate evaporites.

Isolated quartz euhedra (up to 0.25 mm in length) occur as length-slow hexagonal prisms with pyramidal shaped ends, or as aggregates of such crystals. They are widespread throughout carbonate and evaporite lithofacies. At their most abundant they comprise up to 7 percent of the rock in recrystallized peloid and ooid grainstones and packstones. Examples from within a matrix of gypsum and anhydrite contain inclusions of the surrounding evaporite. This replacement of evaporite differs somewhat from similar examples described by Friedman and Radke (1979), Friedman and Shukla (1980) and Radke (1982), which were believed to have been formed in voids created by the dissolution of sulphate crystals.

5.4.2 Feldspar overgrowth

Thin rims of authigenic overgrowth are common on detrital feldspar grains from throughout the Ouldburra Formation. The overgrowths rarely

exceed 0.05 mm thick and are generally not in optical continuity with the original detrital nuclei. The abundance of overgrowths is related to the detrital feldspar content, but occurs in a wide variety of host lithofacies including those with calcareous, dolomitic and gypsum matrix/cements.

Braun and Friedman (1969) and Mazzullo (1976) proposed that K-feldspar precipitated on detrital nuclei and replaced dolomite within an alkaline hypersaline environment. Friedman (1985) considered it one of many features diagnostic of hypersalinity in a Palaeozoic epicontinental sea/sabkha setting.

5.4.3 Authigenic glauconite

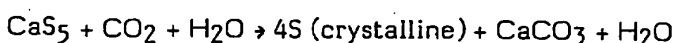
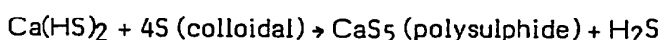
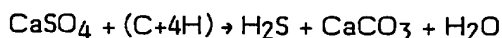
Very rare traces of possible authigenic glauconite have been identified in several thin sections of the Ouldburra Formation carbonates. The ?glauconite occurs as a slightly pleochroic bright green mineral in millimetre scale diffuse patches and wisps. It invariably shows some degree of alteration to ?limonite and occurs only in association with sulphide minerals, ferroan dolomite and stylocumulate. While the presence of detrital glauconite has long been used as an indicator of 'normal marine salinity' (McRae, 1972; Odin and Matter, 1981), the authigenic occurrences in the Ouldburra Formation are of little palaeo-environmental significance.

5.4.4 Native sulphur

Rare traces of elemental sulphur are present in core from 1190 m to 1234 m in the Manya-6 type section, and also occur sporadically in core from drillhole Manya-3. The sulphur occurs in small vugs, fractures and very rarely as millimetre scale laminae. It is commonly associated with gypsum in fractures, and rarely occurs with halite in vugs.

Davis and Kirkland (1979) and Ruckmick *et al.* (1979) proposed a bioepigenetic origin for elemental sulphur which involves postsedimentary

conversion of sulphate evaporite to hydrogen sulphide and subsequent reduction to sulphur. This is accompanied by the oxidation of hydrocarbons to CO_2 . These reactions can be generalized by the following series of equations:-



(Ruckmick et al., 1979).

Sulphate reducing bacteria are believed to be responsible for the initial breakdown of anhydrite. Such bacteria have been cultured from rocks from depths in excess of 500 m. There is also $^{32}\text{S}/^{34}\text{S}$ isotopic evidence to suggest that the reduction of anhydrite is biochemical (Davis and Kirkland, 1979). Such reactions are believed to occur in the presence of hydrocarbons with the petroleum carbon atoms being incorporated into the calcite. This is substantiated on the basis of similar $^{12}\text{C}/^{13}\text{C}$ isotopic ratios in the calcite and petroleum (Davis and Kirkland, 1979).

Similar isotopic studies on examples from the Ouldburra Formation have not been undertaken. However, the association between fracture related migration paths, the presence of gypsum and secondary calcite, and the inferred association with hydrocarbons, are circumstantial evidence supporting a bioepigenetic origin.

5.5 Fracturing

Subsurface fracturing in the Ouldburra Formation can be related to tectonic activity, solution collapse or the volume reduction created by pressure solution.

The most intense fracturing is associated with a fault intersected in the drillhole Middle Bore-1. The smallest fractures are parallel, or at a

low angle, to bedding and commonly exhibit slickensides on the fracture surface. The larger fractures have no preferred orientation with respect to bedding and generally lack slickensides. In some cases individual fractures are partially healed by calcite and also cross cut older calcite veins.

Fracturing in other intersections of the Formation can be related to mechanical brecciation associated with solution collapse. These fractures are small, irregularly anastomosing and often widen downward into calcite filled veins.

Small fractures are also associated with pressure solution textures. The fractures are restricted to areas where pressure solution textures are delimited by a discordant feature such as a pre-existing stylolite or chert nodule. The predominantly vertical volume reduction caused by pressure solution cannot extend into the adjacent non-calcareous zone and small fractures form.

Fractures can greatly enhance the porosity and permeability of the rock. The long irregular fractures which interconnect centimetre scale vugs in core from drillhole Marla-7 are a good example.

5.6 Summary of Diagenesis

The diagenetic history of the Ouldburra Formation shows repeated oscillations between eogenesis and early telogenesis during deposition. These are followed by a long period of deep burial mesogenesis and finally by late telogenesis prior to erosion during the Permo-Carboniferous glaciation. The overall paragenetic sequence shown in Figure 36 is greatly simplified and does not include the repeated superposition of eogenetic and early telogenetic overprints; nor does it include regional variation in the duration and influence of individual diagenetic processes. The overall scenario is similar to that proposed by Radke (1982) for the Ninmaroo Formation in the Georgina Basin, and the following discussion uses the same terminology. Eogenesis is the early burial stage of

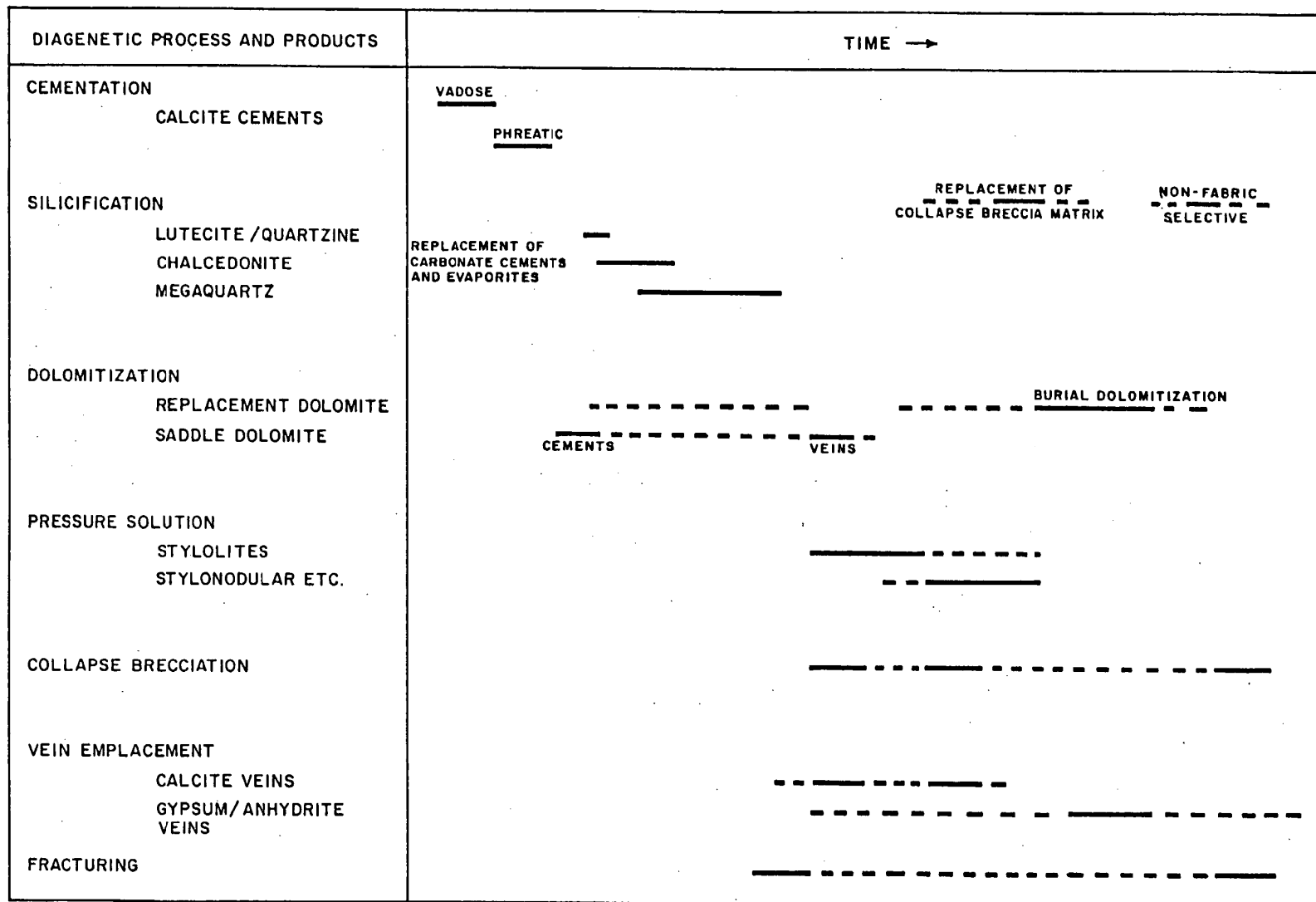


FIGURE 36: GENERALIZED OVERALL PARAGENETIC SEQUENCE FOR THE OULDBURRA FORMATION.

diagenesis where there is interaction with near surface fluids. The eogenetic processes are often penecontemporaneous with deposition and include:-

- i) possible aragonite and Mg-calcite cementation,
- ii) early dolomitization of exposed and shallow carbonates,
- iii) displacive growth of gypsum crystals,
- iv) conversion of gypsum to anhydrite during burial and formation of 'chicken-wire' anhydrite,
- v) early collapse brecciation with plastic deformation of sediments caused by the solution of underlying sulphate evaporite beds.

The transition to early telogenesis is gradual and is characteristic of shallowing-up sedimentation. It exposes the sediments to vadose diagenesis. The important processes in the vadose zone of solution include:-

- i) preferential removal of any aragonite and Mg-calcite,
- ii) development of chalcedonite in voids formed by the solution of sulphate evaporites,
- iii) alteration of some sulphate evaporites to less soluble barite and celestite,
- iv) the possible onset of replacement of sulphate evaporites by various forms of silica and saddle dolomite.

The accumulation of a sufficient amount of sediment and the continued subsidence of the basin heralded the onset of mesogenesis. The regional variation in maturity of organic matter suggests that the effect of mesogenesis varies within the Marla-Manya area. This phase of diagenesis resulted in:-

- i) conversion of most remaining gypsum to anhydrite,
- ii) continued replacement of sulphate evaporites by lutecite and saddle dolomite,

- iii) void fill and continued displacive growth of chalcedonite,
- iv) silicification of carbonate cements,
- v) silicification of the matrix to solution collapse breccias,
- vi) precipitation of drusy and dog tooth calcite cements,
- vii) possible dedolomitization of saddle dolomite,
- viii) remobilization of, and replacement by, barite and celestite,
- ix) rheological remobilization of bedded halite and the anhydrite matrix to solution collapse breccias,
- x) burial dolomitization,
- xi) the formation of calcite and sulphate evaporite veins,
- xii) development of pressure solution textures including stylolites,
- xiii) formation of authigenic minerals,
- xiv) maturation of organic matter, possible hydrocarbon generation and migration.

The last stage of overall diagenesis of the Ouldburra Formation is concerned with the uplift and erosion of the sequence during the Permian-Carboniferous. This late telogenetic phase has not been studied in any detail, but would be expected to result in the normal suite of diagenetic changes associated with a return to vadose and meteoric phreatic conditions. Specific processes would include:-

- i) development of incipient silicification,
- ii) dedolomitization,
- iii) further solution collapse which postdates stylolitization,
- iv) enhancement of existing porosity,
- v) rehydration of anhydrite to gypsum,
- vi) deposition of vadose silt.

In summary, the diagenetic history of the Ouldburra Formation includes a complex interplay of eogenesis, early telogenesis, mesogenesis and late telogenesis. This is reflected in the multiple overprinting of a wide variety of diagenetic processes.

CHAPTER 6

CYCLICITY OF SEDIMENTATION

Cyclic sedimentation consisting of characteristic vertical arrangements of lithofacies or lithologies has been recognized over most of the Ouldburra Formation including the carbonates, mixed carbonate/siliciclastics and evaporites. This study interprets individual shallowing-up cycles in terms of sedimentary and early diagenetic processes. The sedimentary sequence was tested for Markovian tendencies and the validity of some individual empirically derived cycles was checked geostatistically.

Each shallowing-up cycle consists of a characteristic vertical arrangement of lithofacies or lithologies. Six different cycles have been recognized by empirical observation:-

- i) halite/siliciclastic cycle
- ii) halite/mixed carbonate/siliciclastic cycle
- iii) archaeocyath/algal bioherm cycle
- iv) algal bindstone cycle
- v) carbonate sabkha cycle
- iv) mixed carbonate/siliciclastic sabkha cycle.

Table 37 shows the number of complete cycles of each type recognized from several drillhole intersections in the Marla-Manya area. The type section contains 23 complete cycles and dozens of part cycles, often terminated by erosional boundaries. The vertical range of each type of cycle is shown in the summary log (Figure 8). Cyclicity is also obvious in core from Marla-6, where 22 complete cycles were recorded from a 446.2 m intersection of the Ouldburra carbonates. This compares with 38

cycles of similar scale recognized over approximately the same vertical interval of the Ninmaroo Formation from the Georgina Basin (Radke, 1980).

		DRILLHOLE AND THICKNESS (m)		
CYCLE		MANYA-6 1114.2	MARLA-6 446.2	MARLA-7 349.7
(i)	halite/siliciclastic cycle	4	0	0
(ii)	halite/mixed carbonate/ siliciclastic cycle	7	0	0
(iii)	archaeocyath/algal bioherm cycle	0	9	0
(iv)	algal bindstone cycle	2	11	2
(v)	carbonate sabkha cycle	7	2	2
(vi)	mixed carbonate/ siliciclastic sabkha cycle	3	0	0

TABLE 37: NUMBER OF COMPLETE SEDIMENTARY CYCLES IN DRILLHOLE INTERSECTIONS BASED ON EMPIRICAL OBSERVATION.

The vertical distribution of the cycles can, itself, be periodic, as in the case of vertical stacking of the same cycle. The halite/siliciclastic and halite/mixed carbonate/siliciclastic cycles are commonly vertically stacked. They record repeated local shallowing-up events without regional transgression or regression which would have introduced other lithofacies. Other cycles occur episodically, but are often restricted to fairly narrow vertical ranges within the Ouldburra Formation.

Individual cycles also contain evidence of small scale episodic sedimentation such as small scale scour and fill and thin plate breccias within peri-emergent facies. Similarly, the effects of eogenesis and early telogenesis vary between individual cycles of the same type, and where such features are not consistent they have been omitted from the description of cycles. The following descriptions are generalized from a number of each type of cycle in several drillhole intersections of the Ouldburra Formation. The accompanying diagrams show idealized examples or actual cycles from the type section. Those cycles which contain bedded evaporites commonly have a characteristic signature on the gamma, density and neutron logs and the examples shown in Figures 38, 39 and 43 would enable the recognition of these cycles in the Ouldburra Formation in the absence of core data. The consistently unusual neutron response for the bedded halite is believed to be a borehole affect.

6.1 Shallowing-upward Sedimentary Cycles

6.1.1 Halite/siliciclastic cycle

A complete cycle (Figure 38) contains the following lithofacies and lithologies in descending order:-

4. ?algal bindstone as a highly crenulated thin veneer with abundant halite filled fenestrae (this lithofacies is not always preserved);

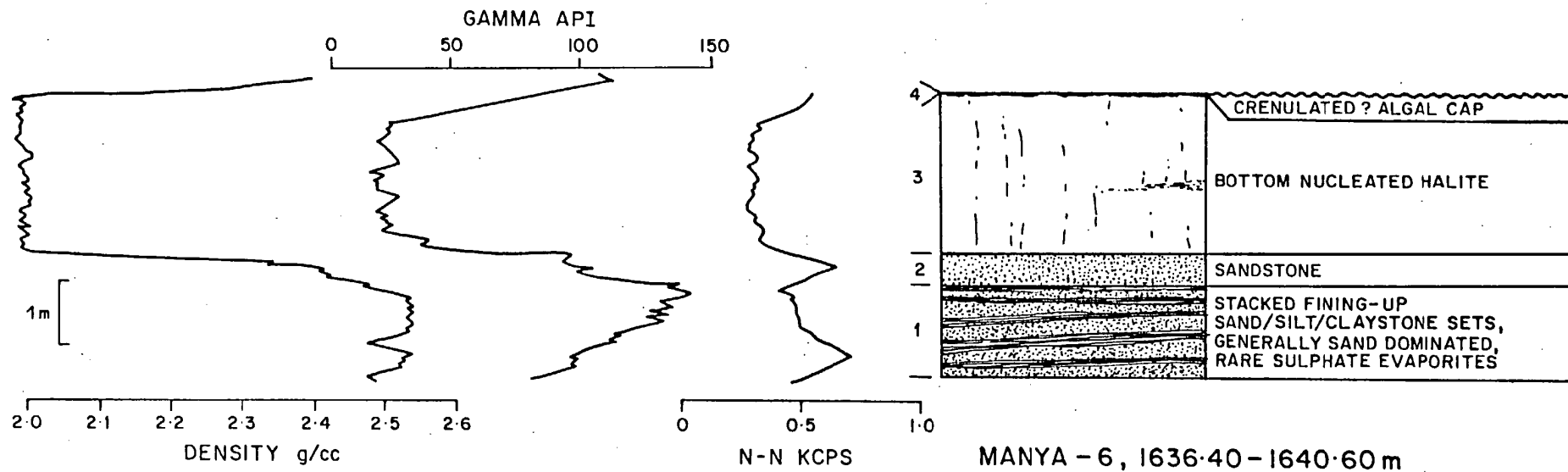


FIGURE 38: TYPICAL HALITE / SILICICLASTIC CYCLE.

3. bedded halite, with a bottom nucleated texture;
2. quartz/feldspathic sandstone, very coarse to fine grained, moderately to poorly sorted, subrounded to well rounded grains, with sporadic planar cross-beds;
1. stacked fining-up sand/silt/claystone sets with sporadic ripple cross-beds, generally sand dominated, rare small sulphate evaporite nodules and isolated crystals, sporadic displacive halite hoppers.

This cycle commonly occurs vertically stacked, with the basal sand/silt/claystone sets being underlain by the top of another halite bed. The contact is generally very sharp. In the absence of an algal bindstone cap, the upper contact is clearly erosional, truncating the halite chevrons. The cycle averages 3.8 m thick, but the total thickness is dependant on the amount of halite preserved. The halite/siliciclastic cycle occurs between 1507 m and 1686 m in the Ouldburra Formation type section.

Interpretation

Deposition of the stacked sand/silt/claystone sets began on a clastic dominated peri-emergent mixed sand/mud flat. Sporadic exposure led to the development of rare nodular sulphate evaporites and displacive halite hoppers within the sediment profile. As deposition continued, the facies became progressively more arenaceous possibly due to the effects of deflation. The sandstone may represent a paralic sand flat or low dunes (Warren, pers. comm., 1984). Bottom nucleated halite was precipitated in small isolated salinas or playas which formed in shallow depressions on the sand flat. The thin crenulated ?algal cap suggests that the shallowing-up cycle was terminated by exposure (Kendall, pers. comm., 1984). Rapid local transgression followed, commonly eroding the halite, before re-establishing the mixed sand/mud flat.

6.1.2 Halite/mixed carbonate/siliciclastic cycle

This cycle (Figure 39) is similar to the previous one but includes regularly emergent mixed carbonate/siliciclastic lithofacies. The lithofacies of an idealized cycle are, in descending order:-

6. laminated carbonate mudstone or ?algal bindstone as a thin cap (not preserved in all examples);
5. bedded halite with bottom nucleated texture and sporadic mudstone stringers;
4. quartz/feldspathic sandstone, very coarse to fine grained, moderately to poorly sorted, subrounded to rounded grains and minor mudstone clasts, stacked laminae defined by variation in grain size, commonly with gypsum/anhydrite as cement and sporadic planar cross-bedding;
3. laminated and silty carbonate mudstone (commonly dolomitic) with sporadic algal bindstone, hosting gypsum/anhydrite nodules, with mudcracks, sheetcracks, small scale teepees and dewatering structures;
2. stacked fining-up sand/silt/mudstone sets, often with small scale ripple cross-stratification grading to the underlying lithofacies;
1. laminated and silty carbonate mudstone as stacked fining-up couplets with sporadic low angle planar cross lamination and ripple cross-stratification.

The cycle occurs between 1283 m and 1562m in the type section, ranging up to 8 m thick. Individual cycles are often incomplete because of erosion or are disrupted by remobilization of the halite.

Interpretation

The deposition of this cycle began on a submergent to sporadically emergent mixed carbonate and siliciclastic mudflat; a setting analogous

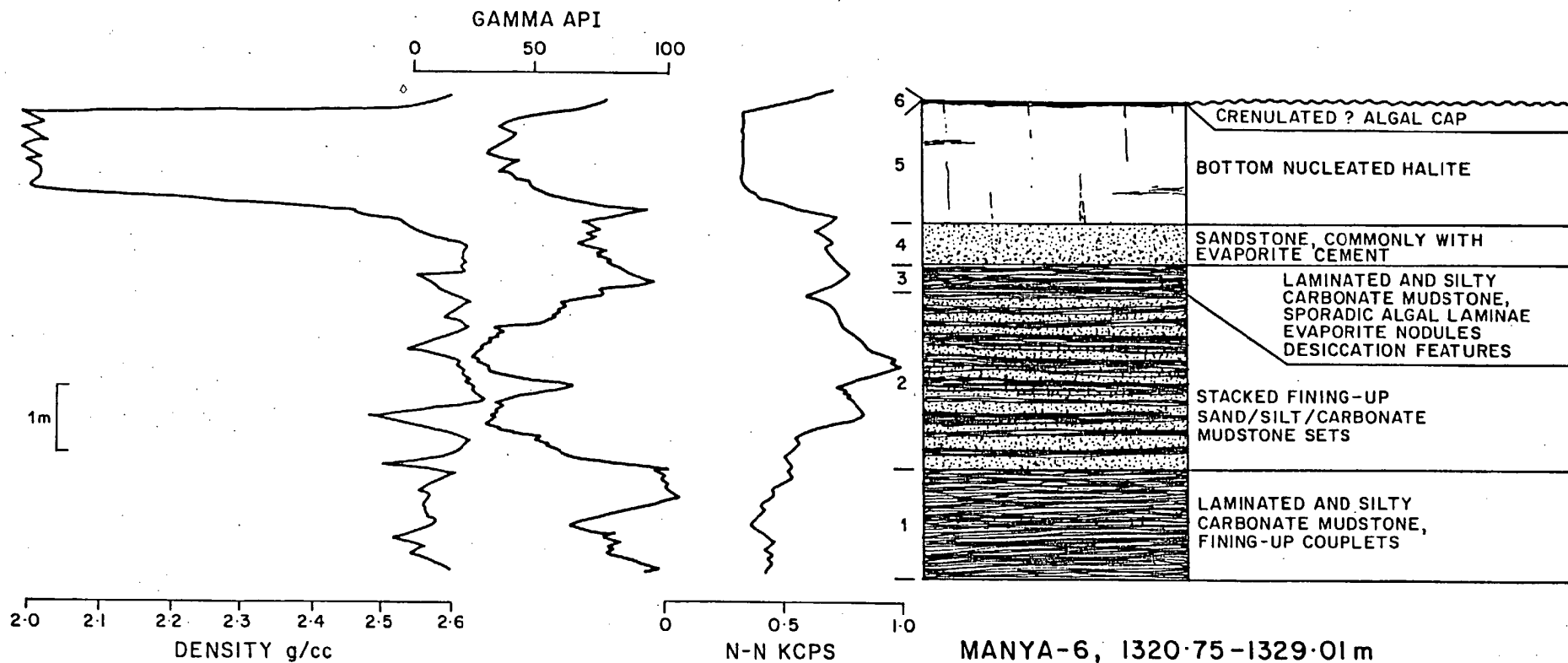


FIGURE 39: TYPICAL HALITE / MIXED CARBONATE / SILICICLASTIC CYCLE.

to modern mixed tidal flats; although sedimentation appears to have been dominated by storm couplets of fining-up laminated and silty carbonate mudstone. This grades up to the more arenaceous 'intertidal' facies consisting of stacked sand/silt/carbonate mudstone sets. The transition to laminated and silty carbonate mudstone with sporadic algal lamination, abundant desiccation features and evaporites is evidence of increasing periods of emergence. These units are overlain by sandstone and halite similar to the examples in the previous cycle; deposition probably occurred in salinas or playa lakes developed on a transitional sand flat or deflation flat. The overall cycle represents a single shallowing-up event.

6.1.3 Archeocyathid/algal bioherm cycle

This cycle (Figure 40) is present from 399.8 m to 543.0 m in the drillhole Marla-6. The cycle averages just over 3 m thick. The lithofacies of an idealized cycle are, in descending order:-

5. thin layers of stromatolitic algal bindstone, either as planar or domed forms with subordinate laminated silty carbonate mudstone (not present in all cycles);
4. archaeocyath bafflestone/framestone, commonly with algal bound clumps, geopetal sediments and internal cements in cavities;
3. thrombolitic algal bindstone;
2. fenestral and stromatactitic carbonate mudstone (not always present);
1. laminated and silty carbonate mudstone, with sporadic low angle planar cross-stratification and ripple cross-lamination.

The cycle generally has an erosional top and, in the absence of the capping algal bindstone, is often overlain by laminated and silty carbonate mudstone. The lower contact is commonly gradational to a thin packstone

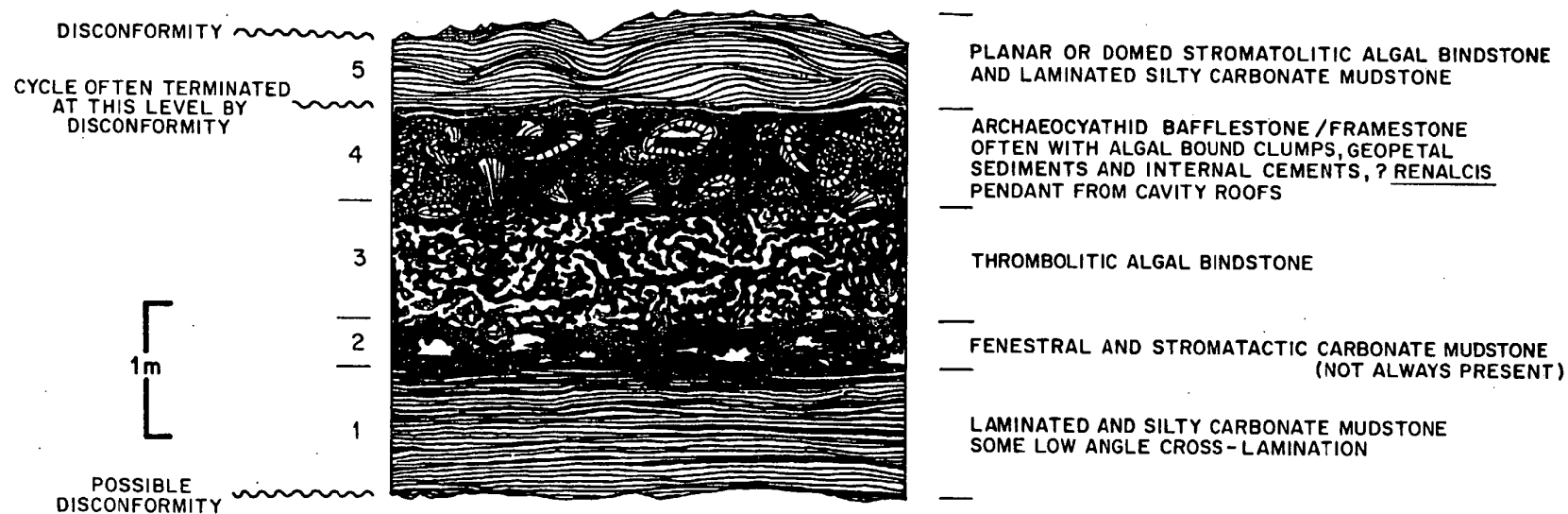


FIGURE 40: IDEALIZED ARCHAEOCYATHID/ALGAL BIOHERM CYCLE.

or wackestone unit. Less commonly, the cycle rests disconformably on clastic channel deposits.

Interpretation

The laminated and silty carbonate mudstone at the base of this cycle generally lacks evidence of desiccation and was probably deposited in a shallow marine environment. Where present, the overlying fenestral and stromatacttic carbonate mudstone is analogous to modern shallow tidal to supratidal fabrics and is probably evidence of shallowing conditions. It may also infer the development of 'mound' facies. Such mounds appear to have been colonized by thrombolitic algae and archaeocyaths, and to be flanked and/or capped by planar or domed stromatolitic algal bindstone and laminated silty carbonate mudstone. Centimetre to decimetre scale cavities within the archaeocyath bafflestone/framestone contain geopetal sediment, a series of internal cements, and algae encrusting the walls and pendant from the roofs. These features are also consistent with the idea that this cycle constituted a bioherm with topographic relief. Similar examples from the Early Cambrian of the Flinders Ranges have also been interpreted as archaeocyath/algal bioherms (Clarke, Gravestock and James, pers. comm., 1985).

The stromatolitic algal bindstone and laminated silty carbonate mudstone which appears to cap the archaeocyath bafflestone/framestone in at least some cycles may represent the overlap of the facies that flanks the adjacent mound. Elsewhere, the cycle appears to terminate with the subaerial exposure of the archaeocyath bafflestone/framestone which gave rise to a complex mixture of vadose and phreatic cements and led to pervasive dolomitization and minor silicification.

6.1.4 Algal bindstone cycle

The algal bindstone cycle (Figure 41) is widespread throughout the Ouldburra carbonates where it averages about 5 m thick. It consists of the following lithofacies in descending order:-

3. laminated and silty carbonate mudstone with sporadic interbeds of stromatolitic algal bindstone and curled algal plates, sporadic small gypsum/anhydrite nodules and other desiccation features, often extensively leached or dolomitized;
2. fenestral and stromatactic carbonate mudstone;
1. thrombolitic algal bindstone.

The top contact of the cycle is generally erosional and the upper lithofacies is overlain by pressure solution textures or clastics. This cycle commonly overlies thin packstone, grainstone or laminated and silty carbonate mudstone lithofacies. The lower contact is sharp and erosional in the first two cases; but may be gradational in the case of the latter lithofacies.

Interpretation

This cycle can be interpreted as resulting from the shoaling-up development of a carbonate mud mound with an algal bindstone cap and flanking packstone, grainstone or laminated carbonate mudstone facies. The presence of desiccation features in the capping lithofacies suggests that the cycle was terminated by exposure. James (pers. comm., 1985) interpreted several very similar examples from Lower Cambrian limestones intersected in the drillhole Minlaton-1 as 'mud mounds'.

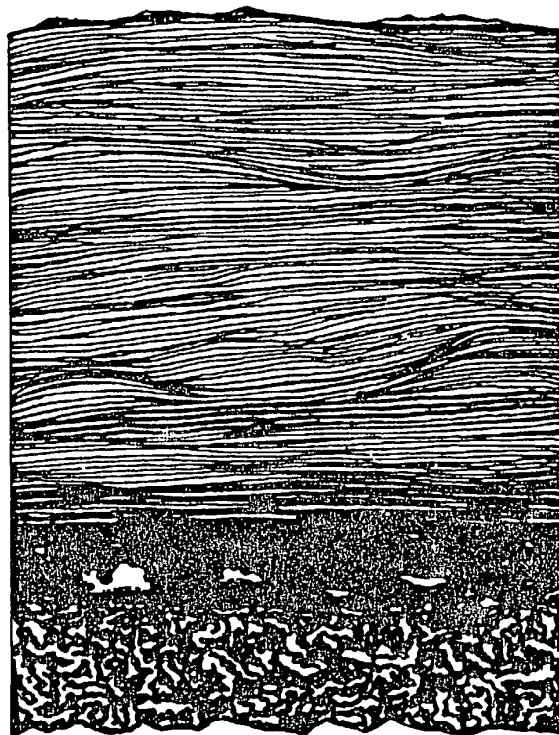
An alternative shallowing-up explanation does not necessarily invoke mounds with topographic relief. The thrombolitic carbonate mudstone is analogous to modern 'intertidal' examples. The desiccated laminated and silty carbonate mudstone and algal bindstone which caps the cycle would have been deposited on regularly emergent carbonate mud and algal flats, analogous to modern high intertidal to supratidal environments.

— EXPOSURE — DISCONFORMITY —

RESULTING IN
DOLOMITIZATION, DEVELOPMENT
OF LEACHED ZONES, GYPSUM /
ANHYDRITE NODULES

3
1m
2
1

— DISCONFORMITY —



LAMINATED CARBONATE MUDSTONE AND
SPORADIC STROMATOLITIC ALGAL BINDSTONE
SOME CURLED ALGAL PLATES
AND DESICCATION FEATURES

FENESTRAL AND STROMATACTIC CARBONATE MUDSTONE

THROMBOLITIC ALGAL BINDSTONE

FIGURE 41: IDEALIZED ALGAL BINDSTONE CYCLE.

Some examples of this cycle terminated with subaerial exposure of sufficient duration to allow the dolomitization and leaching of the capping lithofacies.

6.1.5 Carbonate sabkha cycle

The carbonate sabkha cycle (Figure 42) is widespread in the upper portion of the Ouldburra Formation. It consists of the following lithologies and lithofacies in descending order:-

4. laminated and silty carbonate mudstone, with thin enterolithic layers of evaporites, rare displacive evaporite nodules, mudcracks, dewatering structures and other desiccation features;
3. bedded gypsum/anhydrite, rarely retaining 'chicken-wire' texture, in beds to 0.75 m thick;
2. laminated and silty carbonate mudstone, often with disturbed laminations and thin gradational interbeds of planar laminated stromatolitic algal bindstone, displacive sulphate evaporite nodules;
1. laminated and silty carbonate mudstone with moderately well developed stacked fining-up couplets, ripple cross-lamination, peloids and rare marine fossils.

The overall cycle rarely exceeds 4 m thick and is bounded by sharp contacts; the upper boundary is often a marked transgressive disconformity.

Interpretation

Both Warren and Kendall (pers. comm., 1984) recognized the occurrence of this cycle in the Ouldburra Formation type section. Good examples of both recent and ancient analogues are described by Warren and Kendall (1985). In the scenario favoured by Warren (pers. comm., 1984), the cycle shows the vertical transition from shallow marine

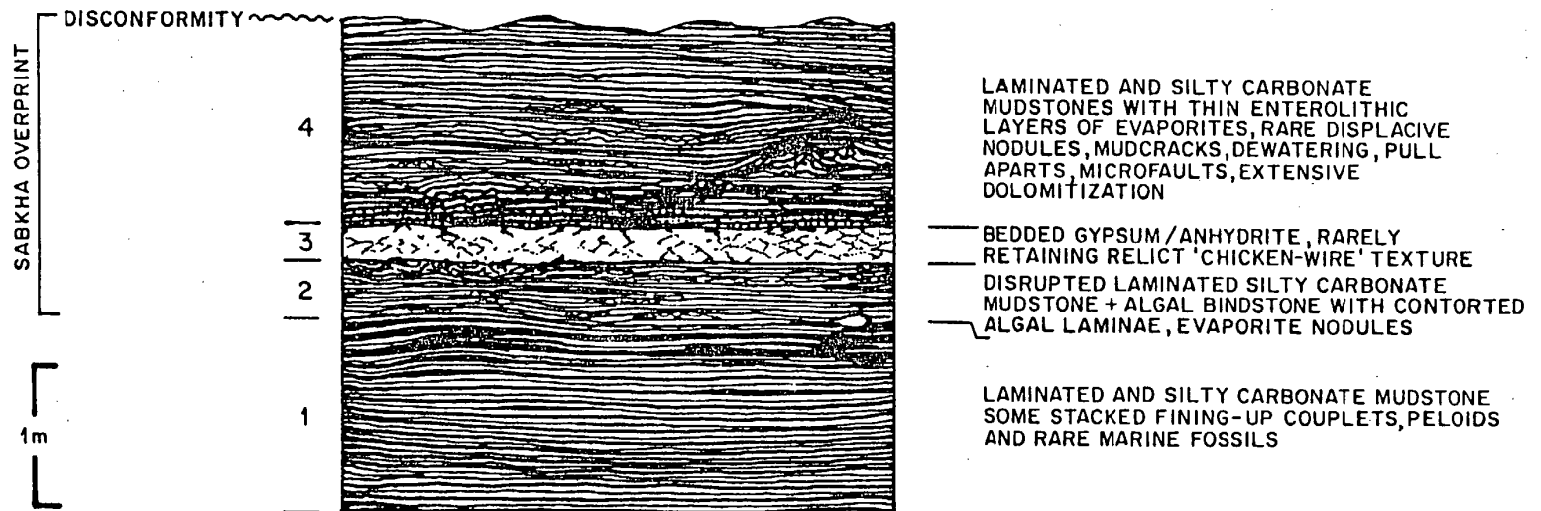


FIGURE 42: IDEALIZED CARBONATE SABKHA CYCLE.

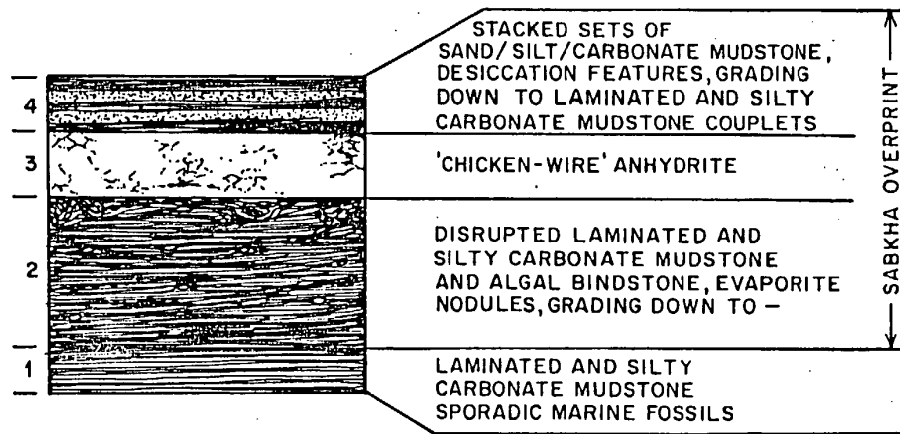
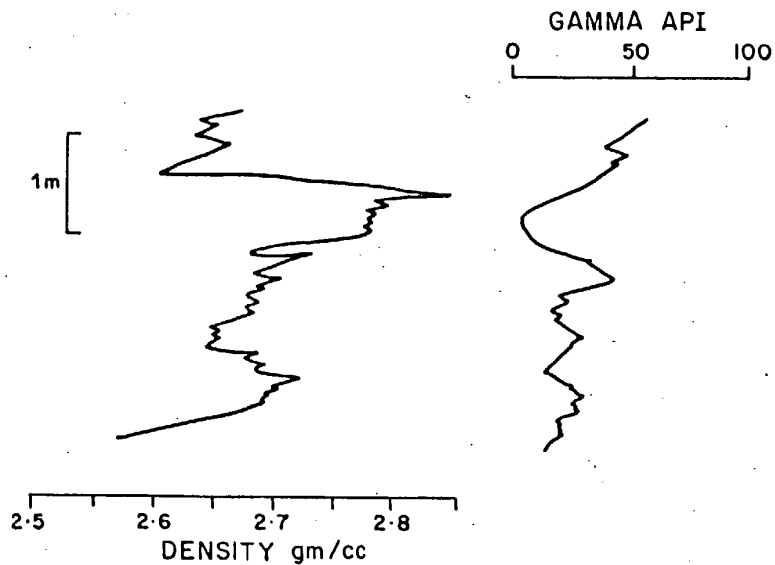
deposition through the sporadically emergent algal flat to an emergent carbonate mud flat. The in situ displacive growth of authigenic evaporites within the upper part of the sediment profile (see Section 3.8.2) produced the sabkha overprint. The overall cycle represents a single shallowing-up event in a carbonate dominated shallow marine to sabkha environment.

6.1.6 Mixed carbonate/siliciclastic sabkha cycle

This cycle (Figure 43) is essentially the same as the previous one with the introduction of a mixed carbonate/siliciclastic lithofacies and a general increase in thickness of the bedded sulphate evaporites. The lithofacies are, in descending order:-

4. sand/silt/mudstone as stacked fining-up sets with mudcracks, dewatering structures and sporadic ripple cross-stratification, in some cases grading down to laminated and silty carbonate mudstone as stacked fining-up couplets;
3. 'chicken-wire' anhydrite with thin discontinuous mudstone stringers, beds to several metres thick;
2. laminated and silty carbonate mudstone, with subordinate stromatolitic algal bindstone, curled algal plates, displacive sulphate evaporite nodules (cauliflower cherts), thin enterolithic evaporite beds, grading to the underlying lithofacies;
1. laminated and silty carbonate mudstone, rare peloids, ooids and bioclastic debris.

This cycle is widespread throughout intersections of the upper Ouldburra Formation. It ranges up to 5 metres thick. The upper contact is sharp and the cycle is commonly overlain by laminated and silty carbonate mudstone or thin collapse breccias.



MANYA-6, 868.60 - 871.75 m

FIGURE 43: TYPICAL MIXED CARBONATE SILICICLASTIC SABKHA CYCLE.

Interpretation

This cycle is interpreted as resulting from a single shallowing-up event on a mixed carbonate/siliciclastic peri-emergent flat and marine sabkha with the growth of bedded sulphate evaporites within the upper sediment profile. The generally thicker development of the 'chicken-wire' anhydrite as compared to the previous cycle could be attributed to a locally thicker capillary zone associated with a greater proportion of clastic sediments in the profile. The thin collapse breccias at the top of some cycles may indicate an ephemeral near-surface crust of evaporites which was removed penecontemporaneously with deposition of marine sediment during the next transgression.

6.2 'Markov Process' Analysis

Markov chain analysis was undertaken to decipher the sedimentation pattern of the Ouldburra Formation. This work utilized a slight modification of the 'Markov process' analysis used by Selley (1970) and Walker (1979). The results were compared using the chi-squared method described by Gingerich (1969). Table 44 shows the data chosen for analysis using these techniques. All major lithofacies and lithologies are incorporated and the depth interval for Manya-6 includes the type section of the Ouldburra Formation with a total of 998 bed to bed transitions. Additionally, where sufficient data is available, a simple chi-squared test was used to compare the observed and predicted frequencies of transitions which constitute individual cycles. This provides a statistical test of the validity of cycles suggested by empirical observation.

The chi-squared test of significance exceeded the limiting value at the 95 percent (or greater) confidence limit in all cases (Table 44). Thus, the null hypothesis that the observed vertical arrangement of lithofacies and lithologies is random can be rejected. The inference that the vertical

Drillhole	Depth interval (m)	Number of lithofacies/ lithologies	Number of transitions	Hypothesis tested	Chi-squared calculated	Chi-squared value confidence level and degrees of freedom
Manya-6	571.4-1284.0 above range of bedded halite	12	635	overall cyclicity	445.5	(0.0005,106)=160.5
Manya-6	1284.0-1685.5	9	363	overall cyclicity	280.9	(0.005,51)=80.7
	range of bedded halite	5	4	validity of the halite	16.8	(0.005,3)=14.1
				mixed siliciclastic/carbonate cycle		
Marla-6	399.8-543.0	6	217	overall cyclicity	56.9	(0.05,24)=36.4
	range of the archaeocyath					
	bafflestone lithofacies	6	8	validity of the	17	(0.05,7)=14.1
				archaeocyath/algal bioherm cycle		

TABLE 44: RESULTS OF 'MARKOV PROCESS' ANALYSIS

arrangement of lithofacies and lithologies form a Markov chain is supported. Individual cycles as determined by empirical observation are supported statistically.

While these techniques demonstrate non-random sedimentation; Carr (1982), Dott (1983), Powers (1984) and Zeller (1964) have pointed out that the interpretation of the results must be treated with a degree of caution. The statistics support the contention, but not necessarily prove, that the sedimentology of the Ouldburra Formation is cyclic.

6.3 Discussion

Examples of shallowing-up shelf cycles are present in clastic, carbonate and evaporitic sequences throughout the geological record and have been well documented in the literature. Mechanisms that could generate such cycles can be divided into autocyclic (intrinsic) and allocyclic (extrinsic). Shinn *et al.* (1969) and Ginsburg (1971) proposed autocyclic mechanisms to explain carbonate sedimentary cycles. However, most examples in the literature (Bulter *et al.*, 1983; Duff *et al.*, 1967; Goldhammer and Elmore, 1984; James, 1979; Kendall and Schlager, 1981; Radke, 1980; Wilson, 1975; Wilson and Pilatzke, 1985) favour allocyclic mechanisms related to eustatic sea-level fluctuations. In proposing their hypothesis of 'Punctuated Aggradational Cycles', Goodwin and Anderson (1980, 1985) described allocyclic shallowing-up sequences as being typically 1-5 m thick and delimited by sharp non-depositional transgressive surfaces. They believed such cycles to be responses to eustatic sea-level changes of a lesser scale than the Sloss-Vail sequences, and as such, to be potentially traceable, basin-wide time-stratigraphic units.

Examples from the Ouldburra Formation are consistent with the criteria for 'Punctuated Aggradational Cycles' and show general

agreement with other documented examples and with the hypothetical allocyclic shallowing-up cycles described by James (1979).

Individual cycles from the Ouldburra Formation cannot be confidently related to eustatic causes (see Section 7.6.1) and may reflect more local passive subsidence. On a broader scale, however, the vertical range of different cycle types does reflect a widespread regression coinciding with the end of carbonate deposition.

CHAPTER 7

SEDIMENTATION MODEL

The deposition of the basal clastics and evaporites of the Ouldburra Formation probably began on marginal-marine siliciclastic sand and mixed carbonate/siliciclastic flats. These contained small isolated halite-salinas in areas of low topographic relief. The overlying shallow marine carbonates are characterised by non-tidal shallowing-up sedimentary cycles through a variety of shallow marine environments which locally included algal-bound carbonate mud mounds and archaeocyath/algal bioherms. The upper portion of the Formation shows the transition to interbedded 'red bed' siltstones and carbonates with subaerially derived sulphate evaporites.

An epeiric sea with a flanking sabkha is proposed as the model of sedimentation for all but the basal portion of the Ouldburra Formation.

7.1 The Epeiric Sea and Flanking Sabkha Model

The global extent of Cambrian to Ordovician epeiric seas and their flanking sabkha facies was noted by Friedman and Radke (1979). This combination of depositional environments has also been proposed in studies by Davidson (1985), Friedman (1985), Lindsay (1985), Lindsay and Kendall (1980) and Radke (1980).

Models of carbonate sedimentation in epeiric seas have been presented by Irwin (1965), Laporte (1969), Mazzullo (1978), and Mazzullo and Friedman (1975). There are no modern epeiric seas. The present 'epeiric' regions are provincial at best and considerable extrapolation of scale is required between epeiric seas of the past and modern analogues (Friedman and Radke, 1979). Examples of ancient and modern marine sabkhat have been well documented in the literature

(Castens-Seidell and Hardie, 1984; Gavish, 1980; Kendall and Skipwith, 1969a,b; Kinsman and Park, 1976; Shinn, 1983b; Warren and Kendall, 1985).

Based on these data, it would be expected that sedimentation in an epeiric sea and on its flanking sabkha would be characterized by the following:-

- i) an epicontinental marine to paralic setting, of appropriate dimensions;
- ii) widespread non-tidal shallow marine conditions;
- iii) prevalence of storm generated deposits;
- iv) hypersaline marine conditions which would result in;
 - a) preservation of cryptalgal mats;
 - b) paucity and reduced diversity of marine fauna;
 - c) widespread deposition of subaerial evaporites as a sabkha overprint to peri-emergent shallow marine deposits;
- v) repeated widespread emergence and inundation, as evidenced by;
 - a) thin (<5 m) - shallowing-up cycles in a range of contemporaneous marine and paralic environments;
 - b) laterally extensive pervasive subaerial exposure surfaces;
- vi) sabkha-type dolomitization, either by seepage/brine reflux or evaporitive pumping.

These points are discussed with respect to the Ouldburra Formation in the following sections.

7.2 Palaeosetting

The known distribution of the Ouldburra Formation is consistent with the Australo-Antarctic palaeogeographic model of Cook (1982) who

postulated a large, shallow epicontinental sea at low palaeolatitudes during the Early Cambrian. Local palaeogeography indicates moderate relief associated with the Gawler Craton and Musgrave Block, and delimits the lateral extent of carbonate, clastic and evaporite facies in the Ouldburra Formation.

7.2.1 Australo-Antarctic palaeogeography

Gondwanaland probably rotated from high paleolatitude (50°N in central Australia) to low latitude (20°N) during the late Precambrian and earliest Cambrian, bringing the Australo-Antarctic region into a north-south orientation straddling the equator (Embleton, 1973; Veevers, 1976). The Ouldburra Formation would have been deposited at a palaeolatitude of 0-15°N (Figure 46).

If global climatic patterns in the Early Cambrian were similar to those of the present; low palaeolatitudes and a low relief epicontinental setting would suggest tropical and possibly arid conditions.

Cook (1982) and Veevers (1976) proposed an Early Cambrian palaeogeography (Figure 45) including an epeiric sea which extended from northern central Australia, through the Flinders Ranges, into Antarctica. The area to the west was believed to be a continental landmass. Open marine deep water conditions prevailed almost 1,000 km to the east. Carbonate deposition dominated the sedimentation over a large proportion of the epeiric sea. Early Cambrian shallow marine faunas, including trilobites and archaeocyaths have been recognized in a zone extending through the present trans-Antarctic Mountains and the Flinders Ranges, into the northeastern Officer Basin. Archaeocyath/algal bioherms were developed in the Marla-Manya area and the Bunkers Graben in the Flinders Ranges.

KEY TO FIGURE 45

1. Ouldburra Formation, Marla-Manya area, northeastern Officer Basin. Early Cambrian carbonates, mixed carbonate/siliciclastics, evaporites including halite. Shallow marine fauna with archaeocyath bioherms.
2. The Cootanoorina Formation, the Andamooka Limestone and other un-named sub-Arckaringa Basin outliers are possible ?Cambrian marine carbonates.
3. Wilkawillina Limestone and its equivalents in the Flinders Ranges. Early Cambrian carbonates. Shallow marine fauna with archaeocyath bioherms. Overlain by Billy Creek Formation 'red beds'.
4. Early Cambrian carbonates on Yorke Peninsula. Shallow marine fauna including trilobites.
5. Rare protolenids and archaeocyaths in sediments in Heathcote Greenstone.
6. Possible Early Cambrian sediments in Molar Formation, Bowers Mountains.
7. Possible Early Cambrian dolomites and clastics in Smithton Basin and Dundas Trough.
8. Shackleton Formation subtidal to supratidal Early Cambrian carbonates. Archaeocyaths.
9. Un-named ?Early Cambrian archaeocyath limestone, clastics and volcanics. Ellsworth Mountains.
10. Possible un-named archaeocyath limestone, clastics. Vicinity of Argentina Range.
11. Bukalara Sandstone, Daly River Basin. Possible Early Cambrian age inferred from microfossils.
12. Buckingham Bay Sandstone, Arafura Basin. Possible Early Cambrian age suggested by trace fossils.

(data from Moore, 1982; and Shergold et al., 1985).

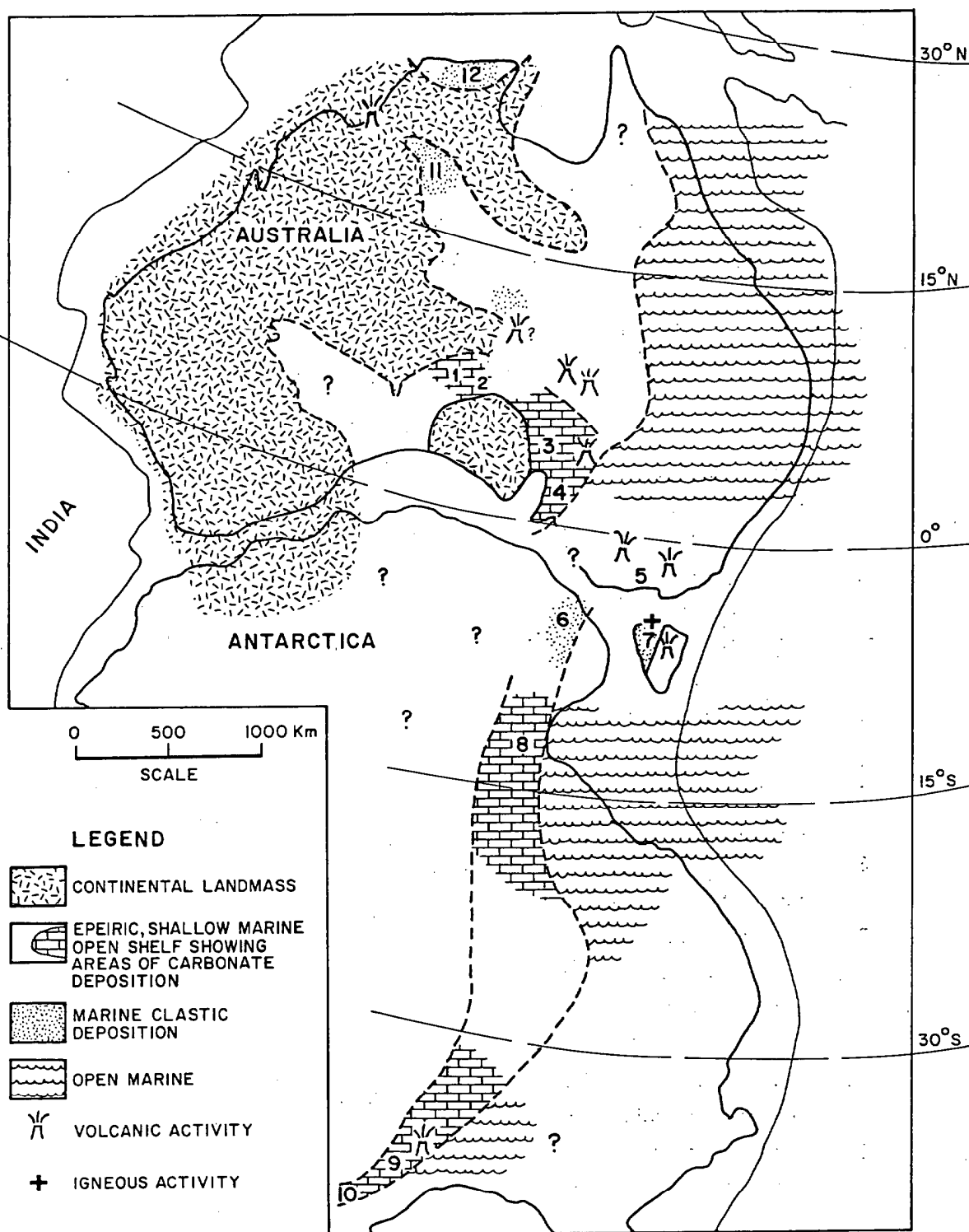


FIGURE 45: EARLY CAMBRIAN AUSTRALO-ANTARCTIC PALAEOGEOGRAPHY.

(Based on Cook, 1982; Veevers, 1976; and Shergold *et al.*, 1985).

7.2.2 Local palaeogeography

An interpretation of the Early Cambrian palaeogeography of the northeastern Officer Basin is presented in Figure 46. The emergent Musgrave Uplands to the north and the Gawler Lowlands to the southeast were separated by at least 200 km, presumably most of the low relief area between would have been inundated by the marine transgression. Islands were probably present in the Ammaroodinna area and to the southeast of the Manya area. These emergent areas would have been locally significant as a source of terrigenous clastic sediments shed as alluvial fans. Further south of the Manya area, a very shallow clastic-dominated shelf approximately 100 km wide flanked the Gawler Lowlands.

During the regression of the sea (mid to Upper Ouldburra Formation), a marginal marine sabkha extended across the areas of topographic relief. The development of the sabkha facies would have been diachronous prograding into the seaway from the north and south. The sabkha was carbonate-dominated closer to the coast and graded to a 'red-bed' mixed carbonate/siliciclastic sabkha further inland. Apart from the moderate to high relief associated with the exposed Precambrian uplands; the sabkha was probably very flat with little or no appreciable change in slope into the epeiric sea. Fluvial clastic sediments would have spread cross the sabkha in sheet-floods or very wide, high sinuosity channels.

The epeiric sea probably had a very small degree of depositional slope. Assuming no relative syndepositional uplift, a bottom slope of one degree will account for the difference in thicknesses of the Ouldburra Formation intersected in the drillholes Manya-6 and Marla-3, which are approximately 45 km apart.

7.3 Non-tidal sedimentation

Very little is known about the effect or periodicity of lunar tidal influences in Cambrian epeiric seas (Carey, 1976; Lamar and Merifield,

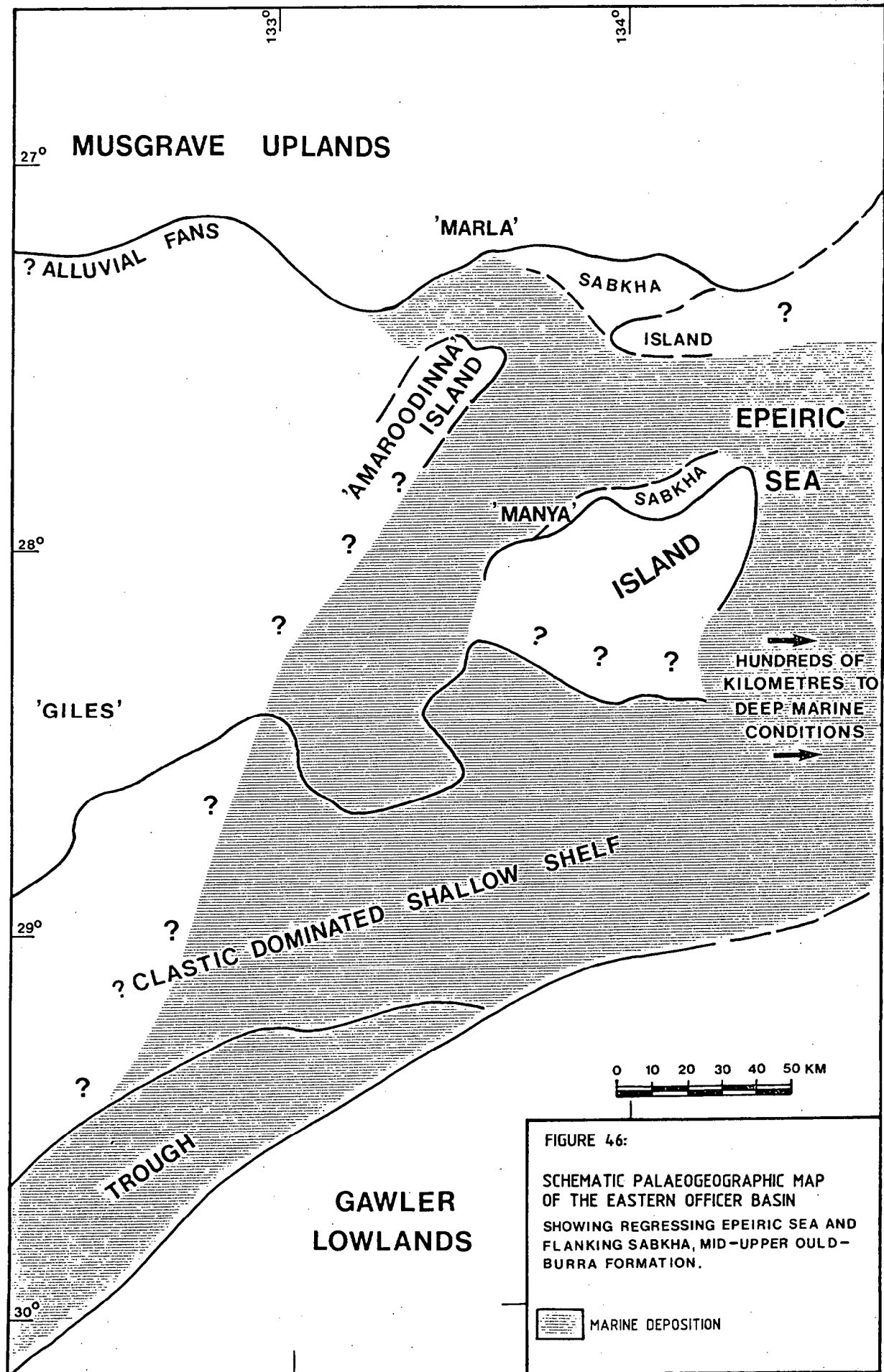


FIGURE 46:

SCHEMATIC PALAEOGEOGRAPHIC MAP OF THE EASTERN OFFICER BASIN SHOWING REGRESSING EPEIRIC SEA AND FLANKING SABKHA, MID-UPPER OULD-BURRA FORMATION.

MARINE DEPOSITION

1976; Munk and MacDonald, 1960). In contrast with modern shallow marine environments which are dominated by tidal sedimentation, epeiric seas appear to be characterized by non-tidal shoaling sedimentation (Kennard, 1981; Mazzullo, 1978). The paucity of tidal features, eg. bimodal or herringbone cross-stratification, in a very shallow marine sequence has been used, in conjunction with other evidence, to infer deposition in an epeiric sea (Kennard, 1981; Radke, 1980).

Bimodal current features are very rare in the Ouldburra Formation. Centimetre scale examples occur in association with ripple cross-laminae and small festoon cross-beds in the clastic-dominated base of the Formation intersected in drillholes Manya-6 and Marla-3. Absence of bimodal current features from elsewhere in the Formation may suggest non-tidal sedimentation.

7.4 Storm Deposits

In modern analogues to epeiric seas, the dominant source of energy in the peri-emergent zones is storm generated. This results in the highest rates of sediment accumulation locally (Kumar and Sanders, 1976; Sepkoski, 1982).

The Ouldburra Formation contains two prominent and widespread lithofacies which are interpreted as storm deposits. These are fining-upward laminated and silty carbonate mudstone couplets and plate breccias.

7.5 Hypersalinity

Where there is no appreciable influx of rain or river water to the shoreward part of an epeiric sea, heating and evaporation of essentially stagnant sea water will result in the development of hypersalinity (Irwin, 1965; Tucker, 1976). Increased salinity is indicated by a reduced diversity in fauna; abundance and widespread preservation of algal mats and the

presence of widespread marginal-marine evaporite deposits (Kennard, 1981).

7.5.1 Preservation of cryptalgal mats

The proliferation of algae and/or cyanobacteria and the preservation of resultant cryptalgal fabrics have an antipathetic relationship to the activities of grazing organisms. Conditions of elevated salinity enable the algae to grow in the absence of less-halophilic first order heterotrophic organisms, (Curtis et al., 1963; Garret, 1970; Kendall and Skipwith, 1968). Cryptalgal textures are commonly preserved in the Ouldburra Formation. They lack inbound fauna, and are often intimately associated with evaporites.

7.5.2 Paucity and reduced diversity of marine fauna

The Ouldburra Formation has a paucity and reduced diversity of marine fauna in comparison with the biostratigraphically equivalent Early Cambrian marine carbonates from the Flinders Ranges. Decreased faunal diversity has been attributed to the adverse conditons of hypersalinity (Logan, 1961; and Kendall and Skipwith, 1968,9a). Radke (1980) suggested that the apparent order of increasing salinity tolerance is:- echinoderms, sponges, archaeocyaths, gastropods, trilobites, brachiopods, infaunal suspension feeders, ostracods and blue green algae. Of these; echinoderms, gastropods and brachiopods have not been recorded from the Ouldburra Formation.

7.5.3 Widespread evaporite deposition

The upper Ouldburra Formation contains ubiquitous sulphate evaporites either as isolated crystals, nodules or displacive beds. Cauliflower cherts and solution collapse are also evidence of former evaporites. This widespread deposition of sulphate evaporites indicates that sea water had been concentrated at least to the point of gypsum

precipitation (ie. 5 times the concentration of modern seawater).

Such concentrations are approached in modern impounded bodies of marine water, and would theoretically, be expected in epeiric seas. Irwin (1965) reasoned that evaporite precipitation would occur where low order slopes, great width of shelves, and shallow depth of water are sufficient to restrict or eliminate circulation.

The point of gypsum precipitation is also commonly reached by the interstitial pore fluids in modern marine sabkha sediments. These brines range up to 10 times as concentrated as the seawater from which they were derived (Kinsman, 1969). Thus, the combination of both epeiric marine conditions and a flanking sabkha provide an ideal environment to produce widespread sulphate evaporites, as seen in the upper Ouldburra Formation.

7.6 Emergence and Inundation

Regional emergence from an epeiric sea may result from shallowing due to shoaling-up sedimentation, or water removal by evaporation and/or migration before strong prevailing winds. Obviously, the duration of emergence will influence the characteristics of the stratigraphic discontinuity produced, whether just desiccation, dolomitization, sabkha overprint, induration, solution, erosion or any combination of these (Friedman and Radke, 1979).

The Ouldburra Formation shows repeated and widespread evidence of 1-5 m thick shallowing-up cycles which often terminate with emergence. There are also more-pervasive subaerial exposure events which may be correlated over tens of kilometres.

7.6.1 Correlation of shallowing-up cycles and transgressive 'kick-backs'

According to the theoretical model of Irwin (1969), the regression of an epeiric sea is usually sufficiently slow to enable the formation of a

regular succession of sediment types (the shallowing-up cycle). Such a cycle would be analogous to the 'Punctuated Aggradational Cycle' of Goodwin and Anderson (1980, 1985) and would be a potentially traceable diachronous event through a series of lateral facies equivalents across the basin.

In contrast, transgression in an epeiric sea/sabkha setting is rapid and often results in an abrupt change from emergent to shallow marine. Irwin (1965) referred to such an abrupt transgression as a 'kick-back' and suggested that such events could be traced over considerable distances. Minor fluctuations between transgressive and regressive sequences should also be able to be correlated locally.

These minor fluctuations are brought about by local changes in the rate of subsidence or emergence relative the rate of deposition; when the rate of subsidence is greater than the rate of deposition, transgressive sequences result, and when the rate of subsidence is less than the rate of deposition, regressive successions form. Care must be taken to differentiate between local variations, which may be the result of this process, and regional 'kick-backs' brought about by regional transgressions and regressions (Irwin, 1965).

Unfortunately, the paucity and widespread distribution of drillhole intersections of the Ouldburra Formation preclude detailed correlation of the numerous shallowing-up cycles and small scale transgressions. However, there are several regional events which appear to correlate between drillholes Marla-6, Marla-7, Manya-6 and possibly to Manya-3 (Figure 48), a total distance of over 60 km. Each event is associated with widespread shallowing-up followed by a transgressive 'kickback'.

The shallowing-up sedimentation produced varying degrees of sabkha overprint culminating in pervasive subaerial exposure (see following section) and/or the deposition of non-marine 'red-bed' siltstones. The

progradation of the 'red-beds' is evident in core from drillholes Marla-7 and Manya-6, but not in Manya-3 or Marla-6 (horizon 1 on Figure 47). This is consistent with the closer proximity of the former two holes to an emergent land mass as suggested by the palaeogeography.

The transgression which followed resulted in a rapid, and widespread return to marine carbonate deposition. Thin ooid grainstones interbedded with shallower-water facies were intersected in Marla-6. These probably indicate nearby higher energy conditions. The carbonates which constitute the transgressive unit in Manya-6 have been altered by pressure solution but contain fragmentary shallow marine fossils. Marla-7 shows the least marked transition. Typical low energy peri-emergent marine carbonates with a desiccation overprint overlie the 'red bed' siltstones.

A second and similar regression/transgression event can also be correlated between drillholes Marla-7 and Manya-6 (horizon 2 on Figure 47). The regression again led to the deposition of 'red bed' siltstones which are overlain by shallow marine carbonates.

The final and most obvious regression marks the end of carbonate deposition as the sabkha prograded basinwards to deposit the Observatory Hill Formation 'red beds'.

7.6.2 Correlation of pervasive subaerial exposure surfaces

The Ouldburra Formation contains evidence of subaerial exposure varying in both intensity of diagenesis and the time of formation.


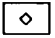
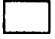


Local subaerial exposure associated with shallowing-up sedimentation produced vadose cementation, and concretionary pisoids, dolomitization and leaching of the exposed carbonates. More pervasive examples are characterized by incipient silicification and dolomitization followed by minor dedolomitization. This resulted in the formation of metre scale laminated and bleached caliche-like carbonate zones underlain by zones of secondary porosity. These intraformational

OBSERVATORY
HILL FORMATION 'red beds' 571
OULDBURRA FM.

MANYA-6

MARLA-7

KEY

-  NON MARINE 'RED BED' SILTSTONE
-  SEDIMENTARY BRECCIA
-  MARINE CARBONATES
-  TRANSGRESSIVE 'KICKBACK'
-  REGRESSION

SCALE

5 km

0

10

20

30

40

50

DEPTH
(m)

HORIZON-2

>> FINAL REGRESSION >>
NUMEROUS LOCAL
SHALLOWING-UP EVENTS
AND MINOR TRANSGRESSIONS
AND REGRESSIONS

193

MAJOR
REGRESSION

? top Cl. 3 (620 m)

NUMEROUS
LOCAL
SHALLOWING-UP
EVENTS

MANYA-3

TOP OF OULDBURRA
FORMATION ERODED BY
PERMO-CARBONIFEROUS
GLACIALS

174

PERVASIVE
SUBAERIAL
EXPOSURE

*lam carbonate mudstone
oid granitic brecciated
radiolaria thrombolite bone striae*

Net to scale

Actually

368-376m

Probably correct subaerial zone (Horizon 1)

is @ 699m

*lobonitised
cryptalgal lum
lst*

843

HORIZON-1

849-865

*lobonitised
carbonate mudstone*

469

467-473

MARLA-6

256

*cryptalgal lum lst
oolite*

PERVASIVE
SUBAERIAL
EXPOSURE
363-368

FIGURE 47 : DRILLHOLE CORRELATION DIAGRAM SHOWING MAJOR TRANSGRESSIONS AND REGRESSIONS (upper Ouldburra Formation only shown).

examples were the product of eogenesis and early telogenesis and formed as marine carbonates underwent sabkha diagenesis in conjunction with subaerial exposure.

The transition from the Ouldburra Formation to the overlying Observatory Hill Formation was also associated with subaerial exposure and erosion of the Ouldburra carbonates, at least locally. The contact of the two formations intersected in drillhole Marla-6 is a 6 m thick breccia (rudstone) which disconformably overlies Ouldburra carbonates. The clasts within the breccia have dedolomitization textures and rarely show non-fabric selective silicification.

During the Permian, late telogenesis resulted in the exposure and erosion of the Ouldburra Formation to the east of the Marla-Manya area. This exposure was probably associated with glaciation and produced only minor dolomitization, but pervasive silicification resulted in the formation of characteristic chert concretions, discrete thin chert beds and zones of incipient silicification.

Apart from work by Chafetz (1972) and Jaanusson (1961), examples of subaerial exposure surfaces older than Silurian are not well documented in the literature. Esteban and Klappa (1983) suggest that pre-Silurian karst and caliche facies which formed without the influence of higher plants had different features to younger examples. The intraformational examples from the Ouldburra Formation bear some similarities to subaerial exposure surfaces described by Chafetz (1972), Harrison and Steinen (1978), Nagtegaal (1969) and Walls et al. (1975). The Ouldburra examples warrant further study, since the more pervasive examples, at least, appear to be excellent marker horizons for correlation between drillholes.

The most intense diagenesis attributable to intraformational subaerial exposure is associated with a regional regression. As discussed in

the previous section, subaerially exposed carbonates and an overlying 'red bed' siltstone unit can be correlated over the 17 km from the Manya-6 type section to the drillhole Marla-7 (horizon 1 on Figure 47). The same event may be represented by an unusual intraformational breccia intersected in drillhole Marla-6. Carbonates with typical caliche-type lamination are overlain by a highly altered pale brown carbonate floatstone which contains angular clasts of bleached chert (see Figure 20a). This event also appears to be represented by a strong reflector on seismic sections and can be traced as an approximate time line within the Ouldburra Formation throughout most of the Marla-Manya area.

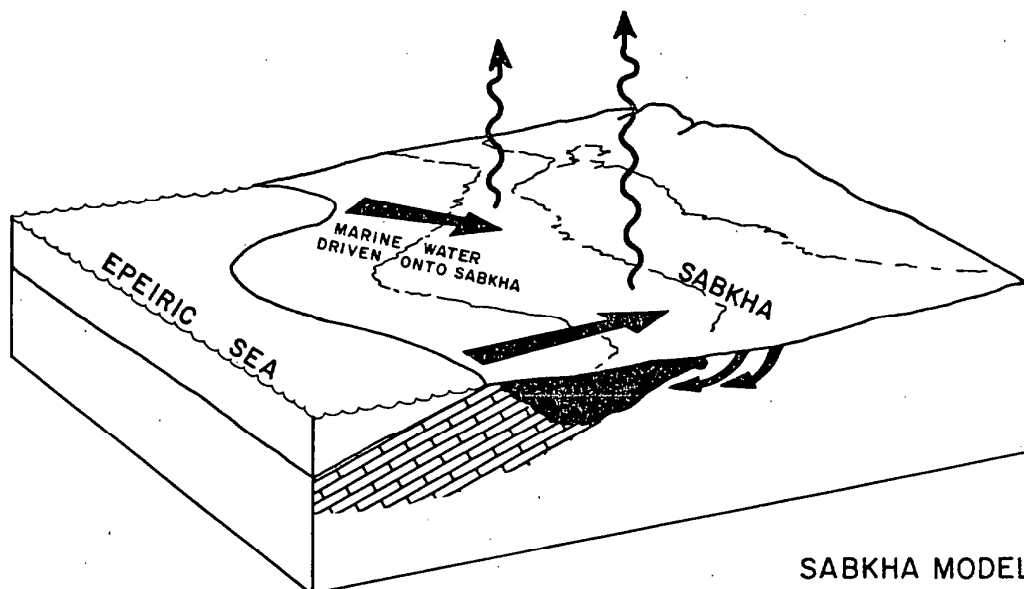
The combination of widespread subaerial exposure, sabkha overprint and non-marine 'red bed' siltstones in a predominantly shallow marine carbonate sequence records the rapid regression and transgression of a shallow sea flanked by an emergent sabkha.

7.7 Sabkha Dolomitization Models

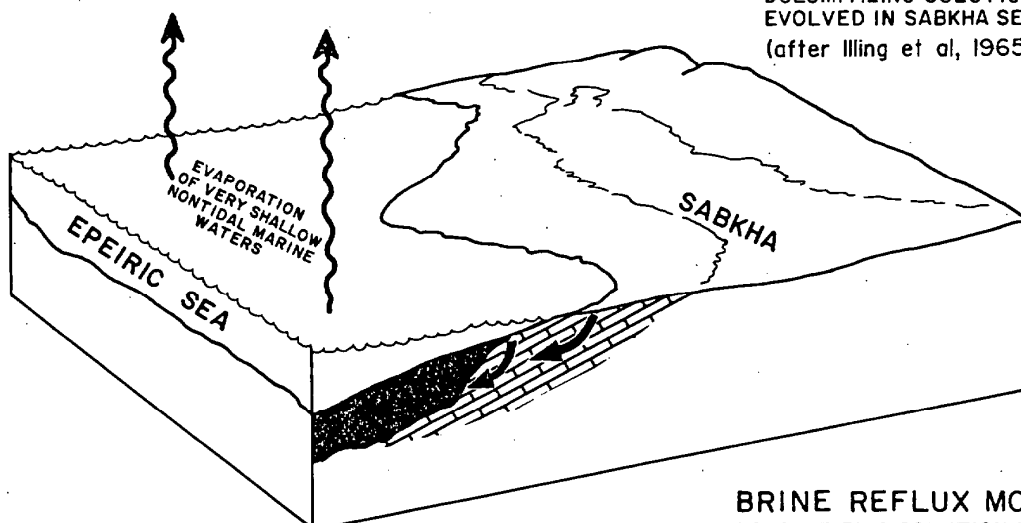
'Primary' dolomite (sensu Zenger et al., 1980) has not been recognized in the Ouldburra Formation. Although, finely laminated or thinly bedded aphanitic dolostones, such as occur in the Ouldburra carbonate facies, may be interpreted as the result of penecontemporaneous or syngenetic dolomitization (Friedman and Sanders, 1967). Other evidence of early dolomitization is the repeated intercalations of metre scale stratiform replacement dolostone and calcareous marine carbonate, and the presence of lithic clasts of dolostone in lithofacies with an unaltered calcareous matrix.

In contrast, the presence of late stage saddle dolomite and the widespread occurrence of reactate dolomite in pressure solution textures suggests deep burial late diagenetic dolomitization.

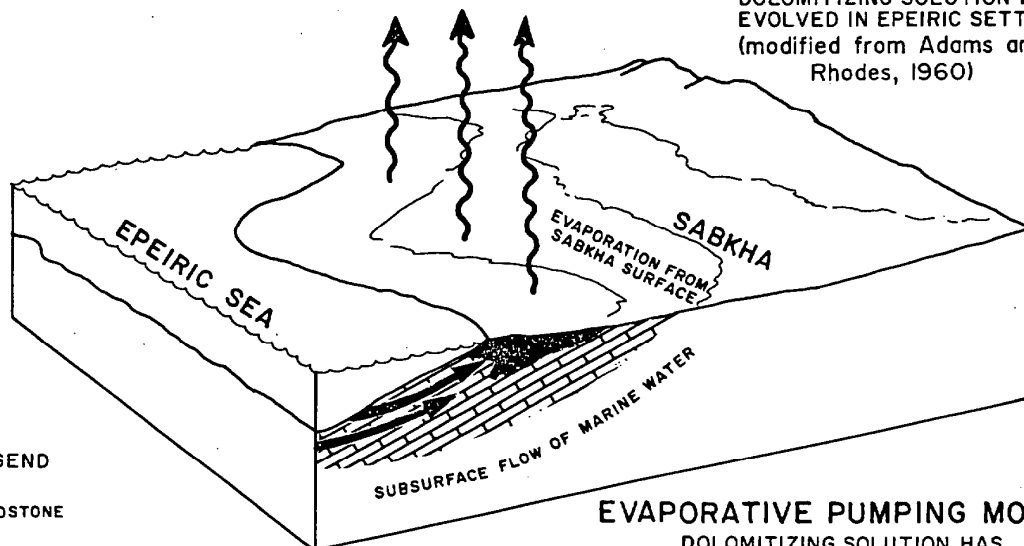
The following discussion outlines the applicability of various models of dolomitization to explain the occurrences of dolostone in the Ouldburra



SABKHA MODEL
DOLOMITIZING SOLUTION HAS
EVOLVED IN SABKHA SETTING
(after Illing et al, 1965)

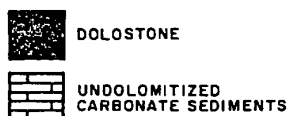


BRINE REFLUX MODEL
DOLOMITIZING SOLUTION HAS
EVOLVED IN EPEIRIC SETTING
(modified from Adams and
Rhodes, 1960)



EVAPORATIVE PUMPING MODEL
DOLOMITIZING SOLUTION HAS
EVOLVED IN EPEIRIC SETTING
(Hsu and Schneider, 1973)

LEGEND



**FIGURE 48: SCHEMATIC DIAGRAMS SHOWING VARIOUS MODELS
OF DOLOMITIZATION (NOT TO SCALE).**

Formation. Each of these models have their proponents in the literature (Longman, 1982; Zenger *et al.*, 1980). Evidence for the sabkha-type models based on either brine reflux or evaporative pumping would support the overall concept of an epeiric sea and flanking sabkha.

The presence of abundant primary evaporites throughout most intersections of the Ouldburra Formation indicates that those portions of the sequence have not been flushed by fresh water, at least to shallow burial depths. This precludes the mixing-zone and Coorong dolomites as possible models of dolomitization (Warren, pers. comm., 1985). The remaining models; sabkha, brine reflux and deep burial dolomitization (Figure 48); suggest different scenarios for the source of the Mg-rich solutions. In the sabkha model (Illing *et al.*, 1965) the dolomitizing solutions are initially produced from seawater driven up onto the sabkha flat during storms. Evaporation concentrates the water to the point where aragonite and then gypsum are precipitated. The Ca thus removed; the dense Mg-rich solution becomes heavier than the pore-water surrounding it. It seeps downward and seaward through the previously deposited sabkha carbonates, causing their dolomitization (Longman, 1982).

The brine reflux model uses a very similar mechanism but involves a restricted lagoon behind some sort of physical barrier to the free inflow of marine waters. The reflux dolomite forms as the hypersaline Mg-rich lagoonal brine becomes heavy enough to displace the connate water and seeps downward and seaward, again dolomitizing the carbonate sediments. Unlike the sabkha model which explains thin supratidal dolostones, the brine reflux model is used to explain thick, laterally extensive, ancient dolostones when they are associated with shelf evaporites (Warren, pers. comm., 1984). Although this model, as originally proposed by Adams and Rhodes (1960), uses impounded lagoonal waters, it may be applied equally well to the epeiric sea/sabkha model, as shown in Figure 48.

The evaporative pumping model of dolomitization (Hsu and Schneider, 1973) involves a hydrological model almost the reverse of seepage reflux. A continuous subsurface flow of marine water replaces groundwater lost by evaporation from the sabkha surface and dolomitizes the sabkha carbonate sediments.

Finally, in the case of burial stage dolomitization (Mattes and Mountjoy, 1980), hot organic and Mg-rich solutions are derived from clay mineral transformations associated with the dewatering of shales deeper in the basin. Saddle dolomite is taken to be an indicator of burial stage dolomitization, and its widespread occurrence in the Ouldburra Formation carbonates probably reflects later phases of dolomitization. Thus, its presence does not necessarily preclude an original sabkha-type model of dolomitization.

This is supported by the recent work of Machel and Mountjoy (1986) which suggests that massive dolostones associated with shallowing-up cycles and capped by regional unconformities result from either of two possibilities:-

- i) small quantities of dolomite (cement or replacement) are formed during exposure and act as nuclei for later, and more extensive subsurface dolomitization
- ii) large-scale dolomitization may take place in shallow subtidal environments of moderate to strong hypersalinity.

The dolomitization of original carbonate mudstone fabrics is a consistent feature of shallowing-up sabkha cycles from the upper most portion of the Ouldburra Formation. The pale brown aphanitic to finely recrystalline dolostones up to 4 m thick could be equally well explained using the seepage reflux, evaporative pumping or Machel and Mountjoy (1986) models.

CHAPTER 8

HISTORY OF SEDIMENTATION

Deposition of the Ouldburra Formation began as part of a widespread marine transgression which inundated the area between the Gawler Craton and the Musgrave Block. In the Marla area, the marginal marine Relief Sandstone was overlain directly by Early Cambrian shallow marine carbonates.

To the south, deposition of the Ouldburra Formation began in small isolated halite-salinars (Figure 50c). These were developed in shallow depressions on peri-emergent siliciclastic sand flats. Impounded marine-derived water was evaporated to produce metre thick beds of bottom nucleated halite. Isolated halite hoppers and rare sulphate evaporites grew displacively within the sediment profile surrounding the salinas. Sedimentation appears to have been cyclic with repeated sand flat/salina alternations. As deposition continued a submergent to sporadically emergent mixed carbonate and siliciclastic mudflat developed. Shallowing-up sedimentation produced repeated cycles of mixed carbonates/siliciclastics, clastics and evaporites which show the transition from submergent shallow marine to salina.

The cessation of halite precipitation was followed by the widespread deposition of shallow marine carbonates throughout the Marla-Manya area (Figure 50b). This marked the onset of epeiric sedimentation during the ?Botoman Stage of the Cambrian. Archaeocyath/algal bioherms, stromatolitic and thrombolitic algal/mud mounds and thin ooid shoals were developed offshore. Trilobites, sponges and other shallow marine fauna were present, but not abundant. A very low angle of depositional slope resulted in a broad low energy, very shallow marine zone near shore. Sedimentation in this area was probably non-tidal, and deposition in both

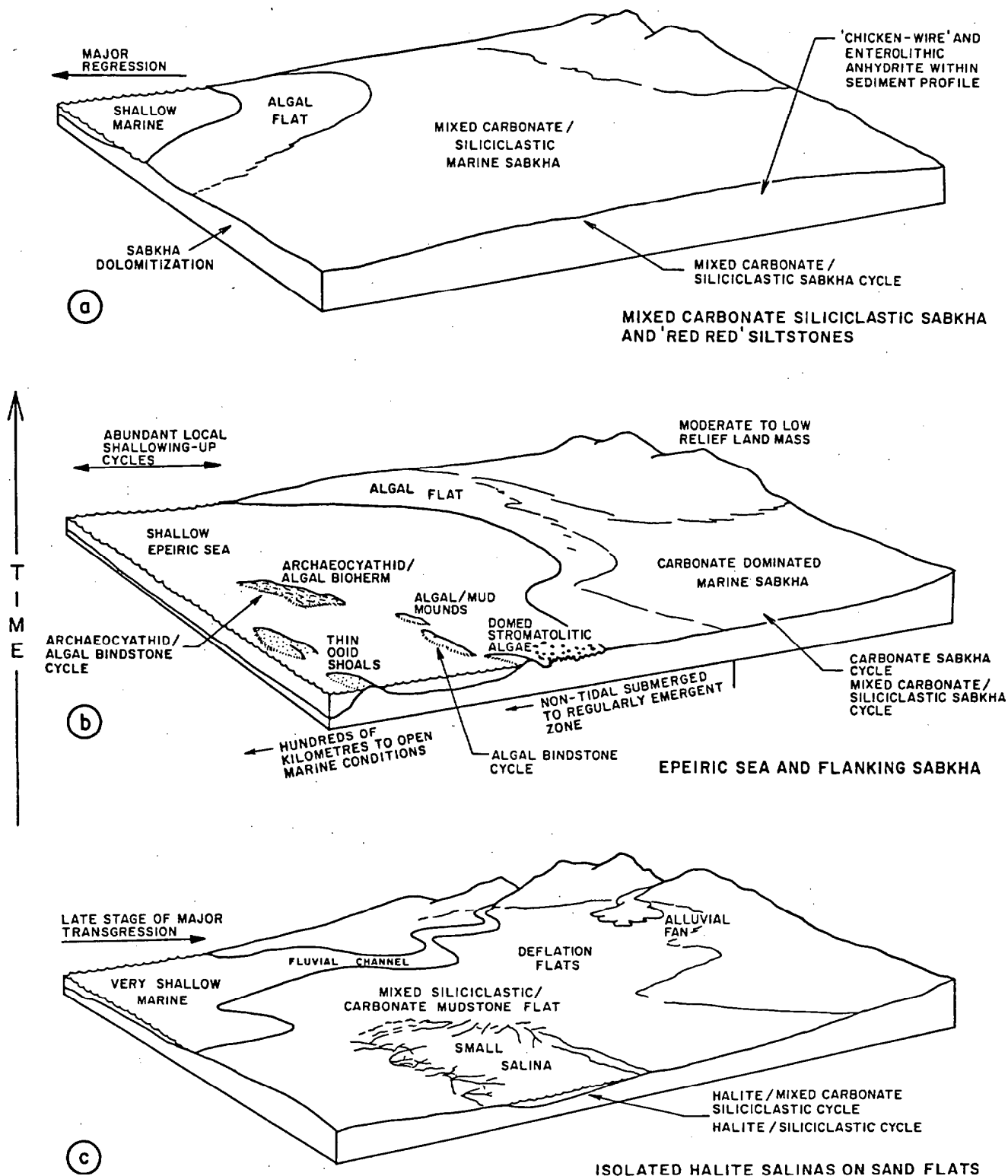


FIGURE 49: REGIONAL SEDIMENTATION MODEL OF THE OULDBURRA FORMATION, (NOT TO SCALE).

shallow submergent and regularly emergent areas was dominated by storm deposited fining-up siltstone/carbonate mudstone couplets. Algal flats were widespread in this zone in the absence of grazing fauna. Small scale regressions related to local differences in the rate of sedimentation relative to subsidence resulted in a desiccation overprint with the formation of plate breccias, mudcracks, dewatering structures and small sulphate evaporite nodules. The bioherms and mounds also show some evidence of having developed during shallowing-up conditions, commonly terminating with subaerial exposure.

As deposition continued, a marine sabkha developed in areas of greatest topographic relief flanking the Musgrave Uplands, the Gawler Lowlands and several islands in the Marla-Manya area (Figure 50a). The sabkha was initially carbonate dominated. Regional shallowing-up events produced a number of sabkha cycles showing the transition from shallow marine sedimentation to the development of sulphate evaporite nodules and enterolithic and 'chicken-wire' anhydrite within the emergent sediment profile. Sabkha dolomitization, by either seepage reflux of sabkha derived brines or evaporative pumping of evolved marine water, produced stratiform dolostones up to 4m thick.

As the large scale regression of the epeiric sea began, presumably in the late Early Cambrian, the sabkha prograded basinwards from both the north and south. The sabkha sedimentation included an increasing clastic component in the form of stacked sand/silt/carbonate mudstone sets and 'red bed' gypsiferous siltstones. Laterally extensive pervasive subaerial exposure resulted in dolomitization followed by limited dedolomitization to produce zones of chalky bleached carbonate. This was accompanied by incipient silicification and the development of significant secondary porosity in the underlying carbonates. In some areas within the Marla-Manya region, the Ouldburra Formation carbonates were exposed and

eroded prior to the deposition of the overlying Observatory Hill Formation. Elsewhere, the 'red bed' siltstones of the Observatory Hill Formation interdigitate with Ouldburra Formation.

ACKNOWLEDGEMENTS

The author gratefully acknowledges the support of Comalco Aluminium Limited. The typing and drafting of the many versions of this thesis were undertaken by the staff of Comalco Exploration's Adelaide Office. My colleagues in both Adelaide and Brisbane have also provided useful discussions. Computer drafting of the detailed sedimentological logs used modified AUSLOG software from Technical Computer Systems.

The inchoation of this study owes much to the inspiration of Drs. Chris Kendall, Bob Sneider and John Warren who briefly consulted with Comalco during 1984 and 1985.

Jonathan Clarke, Colin Gatehouse, Drs. David Gravestock, Jim Jago and Wolfgang Preiss have assisted with identification of fossils.

This thesis also owes a great deal to the enthusiasm and helpful criticism of my supervisor Dr. Victor Gostin.

REFERENCES

- Adams, J.E.; and Rhodes, M.L. (1960) Dolomitization by seepage refluxion. American Association of Petroleum Geologists Bulletin 44, 1912-1920.
- Ahr, W.M. (1971) Palaeoenvironments, algal structures, and fossil algae in the Upper Cambrian of Central Texas. Journal of Sedimentary Petrology 41 (1), 205-216.
- Aitken, J.D. (1967) Classification and environmental significance of cryptalgal limestones and dolomites, with illustrations from Cambrian and Ordovician of Southwestern Alberta. Journal of Sedimentary Petrology 37 (4), 1163-1178.
- Allchurch, P.D.; Wopfner, H. (1973) Cootanoorina No 1 well. Well completion report. South Australian Department of Mines Report of Investigations 40.
- Ambrose, G.J.; and Flint, R.B. (1981) Billa Kalina, South Australia. Explanatory Notes. 1:250 000 Geological Series Sheet SH/53-7. Geological Survey South Australia.
- Anon, Continental Oil Company of Aust. Ltd (1969) Munyarai No 1 well, South Australia, stratigraphic drilling project. Well completion report. South Australian Department Mines and Energy open file Env. 979 (unpublished).
- Anon, Phillips Australian Oil Company (1984) Technical evaluation of Officer Basin open acreage South Australia. Phillips Australian Oil Company. Perth. October, 1984 (unpublished).
- Austin, P.M.; and Williams, G.E. (1978) Tectonic development of the Late Precambrian to Mesozoic Australia through plate motions possibly influenced by the Earth's rotation. Journal of the Geological Society of Australia 25 (1), 1-21.
- Ball, M.M.; Shinn, E.A.; and Stockman, K.W. (1963) Geologic effects of Hurricane Donna. Abstract, American Association of Petroleum Geologists Bulletin 47, 349.
- Balsam, W.L.; and Vogel, S. (1973) Water movement in archaeocyathids : evidence and implications of pressure flow in models. Palaeontology 47, 979-984.
- Bechstadt, T. (1974) Sind Stromatactics und radiaxial - Fibroser calcit Faziesindikatoren? Neues Jahrbuch fuer Geologie und Palaeontologic. Monatshefte. 174(11), 643-663.
- Bechstadt, T; and Dohler-Hirner, B. (1983) Lead-zinc deposits of Bleiberg-Kreth IN Scholle et al. (1983) p55-63.
- Benbow, M.C. (1980) Marla 1A, 1B well completion report. Report No 5 of Officer Basin Study Group. South Australian Department Mines and Energy Report 80/22.
- Benbow, M.C. (1982) Stratigraphy of the Cambrian ?Early Ordovician, Mount Johns Range, NE Officer Basin, South Australia. Transaction Royal Society South Australia 106(4), 191-211.

- Bingham, M.P.; and Bailey, R.H. (1985) Depositional environment of Lower Cambrian Limestones, Nahant, Massachusetts. Abstract of paper presented at American Association of Petroleum Geologists, Annual Convention, March 24-27, 1985. American Association of Petroleum Geologists Bulletin 69 (2), 238.
- Blount, D.M.; and Moore, C.H. (1969) Depositional and nondepositional breccias, Chiantla Quadrangle, Guatamal. Geological Society of America Bulletin 80, 429-442.
- Bourque, P.A.; and Gignac, H. (1983) Sponge-constructed Stromatactis mud mounds, Siberian of Gaspé, Quebec. Journal of Sedimentology Petrology 53(2), 521-532.
- Braun, M.; and Friedman, G.M. (1969) Carbonate lithofacies and environments of the Tribes Hill Formation (Lower Ordovician) of the Mohawk Valley, New York. Journal of Sedimentary Petrology 39, 113-115.
- Brett, C.E. (1983) Sedimentology, facies and depositional environments of the Rochester Shale (Silurian: Wenlochan) in western New York and Ontario. Journal of Sedimentary Petrology 53 (3), 947-971.
- Brewer, A.M. (1985) Base metal geochemical data from the 1984 diamond drilling programme. E.L.'s 1070 and 1076. Eastern Officer Basin. Open File report to the South Australian Department of Mines and Energy (unpublished).
- Brewer, A.M.; Dunster, J.N.; Gatehouse, C.G.; Henry, R.L.; and Weste, G. (in prep.) Revision of the stratigraphy of the north-eastern Officer Basin.
- Budros, R.; and Briggs, L.I. (1977) Depositional environment of Ruff Formation (Upper Silurian) in Southeastern Michigan. IN Fisher (1977) pp 53-71.
- Busson, G. (1980) Carbonated, anhydritic and saliferous sequences in the Middle Devonian of wells in north-eastern Alberta (West Canada). Chapter 4 IN Evaporite Deposits - Illustration and Interpretation of some Environmental Sequences. Comité des Techniciens. Chambre Syndicale de la Recherche et de la Production du Pe'trole et du Gaz Naturel. Editions Technip, Paris.
- Butler, G.P.; Harris, P.M.; and Kendall, C.G. St. C. (1983) Recent evaporites from the Abu Dhabi coastal flats, Persian Gulf. Shale Shaker 44-68.
- Buxton, T.M.; and Sibley, D.F. (1981) Pressure solution features in a shallow buried limestone. Journal of Sedimentary Petrology 51, 27-36.
- Carr, T.R. (1982) Log-linear models, Markov chains, and cyclic sedimentation. Journal of Sedimentary Petrology 52, 905-912.
- Carey, S.W. (1976) The expanding earth. Developments in geotectonics; 10. Elsevier Scientific Publishing Company. Amsterdam.

- Castens-Seidell, B. (1984) Morphologies of gypsum on a modern sabkha: clues to depositional conditions. Abstract of Paper presented at the American Association of Petroleum Geologists Annual Convention, May 20-23, 1984. American Association of Petroleum Geologists Bulletin 68 (4), 460.
- Castens-Seidell, B.; and Hardie, L.A. (1984) Anatomy of a modern marine sabkha in a rift valley setting, Northwest Gulf of California, Baja California, Mexico. Abstract of Paper presented at the American Association of Petroleum Geologists Annual Convention, May 20-23, 1984. American Association of Petroleum Geologists Bulletin 68 (4), 460.
- Chafetz, H.S. (1972) Surface diagenesis of limestone. Journal of Sedimentary Petrology 42 (2), 325-329.
- Chowns, T.M.; and Elkins, J.E. (1974) The origin of quartz geodes and cauliflower cherts through the silicification of anhydrite nodules. Journal of Sedimentary Petrology 44, 844-1003.
- Coniglio, M.; and James, N.P. (1984) Algal origin of peloids, peloidal intraclasts, and structure grumeleuse in Palaeozoic Limestones: Evidence from Cow Head Group, Western Newfoundland. Abstract of paper presented at the American Association of Petroleum Geologists Annual Convention, May 20-23, 1984. American Association of Petroleum Geologists Bulletin 68 (4), 464.
- Cook, P.J. (1982) The Cambrian palaeogeography of Australia and opportunities for petroleum exploration. Journal of Australian Petroleum Exploration Association 22 (1) Technical Papers. APEA Conference Sydney 9-12th May, 1982.
- Curtis, R.; Evans, A.; Kinsman, D.J.J.; and Shearman, D.J. (1963) Association of dolomite and anhydrite in the Recent sediments of the Persian Gulf. Nature 197, 679-680.
- Cussey, R. (1980) Diagenetic anhydrite of carbonate sabkha in the Tertiary of Iraq. Chapter VIII IN Evaporite Deposits - Illustration and Interpretation of some Environmental Sequences. Comite' des Techniciens. Chambre Syndicale de la Recherche et de la Production du Petrole et du Gaz Naturel. Editions Technip, Paris.
- Daily, B. (1972) The base of the Cambrian and the first Cambrian faunas. University of Adelaide Centre for Precambrian Research Special Paper 1, 13-42.
- Davidson, W.T. (1985) Depositional and diagenetic aspects of siliciclastic and carbonate reservoirs in Gloriet Formation (Permian), North Midland Basin, Texas. Abstract of Paper presented at American Association of Petroleum Geologists Annual Convention, March 24-27, 1985. American Association of Petroleum Geologists Bulletin 69 (2), 248.
- Davis, J.B.; and Kirkland, D.W. (1979) Bioepigenetic sulfur deposits. Economic Geology 74, 462-468.
- Dean, W.E.; and Schreiber, B.C. (ed) (1978) Marine evaporites. Lecture notes for short course No. 4. Society of Economic Palaeontologists and Mineralogists. April, 1978. 188 pp. Tulsa, Oklahoma.

- Demicco, R.V. (1983) Wavey and lenticular - bedded carbonate ribbon rocks of the Upper Cambrian Conococheague Limestone, central Appalachians. Journal of Sedimentary Petrology 53 (4), 1121-1132.
- Dott, R.H. (1983) 1982 SEPM Presidential Address: Episodic sedimentation - How normal is average? How rare is rare? Does it matter? Journal of Sedimentary Petrology 53 (1), 5-23.
- Douth, H.F.; and Nicholas, E. (1978) The Phanerozoic sedimentary basins of Australia and their tectonic implications. Tectonophysics 48, 365-385.
- Duff, P. Mc L.D.; Hallam, A.; and Walton, E.K. (1967) Cyclic sedimentation. Developments in Sedimentology 10. Amsterdam. Elsevier.
- Duff, P. Mc L.D.; and Walton, E.K. (1962) Statistical basis for cyclothems: a quantitative study of the sedimentary succession in the East Pennine Coalfield. Sedimentology 1, 235-235.
- Dunham, R.J. (1962) Classification of carbonate rocks according to depositional texture. Memoir American Association Petroleum Geologists 1, 108-121, Tulsa.
- Einsele, G.; and Sielacher, A. (1982) Cyclic and event stratification. Berlin. Springer-Verlag, 536p.
- Embleton, P.J.J. (1973) The palaeolatitude of Australia through Phanerozoic time. Journal of the Geological Society of Australia 19, 475-482.
- Embry, A.F.; and Klovan, J.E. (1971) A Late Devonian reef tract on northeastern Banks Island, Northwest Territories. Canadian Petroleum Geology Bulletin 19, 730-781.
- Esteban, M.; and Klappa, C.F. (1983) Subaerial exposure environment. IN Scholle et al. (1983) p2-54.
- Evamy, B.D. (1967) Dedolomitization and the development of rhombohedral pores in limestones. Journal of Sedimentary Petrology 37, 1204-1215.
- Evamy, B.D. (1969) The precipitational environment and correlation of some calcite cements deduced from artificial staining. Journal of Sedimentary Petrology 39, 787-793.
- Fischer, A.G. (1964) The Lofer cyclothems of the Alpine Triassic. IN Merriam (1964).
- Flint, R.B.; and Parker, A.J. (Compilers) (1982) Tectonic Map of South Australia. 1:2 000 000 scale. South Australian Department Mines and Energy.
- Flügel, E. (1982) Microfacies analysis of limestones. Springer-Verlag, Berlin.
- Folk, R.L. (1959) Practical petrographic classification of limestones. American Association of Petroleum Geologists Bulletin 43, 1-38, Tulsa.

- Folk, R.L.; and Pittman, J.S. (1971) Length-slow chalcedony: a new testament for vanished evaporites. Journal of Sedimentary Petrology 41, 1045-58.
- Freytag, I.B. (1966) Proposed rock units for marine Lower Cretaceous sediments in the Oodnadatta region of Great Artesian Basin. Quarterly Geological Notes, Geological Survey of South Australia 18, 3-7.
- Friedman, G.M. (1965) Terminology of crystallization textures and fabrics in sedimentary rocks. Journal of Sedimentary Petrology 35 (3), 643-655.
- Friedman, G.M. (ed) (1969) Depositional environments in carbonate rocks - A symposium. Special Publication No 14. Society of Economic Palaeontologists and Mineralogists.
- Friedman, G.M. (1985) Setting of Early Ordovician (Arenigian) carbonate sedimentation in Appalachian Basin: Arid climatic epicontinental seas interrupted by intermittent conditions of emergence. Abstract. American Association of Petroleum Geologists 69(9), 1437.
- Friedman, G.M.; and Radke, B. (1979) Evidence for sabkha overprint and conditions of intermittent emergence of northeastern North America and Queensland, Australia. Northeastern Geology (1).
- Friedman, G.M.; and Sanders, J.E. (1967) Origin and occurrence of dolostones IN Carbonate rocks: Developments in sedimentology 9A. Amsterdam, Elsevier Publishing Company. p267-348.
- Friedman, G.M.; and Shukla, V. (1980) Significance of authigenic quartz euhedra after sulfates: example from the Lockport Formation (Middle Silurian) of New York. Journal of Sedimentary Petrology 50 (4), 1299-1304.
- Garret, P. (1970) Phanerozoic stromatolites: Noncompetitive ecologic restriction by grazing and burrowing animals. Science 169, 171-173.
- Gatehouse, C.G. (1976) A fossil in the Observatory Hill Beds, South Australia. Quarterly Geological Notes, Geological Survey of South Australia 60, 5-8.
- Gatehouse, C.G. (1979) Well completion report Wilkinson No 1. South Australian Department of Mines and Energy Report No 79/88 (unpublished).
- Gavish, E. (1980) Recent sabkhas marginal to the southern coasts of Sinai, Red Sea Chapter 16. IN Nissenbaum (1980).
- Gingerich, P.D. (1969) Markov analysis of cyclic alluvial sediments. Journal of Sedimentary Petrology 39 (1), 330-332.
- Ginsburg, R.N. (1971) Landward movement of carbonate mud. New model for regressive cycles in carbonates (abstract). American Association of Petroleum Geologists Bulletin 52, 340.

- Goddard, E.N.; Trask, P.D.; De Ford, R.K.; Rove, O.N.; Singewald, J.T.; and Overbeck, R.M.; (1979) Rock colour chart. Prepared by the Rock Colour Chart Committee 1948. Distributed by The Geological Society of America, Boulder, Colorado.
- Goldhammer, R.K.; and Elmore R.D. (1984) Paleosols capping regressive carbonate cycles in the Pennsylvanian Black Prince Limestone, Arizona. Journal of Sedimentary Petrology 54 (4) 1124-1137.
- Goodwin, P.W., and Anderson, E.J. (1980) Punctuated aggradational cycles: a general hypothesis of stratigraphic accumulation (abs) Geological Society of America. Abstracts. 1980 Annual Meeting. P436.
- Goodwin, P.W.; and Anderson, E.J. (1985) Punctuated aggradational cycles: a general hypothesis of episodic stratigraphic accumulation. Journal of Geology 93 (5), 515-533.
- Gravestock, D.I. (1984) Archaeocyatha from lower parts of the Lower Cambrian sequence in South Australia. Memoir of the Association of Australasian Palaeontologists 2, 1-139.
- Gregg, J.M. (1983) On the formation and occurrence of saddle dolomite - discussion. Journal of Sedimentary Petrology 53 (3) 1025-1033.
- Gregg, J.M.; and Sibley, D.F. (1984) Epigenetic dolomitization and the origin of xenotopic dolomite texture. Journal of Sedimentary Petrology 54, 908-931.
- Guillemin, Y. (1980) Petrographical data of Oligocene evaporites in the Bresse and Valence Basins (Eastern France). Chapter VII IN Evaporite Deposits - illustration and interpretation of some environmental sequences. Comité des Techniciens. Chambre Syndicale de la Recherche et de la Production du Pétrole et du Gaz Naturel. Editions Technip. Paris.
- Halley, R.B.; and Loucks, R.G. (eds) (1980) Carbonate reservoir rocks. Notes for SEPM core workshop No 1. Denver, Colorado, 1980. Society of Economic Palaeontologists and Mineralogists. Denver, Colorado.
- Handford, C.R. (1981) Coastal sabkha and salt pan deposition of the Lower Clear Fork Formation (Permian), Texas. Journal of Sedimentary Petrology 51(3), 761-778.
- Harris, W.K. (1968) Munyarai No. 1 Well, palynological examination of cores. South Australian Department Mines Report 754. IN Anon., Continental Oil Co. of Aust. Ltd (1969).
- Harrison, R.S.; and Steinen R.P. (1978) Subaerial crusts, caliche profiles, and breccia horizons; comparison of some Holocene and Mississippian exposure surfaces, Barbados and Kentucky. Geological Society of America Bulletin 89, 385-396.
- Haslett, P.G. (1975) Lower Cambrian stromatolites from open and sheltered intertidal environments, Wirrealpa, South Australia. IN Walter, M.R. (ed.) Stromatolites, 565-584, Elsevier, Amsterdam.

- Heckel, P.H. (1972) Possible inorganic origin for stromatactis in calcilutite mounds in the Tully Limestone, Devonian of New York. Journal of Sedimentary Petrology 42(1), 7-18.
- Hibburt, J. (1984) Review of exploration activity in the Arckaringa Basin Region 1858-1983. Department Mines and Energy Report No 84/1(unpublished).
- Hsu, K.J.; and Schneider, J. (1973) Progress report on dolomitization of Abu Dhabi Sabkhas, Arabian Gulf, IN Purser (1973), 409-422.
- Illing, L.V. (1959) Deposition and diagenesis of some upper Palaeozoic carbonate sediments in western Canada. Proceedings of the Fifth World Petroleum Congress, Sec. 1, Paper 2.
- Illing, L.V.; Wells, A.V.; Taylor, J.C.M (1965) Penecontemporaneous dolomite in the Persian Gulf IN Pray and Murray (1965) p 89-111.
- Irwin, M.L. (1965) General theory of epeiric clear water sedimentation. American Association of Petroleum Geologists Bulletin 49 (4), 445-59.
- Jaannussan, V. (1961) Discontinuity surfaces in limestones, Mineralogista Geologista Institution Bulletin University Uppsala 40, 221-241.
- Jackson, M.J.; and Muir, M.D. (1981) The Babbagoola Beds, Officer Basin, Western Australia: correlations, micropalaeontology and implications for petroleum prospectivity. BMR Journal of Australian Geology and Geophysics 6, 81-93.
- Jackson, M.J.; and van de Graff, W.J.E. (1981) Geology of the Officer Basin. Bureau of Mineral Resources Bulletin 206.
- Jago, J.B.; and Youngs, B.C. (1980) Early Cambrian trilobites from the Officer Basin, South Australia. Transactions of the Royal Society of South Australia 104 (6), 197-199.
- James, N.P. (1979) Shallowing - upward sequences in carbonates, facies models 8: Geoscience Canada, 4, 126-136.
- James, N.P.; and Klappa, C.F. (1983) Petrogenesis of Early Cambrian Reef Limestones, Labrador, Canada. Journal of Sedimentary Petrology 53 (4), 1051-1096.
- Kendall, A.C. and Tucker, M.E. (1973) Radial fibrous calcite: a replacement after acicular carbonate. Sedimentology 20, 365-389.
- Kendall, C. G. St.C. and Schlager, W. (1981) Carbonates and relative changes in sea level. Marine Geology 44, 181-212.
- Kendall, C.G. St.C.; and Skipwith, P.A. d'E (1968) Recent algal mats of a Persian Gulf lagoon. Journal of Sedimentary Petrology 38, 1040-1058.
- Kendall, C.G. St.C.; and Skipwith, Sir P.A.d'E (1969a) Holocene shallow-water carbonate and evaporite sediments of Kor al Bozam, Abu Dhabi southwest Persian Gulf. American Association of Petroleum Geologists Bulletin 53, 841-869.

- Kendall, C.G. St. C. and Skipwith, Sir P.A. d'E (1969b) Geomorphology of a Recent shallow-water carbonate province. Khor Al Bazam, Trucial Coast, Southwest Persian Gulf. Geological Society of America Bulletin 80, 865-892.
- Kennard, J. (1981) The Arrinthrunga Formation, Georgina Basin, central Australia. Bureau of Mineral Resources, Australia, Bulletin 211.
- Kinsman, D.J. (1969) Modes of formation, sedimentary associations and diagnostic features of shallow-water and supra-tidal evaporites. American Association of Petroleum Geologists Bulletin 53, 830-840.
- Kinsman, D.J.; and Park, R.K. (1976) Algal belt and coastal sabkha evolution. Trucial Coast, Persian Gulf. IN Walter, M.R. (1976) Stromatolites pp. 790. Elsevier, Amsterdam.
- Krieg, G.W. (1969) Geological development in the eastern Officer Basin of South Australia. Australian Petroleum Exploration Association Journal 9, 8-13.
- Krieg, G.W. (1972) The Ammaroodinna Inlier. Quarterly Geological Notes, Geological Survey of South Australia 41, 3-7.
- Krieg, G.W. (1973) Everard, South Australia: Explanatory Notes, 1:250 000 Geological Series, Sheet SG/53-13: Adelaide, Geological Survey of South Australia.
- Kumar, N.; and Sanders, J.E. (1976) Characteristics of shoreface storm deposits. Modern and ancient examples. Journal of Sedimentary Petrology 46, 145-162.
- Kyle, R.J. (1983) Economic aspects of subaerial carbonates IN Scholle et al. (1983) p. 73-92.
- Lamar, D.L.; and Merifield, P.M. (1967) Cambrian fossils and origin of earth-moon system. Geological Society of America Bulletin 78, 1359-1367.
- Lambeck, K. (1984) Structure and evolution of the Amadeus, Officer and Ngalia Basins of central Australia. Australian Journal of Earth Sciences 31 (1), 25-49.
- Lambert, I.B.; Donnelly, T.H.; Southgate, P.N.; and Etminan, H.; and Weste, G. (1986) Isotopic and fluid inclusion studies of Cambrian palaeoenvironments, eastern Officer Basin, South Australia. Abstract of paper presented at Eighth Australian Geological Convention. Flinders University, February 1986. Abstracts Geological Society of Australia 15, 118.
- Laporte, L.F. (1969) Recognition of a transgressive carbonate sequence within an epeiric sea; Heldenberg Group (Lower Devonian) of New York State. IN Friedman (1969).
- Laut, P.; Keig, G.; Lazarides, M.; Loffler, E.; Margules, C.; Scott, R.M.; and Sullivan, M.E. (1977) Environments of South Australia Province 8: Northern Arid. CSIRO Division of Land Use Res., Canberra.

- Lindsay, R.F.; and Kendall, C. G. St.C. (1980) Depositional facies, diagenesis and reservoir character of the Mission Canyon Formation (Mississippian) of the Williston Basin at Little Knife Field, North Dakota. IN Halley and Loucks (1980), p 79-104.
- Lindsay, R.F. (1985) Anatomy of a dolomitized carbonate reservoir - Mission Canyon Formation at Little Knife Field, North Dakota. Abstract. American Association of Petroleum Geologists Bulletin 69 (5), 854.
- Logan, B.W. (1961) Cryptozoon and associated stromatolites from the Recent, Shark Bay, Western Australia. Journal of Geology 69, 517-533.
- Logan, B.W. (1984) Pressure responses (deformation) in carbonate sediments and rocks - analysis and application, Canning Basin. IN Purcell (1984).
- Logan, B.W.; Rezak, R.; Ginsbury, R.N. (1964) Classification and environmental significance of algal stromatolites. Journal of Geology 72 (1), 68-83.
- Logan, B.W.; and Semenuik, V. (1976) Dynamic metamorphism; processes and products in Devonian carbonate rocks. Canning Basin, Western Australia. Geological Society of Australia Special Publication 6, 138p.
- Longacre, S.A. (1980) Dolomite reservoirs from Permian biomicrites. IN Halley and Loucks (1980), p 105-17.
- Longman, M.W. (1980) Carbonate diagenetic textures from nearsurface diagenetic environments. American Association of Petroleum Geologists Bulletin 64 (4), 461-487.
- Longman, M.W. (1982) Carbonate diagenesis as a control on stratigraphic traps (with examples from the Williston Basin). Presented at the 1981 AAPG Fall Education Conference in Calgary, Canada. Education Course Note Series No 21. American Association of Petroleum Geologists Tulsa. pp 159.
- Machel, H.-G.; and Mountjoy, E.W. (1986) Chemistry and environments of dolomitization - A reappraisal. Earth Science Reviews 23, 175-222.
- Lydyard, A.J. (1979) A petrographic study of the sediments in seven Officer Basin stratigraphic wells. South Australian Department Mines and Energy Report 79/55 (unpublished).
- Maleev, M.N. (1972) Diagnostic features of spherulites formed by splitting of a single-crystal nucleus. Growth mechanism of chalcedony. Mineral. Petrog. Mitt. 18, 1-16.
- Mattes, B.W.; and Mountjoy, E.W. (1980) Burial dolomitization of the Upper Devonian Miette Buildups Jasper National Park, Alberta. IN Zenger et al. (1980).
- Mazzullo, S.J. (1976) Significance of authigenic K-feldspar in Cambro-Ordovician rocks of the Proto-Atlantic Shelf in North America: A discussion. Journal of Sedimentary Petrology 46, 1035-1038.

- Mazzullo, S.J. (1978) Early Ordovician tidal flat sedimentation, Western margin of Proto-Atlantic Ocean. Journal of Sedimentary Petrology 48, 49-62.
- Mazzullo, S.J. and Friedman, G.M. (1975) Conceptual model of tidally influenced deposition on margins of epeiric seas; Lower Ordovician (Canadian) of eastern New York and southwestern Vermont. American Association of Petroleum Geologists Bulletin 59, 2123-2141.
- McCave, I. (1970) Deposition of fine-grained suspended sediment from tidal currents. Journal of Geophysical Research 75, 4151-4159.
- McKirdy, D.M.; Kantsler, A.J.; Emmett, J.K.; and Aldridge, A.K. (1984) Hydrocarbon genesis and organic facies in the Cambrian carbonates of the Eastern Officer Basin, South Australia. IN Palacas, J.G. (1984) Petroleum geochemistry and source rock potential of carbonate rocks. American Association of Petroleum Geologists Studies in Geology. No. 18, 13-31.
- McRae, S.G. (1972) Glauconite. Earth - Science Review 8, 397-440.
- Merriam, D.F. (ed) (1964) Symposium on Cyclic Sedimentation. Geological Survey Kansas Bulletin 169 (2), 631-636.
- Meyers, W.J. (1974) Carbonate cement stratigraphy of the Lake Valley Formation (Mississippian) Sacramento Mountains, New Mexico. Journal of Sedimentary Petrology 44 (3), 837-861.
- Middleton, G.V. (1961) Evaporite solution breccias from the Mississippian of southwest Montana. Journal of Sedimentary Petrology 31, 189-195.
- Milanovsky, E.E. (1981) Aulacogens of ancient platforms: problems of their origin and tectonic development. Tectonophysics 73, 213-248.
- Milton, B.E.; and Parker, A.J. (1973) An interpretation of geophysical observations on the northern margin of the eastern Officer Basin. Quarterly Geological Notes, Geological Survey of South Australia 46, 10-14.
- Moore, A.C.; and Goode, A.D.T. (1978) Petrography and origin of granulite-facies rocks in Western Musgrave Block, Central Australia. Journal of Geological Society of Australia 25 (6), 341-358.
- Moore, C.H. (1971) Pseudospar dedolomite "cements" of evaporite solution collapse breccias. IN Bricker, O.P. (ed.) Carbonate cements. John Hopkins University Press, Baltimore, 347-351.
- Moore, P.S. (1982) Hydrocarbon potential of the Arckaringa region, central South Australia. Journal of the Australian Petroleum Exploration Association 22 (1), 237-253.
- Muir, M. (1979) Palynological examination of microfossils from the Observatory Hill Beds, Wilkinson No. 1. DDH, Officer Basin, South Australia. IN Gatehouse 1979(b).
- Munk, W.H.; and MacDonald, G.J.F. (1960) The rotation of the earth. Cambridge University Press, London, 323.

- Nagtegaal, P.J.C. (1969) Microtexture in recent and fossil caliche. Leidse Geologische Mededelingen 42, 131-142.
- Nichol, D. (1971) Opal occurrences near Welbourn Hill Homestead Mineral Resources Review South Australia 135, 164-168.
- Odin, G.S.; and Matter, A. (1981) De glauconiarum origine. Sedimentology 28, 611-641.
- Opik, A.A. (1975) Cymbric Vale Fauna of New South Wales and early Cambrian biostratigraphy. Bulletin Bureau of Mineral Resources Geology and Geophysics Australia 159.
- Palacas, J.G. (1983) Carbonate rocks as sources of petroleum: geological and chemical characteristics and oil-source correlations. Proceedings 11th World Petroleum Congress Meeting. London, England.
- Park, R.K. (1973) Algal belt sedimentation of the Trucial Coast, Arabian Gulf. PhD. Thesis, University of Reading, England (not sighted).
- Parker, A.J. (1979) The Gawler Craton Extended Abstracts. Geological Society of Australia S.A. Division Symposium on the Gawler Craton Dec. 1979.
- Parker, A.J. and Lemon, N.M. (1982) Reconstruction of the Early Proterozoic stratigraphy of the Gawler Craton, South Australia. Journal Geological Society of Australia 29 (2) 221-238.
- Pfeil, R.W.; and Read, J.F. (1980) Cambrian carbonate platform margin facies, Shady Dolomite, Southeastern Virginia, U.S.A. Journal of Sedimentary Petrology 50 (1), 91-116.
- Pitt, G.M. (1978) Murloocoppie, South Australia. Explanatory Notes, 1:250,000 geological series. Sheet SH/53-2. Geological Survey of South Australia.
- Pitt, G.M.; Benbow, M.C.; and Youngs, B.C. (1980) A review of recent geological work in the Officer Basin, South Australia. Journal of Australian Petroleum Exploration Association 20, 209-220.
- Pluim, S. (1984) Timing of saddle dolomite in Tuscaloosa Formation, Mississippi. Abstract of Paper presented at the American Association of Petroleum Geologists Annual convention, May 20-23, 1984. American Association of Petroleum Geologists Bulletin 68 (4), 517.
- Powers, D.W. (1984) Order and randomness in sedimentary sequences. Abstract of Paper presented at the American Association of Petroleum Geologists Annual Convention, May 20-23, 1984. American Association of Petroleum Geologists Bulletin 68 (4), 519.
- Purcell, P.G. (ed) (1984) The Canning Basin, W.A.: Proceedings of the Geological Society Australia / Petroleum Exploration Society of Australia Symposium, Perth, 1984.
- Radke, B.M. (1980) Epeiric carbonate sedimentation of the Ninmaroo Formation (Upper Cambrian-Lower Ordovician). Georgina Basin. Bureau of Mineral Resources, Australia, Geology and Geophysics Journal (5), 183-200.

- Radke, B.M. (1982) Late diagenetic history of the Ninmaroo Formation (Cambro-Ordovician), Georgina Basin, Queensland and Northern Territory. Bureau of Mineral Resources, Australia, Geology and Geophysics Journal (7), 231-254.
- Radke, B.M.; and Mathis, R.L. (1980) On the formation and occurrence of saddle dolomite. Journal of Sedimentary Petrology 50 (4), 1149-1168.
- Raup, O.B. (1970) Brine mixing: an additional mechanism for formation of basin evaporites. American Association of Petroleum Geologists Bulletin 54 (12), 2246-2259.
- Raup, O.B.; and Hite, R.J. (1978) Bromine distribution in marine halite rocks IN Dean and Schreiber (1978), p105-123.
- Read, J.F.; and Pfeil, R.W. (1983) Fabrics of allochthonous reefal blocks, Shady Dolomite (Lower to Middle Cambrian), Virginia Appalachians. Journal of Sedimentary Petrology 53 (3), 761-778.
- Reineck, H.E., and Singh, I.B. (1972) Genesis of laminated sand and graded rhythmites in storm-sand layers of shelf mud. Sedimentology 18, 123-128.
- Reineck, H.E.; and Singh, I.B. (1980) Depositional sedimentary environments. With reference to terrigenous clastics. Second edition. Springer-Verlag. Berlin.
- Robertson C.S.; Mayne, S.J.; and Townsend, D.G. (1980) A review of the geology, petroleum exploration, and petroleum prospects of the Officer Basin Region. Bureau of Mineral Resources, Record, 1980/26.
- Ruckmick, J.C.; Wimberly, B.H.; and Edwards, A.F. (1979) Classification and genesis of biogenic sulphur deposits. Economic Geology 74, 469-474.
- Schmidt, V. (1965) Facies, diagenesis, and related reservoir properties in the Gigas Beds (upper Jurassic), Northwestern Germany. IN Pray and Murray (1965), p124-168.
- Schmidt, V.; McDonald, D.A.; and McIlreath, I.A. (1980) Growth and diagenesis of Middle Devonian Keg River cementation reefs, Rainbow Field, Alberta. IN Halley and Loucks (1980), pp43-63.
- Scholle, P.A.; Bebout, D.G.; and Moore, C.H. (1983) Carbonate depositional environments. AAPG Memoir 33. American Association of Petroleum Geologists.
- Selley, R.C. (1970) Studies of sequence in sediments using a simple mathematical device. Quarterly Journal of the Geological Society of London 125 (4), 557-581.
- Semeniuk, V. (1971) Subaerial leaching in the limestones of the Bowan Park Group (Ordovician) of Central Western New South Wales. Journal of Sedimentary Petrology 41 (4), 939-950.
- Sepkoski, J.J. (1982) Flat pebble conglomerates, storm deposits and the Cambrian bottom fauna. IN Einsele and Seilacher (1982), 371-385.

- Shearman, D.J. (1978) Evaporites of coastal sabkhas. Section 2 IN Dean and Schrieber (1978).
- Shergold, J.; Jago, J.; Cooper, R.; and Laurie, J. (1985) The Cambrian System in Australia, Antarctica and New Zealand. Correlation charts and explanatory notes. International Union of Geological Sciences. Publication No 19.
- Shinn, E.A. (1968) Practical significance of birdseye structures in carbonate rocks. Journal of Sedimentary Petrology 38 (1), 215-223.
- Shinn, E.A. (1983a) Birdseyes, fenestrae, shrinkage pores, and loferites: a re-evaluation. Journal of Sedimentary Petrology 53 (2), 619-628.
- Shinn, E.A. (1983b) Tidal flat environment. Chapter 4 IN Scholle et al. (1983).
- Shinn, E.A.; Lloyd, R.M.; and Ginsburg R.N. (1969) Anatomy of a modern carbonate tidal flat, Andros Island, Bahamas. Journal of Sedimentary Petrology 39, 1202-1228.
- Shinn, E.A.; and Robbin, D.M. (1983) Mechanical and chemical compaction in fine-grained shallow-water limestones. Journal of Sedimentary Petrology 53 (2), 595-618.
- Siedlecka, A. (1972) Length-slow chalcedony and relics of sulphates - evidence of evaporitic environments in the Upper Carboniferous and Permian beds of Bear Island, Svalbard. Journal of Sedimentary Petrology 42, 812-816.
- Siedlecka, A. (1976) Silicified Precambrian evaporite nodules from Northern Norway. A preliminary report. Sedimentary Geology 16, 161-175.
- Simpson, J. (1985) Stylolite-controlled layering in an homogeneous limestone : pseudo-bedding produced by burial diagenesis Sedimentology 32, 495-505.
- Southgate, P.N. (1982) Cambrian skeletal halite crystals and experimental analogues. Sedimentology 29, 391-407.
- Spizharsky, T.N.; Yergaliyev, G.Kh; Zhuravleva, I.T.; Repina, L.I.; Rozanov, A. Yu; and Chernysheva, N.Ye (1984) A scale of stages for the Cambrian system. International Geology Review 26, May, 506-522.
- Swanson, R.G. (1981) Sample examination manual. Methods in exploration series. American Association of Petroleum Geologists. Tulsa, Oklahoma, USA.
- Thornton, R.C.N. (1971) Mt. Willoughby No 1 Well completion report. South Australian Department of Mines Report. 71/37 (unpublished).
- Thornton, R.C.N. (1975) Manya No 1 and Marla No 1 Well completion report. South Australian Department of Mines Report 75/106. G.S. 5639, D.M. 1035/74 (unpublished).

- Thornton, R.C.N. (1978) The geological results of the drilling of Manya No. 1 and Marla No. 1. Mineral Resources Review South Australia 143, 47-65.
- Tissot, B.; and Welte, D.H. (1978) Petroleum Formation and Occurrence. Springer-Verlag, Berlin.
- Townsend, I.J. and Ludbrook, N.H. (1975) Revision of the Permian and Devonian nomenclature of four formations in and below the Arckaringa Basin. Quarterly Geological Notes of the Geological Survey of South Australia 54, 2-5.
- Tucker, M.E. (1976) Replaced evaporites from the Late Cambrian of Finnmark, Arctic Norway. Sedimentary Geology 16, 193-204.
- Veevers, J.J. (1976) Early Phanerozoic events on and alongside the Australian - Antarctic platform. Journal of the Geological Society of Australia 23, 183-206.
- Veevers, J.J.; Jones J.G.; and Powell, C.McA. (1982) Tectonic framework of Australia's sedimentary basins. Journal of the Australian Petroleum Exploration Association Journal 22 (1), 283-300.
- Vozoff, K.; and Cull, J.P. (1981) An electro-magnetic method for rapid basin evaluation and some special problems. Journal of the Australian Petroleum Exploration Association 21 (1), 167-174.
- Walker, R.G. (ed) (1979) Facies Models. Geoscience Canada, Reprint Series 1, Geological Association of Canada 1-7.
- Walker, R.N.; Muir, M.D.; Diver, W.C.; Williams, N.; and Wilkins, N. (1977) Evidence of major sulfate evaporite deposits in the Proterozoic McArthur Group, Northern Territory, Australia. Nature 265 (5594), 526-529.
- Walker, T.R. (1962) Reversible nature of chert-carbonate replacement in sedimentary rocks. Geological Society of America Bulletin 73, 237-242.
- Walls, R. A.; Harris, W.B.; and Nunan W.E. (1975) Calcareous crust (caliche) profiles and early subaerial exposure of Carboniferous carbonates, northeastern Kentucky. Sedimentology 22, 417-440.
- Wanless, H.R. (1979) Limestone response to stress: pressure solution and dolomitization. Journal of Sedimentary Petrology 49, 437-462.
- Wanless, H.R. (1982) Limestone response to stress: pressure solution and dolomitization - Reply. Journal of Sedimentary Petrology 52, 328-332.
- Warren, J.K.; and Kendall, C.G. St.C. (1985) Comparison of sequences formed in marine sabkha (subaerial) and salina (subaqueous) settings; modern and ancient. American Association of Petroleum Geologists Bulletin 69 (6), 1013-1023.
- Wentworth, C.K. (1922) A scale of grade and class terms for clastic sediments. Journal of Geology 30, 377-392.

- West, I.M.; Ali, Y.A.; and Hilmy, M.E. (1979) Primary gypsum nodules in a modern sabkha on the Mediterranean coast of Egypt. Geology 7, 354-358.
- Weste, G.; Summons, R.E.; McKirdy, D.M.; Southgate, P.N.; Henry, R.L.; and Brewer, A.M. (1984) Cambrian palaeoenvironments and source rocks of the Eastern Officer Basin. Geological Society of Australia, Abstract Series 12, 542-544.
- White, A.H.; and Youngs, B.C. (1980) Cambrian alkali-playa lacustrine sequence in the northeastern Officer Basin, South Australia. Journal of Sedimentary Petrology 50 (4), 1279-1286.
- Wilson J.L. (1975) Shoaling upward shelf cycles and shelf dolomitization. Chapter X IN Wilson (ed) (1975) Carbonate facies in geologic history. Springer-Verlag.
- Wilson, J.L.; and Jordan, C. (1983) Middle Shelf Environment. Chapter 7 IN Scholle et al. (1983).
- Wilson, J.L.; and Pilatzke, R.H. (1985) Carbonate-evaporite cycles in Lower Duperow Formation of Williston Basin - Abstract American Association of Petroleum Geologists Bulletin 69 (5), 870-871.
- Wilson, R.C.L. (1966) Silica diagenesis in Upper Jurassic limestones of Southern England. Journal of Sedimentary Petrology 36 (4), 1036-1049.
- Wolf, K.H.; (1965) Littoral environment, indicated by open-space structures in algal limestones. Palaeontology 3 (1), 183-223.
- Wopfner, H. (1969) Lithology and distribution of the Observatory Hill Beds, eastern Officer Basin: Transactions of the Royal Society of South Australia 93, 169-188.
- Wopfner, H.; Freytag, I.G.; and Heath, G.R. (1970) Basal Jurassic - Cretaceous rocks of western Great Artesian Basin, South Australia. Stratigraphy and environment. American Association of Petroleum Geologists Bulletin 54, 383-416.
- Youngs, B.C. (1980) Lithologies and interpretations of the Observatory Hill Beds, Marla-1A and -1B. Report No. 10 of the Officer Basin Study Group. Department of Mines and Energy South Australia Report 80/79.
- Zeller, E.J. (1964) IN Merriam (1964) p. 631-636.
- Zenger, D.H.; Dunham, J.B; and Ethington, R.L. (eds) (1980) Concepts and models of dolomitization. Society of Economic Palaeontologists and Mineralogists. Special Publication No 28.

APPENDIX I

PETROGRAPHIC CLASSIFICATIONS









ALLOCHTHONOUS LIMESTONES ORIGINAL COMPONENTS NOT ORGANICALLY BOUND DURING DEPOSITION						AUTOCHTHONOUS LIMESTONES ORIGINAL COMPONENTS ORGANICALLY BOUND DURING DEPOSITION		
LESS THAN 10% >2mm COMPONENTS				GREATER THAN 10% > 2 mm COMPONENTS		BOUNDSTONES		
CONTAINS CARBONATE MUD			NO CARBONATE MUD	MATRIX SUPPORTED	> 2 mm COMPONENT SUPPORTED	BY ORGAN- ISMS WHICH ACT AS BAFFLES	BY ORGAN- ISMS WHICH ENCRUST AND BIND	BY ORGAN- ISMS WHICH BUILD A RIGID FRAME WORK
MUD SUPPORTED		GRAIN SUPPORTED				BAFFLE- STONE	BIND- STONE	FRAME- STONE
LESS THAN 10 % GRAINS	GREATER THAN 10% GRAINS							
MUD- STONE	WACKE- STONE	PACK- STONE	GRAIN- STONE	FLOAT- STONE	RUD- STONE	BAFFLE- STONE	BIND- STONE	FRAME- STONE
								

FIGURE 50: CARBONATE CLASSIFICATION
(from Embry and Klovan, 1971;
after Dunham, 1962).

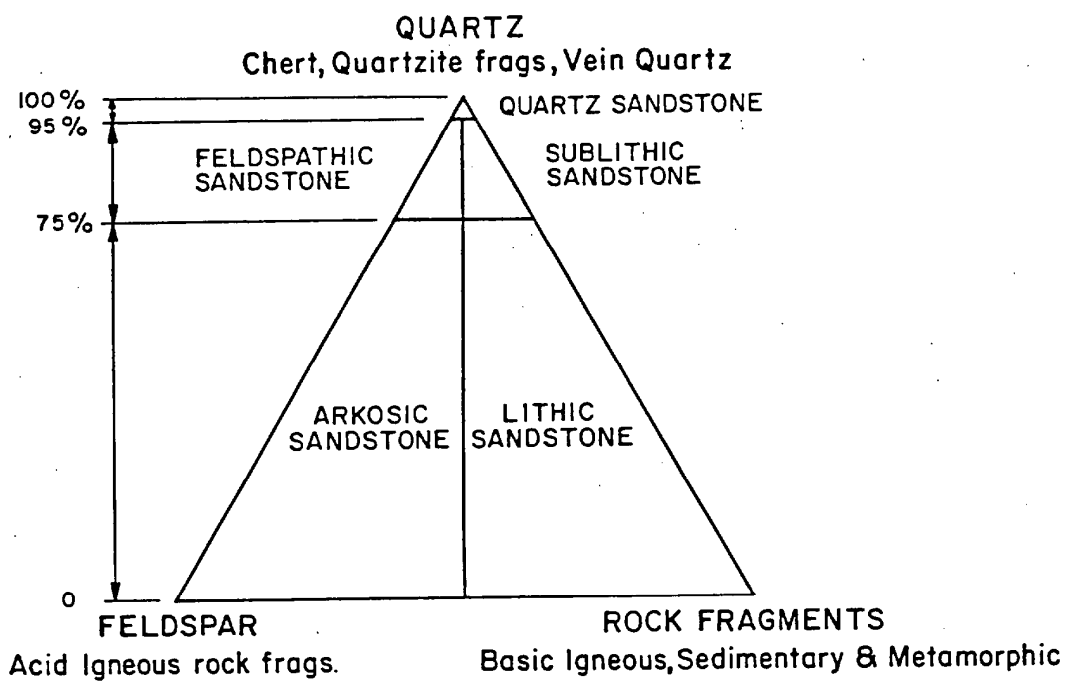


FIGURE 51: COMPOSITIONAL CLASSIFICATION OF SANDSTONES
(from Swanson, 1981).

APPENDIX II

CATALOGUE OF SPECIMENS

INDEX TO THIN SECTIONS

Key to Abbreviations

COM = thin section stored in the collection of
Comalco Exploration, Glenside

SEM = scanning electron microscope study

Sample Number	Drillhole	Depth (m)	Lithology/Lithofacies	Figure
COM511	Manya-3	239.70	Laminated and silty carbonate mudstone	17d
COM516	Manya-3	299.70	Stylonodular carbonate mudstone	
COM520	Manya-3	353.70	Laminated and silty carbonate mudstone	
COM527	Manya-3	685.90	Microfaulted dolostone, laminated mudstone texture	
COM528	Manya-3	739.00	Quartz feldspar packstone, dolomite/calcite/anhydrite cement/matrix	
COM530	Manya-3	795.80	Dolostone, stylolaminated mudstone texture, with cauliflower chert	
COM627	Manya-6	928.50	Bioclastic wackestone (hyolithid debris)	19d
COM628	Manya-6	728.55	Sand/silt/carbonate mudstone set	22d
COM630	Manya-6	869.85	Anhydrite, 'chicken-wire' texture	19d
COM633	Manya-6	954.44	Thrombolitic algal bindstone	
COM634	Manya-6	976.50	Oncoid wackestone	
COM637	Manya-6	1032.00	Stylolaminated carbonate mudstone	
COM639	Manya-6	1039.90	Laminated carbonate mudstone	
COM640	Manya-6	1045.65	Stylonodular carbonate mudstone	
COM648	Manya-6	1263.70	Bioclastic peloid grainstone	33a
COM650	Manya-6	1323.00	Quartz feldspathic wackestone/carbonate mudstone	
COM651	Manya-6	1334.05	Stromatolitic algal bindstone, pressure solution texture	
COM652	Manya-6	1373.00	Sand/silt/carbonate mudstone sets	
COM653	Manya-6	1392.30	Laminated silty carbonate mudstone	
COM655	Manya-6	1676.75	Feldspathic sandstone, halite cement	
COM670	Marla-7	364.50	Gypsum and anhydrite vein	33a
COM673	Marla-7	410.86	Carbonate mudstone hosting chert nodules	
COM676	Marla-7	468.11	Granule conglomerate/coarse feldspathic sandstone, gypsum cement	
COM677	Marla-7	470.13	Coarse to very coarse feldspathic sandstone, gypsum cement	

COM681	Marla-7	492.60	Medium grained feldspathic sandstone, dolomite cement/matrix	
COM682	Marla-6	679.33	Ooid aggregate grain grainstone/packstone partly silicified and Feldspathic sandstone, dolomitic matrix/cement	
COM686	Marla-6	308.30	Massive secondary dolostone, no relict texture	
COM688	Marla-6	366.60	Chert and carbonate mudstone breccia, floatstone/rudstone texture	
COM691	Marla-6	457.75	Relict micritized intraclastic ooid peloid grainstone	29e,f
COM692	Marla-6	471.20	Sand/silt/carbonate mudstone sets	
COM698	Marla-6	510.14	Dolostone, relict ?intraclastic wackestone texture	
COM699	Marla-6	512.66	Relict ooid grainstone/packstone	
COM705	Marla-6	614.00	Dolostone, relict archaeocyath bafflestone/framestone	
COM706	Marla-6	616.15	Dolostone, relict archaeocyath bafflestone/framestone	15
COM707	Marla-6	669.75	Dolostone, relict thrombolitic algal texture	
COM719	Manya-6	1085.86	Bioclastic peloid grainstone, tubular fossils	
COM720	Manya-6	1208.33	Bioclastic peloid grainstone, tubular fossils	
COM730	Manya-3	401.60	Collapse breccia	
COM731	Manya-3	401.90	Collapse breccia	
COM732	Marla-6	546.88	Fenestral and stromatactitic carbonate mudstone	18b
COM733	Manya-6	936.60	Fenestral and stromatactitic carbonate mudstone	18d
COM739	Manya-6	896.46	Laminated carbonate mudstone with saddle dolomite and chert after evaporites	33c
COM740	Manya-6	897.13	Carbonate mudstone hosting concentric-zoned chert after evaporites	
COM747	Manya-3	353.35	Relict ooid grainstone	29c
COM748	Manya-3	357.86	Bioclastic wackestone, tubular fossils	29a,b
COM749	Manya-3	324.13	Relict ooid grainstone	
COM750	Manya-3	537.20	Laminated carbonate mudstone with cauliflower cherts	

SEM750	Manya-3	537.20	Laminated carbonate mudstone with cauliflower cherts	33b
COM766	Marla-3	557.60	Chert	
COM768	Marla-6	309.95	Carbonate mudstone with partly silicified nodule of sulphate evaporites	
COM769	Marla-6	377.38	Stromatolitic algal bindstone and ooid grainstone	21d
COM779	Marla-6	457.60	Dolostone	26c
COM782	Marla-6	648.10	Dolostone	26d
COM788	Marla-7	437.80	Dolostone	26b

INDEX TO POLISHED SLABS

Drillhole	Depth (m)	Lithofacies/Lithology	Figure
Manya-2	642.89	Rudstone	
Manya-3	299.30	Stylonodular carbonate mudstone, stained with potassium ferricyanide	
	369.11	Floatstone, dolomitic clasts in calcareous matrix	
	388.50	Stylonodular carbonate mudstone (unpolished slab)	
	390.36	Stylonodular carbonate mudstone, stained with potassium ferricyanide	
	401.60	Collapse breccia (unpolished slab)	
	401.90	Collapse breccia (unpolished slab)	
	413.92	Collapse breccia	
	512.70	Laminated and silty carbonate mudstone with abundant dewatering structures	17c
	537.35	Laminated and silty carbonate mudstone	
	556.56	Fenestral and thrombolitic carbonate mudstone	
	761.15	Sandstone with pseudomorphs of displacive halite hoppers	
	789.60	?Pagoda halite pseudomorphs in laminated and silty carbonate mudstone	
	790.00	Euhedral sulphate evaporite crystals in laminated and silty carbonate mudstone	
Manya-6	625.45	Disturbed (?burrowed) carbonate mudstone with stylolites	
	842.74	'Red-bed' siltstone and claystone	22a
	869.62	Anhydrite, 'chicken-wire' texture	25
	936.60	Stromatacttic carbonate mudstone	18c
	1036.50	Plate breccia	20c
	1070.73	Microlaminated carbonate mudstone	17a
	1074.59	Stylobanded carbonate mudstone	
	1085.86	Bioclastic peloid grainstone with tubular (?sponge) fossils	
	1106.56	Stylonodular carbonate mudstone, stained with potassium ferricyanide	
	1107.43	Stylomottled to stylonodular carbonate mudstone	
	1136.02	Thrombolitic algal bindstone, leached and dolomitized	

	1142.30	Stylolaminated carbonate mudstone	
	1208.33	Bioclastic peloid grainstone with tubular (?sponge) fossils	
	1228.41	Pagoda halite in laminated and silty carbonate mudstone	24c
	1243.22	Ooid packstone/grainstone, silicified	
	1453.20	Sand/silt/claystone sets	22c
	1504.35	Sand/silt/claystone set, cross stratified, minor halite	
	1567.70	Granule conglomerate and claystone	
	1598.70	Displacive halite hopper in fine grained sandstone	24a
	1607.27	Sand/silt/claystone sets	
	1649.98	Skeletal halite hopper in silty claystone	24b
	1656.40	Bedded halite (specimen destroyed for analysis)	24d
Marla-3	557.60	Chert layer in carbonate mudstone	
	559.60	Leached ?burrow mottled carbonate mudstone	
	571.40	Thrombolitic algal bindstone, burrowed	21c
	593.24	Sandstone and granule conglomerate, cross-stratified	22b
	601.06	Sandstone and siltstone, ripple cross-stratified	
	613.18	Ooid packstone/grainstone, stylolites	
Marla-6	258.10	Rudstone and 'red bed' siltstone	
	265.79	Rudstone	20b
	273.60	Dolostone, massive	26a
	301.45	Laminated and silty carbonate mudstone, early solution collapse brecciation	
	309.95	Laminated and silty carbonate mudstone with sulphate evaporite nodules	25b
	360.15	Intraclastic packstone, silicified	
	362.90	Floatstone, leached chert clasts in carbonate matrix	20a
	373.20	Stromatolitic algal bindstone, leached and dolomitized	

373.50	Stromatolitic algal bindstone, dolomitized	
377.38	Stromatolitic algal bindstone with ooid grainstone lens	21a
394.30	Quartz feldspar packstone and massive secondary dolostone	
437.92	Dolostone, relict laminated carbonate mudstone texture	
442.95	Sand/silt/carbonate mudstone set	
450.89	Sand/silt/carbonate mudstone set	
457.80	Intraclastic ooid peloid grainstone, silicified	
471.25	Sand/silt/carbonate mudstone sets, chert after evaporites	
475.60	Laminated carbonate mudstone	
485.40	Laminated and silty carbonate mudstone, fining-up couplets	
512.66	Ooid grainstone/packstone	
546.88	Fenestral and stromatactic carbonate mudstone	18a
576.25	Sand/silt/carbonate mudstone sets	
584.70	Massive carbonate mudstone, incipient stylolitization and chertification	
609.16	Laminated carbonate mudstone	
616.15	Archaeocyath bafflestone/framestone, dolomitized	21b
617.18	Oncoid wackestone/packstone	19a
643.60	Intraclastic wackestone/grainstone	
646.72	Thrombolitic algal bindstone	
646.82	Oncoid wackestone	19b
662.48	Sandstone, granule conglomerate	
667.38	Laminated carbonate mudstone with columnar stylolites	
669.75	Thrombolitic algal bindstone, ?burrowed	
696.15	Sandstone, medium to fine grained, cross-stratified	
400.80	Laminated and silty carbonate mudstone, fining-up couplets	17b

APPENDIX III

PETROGRAPHIC DESCRIPTIONS

LAMINATED AND SILTY CARBONATE MUDSTONE

Description

In hand specimen, this rock varies from thinly bedded to laminated grey (N7,N5,N6) and is cut by a thin vein. The sample comes from a sequence of stacked fining-up silt/carbonate mudstone couplets.

Microscopically, the bulk of this rock consists of microcrystalline to amorphous turbid dolomite with laminae defined by varying concentrations of detrital silt to sand sized quartz, feldspar and carbonate grains and by thin discontinuous carbonaceous wisps and laminae. Rare, randomly oriented, highly birefringent crystals which appear acicular in cross-section may be anhydrite.

The terrigenous clasts average 0.2 mm diameter but range up to 0.8 mm. The larger clastic grains are well rounded but vary from low to high sphericity. Some of the smaller quartz grains have syntaxial overgrowths. The larger carbonate grains are dolomite and are well rounded with high sphericity.

Sporadic fine grained accessory opaque minerals are also present.

Incipient stylolitization is visible in thin section. It has concentrated the detrital clastic grains and abundant small euhedral dolomite rhombs.

The rock is cut by a 1 mm wide sparry calcite vein with thinner conformable continuations.

Interpretation

Each fining-up couplet probably formed during a single pulse of high energy. As the current velocity waned, the progressively finer grained particles settled out. The texture has been partly enhanced by later dolomitization and stylolitization.

STYLONODULAR CARBONATE MUDSTONE

Description

This specimen comes from a unit several metres thick and is composed of boudin-like bodies of pale grey (N6) material in a very finely laminated dark grey (N4) matrix. The fine laminations appear to enclose the boudin-like nodules.

In thin section, the dark material is revealed to be a clayey ferroan dolomitic mudstone with abundant very fine grained to silt-sized ?detrital quartz, feldspar and carbonate grains concentrated in laminae. The majority of the carbonate is very finely crystalline dolomite, but ?detrital calcite grains, and larger secondary euhedral dolomite rhombs up to 0.1 mm across, are also present.

Staining with Alizarin Red-S shows that the paler boudin-like nodules are microcrystalline to amorphous very slightly dolomitic calcite with highly disturbed fining-up laminae containing abundant ?detrital quartz, feldspar and ?detrital calcite. These grains range in size up to 0.15 mm (fine grained). Vertically oriented areas within the mudstone contain terrigenous grains and an anomalous concentration of well rounded dolomitic ?peloids averaging just under 0.1 mm diameter. These vertical structures are almost certainly burrows. The nodules also contain some microfractures with secondary calcite spar infill. The fractures do not continue into the surrounding dolomitic material.

Interpretation

The presence of ?peloid filled burrows supports a shallow subtidal environment of deposition for the original calcareous sediment. The extensive ferroan dolomite and associated detrital grains represent reactate and stylocumulate respectively. They formed as a result of pressure solution and maybe accentuating an original difference in lithology. The small calcite spar filled fractures preceded pressure solution.

LAMINATED AND SILTY CARBONATE MUDSTONE

Description

This rock is a grey (N5) extremely fine grained to silty carbonate mudstone. Laminations are visible at 70° to 80° to the core length. It comes from a sequence of laminated carbonate mudstones with disturbed laminations, possible burrowing and some incipient stylolitic pressure dissolution.

In thin section, this rock primarily consists of very finely crystalline to amorphous dolomite with very small sporadic patches of calcite. This is interbedded with thin beds and laminae of fining-up silty dolomitic calcite. The lower edges of these interbeds are noticeably more calcareous. They contain fine grained to silt-sized calcite grains with subordinate (less than 15 percent) detrital quartz and feldspar. The grains are angular to subangular with low to moderate sphericity.

The slide also shows moderately well developed irregular microstylolites; some showing columnar structures up to 0.2 mm high. A possible burrow or soft sediment injection of a sandier layer is also evident.

Interpretation

The primary texture of fining-up couplets probably resulted from repeated pulses of higher energy. The fact that the cap of each couplet is more dolomitic may suggest the formation of primary dolomite. The texture has been enhanced by subsequent stylolitization.

MICROFAULTED DOLOSTONE, LAMINATED MUDSTONE TEXTURE

Description

This is an aphanitic grey dolostone with alternate light (N5) and dark (N3) (5YR 6/1) thin beds and laminae at about 70° to the core length.

In thin section, the paler thin beds and laminae consist of fine grained to microcrystalline dolomite with an average crystalsize less than 0.02 mm, and containing isolated individual crystals to 0.9 mm (coarse grained), and patches of very fine to medium grained dolomite and rare opaque heavy minerals. Patches of coarsely crystalline sparry calcite and very fine grained to silty quartz, feldspar and detrital ?biotite are also scattered throughout these paler beds.

The thin dark beds consist of very finely crystalline dolomite and a brown ?limonitic material possibly with some incipient stylolitic concentration.

The rock is cut by a gently curved microfault at about 30° to the lamination, with a vertical displacement of 2 mm.

Indistinct, possible algal lamination is also present in one corner of the thin section.

Interpretation

This rock shows repeated alternations of provenance with regular input of clays; and separate, very limited, influx of fine grained detrital terrigenous clastics. The dolomitization is a secondary recrystallization texture, it is not certain whether the precursor was calcareous or an earlier generation of dolomite.

QUARTZ FELDSPAR PACKSTONE, DOLOMITE/CALCITE/ANHYDRITE
CEMENT/MATRIX

Description

This hand specimen comes from an interbed in a sequence of stacked sand/silt/mudstone sets. The colours vary from grey (N6) to pale green (5GY 6/1).

A complex composition is revealed in thin section. Roughly one third of the slide is a laminated to thinly bedded secondary dolomite with scattered detrital quartz (including metamorphic grains) and feldspar grains - a QUARTZ FELDSPAR WACKESTONE, REPLACEMENT DOLOMITE MATRIX. This grades down to QUARTZ FELDSPAR PACKSTONE, with patches of ?secondary coarse grained sparry calcite cement (strictly a QUARTZ FELDSPAR GRAINSTONE) and patches of replacement anhydrite cement.

The quartz and feldspar grains never exceed 40 percent of the total composition and range from a maximum dimension of 0.8 mm (coarse grained) to 0.06 mm (silt-sized) indicating poor sorting. Feldspar grains are dominant in several of the laminae; but quartz is more common overall. The grains show a complete range of sphericity and roundness. The medium sized and larger grains are well rounded with moderate to high sphericity. The smaller grains are more angular and less spherical. Some of the quartz grains show optically continuous overgrowths. Sporadic well rounded spherical microcrystalline dolomite clasts and poorly preserved ooids and peloids are also present. The ooids are about 0.17 mm diameter and have a poorly preserved multi-walled structure with a radial fabric.

The sample is cut by a number of small ?syndepositional microfaults and has generally disturbed lamination and bedding.

Interpretation

This specimen is interpreted as representing fluctuating energy conditions, regularly emergent from shallow marine. The anhydrite cement is probably replacive and may be a later remobilization of original sulphate evaporites. The terrigenous clastics indicate a metamorphic provenance.

DOLOSTONE, STYLOLAMINATED MUDSTONE TEXTURE, WITH
CAULIFLOWER CHERT CONTAINING CONCRETIONARY PISOIDS

Description

This hand specimen is a laminated grey (N5) carbonate mudstone with several thin dark ferruginous seams and a siliceous ?displacive nodule (a cauliflower chert).

Microscopically, the laminations in the carbonate mudstone are clearly stylolitic. The bulk of the rock is fine grained to microcrystalline turbid dolomite with up to 20 percent fine grained to silt-sized corroded detrital quartz and feldspar.

The dolomite hosts a ?displacive cauliflower chert containing secondary coarse grained sparry calcite with saddle dolomite, sparse euhedral authigenic and xenotopic megaquartz crystals and radiating fibrous quartzine and length-slow lutecite, in turn ?replacing the calcite. Patches of primary anhydrite, replacement barite and possible celestite are associated with opaque heavy minerals. Individual lathes of anhydrite are commonly enclosed poikilotopically in megaquartz. Rare poorly preserved relict concretionary ?pisoids up to 1.2 mm diameter are discernible as ghosts in the coarse calcite spar in the nodule. They are best observed in reduced intensity plane polarized light and are least altered near the edge of the slide. The internal structures are weakly birefringent and are only obvious at 180° rotations of the stage. The ?pisoids have up to 10 dark concentric shells, no obvious radial structure and lack a nucleus. They are almost certainly concretionary in nature; the calcite spar being a replacement of a pre-existing spherulitic structure. However, it is not possible to determine the original mineralogy of the concretionary ?pisoids.

Interpretation

This texture is interpreted as a siliceous replacement of an original evaporite nodule.

Paragenesis

The suggested paragenesis for this sample involves replacement of sulphate evaporite by saddle dolomite, calcite spar and various forms of silica. The relative timing of the different generations is difficult to ascertain but it appears that an original anhydrite nodule has been altered to barite which was in turn partially replaced by a rim of penecontemporaneous saddle dolomite and sparry calcite. Pseudo-fibrous lutecite, fibrous quartzine and xenotopic quartz then corroded and replaced some of the dolomite and calcite. The saddle dolomite is also being replaced by coarse calcite spar.

SAND/SILT/CARBONATE MUDSTONE SET

Description

Macroscopically, this specimen consists of thin interbeds (to 1.0 cm) of olive grey (5Y 4/1) carbonate mudstone, light olive grey (5YR 5/2) sandstone and siltstone, and light olive grey (5Y 6/1) silty carbonate mudstone. These are arranged as stacked fining-up triplets.

In thin section, the carbonate mudstones show minor dolomitization and vague incipient stylolitic pressure dissolution.

The sandstone is poorly sorted and ranges from quartzose to feldspathic with a closed framework and a mixture of micritic and sparry calcite cement. The largest grains are medium grained and the unit fines up through siltstone with increasing carbonate mud matrix to a silty carbonate mudstone. Rare fine grained quartz and feldspar clasts are present throughout the set.

Interpretation

These sand/silt/mudstone sets are analogous to similar examples from modern intertidal to subtidal mixed sand-mud flats.

ANHYDRITE, 'CHICKEN-WIRE' TEXTURE

Description

This specimen was taken from a bed of 'chicken-wire' anhydrite. It is mottled light (N7) to medium light grey (N6) in hand specimen.

In thin section, the rock consists of interlocking acicular to fibrous anhydrite crystals. Rare irregular silty carbonate mudstone inclusions are present.

The felted mass of anhydrite crystals shows an undulating preferred parallel orientation with respect to bedding. On a larger scale this lineation is locally disturbed and the long axes of the anhydrite crystals form concentric zones sub-parallel to the edges of centimetre sized areas which are defined by stringers of mudstone inclusions.

Interpretation

This fabric suggests an original 'chicken-wire' texture similar to that found in gypsum/anhydrite beds on modern sabkhat. The evaporite grew displacively in the sediment, starting with individual clumps of crystals. The crystals initially became oriented in layers; then as the nodules coalesced, the crystal orientation changed to define the edges of individual nodules. The thin mudstone stringers between the nodules are remnants of the host sediment which has been displaced by the growth of the evaporite.

THROMBOLITIC ALGAL BINDSTONE

Description

This sample is massive dark grey (N3) with vague medium grey (N5) mottles and has a texture most resembling thrombolitic algal bindstone in hand specimen.

Mineralogically, the thin section consists of roughly equal amounts of turbid microcrystalline to finely crystalline secondary dolomite intermixed with irregular mottles of more coarsely crystalline calcite. Some of the larger calcite mottles contain incipient silicification including colloform and fibrous chalcedonite. Thin dark irregular laminae between areas of different crystalsize are probably a relict algal fabric although no individual filaments have been preserved.

Interpretation

This texture has been described as 'grumeleuse' and represents a relict clotted algal fabric. The rock has been subsequently dolomitized and partly silicified.

ONCOID WACKESTONE

Description

In hand specimen, this rock is medium dark grey (N4) mottled by abundant black (N1) parallel sets of irregular stylolites. Vaguely defined rounded features up to 2.5cm diameter are present. These are interpreted as oncoids or algal balls.

In thin section, the oncoids consist of overlapping poorly preserved cryptalgal coatings around a mottled and disturbed carbonate mudstone nucleus.

The surrounding micritic carbonate mudstone contains poorly preserved peloids and small fragments of bioclastic debris, including possible trilobite fragments.

The sample also contains numerous stylolites and patches of secondary chert.

Interpretation

The presence of oncoids, peloids and other bioclastic debris in a micritic matrix suggests deposition in quiet water shallow marine conditions. The stylolites and chert are diagenetic.

STYLOLAMINATED CARBONATE MUDSTONE

Description

This sample is a laminated to thinly bedded carbonate mudstone in hand specimen; alternating from an internally microlaminated dark grey (N3) to medium grey (N5).

In thin section, the dark microlaminations are stylolitic in nature and consist of turbid clayey ferroan dolomite with local concentrations of corroded silt-sized detrital clastics and very finely crystalline euhedral dolomite rhombs. The stylocumulate material occurs as discontinuous wispy lens often terminating in horse-tail stylolites, or as relatively discrete thin beds which follow original variations in lithology.

The paler laminae and thin beds range from silty micritic carbonate mudstone to bioclastic mudstone and wackestone. Well rounded micritic spheroids to 0.1 mm diameter (?calci-spheres) and elongate bioclasts including trilobite hooks and fragments of carapace are present. Burrowing is also evident.

Interpretation

The presence of burrows and fossils suggests a shallow marine origin. The silt-sized detrital clastic grains indicate some allochthonous input. This variation in lithology has been enhanced by pressure solution, resulting in the alternation of the stylocumulated clastics and reactate ferroan dolomite with the unaltered silty micrite.

LAMINATED CARBONATE MUDSTONE

Description

In hand specimen, this is a well laminated dark grey (N3) to medium dark grey (N4) carbonate mudstone with small scale cross laminations and rare smooth, well defined stylolites.

In thin section, the laminations appear to result from different degrees of dolomitization of intrinsically different carbonate mudstones defined by variations in crystal sizes. Several of the laminae also contain slightly more of the sporadic fine grained quartz and quartz silt or local concentrations of peloids. Most of the terrigenous material is detrital and some small euhedral grains may be syntaxial overgrowth.

Vaguely defined burrows or water escape structures are present.

Interpretation

A shallow marine environment of deposition is inferred. The different degrees of dolomitization which now define the laminae probably reflects an original lamination of micritic and more coarsely crystalline calcite.

STYLONODULAR CARBONATE MUDSTONE

Description

In hand specimen, this rock shows irregular shaped boudin-like medium grey (N4) and dark grey (N3) mottles about 1 cm thick in dark grey (N3) laminated matrix.

In thin section, the dark patches are clayey stylolaminated ferroan dolomite. The boudin-like nodules are laminated to thinly bedded slightly dolomitic to micritic clayey carbonate mudstone. Some of micritic laminae contain local concentrations of peloids. Sporadic biocalstic debris including fragments of trilobites occurs throughout. Possible bioturbation or water escape structures are also evident.

Interpretation

This stylonodular texture consists of isolated nodules of original micritic carbonate mudstone in a matrix of reactate. Pressure solution appears to have accentuated an original difference in lithology. At least one irregular unstylolitic contact between partly dolomitized clay-rich carbonate mudstone and a paler carbonate mudstone with abundant fine grained to silt-sized quartz remains unaltered.

QUARTZ FELDSPATHIC WACKESTONE/CARBONATE MUDSTONE

Description

This specimen is a speckled medium light grey (N6) arenaceous carbonate mudstone grading to wackestone.

Microscopic examination shows that the turbid micritic carbonate mudstone matrix contains sporadic to locally common (>25 percent) fine grained to silt-sized detrital quartz and feldspar clasts. These grains are slightly corroded, rounded to well rounded with moderate to high sphericity. Rare carbonate intraclasts, euhedral dolomite rhombs, sporadic ?detrital opaque heavy minerals and ?detrital muscovite and biotite are also present. Where the clasts are locally concentrated, the rock has a wackestone texture.

Staining with Alizarin Red-S and potassium ferricyanide shows that the matrix consists of clay-rich micrite and ferroan dolomite.

The sample contains sporadic small pores up to 0.6 mm across. The walls of the pores are often stained by oxides.

Interpretation

The presence of detrital terrigenous clastic grains in a micritic carbonate mudstone is a textural inversion, indicating very sporadic periods of higher current energy or possibly aeolian input, into a predominantly quiet water environment. The detrital quartz, feldspar, mica and heavy minerals suggests an igneous or metamorphic provenance.

STROMATOLITIC ALGAL BINDSTONE, PRESSURE SOLUTION TEXTURE

Description

In hand specimen, this rock is a mottled medium grey (N5) partly dolomitized micrite with abundant thin greyish black (N2) draped laminae and internally disturbed nodular areas. The texture suggests an original laminated algal fabric.

Staining with Alizarin Red-S and potassium ferricyanide highlights areas of ferroan dolomitization which occur preferentially in the zones of most concentrated fine lamination. In thin section, some of the fine dark laminae appear to be stylolitic overprints but the laminae grade laterally into the primary micrite where they are interpreted to be of cryptalgal origin. The fabric is defined by stacked layers of carbonaceous material, clay and micrite alternating with more coarsely crystalline carbonates and detrital clastic grains. Micro-fenestrae are abundant in the crenulated cryptalgal laminae and sporadic throughout the remainder of the slide.

Some of the patches of disturbed lamination in the nodular areas contain abundant peloids and are interpreted as burrows; others appear to be dewatering structures.

Interpretation

This sample is interpreted as an original cryptalgal laminated stromatolitic algal bindstone which has been partly dolomitized as a result of pressure solution. The original silty, more coarsely crystalline calcite laminae have been preferentially removed, resulting in compaction of the areas of stylolite and reactite relative to the unaltered areas. This results in a texture reminiscent of a stylonodular texture.

SAND/SILT/CARBONATE MUDSTONE SETS

Description

In hand specimen, this rock consists of thinly interbedded sets of greyish orange pink (5YR 7/2), light olive grey (5Y 5/2) and olive grey (5Y 4/1) sandstone, siltstone and mudstone.

Cyclic fining-upwards sets of thinly bedded sand/silt/carbonate mudstone are evident in thin section. Sets range from over 2 cm to less than 1 cm thick. The base of the sandstone is erosional in some cases. The grains include abundant carbonate intraclasts, detrital quartz, feldspar and rare ooids and peloids. The terrigenous clastic grains range from medium to fine grained. The majority of the quartz is monocrystalline grains, but composite, recrystallized metamorphic and stretched metamorphic grains are also present. These are accompanied by very coarse to very fine grained carbonate clasts. Sorting is moderate to poor. The clasts are angular to subrounded with sphericities ranging from low to moderate. Rare anhydrite is present in clumps in the sandstone at the bottom of the slide. Sporadic heavy minerals occur throughout and are locally concentrated toward the base of the sandstones.

In each set, the sandstone grades to siltstone. The silt-sized grains are angular to subangular and have moderate to low sphericity. Laterally discontinuous carbonate mudstone ripples are present as drapes in the siltstone.

The siltstone is overlain by clayey mudstone which also contains sporadic very fine silt and rare finely crystalline calcite. The tops of some of the mudstone units have very small scale mudcracks.

Interpretation

The stacked sand/silt/mud sets are interpreted as having been deposited on clastic-dominated mixed siliciclastic/carbonate 'tidal' flats. The detrital clastics were derived from a metamorphic terrain. The mudcracks and clumps of anhydrite suggest subaerial exposure.

LAMINATED AND SILTY CARBONATE MUDSTONE

Description

This rock is a thinly bedded to vaguely laminated greyish black (N2) to black (N1) carbonate mudstone.

Laminations become clearer in thin section. The rock consists of turbid dolomitic carbonate mudstone with fine grained to silt-sized quartz and feldspar grains. The darker thin beds and laminae are defined by diffuse clays and authigenic ?haematite. Very fine grains of other opaque isotropic heavy minerals and possible sponge spicules occur sporadically throughout.

Interpretation

This sample was probably deposited in relatively quiet water conditions with limited terrigenous clastic input.

FELDSPATHIC SANDSTONE, HALITE CEMENT

Description

This rock is a speckled greyish red (10R 4/2) moderately consolidated sandstone in hand specimen.

In thin section, it consists of a closed framework of detrital quartz (85 percent) and feldspar (to 15 percent) grains in an impure halite cement.

The majority of quartz grains are monocrystalline, extinction varies from slightly to strongly undulose. Lines of inclusions and vacuoles are very common. Microlites are present only in rare grains and, even then, never abundant. Semi composite and composite grains are present. Both stretched metamorphic and recrystallized metamorphic quartz grains are also present, but confined to the larger grain sizes.

The feldspars include, in decreasing order of abundance; orthoclase, microcline, plagioclase. The latter includes quite fresh albite.

The sample varies from medium to fine grained, is moderately to locally well sorted, with subangular to rounded grains. The larger grains are well rounded with moderate to high sphericity. There are also rare well rounded high sphericity carbonate clasts.

The cement is halite (isotropic under crossed nicols) with diffuse clays, minor anhydrite and rare silica cement. The anhydrite occurs as discrete nodules to 5.5 mm across which are comprised of a felted mass of lathes. Rare coarsely crystalline anhydrite also occurs as a cement interstitial to the grains.

Interpretation

The halite cement and anhydrite nodules are believed to be primary, indicating an evaporative environment of deposition. The detrital clastics suggest a reasonably close metamorphic and igneous source.

GYPSUM AND ANHYDRITE VEIN

Description

This sample is from a 3 cm thick multi-layered gypsum/anhydrite vein parallel to bedding. The vein ranges in colour from medium light grey (N5) to very light grey (N8).

Microscopic examination (Figure 52) reveals that the multi-layering of the vein is related to variation in crystal form and mineralogy. The two outer zones are fibrous gypsum and microscopically amorphous anhydrite. The inner zone is composed of tabular gypsum crystals.

The fibrous gypsum (1) is arranged with bundles of fibres perpendicular to the vein. Rare anhydrite needles occur sporadically dispersed between the gypsum fibres, and some of the fibrous gypsum shows alteration to an almost isotropic very pale brown translucent mineral (2). A thin disturbed zone (3) of intermixed matted fibres and anhedral gypsum crystals separates the fibrous gypsum from the large tabular gypsum crystals (4). The latter crystals range up to 3 mm long and are oriented perpendicular to the vein. Twinning is common. The contact between the tabular gypsum and the anhydrite is irregular with embayments corresponding to the terminations of the gypsum crystals. The anhydrite (5) displays typically high birefringence and occurs as interlocking lathes.

Interpretation

This vein shows the co-existence of gypsum and anhydrite as late stage vein infill.

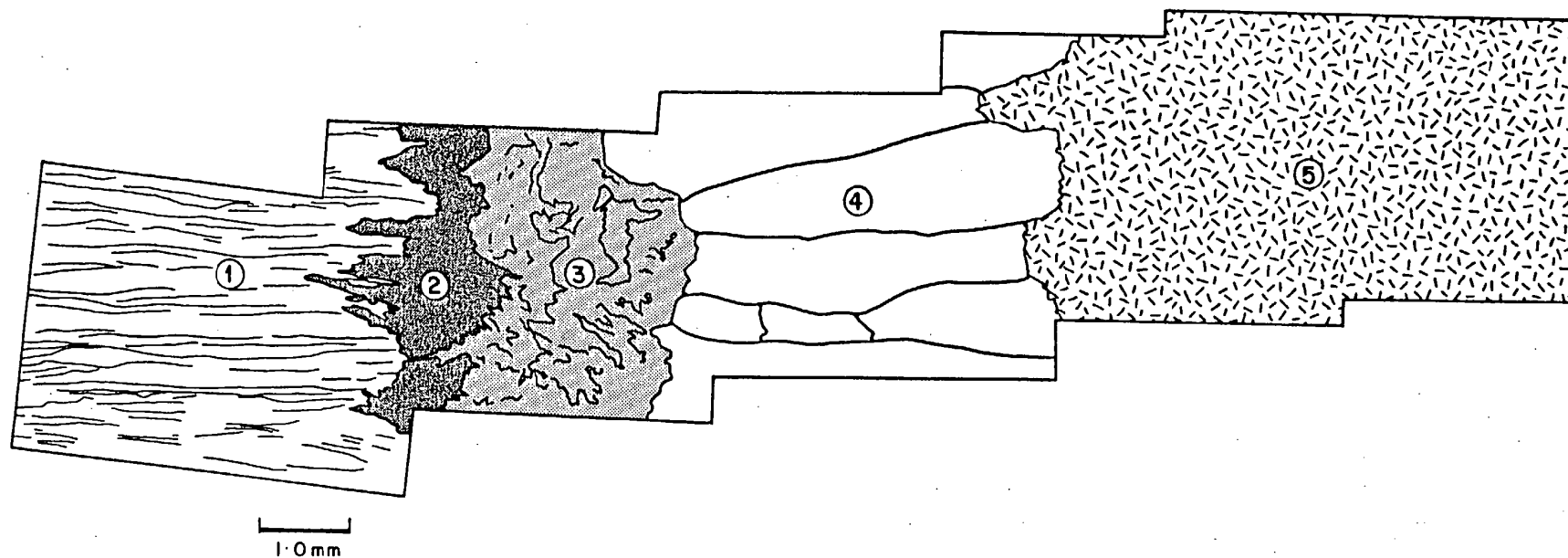


FIGURE 52: GYPSUM AND ANHYDRITE VEIN
THIN SECTION COM670, MARLA-7, 364.50 m.

- (1) FIBROUS GYPSUM
- (2) GYPSUM ALTERED TO PALE BROWN MINERAL
- (3) MIXED ZONE OF GYPSUM
- (4) TABULAR GYPSUM CRYSTALS
- (5) ANHYDRITE LATHES.

CARBONATE MUDSTONE HOSTING CHERT NODULES

Description

In hand specimen, this rock is laminated dark grey (N3) carbonate mudstone with abundant very light grey (N8) mottles. The mottled area is adjacent to a well developed low amplitude irregular stylolite. Rare disseminated pyrite was also recorded in the vicinity of this sample.

Microscopically, this specimen consists of moderately dolomitized silty micrite with large irregular patches of paler coloured and brown colloform chalcedonic to isotropic opaline silica.

The mudstone contains sporadic ?carbonaceous wisps up to 1 mm across and discontinuous horsetail stylolites parallel to bedding. It also contains abundant sub-angular quartz and feldspar silt and rare ?detrital muscovite.

The silicified areas appear to be replacing anhydrite/gypsum. Many of the chalcedonic colloform spheroids have a nucleus of gypsum which rarely retains a corroded euhedral habit. This gypsum, in turn, contains rare very small euhedral to anhedral anhydrite crystals. Many of the colloform bodies show further generations of 'aggregate' silica overgrowth consisting of an intimate mixture of pseudo-fibrous length-show lutecite and concretionary chalcedonite. These are more evident in plane polarised light. Rarely, these overgrowths include dolomite rhombs and opaque heavy minerals, possibly pyrite.

Interpretation

Possible scenarios for the diagenesis of this rock must include anhydrite/gypsum growth in the original mudstone; replacements of anhydrite/gypsum by colloform chalcedony; followed by several further generations of silicification which may have preceded contemporaneously with dolomitization and pyritization.

GRANULE CONGLOMERATE/COARSE FELDSPATHIC SANDSTONE, GYPSUM CEMENT

Description

This granule conglomerate/sandstone sample comes from a thin bed with an erosional top and bottom. It is overlain by laminated dolomitic mudstone and underlain by grey and reddish brown moderately calcareous mudstone and siltstone.

Greyish brown (5YR 3/2), dark reddish brown (10R 3/4), greenish black (5GY 2/1), greenish grey (5GY 6/1) and pale red (10R 6/2) clasts are visible in hand specimen. The matrix/cement is translucent pale red (10R 6/2).

In thin section, this specimen consists of very poorly sorted detrital granules to very fine grains of quartz, feldspar, basaltic rock fragments, chert, and detrital muscovite and chlorite in an altered gypsiferous, silty to clayey dolomitic carbonate matrix/cement.

The detrital quartz includes monocrystalline, semicomposite, composite, stretched metamorphic, recrystallized metamorphic and rare ?vein quartz grains. Microcline, orthoclase, plagioclase and perthitic grains are all represented amongst the feldspars. Lithic grains include basaltic rock fragments, chert, silicified and partly silicified dolostone, dolostone with a relict peloidal texture, and calcareous carbonate mudstone.

The grain size shows a bimodal distribution. The larger framework clasts range from about 0.6 mm diameter to a maximum of 4 mm diameter, with an average of about 2 mm diameter (coarse grained). This population is rounded to well rounded; although some grains show diagenetically corroded edges. Sphericity varies from moderate to high. The micritic and dolomitic carbonate mudstone clasts are rounded to well rounded.

The second population of grain size ranges from just over 0.1 mm (very fine) to silt-sized and constitutes up to 40 percent of the matrix. These grains are angular to subrounded and have moderate to low sphericity.

Seventy percent of the matrix/cement consists of altered gypsum. This material is pale brown in plane polarized light and isotropic in part, and includes small clumps of anhydrite; rarely euhedral. Several feldspar grains appear to be breaking down in situ and being replaced by gypsum. Patches of the matrix/cement are carbonate; varying from silty and clayey microspar to micrite with moderate dolomitization.

Interpretation

The presence of euhedral sulphate evaporites and cements indicates an evaporative environment of deposition. The source of the bimodal terrigenous clastics indicates a diverse provenance; but the bimodal size distribution with well rounding and high sphericity of one size fraction might suggest reworking.

COARSE TO VERY COARSE FELDSPATHIC SANDSTONE, GYPSUM CEMENT

Description

This sample is a mottled greyish red (10R 4/2) and moderate red (5R 5/4) moderately well consolidated sandstone with a pale red to translucent cement.

In thin section, the rock consists of detrital quartz and feldspar grains and carbonate clasts in a fine grained matrix with altered gypsum and dolomitic carbonate cements. The grains are poorly sorted, ranging in size from 3.0 mm diameter (granule) to 0.125 mm diameter (fine grained) with an average of about 1 mm (coarse to very coarse). The quartz includes mono and polycrystalline grains. The feldspars include microperthites, antiperthites, microcline and orthoclase. Rare ?metamorphic and ?basaltic rock fragments and clasts of dolomitic carbonate are also present. Some of the dolomitic clasts range from well rounded to subangular; the coarser grains tending to be better rounded with higher sphericity. Rare peloids and micritized ooids are also present.

The gypsiferous matrix/cement contains fine grained to silty subangular to subrounded grains of quartz and K-feldspar. Minor carbonate cement is also present. The gypsum is altered to a brown near isotropic state with sporadic small euhedral to anhedral anhydrite crystals throughout. The subordinate carbonate cement occurs as laminae and diffuse patches. It is moderately dolomitic, with sporadic small internally-zoned euhedral rhombs.

Interpretation

The provenance of the detrital terrigenous clastics suggests a diverse source including metamorphic, basaltic, igneous, and carbonate terrains. The gypsum cement shows some evidence of remobilization but the presence of euhedral crystals indicates deposition in evaporitic conditions.

MEDIUM GRAINED FELDSPATHIC SANDSTONE, DOLOMITIC
CEMENT/MATRIX

Description

This sample comes from a one metre thick sandstone and siltstone bed. Large dolomitic mudstone clasts are a feature of this unit. In hand specimen, the rock is speckled medium dark grey (N4).

In thin section, this rock consists of detrital quartz, feldspar and carbonate grains in a silty dolomitic matrix/cement.

The carbonate grains range in size from up to 2.0 mm diameter (very coarse grained) to less than 0.125 mm diameter (very fine grained). The terrigenous grains range from up to 1.25 mm diameter (very coarse grained) to less than 0.25 mm (fine) averaging about 0.3 mm diameter (medium grained). Sorting is moderate. The grains are subangular to subrounded with some larger rounded grains. Sphericity ranges from low to high; the larger grains also tending to have the higher sphericity. The feldspars include orthoclase, microcline, and sporadic perthite/ antiperthite. Locally, the feldspars exceed 30 percent of the total composition and these areas are strictly ARKOSIC SANDSTONE. The quartz is mono and polycrystalline with undulose extinction. Staining indicates that the carbonate clasts are micrite. Some have gypsum inclusions/replacements and several contain ooids and peloids.

The matrix/cement includes fine grained to silt-sized quartz and feldspar grains and clays. It is predominantly dolomitic with minor recrystallization textures and possible haematitic staining.

Interpretation

The large amount of feldspar and metamorphic quartz suggests a metamorphic/igneous provenance. The angularity of some of the feldspar grains indicates only moderate maturity. The presence of primary sulphate evaporites in angular carbonate clasts shows the proximity of an evaporitive terrain, while the ooids and peloids probably indicate a shallow marine origin.

OOID AGGREGATE GRAIN GRAINSTONE/PACKSTONE PARTLY SILICIFIED
FELDSPATHIC SANDSTONE, DOLOMITIC MATRIX/CEMENT

Description

This sample was taken from a thin lenticular bed of silicified ooid grainstone within a dolomitic sequence containing algal bindstones, imbricated intraclasts, disturbed laminae, stylolites and gypsum/flourite/calcite veins.

The hand specimen is mottled to speckled medium dark grey (N4) with areas of dusky yellow (5Y 6/4) to moderate brown (5YR 4/4).

The thin section shows two main lithologies with a complex diagenetic history. The bulk of the specimen consists of:

OOID GRAINSTONE, PARTLY TO WHOLLY SILICIFIED, MINOR SPHALERITE.

The ooids occur in a moderately open relict grainstone framework and consistently average about 0.8 mm diameter and vary from completely to slightly chertified. A relict multiwalled fabric is visible in plane polarized light. Radial fabric is only rarely preserved. Up to 6 concentric walls are discernible; the nucleus varies from less than one third to up to two thirds of the overall diameter and consists of relict micritic material, small aggregate grains or less commonly a euhedral dolomite rhomb (possibly recrystallized in situ). Relict aggregate grains containing up to 8 ooids are also present.

Interpretation

The cement fabric is believed to represent original carbonate cements, of both vadose and phreatic origin, now pseudomorphed by silica.

The initial open framework of ooids, coated aggregate grains and carbonate clasts are shown in Figure 53a. The aggregate grains have a micritic matrix which contains faint outlines of a possible multilayered concentric cement. Therefore, these clasts may, themselves, represent reworked micritized grainstones. The first generation of cement, visible in the lower portion of Figure b forms a thin brown ?isopachous rim to the larger aggregate grains and isolated ooids. No relict texture is visible. Figure c shows a

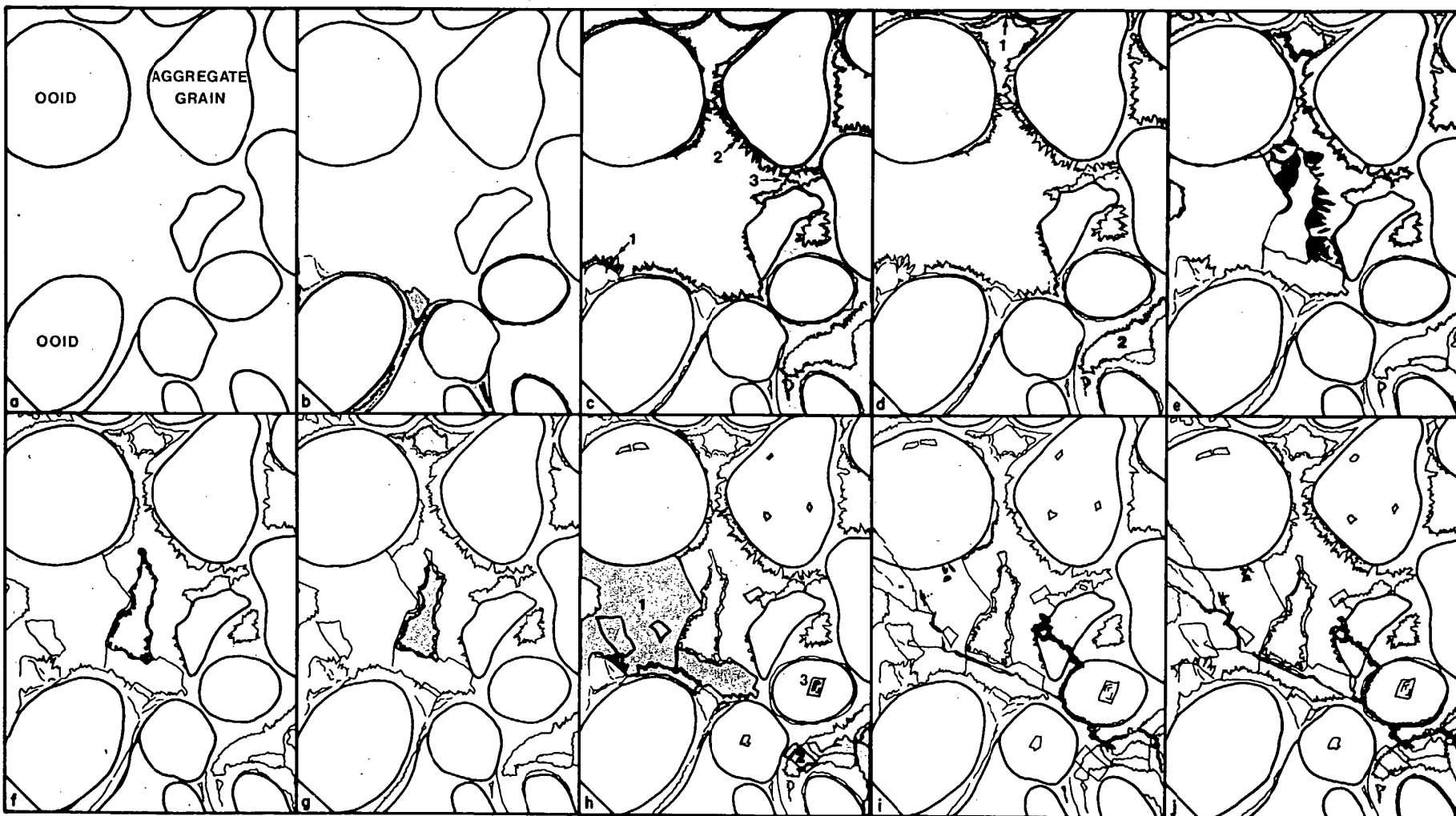


FIGURE 53: HISTORY OF CEMENTATION OF AN OOID GRAINSTONE LENS,
THIN SECTION COM682, MARLA-6, 679-33m.

transparent meniscus cement. It bridges gaps between adjacent grains, is thicker and of less uniform crystal size where the grains are close, and is discontinuous or absent from the walls of the larger voids. At least two crystal morphologies can be identified. The most abundant is bladed dog-tooth spar (Flügel, 1982) (1). Accumulations of opaque heavy minerals occur within the base of some of these bladed crystals (2). This texture grades to botryoidal cement (3). This difference cannot be attributed to orientation. Such meniscus cement originates in the vadose zone by carbonate precipitation from capillary films (Longman, 1982). The dog-tooth crystal form is somewhat unusual in a vadose setting, it is normally taken as indicative of meteoric water, possibly in the subtidal and intertidal zones (Flügel, 1982). The third generation of cement is pendant from the roof of some cavities (Figure d, 1) and completely infills smaller isolated voids (2). It consists of clear blocky crystals and represents a continuation of vadose precipitation. The fourth generation shown in Figure e is a dark brown botryoidal cement, now consisting entirely of silica. The crystals are arranged with the long axes diverging into the cavity, and have a characteristic fan-like undulose extinction. If this represents a relict radial fibrous ferroan calcite cement, it may be interpreted as submarine (Kendall and Tucker, 1973) or vadose (Bechstadt, 1974). Figure f shows a very thin, often discontinuous rim of clear stubby bladed spar and dog-tooth spar which constitutes the fifth generation cavity lining. This cement may have been precipitated under phreatic conditions. The final cavity fill shown in Figure g consists of clear anhedral to subhedral crystals of secondary quartz with larger crystals in the cavity centre. Extinction is uniform and 180° enfacial junctions are common. Drusy calcite cements with such textures may form in submarine or subaerial conditions with the crystals growing from free surfaces in supersaturated solution (Flügel, 1982).

Figure h (1) shows the first evidence of diagenesis which destroys the original fabric. The stippled area consists of a slightly turbid intimate mixture of calcite, dolomite and silica which partly pseudomorphs pre-existing cements and partly obscures previous textures. Coeval euhedral rhombs of dolomite and silica after dolomite occur as non-fabric selective recrystallizations of previous cements (2), and as possible recrystallizations of original ooid nuclei (3). Many of the rhombs have an internal curved plane of extinction and concentric internal zonation, suggesting saddle dolomite. Sphalerite has formed preferentially along crystal boundaries or microfractures (Figure i). Elsewhere in the thin section, sphalerite almost completely replaces pre-existing cements and ooids. Figure j shows the superimposed cements as traced from a photograph.

The sample is cut by a thin deformed area parallel to the bedding of the surrounding strata. In this zone, secondary dolomitization and iron oxides have preserved the strongly deformed ooids (spastoliths).

A zone of incipient stylolitization; now overprinted by sphalerite; separates the ooid packstone from the next lithotype.

FELDSPATHIC SANDSTONE, DOLOMITIC MATRIX/CEMENT.

This lithotype consists of a microcrystalline to fine grained recrystallized turbid (possibly carbonaceous) dolomite matrix containing very poorly sorted detrital quartz, feldspar and carbonate grains. The detrital quartz and feldspars range from highly angular, low sphericity grains to rounded, moderate sphericity grains; and from in excess of 2 mm (granule) to silt-sized. Locally, they are subordinate to the dolomitic matrix and these areas are strictly QUARTZ FELDSPAR PACKSTONE.

MASSIVE SECONDARY DOLOSTONE, NO RELICT TEXTURE

Description

This sample was taken from a 1.7 m thick bed containing abundant stylolites, calcite veins and small calcite nodules.

It is an aphanitic massive medium dark grey (N4) carbonate mudstone in hand specimen.

In thin section, 80 percent of the rock consists of xenotopic equigranular very finely crystalline (up to 0.07 mm) turbid dolomite. Larger euhedral dolomite rhombs are moderately abundant and scattered throughout. The remaining 20 percent of the specimen is gradational to an idiomatic texture with secondary calcite spar. The calcite is locally concentrated into small irregular patches which make up a thin discontinuous veinlet across the slide. In places, this sparry calcite includes euhedral dolomite rhombs.

What little visible porosity the rock does display is in rare scattered very small vugs bordered by discrete dolomite crystal faces.

Interpretation

This dolomite shows a diagenetic recrystallization texture.

CHERT AND CARBONATE MUDSTONE BRECCIA, FLOATSTONE/RUDSTONE TEXTURE

Description

This sample contains angular clasts of moderate orange pink (10R 7/4) and light olive grey (5Y 5/2) mudstone and banded grey (N7 to N5) chert in a yellowish grey (5Y 7/2) matrix. The overall unit is about 2 m thick. At its base, the matrix of the unit grades down to a fine grained light brownish grey dolomitic sandstone which disconformably overlies a thick carbonate sequence. The clasts decrease in abundance towards the top of the breccia and it grades to a grey limestone with a mudstone texture. The largest clasts in hand specimen exceed 2.5 cm across. This sample has a strong bright yellow natural fluorescence under long wavelength UV light.

In thin section, at least 65 percent of the sample consists of a random, open framework of angular to subangular, low to moderate sphericity clasts with a size range of 1 mm to 15 mm. These clasts consist of leached chert and carbonate mudstone. The siliceous clasts include microcrystalline, fine grained, and cherty quartzites, the edges are often corroded. The microcrystalline clasts include abundant small voids and rare small euhedral dolomite rhombs, probably indicating subaerial weathering. The carbonate mudstone clasts vary from recrystallized microcrystalline dolomite to slightly dolomitic turbid limestone.

The matrix/cement consists of subhedral to euhedral sparry calcite crystals, averaging about 0.3 mm across. This incorporates scattered euhedral dolomite rhombs (to 0.05 mm) and patches of chalcedonic silica. The matrix/cement has rare small visible voids often bordered by idiomorphic faces of large calcite crystals, but may have considerable intercrystalline porosity as well. In combination with the leached chert clasts; the overall rock has quite good porosity.

Interpretation

This rock was originally a sedimentary breccia which contained chert and carbonate mudstone clasts in a calcareous matrix. The sample has been leached

during diagenesis with dolomitization of the calcareous clasts and matrix and corrosion of the cherts. The formation of the calcite spar was an on-going replacement of other minerals and as a partial void filling cement.

RELICT MICRITIZED INTRACLASTIC OOID PELOID GRAINSTONE

Description

The matrix of this hand specimen grades from mottled greyish black (N2) to light to very light grey (N7 to N8), and contains abundant angular to well rounded greyish black clasts.

In thin section, the paler matrix colours can be attributed to a replacive siliceous cement; the darker colours are porous dolomite matrix/cement. The clasts consist of rounded to well rounded intraclasts, possible relict ooids and peloids. The relict ooids average just over 0.5 mm diameter. They are almost all replaced by dolomite or silica (?micritized then dolomitized or silicified); their original structure can only be inferred from a few individuals which retain a relict radial and concentric fabric and from the similarity in size of these coated particles.

The preservation and type of cement varies across the sample. Lower in the specimen, a very thin isopachous cement is replaced by a clear radially fibrous chalcedonic silica; this is superseded by a thicker isopachous turbid pale brown botryoidal to pseudo-colloform silica cement. The final cavity fill is now a transparent equigranular fine grained quartz, with the largest crystals in the centre of the cavity.

Several larger inter-oid cavities are lined by a relatively thick rind of pale brown isopachous cement. This cement shows a concentric zonation in plane polarized light. Under crossed nicols, this is evident as a superimposition of areas of fan like undulose extinction.

A vuggy recrystallized ?xenotopic dolomitic cement remains at the very top of this thin section; it provides good porosity. Elsewhere in the hand specimen, the ooids/peloids/intraclasts have been selectively leached resulting in excellent oomoldic porosity.

Interpretation

It is assumed that the relict cement textures can be attributed to original

calcite cements since the whole rock, including both cement and clasts, has been pseudomorphed by silicification. This being the case, the sample was probably a shallow marine deposit in an area of moderate energy, possibly a small debris flow. The complex diagenetic history includes micritization (?stagnant marine phreatic zone) and dolomitization (?mixing zone). The isopachous rinds may indicate active marine phreatic cementation. The final cavity fill may be subsurface late diagenetic or possibly an active freshwater phreatic zone cement. The rock has then been partly silicified.

SAND/SILT/CARBONATE MUDSTONE SETS

Description

This hand specimen shows stacked fining-up sets of grey (N4 to N7) sand/silt/carbonate mudstone. One thin sandstone interbed is reverse graded. There are abundant large rip-up clasts of carbonate mudstone and some light grey (N7) chert, possibly after nodular evaporites.

In thin section, the carbonate mudstones are mostly massive and amorphous to rarely microcrystalline slightly calcareous dolomites, which become more calcareous toward the top of the unit.

The reverse graded clastic-rich interbed grades up from the underlying carbonate mudstone as detrital quartz, feldspar and dolomitic limestone intraclasts increase in abundance. They range from silt-sized at the base of the unit, to 1.7 mm diameter (very coarse) at the top. The grains are mostly subangular to angular, with low to moderate sphericity. Some of the larger clasts are better rounded. The matrix of the unit is altered dolomitic carbonate mudstone.

This unit is overlain by a laminated carbonate mudstone. The contact is sharp. Many of the sand grains protrude up into mudstone and there are sporadic individual sand sized grains in the basal carbonate mudstone. The dolomitic carbonate mudstone appears to be contiguous with the unaltered matrix of the sandstone. There are thin wavy silty laminae throughout the carbonate mudstone, increasing in abundance towards the top of the unit. Randomly oriented lathes and needles (averaging 0.13 mm long) of a dark brown isotropic mineral also increase in abundance towards the top of the unit. The hand specimen shows a corresponding paler colour change and it is suggested that this mineral was originally gypsum or anhydrite which has been altered during the preparation of the slide. The top contact of this carbonate mudstone also shows possible mudcracks.

The overlying clastic sandstone exhibits a complex series of variations in grain size; possibly due to eddy effects around the large (up to 6 cm x 1 cm) mudstone clasts. The overall grain size change is a poorly sorted fining upward sequence. The largest of the quartz and feldspar grains exceed 2.5 mm

(granular) and range to silt-sized. The majority of the grains are moderately to well rounded, but show a complete range of sphericities.

There are small patches of knotted gypsum scattered throughout the sandstone/siltstone. In places it has been altered to the dark brown isotropic condition mentioned above; elsewhere it grades to anhydrite. It hosts a lens-shaped area of slightly turbid chalcedonic to microcrystalline silica. Larger areas of chert after evaporites are visible in hand specimen.

The sandstone/siltstone set is overlain by another carbonate mudstone. The contact is sharp but irregular.

Interpretation

The presence of original evaporite in stacked sand/silt/mud sets indicates an evaporite environment of deposition with fluctuations of energy conditions and periodic emergence.

DOLOSTONE, RELICT ?INTRACLASTIC WACKESTONE TEXTURE

Description

This sample is mottled medium dark grey (N4) to medium light grey (N6) wackestone with vague well rounded dark grey (N3) structures visible in hand specimen.

Mineralogically, the sample consists entirely of recrystallized xenotopic dolomite. Crystalsize varies in patches across the slide from microcrystalline to very coarsely crystalline. Some of larger crystals are subhedral and may be saddle dolomite. These patches partly correspond to a relict intraclastic wackestone texture clearly visible in hand specimen but just discernible in thin section under plane polarized light. The intraclast ghosts vary in size from 6 mm to less than 1 mm; are generally well rounded; and lack any visible outer coats or internal structures. Less than 10 percent of the clasts exceed 2 mm across. They are inferred to have been original carbonate mudstone clasts.

This slide shows quite good visual porosity in small scattered rounded pores averaging 0.13 mm diameter, which bear no relationship to the original texture.

Interpretation

The present mineralogy of this sample has resulted from wholesale replacement by dolomite. The dolomitization has only partly preserved the original texture.

RELICT OOID GRAINSTONE/PACKSTONE

Description

This ooid grainstone sample was taken from a thin interbed with an erosional top and which grades down to the underlying thinly bedded carbonate mudstone. The hand specimen shows two distinct secondary colour phases. One is a light grey (N7) matrix/cement containing greyish red (5 R 4/2) ooids; the other is a medium grey (N5) matrix/cement containing greyish black (N2) mottles.

In thin section, the lighter colour matrix/cement is revealed to be very fine to medium crystalline ?replacement siliceous cement. It contains silicified ooids with a preserved concentric multiwalled structure and a nucleus varying from one third to two thirds of the overall diameter. No radial fabric is visible. The ooids range in size from just under 0.5 mm to 1.5 mm diameter, averaging about 0.8 mm. Sporadic relict micritic intraclasts (because this is a horizontal section the 'intraclasts' may be the top of underlying bed) and rare aggregate grains containing two or three ooids are also present. The ooids commonly contain haloes of heavy minerals. There is some intraooid porosity.

The cements include a thin coat of very finely crystalline clear acicular to bladed silica arranged radially to the ooids. Interoid cavities are infilled by coarser interlocked clear equigranular quartz crystals. Presumably, the silica is pseudomorphing original carbonate cements.

The remainder of the slide corresponds to the darker colour phase visible in hand specimen. In thin section, this material is an irregularly mottled texture produced by almost complete dolomitization or micritization of the ooids and subsequent silicification. The fringing cement is absent, most of the clear silica is equigranular and medium grained. There are also areas of extremely turbid medium grained to amorphous ?chalcedonite and quartzine which rim the irregular mottles of relict dolomitic texture. This may also be a relict carbonate cement.

Interpretation

This specimen was probably originally gradational from ooid grainstone to

oid packstone. The ooids in the grainstone texture have been dolomitized or micritized and then silicified. The silica cements now present may be pseudomorphing original carbonate cements. The original micritic matrix and ooids in the packstone have also been partly recrystallized, possibly to dolomite, and then silicified.

DOLOSTONE, RELICT ARCHAEOCYATH BAFFLESTONE/FRAMESTONE

Description

This sample was taken from a 3 metre thick essentially unbedded sequence of archaeocyath bafflestone/framestone. The hand specimen is grey (N5 to N7) to pale olive grey (5Y 6/1).

Mineralogically, most of this specimen is amorphous to finely crystalline equigranular xenotopic secondary dolomite with very scattered euhedral rhombs to 0.5 mm across (medium to coarsely crystalline). Brown colloform and chalcedonic chert nodules averaging about 0.3 mm across occur sporadically throughout the samples. There are also locally abundant areas of drusy calcite spar and rare saddle dolomite associated with voids in the relict archaeocyath bafflestone texture. A poorly preserved algal mottled fabric is also present.

Individual archaeocyaths are only very poorly preserved in this section. One transverse section visible in hand specimen is represented in the thin section, but recrystallization has entirely obscured any microstructure.

Microstylolites are moderately common, they separate areas of different crystalsize and often outline the inner and outer walls of the archaeocyaths.

This specimen shows good porosity in vugs up to 5 mm across. They are scattered throughout the sample and are generally bounded by discrete dolomite crystal faces.

Interpretation

The original archaeocyath bafflestone/framestone texture of this sample has been largely obscured by dolomitization. The primary cavities have been filled by saddle dolomite and void-filling chalcedonite. Most of the saddle dolomite has been replaced by secondary calcite.

DOLOSTONE, RELICT ARCHAEOCYATH BAFFLESTONE/FRAMESTONE

Description

This sample comes from an essentially unbedded sequence of grey (N5 to N6) stylolitic fenestral archaeocyath bafflestone/framestone with good vuggy porosity.

Mineralogically, the large thin section is predominately amorphous turbid dolomite with irregular patches of chalcedonite; subordinate coarsely crystalline calcite (drusy) spar; coarse to granule sized euhedral (?saddle) dolomite rhombs; and rare euhedral quartz. The last three minerals also occur as infill to the archaeocyaths. The calcite spar also occurs in discontinuous veinlets which cut the other fabric.

At least fourteen individual archaeocyaths are visible in this sample. The thin section provides a range of transverse to longitudinal sections. Most archaeocyaths appear to be intact, but there is no obvious preferred growth position. Many of the archaeocyaths are surrounded by an indistinct texture of possible algal origin. A similar texture forms the lining to a cavity, where is tentatively attributed to Renalcis. Some of the archaeocyath cavities also contain geopetal sediments and overlying cavity filling cements. Boring and burrowing occur sporadically in the archaeocyath framework and algal binding, as well as in the geopetal sediments.

Interpretation

The presence of the archaeocyaths and algae indicates a shallow submarine environment of deposition. The diagenesis includes original wholesale dolomitization; formation of the ?saddle dolomite and chalcedony in original vugs and archaeocyath cavities; and the replacement of some dolomite by coarse secondary calcite spar. This calcite is the same generation as present in veinlets.

DOLOSTONE, RELICT THROMBOLITIC ALGAL TEXTURE

Description

This hand specimen shows a typical thrombolitic texture, with a brownish grey (5YR 4/1) and medium dark grey (N4) clotted to rarely digitate fabric with very light grey (N8) sparry calcite in irregular tubular fenestrae and birdseyes.

Mineralogically, the sample consists of 'grumeleuse' patches of microcrystalline and equigranular finely crystalline secondary dolomite. There are also patches of medium to coarsely crystalline internally zoned ?saddle dolomite. Equigranular intergrown xenotopic calcite occurs in association with the finer dolomite. Rarely, the ?saddle dolomite hosts extremely small euhedral calcite crystals. The rock also contains scattered silt-sized cloudy quartz and ?feldspar grains. These are bound together by thin discontinuous anastomosing dark brown accumulations of ?carbonaceous material which also contains small open fenestrae.

Interpretation

The overall texture is inferred to be of algal origin. The crystalsize of the dolomite reflects an original clotted thrombolitic texture. The dolomite and calcite filled tubular fenestrae may be after burrows or borings.

BIOCLASTIC PELOID GRAINSTONE/TUBULAR FOSSILS

Description

This specimen comes from an 8 cm thick bed of grey (N4 to N7) calcareous bioclastic grainstone and packstone. The bed has stylolitic upper and lower boundaries.

Tubular fossils up to 1cm diameter are visible in hand specimen and constitute up to 40 percent of the rock. Many contain geopetal infill and internal cements.

In thin section, the walls of the tubular fossils contain abundant ?tetraxon spicules. Some of the spicules are linked together forming a network.

The tubes are surrounded by finely crystalline calcite spar which contains up to 70 percent peloids and rare trilobite fragments.

Interpretation

The tubes have been interpreted as sponge body fossils. These and the accompanying trilobite fragments and peloids indicate a shallow marine setting. Since the tubes show little evidence of compaction, the cement infill must have been very early.

BIOCLASTIC PELOID GRAINSTONE/TUBULAR FOSSILS

Description

This sample comes from a 7 cm thick grey (N5 to N6) calcareous bed with abundant macroscopic tubular fossils which contain geopetal sediment and internal cement. They constitute 30 to 40 percent of the rock.

In thin section, the walls of the tubes contain sporadic tetraxon spicules.

The tubes are surrounded by finely crystalline spar with abundant peloids and trilobite fragments.

Interpretation

A shallow marine environment of deposition is inferred. The tubes might represent sponge body fossils but in contrast to the previous sample, no interlocking of spicules can be demonstrated. Cementation within the tubes was very early.

COLLAPSE BRECCIA

Description

The original fabric of this rock was a dark grey (N3) finely laminated silty carbonate mudstone with stacked fining-up couplets. The hand specimen shows collapse brecciation with sparry calcite cement in abundant thin veins and filling the voids between clasts. Macroscopic stylolites are also visible.

In thin section, the base of the larger cement-filled cavities contain ?diagenetic or ?geopetal sediment intimately associated with the coarse non-ferroan calcite spar cement. Rare poorly preserved spheroids with a fringing bladed dog-tooth cement are present within this sediment.

The stylolites cut across ?diagenetic/geopetal sediments, calcite cements and the original laminated fabric.

Interpretation

Lack of definitive marine elements in the geopetal sediment make it impossible to distinguish penecontemporaneous marine deposition and cementation from later ?diagenetic/vadose sediment and cementation. However, there is little evidence to support the original presence of evaporites within the cavity and collapse was probably initiated by chemical and/or mechanical breakdown of the original laminated silty carbonate mudstone. The relationship to the stylolites suggests that collapse and cementation preceded stylolitization.

COLLAPSE BRECCIA

Description

This sample comes from an extensive zone of veined and solution collapsed dark grey (N3) laminated silty mudstone. Macroscopic stylolites are also present.

In thin section, the matrix to the solution collapse breccia consists of coarsely crystalline non-ferroan calcite spar. The base of some of the larger areas of cement contain intermixed ?geopetal and diagenetic collapse sediment, including angular clasts up to 3 mm across. The larger fragments have been rotated and moved several millimetres from their original orientation.

Stylolitization has overprinted the solution collapse; many of the clasts are now rimmed by microstylolites and smooth low amplitude macrostylolites cross-cut the host silty mudstone, geopetal sediment and cement. The area of collapse brecciation grades laterally to horsetail stylolites.

Interpretation

This texture is believed to have been formed by the mechanical brecciation and chemical solution of carbonate mudstone. The initial collapse probably resulted from the removal of evaporites lower in the sequence, although there is no evidence of original evaporites in this particular cavity. The rotation and rearrangement of clasts suggests that the cavity was fluid filled prior to cementation. The cavity-fill of coarse calcite spar preceded stylolitization.

FENESTRAL AND STROMATACTIC CARBONATE MUDSTONE

Description

This hand specimen comes from a thick unit of olive grey (5Y 3/2) stylolitic dolostones which contain a variety of different shapes of calcite filled fenestrae. Macroscopically, the host mudstone is predominantly dark olive grey (5Y 3/2) with irregular mottles of light olive grey (5Y 5/2). The calcite filled fenestrae occur within the lighter coloured areas. The calcite cement in the fenestrae shows a sub-horizontal layering in hand specimen; with medium grey (N5) being overlain by very light grey (N8).

In thin section, the differences in colour in the host mudstone are produced by subtle differences in the average grain size and turbidity of the dolomite and are often accentuated by stylolitization. The dolomitization has obscured any more definitive differences in primary texture.

Low amplitude irregular stylolites interconnect many of the small lens of calcite and delimit the base of the larger calcite filled fenestrae and stromatactis.

The calcite cement in the top of the cavities is very coarse to coarsely crystalline ferroan spar. Sixty degree infacial angles are common. The darker coloured calcite visible in hand specimen consists of fine to very fine crystals. It also appears to be slightly less ferroan and contains sporadic heavy minerals, disseminated clays and inclusions of the host mudstone.

Interpretation

The origin of fenestral and stromatactic fabrics remains obscure. It is impossible to ascertain the timing of the cement infill in the cavities without a more detailed cathodoluminescence study.

FENESTRAL AND STROMATACTIC CARBONATE MUDSTONE

Description

This hand specimen is a mottled light olive grey (5Y5/2) and dark grey (N3) carbonate mudstone. This sample contains fenestrae and stromatactis which have a coarsely crystalline very light grey (N8) infill often with a thin light olive grey (5Y5/2) area on the floor of the cavity.

Mineralogically, the host mudstone consists of intermixed non-ferroan dolomite and calcite with a vaguely defined 'grumeleuse' to peloidal texture. The pale coloured cement is coarsely crystalline non-ferroan idiopathic saddle dolomite with characteristic curved crystal faces, cloudy appearance and undulose extinction. The mineralogy was confirmed by XRD analysis. The areas of light olive grey on the floors of the cavities are finely crystalline saddle dolomite. The saddle dolomite occurs as subhedral rhombs with slightly curved compromise boundaries.

Very fine opaque heavy minerals occur sporadically throughout.

Interpretation

Saddle dolomite commonly occurs as a diagenetic cavity fill in fenestral and stromatactic fabrics. The timing and nature of its formation remains problematical.

LAMINATED CARBONATE MUDSTONE WITH SADDLE DOLOMITE AND CHERT AFTER EVAPORITES

Description

This hand specimen is a mottled to laminated medium dark grey (N4) carbonate mudstone with highly disturbed bedding. Small tepees and sporadic irregularly shaped areas of cavity fill which host concentric-zoned cherts are locally abundant.

In thin section, the host mudstone is a laminated to thinly bedded medium to finely crystalline calcite with a possible relict peloidal texture and rare rounded ?bioclastic debris. The original laminations, delineated by changes in crystalsize and incipient stylolitization, are now highly contorted.

The mudstone hosts irregularly shaped patches of coarsely crystalline saddle dolomite and calcite spar with concentric zones of chalcedonite. The largest (approx. 1 cm across) of these patches visible on the thin section contains an outer zone of very coarsely crystalline xenotopic saddle dolomite cement with characteristic turbidity, incomplete undulose extinction and curved crystal faces. The crystals range from subhedral to anhedral; the larger subhedral forms have straight to gently curved rational crystal faces. Rare scimitar-like terminations are also present. About 10 percent of this material is replaced by non-ferroan calcite which pseudomorphs all the textures of the saddle dolomite.

A second zone; roughly concentric and internal to; the saddle dolomite, consists of alternating very fine dark brown concentric microlaminated and radially fibrous ?length-slow chalcedonite. It is slightly pleochroic and has a pervasive sweeping but incomplete extinction. The chalcedonite does not corrode the adjacent saddle dolomite crystals, but its growth appears to have been slightly displacive.

Within the chert is another coarsely crystalline saddle dolomite and calcite zone. The core of the area is occupied by dark brown chert (?quartzine) with inclusions of finely crystalline calcite, rare sulphate evaporite (possibly barite), and extremely small euhedral quartz crystals.

Interpretation

The areas of saddle dolomite and chert are believed to be replacements of an original sulphate evaporite which was associated with small tepees.

Paragenesis

A possible paragenesis includes partial in situ replacement and partial infill after solution of pre-existing cavity fill. The euhedral curved faces and scimitar-like terminations of some of the saddle dolomite are characteristics of pore-lining cement, and the chalcedonite also appears to be a later generation of cavity fill.

CARBONATE MUDSTONE HOSTING CONCENTRIC-ZONED SILICA

Description

This rock is a massive to thinly bedded medium grey (N5) to medium dark grey (N4) carbonate mudstone which hosts small irregular shaped areas of concentrically zoned silica in small cement-filled veins and as infill in mudcracks.

The host mudstone is finely crystalline calcite with rare peloids, opaque heavy minerals, and thin secondary calcite spar-filled veins.

The silica occurs as concentric zoned ?quartzine, pseudo-fibrous length-slow lutecite and xenotopic megaquartz. The first two forms occur in intimate association with medium to coarsely crystalline corroded calcite spar in millimetre sized concentric spherules. The megaquartz appears to be restricted to the core of the area, with an irregular contact between the megaquartz and adjacent spherules.

Interpretation

The presence of length-slow quartz, the association with desiccation features and the similarity with thin section COM739, suggests that silicification may be after original sulphate evaporites.

RELICT OOID GRAINSTONE

Description

This sample is a speckled grey (N3 and N4) calcareous rock which contains abundant ooids. Pale irregularly shaped areas to 1.5 cm across are outlined by a black (N1) halo.

The majority of the material represented on the slide is a secondary recrystallization of interlocked subhedral to anhedral calcite crystals which obscures the relict ooid texture and has totally replaced the original cement or matrix. Faint outlines defined by zones of inclusions suggest an original blocky or granular cement. Within this framework, individual ooids may be replaced by an optically single calcite or dolomite crystal. Subhedral to almost euhedral turbid dolomite rhombs occur sporadically throughout. Rare bioclastic debris including possible trilobite fragments is also present.

The paler areas visible in hand specimen are microstylolite-bounded lenses of dolomitization and incipient chertification. The ooids at the base of the lens are very dark in colour, possibly due to iron mineralization.

The ooid ghosts range up to 0.5 mm diameter, and have an originally ?micritic nucleus which varies from one quarter to two thirds of an overall diameter. Concentric multi-layered walls and a radial fabric are only poorly preserved. Some ooids retain their characteristic figure under crossed nicols. Rare coated aggregate grains occur throughout. The ooids form a closed framework.

The sample is cut by a number of thin irregular stylolites which are concentrated in the recrystallized areas but locally reduce the ooids to poorly preserved spastoliths.

Interpretation

Ooid grainstones are usually interpreted as indicating moderately high energy conditions. The bioclastic debris suggests a marine origin.

This sample shows a complex diagenesis including wholesale recrystallization to neomorphic spar, stylolitization, silicification, iron staining and dolomitization.

RELICT OOID GRAINSTONE

Description

This hand specimen is an ooid grainstone which shows three distinct horizontal colour phases varying from dark grey (N3), through medium dark grey (N4) to medium light grey (N6). Irregular macrostylolites are visible in the darker colour phases.

Thin section study shows that the different colour phases are due to varying degrees of chertification.

The lowermost area is still entirely calcareous, although it has undergone recrystallization to interlocking finely crystalline subhedral pseudo-spar. The ooids are clearly visible as outlines of inclusions, but their ultrastructure is obscured. The original fabric of the cement is lost, although sporadic less-turbid areas between the ooids may be relics of the final cavity fill.

The middle area of the sample is entirely chertified. The ooids are preserved as ghosts which retain their figure under crossed nicols and the multilayering of the concentric wall is outlined by local concentrations of small opaque heavy minerals. Faint haloes of inclusions also surround the ooids and may represent an original fringing cement.

The uppermost colour phase corresponds to an area of partial chertification, where the ooids themselves and a first generation meniscus cement are silicified and the final inter-ooid cavity fill is either silica or dolomite. The relict second generation isopachous to botryoidal cement is recrystallized calcite. Coarse to very coarse euhedral ?saddle dolomite rhombs occur throughout this zone. They are entirely non fabric selective, cross-cutting the chertified ooids, silicified areas and calcite cements. Rarely, they include small calcite rhombs which appear to be pseudomorphs of a preceding generation of saddle dolomite. The diagenesis is further complicated because several of the late stage dolomite rhombs appear to be undergoing preferential silicification in relation to adjacent calcite. The ooids consistently average just over 0.5 mm diameter and, in the majority of cases, retain a relict multiwalled structure with an internal radial fabric. Sporadic twinned ooids form coated

aggregate grains and elongate ooids are rare. The ooids form a closed framework.

Interpretation

Ooid grainstones are usually interpreted as moderately high energy shallow marine deposits.

This sample shows a complex diagenesis involving at least two generations of primary calcite cement formed initially in the vadose zone of precipitation and then possibly in marine phreatic conditions. These cements and, to some extent, the ooids themselves have been altered by recrystallization to neomorphic calcite spar, by silicification delimited by a stylolite bounded solution front and by dolomitization. The formation of the dolomite rhombs was penecontemporaneous with silicification.

LAMINATED CARBONATE MUDSTONE WITH CAULIFLOWER CHERTS

Description

This sample is a grey (N5 to N4) laminated carbonate mudstone which contains sporadic millimetre scale irregularly shaped siliceous nodules.

In thin section, the laminae in the carbonate mudstone are defined by variations in the xenotopic dolomite which constitutes 90 percent of the rock. The remainder is composed of silt sized detrital quartz and feldspar with local concentrations of clay in some laminae. Rare traces of ?anhydrite are also present as diffuse patches less than 0.25 mm across in the areas of coarser dolomite.

The siliceous nodules (Figure 54) are composed of xenotopic megaquartz, pseudofibrous length-slow lutecite (1), euhedral rhombs and corroded subhedral crystals of dolomite (2) and calcite (3) isotropic opaque minerals (4) and possible traces of an original evaporite mineralogy. The calcite and dolomite are generally restricted to the outer edges of the nodule, lined by a rim of lutecite with traces of ?evaporite mineral (possibly celestite) and opaque heavy minerals in the remaining central cavity void. Megaquartz occurs as an irregular extension of the nodule. It has a xenotopic fabric in sharp irregular contact with adjacent lutecite and saddle dolomite.

Interpretation

The siliceous nodules, or cauliflower cherts, are interpreted as replacements after sulphate evaporites. This is supported by the presence of possible unaltered anhydrite in the matrix of the host mudstone, the possibility of relict or remobilized evaporites in the core in the nodule, and the abundance of length-slow quartz.

Paragenesis

It appears that the original evaporite mineralogy has been replaced sequentially by dolomite, calcite and silica, with possible remobilization of evaporite minerals and growth of authigenic opaque minerals as late stage ?void fill.

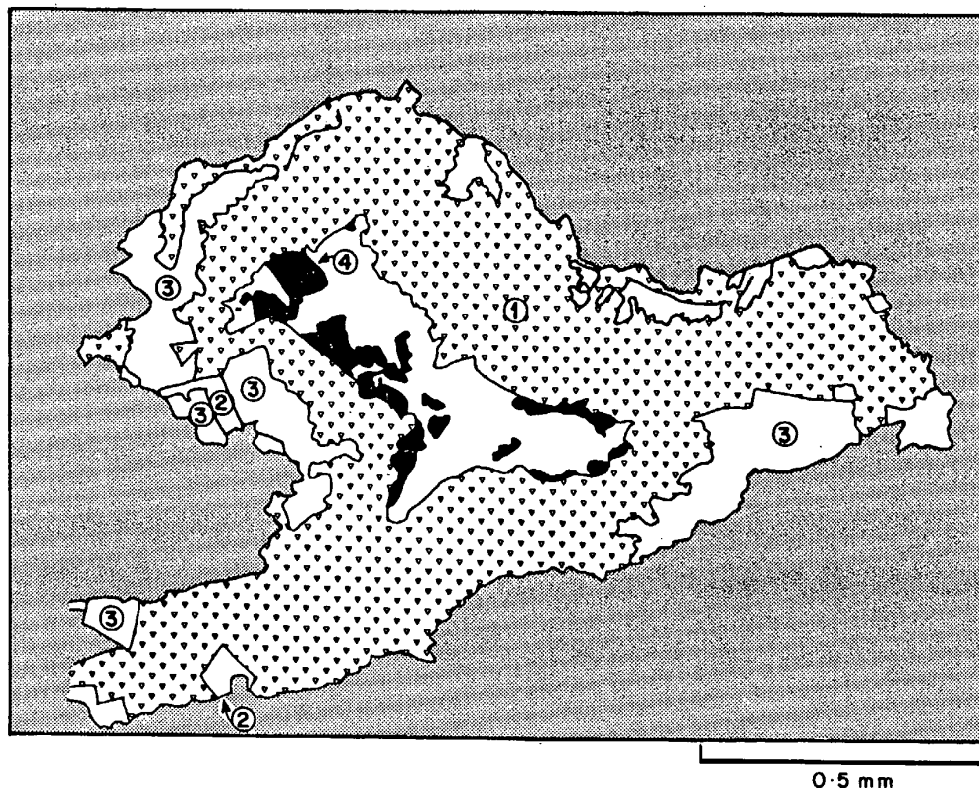


FIGURE 54: CAULIFLOWER CHERT
THIN SECTION COM750, MANYA-3, 537.20m.
(1) PSEUDO-FIBROUS LENGTH-SLOW LUTECITE
(2) DOLOMITE
(3) CALCITE
(4) OPAQUE ISOTROPIC MINERAL.

Note

Cauliflower cherts from this sample were also examined by scanning electron microscopy (see next description).

LAMINATED CARBONATE MUDSTONE WITH CAULIFLOWER CHERTS

Description

This sample is a grey (N5 to N4) laminated carbonate mudstone which contains sporadic millimetre scale irregularly shaped siliceous nodules.

In thin section, the laminae in the carbonate mudstone are defined by variations in the xenotopic dolomite which constitutes 90 percent of the rock. The remainder is composed of silt sized detrital quartz and feldspar with local concentrations of clay in some laminae. Rare traces of ?anhydrite are also present as diffuse patches less than 0.25 mm across in the areas of coarser dolomite.

Examination with a petrological microscope shows a very similar fabric to other nodules from the same sample (see COM750). The siliceous nodules are composed of xenotopic megaquartz, (Figure 55, (3)) pseudofibrous length-slow lutecite (1), euhedral rhombs and corroded subhedral crystals of calcite (2) and possible traces of an original evaporite mineralogy. The calcite and dolomite are generally restricted to the outer edges of the nodule, lined by a rim of lutecite with an ?evaporite mineral at the core.

The SEM study (courtesy of A. Brewer) confirms the identity of the outer zone (2) as calcite, and highlights the scimitar-like curved terminations and stepped faces of the inner most crystals (2a). These crystal forms are usually diagnostic of void filling saddle dolomite cement, which suggests that calcite is pseudomorphing saddle dolomite. The pseudo-fibrous length-slow lutecite is visible in the SEM photograph as a dark grey band. The high strontium count (Figure 56) obtained for the bright mineral at the core of the nodule, (4) confirms its identification as celestite.

Note

This sample was taken from the same thin section as the previous description (COM750) and helps confirm the interpretation and paragenesis.

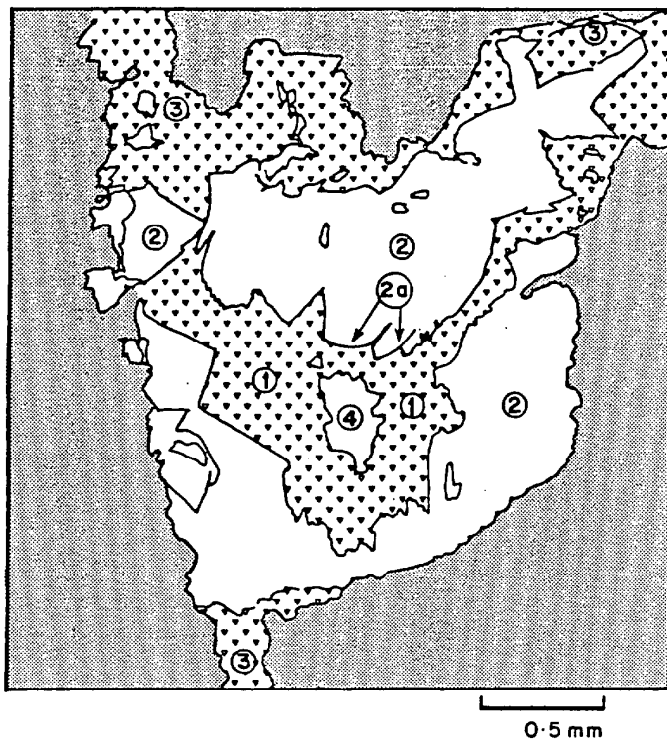


FIGURE 55: CAULIFLOWER CHERT
SEM PHOTO SEM750, MANYA-3, 537-20 m.

- (1) LUTECITE
- (2) CALCITE
- (2a) CURVED CRYSTAL TERMINATIONS
- (3) MEGAQUARTZ
- (4) CELESTITE.

LT = 100 SECS

M3/537.2-X800

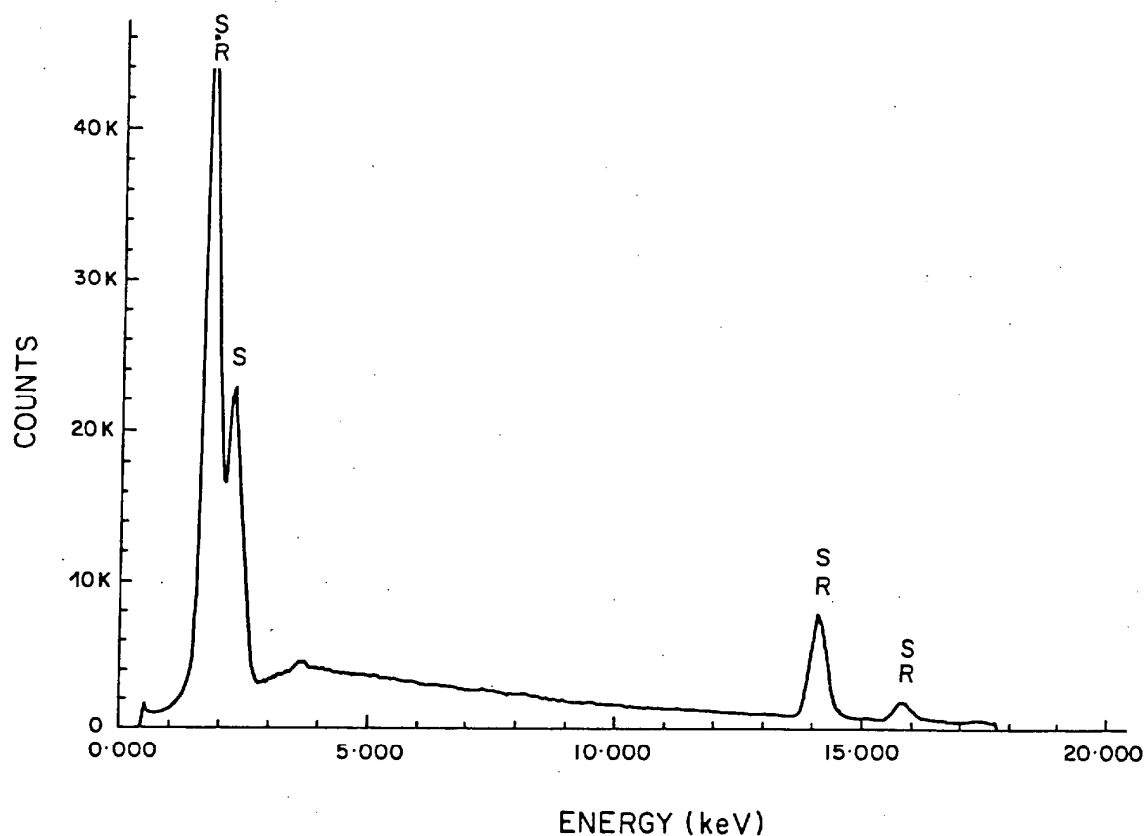


FIGURE 56 : ENERGY DISPERSIVE S.E.M. PLOT OF CORE OF CAULIFLOWER CHERT NODULE, SEM750, MANYA-3, 537.20m, SHOWING INFILLING BY Sr AND S, PROBABLY AS CELESTITE.

CHERT

Description

This sample is from a 8 cm thick chert band or lens in an overall massive carbonate mudstone sequence. The hand specimen shows abundant columnar to irregular anastomosing stylolites which surround the chert lens and separate areas with abundant clastic grains from the predominantly massive carbonate mudstone. The host mudstone is greenish grey (5 G 6/1) and the chert ranges from bluish white (5 B 9/1) to pale blue (5 B 7/2).

This thin section includes the base of the chert and some of the underlying stylolite-bounded clastic-rich zone. This latter area contains a closed framework of ?detrital quartz and feldspar in a very clayey dolomitic matrix. The quartz and feldspar range from just under 1.0 mm (coarse grained) to very fine grained, and includes a complete spectrum of roundness and sphericity. Some of the larger grains have corroded edges and re-entrant angles, others appear to be undergoing in situ alteration along microfractures.

This lithotype is separated from the chert by a 1.5 mm thick stylolite-like band of clastic grains in a dark brown to black opaque matrix.

In plane polarized light, the chert shows a variety of textures defined by the relative abundance of inclusions and pale brown colour phases. Lathes and needles are arranged in a decussate to felted texture. This is intermixed with areas of microspherulitic to concentric fabric. Under crossed nicols, the microspherulites show a typical maltese cross figure produced by radial arranged length-slow ?lutecite. Individual crystals extend beyond the circular areas visible in plane polarized light. Where the crystals are not directly in contact with one another, the area between is filled with xenotopic equant finely crystalline quartz. The areas of decussate texture are composed of equant xenotopic very finely crystalline quartz and ?microspherulites of ?lutecite finely intermixed with a turbid grey pleochroic mineral, possibly siderite. Large areas of this material extinguish at the same point under crossed nicols suggesting it is an original mineralogy being replaced by quartz.

Rare millimetre sized areas resemble cavity infill. The outer wall is defined by pale brown colouration in plane polarized light. Under crossed nicols lutecite spherulites extend from this border grading into a rim of megaquartz with largest crystals toward the ?cavity centre. The core of the area is a void.

Interpretation

The paragenesis of this chert band remains problematical. There is evidence of both void fill and replacement of another mineralogy by different crystal forms, if not different generations, of silica. The relict decussate texture and the occurrence of length-slow quartz may indicate an original sulphate evaporite mineralogy.

CARBONATE MUDSTONE WITH PARTLY SILICIFIED NODULE OF SULPHATE EVAPORITES

Description

This sample comes from a light olive grey (5 Y 6/1) laminated and silty carbonate mudstone which contains 'ghosts' of swallow tail gypsum crystals and millimetre to centimetre scale rounded nodules of sulphate evaporites. The laminae in the host mudstone curve around the nodules. Some of the nodules contain areas of white ?chert while other nodules have a central cavity lined by coarse euhedral crystals.

The carbonate mudstone contains sporadic detrital silt sized to fine grained quartz and feldspar. The laminae are defined by local concentrations of those detrital clastics and by thin ?carbonaceous wisps and clay-rich horizons.

About 70 percent of the nodule consists of very coarsely crystalline celestite with minor barite (Figure 57, (1)). The mineralogy was confirmed by XRD analysis. The crystals form an idiomorphic mosaic with a greater proportion of straight crystal faces in the centre of the nodule. The celestite hosts inclusions of silt-sized ?detrital quartz and rare small patches of anhydrite. Although the areas of anhydrite are discontinuous, they extinguish at the same point under crossed nicols.

The areas of ?chert (2) in the nodule have a distinctive texture in thin section. They consist of a decussate to felted fibrous arrangement of lathes. These are comprised of the following mineralogies in decreasing order of abundance:- black isotropic ?opaline silica, length-slow lutecite, celestite, barite and rare anhydrite. The lathes are grouped into clumps cut by thin 'veins' (3) of barite contiguous with the rest of the nodule.

Interpretation

The partly silicified nodule is believed to be after original sulphate evaporites. As such, it represents an intermediate stage in the formation of a cauliflower chert.

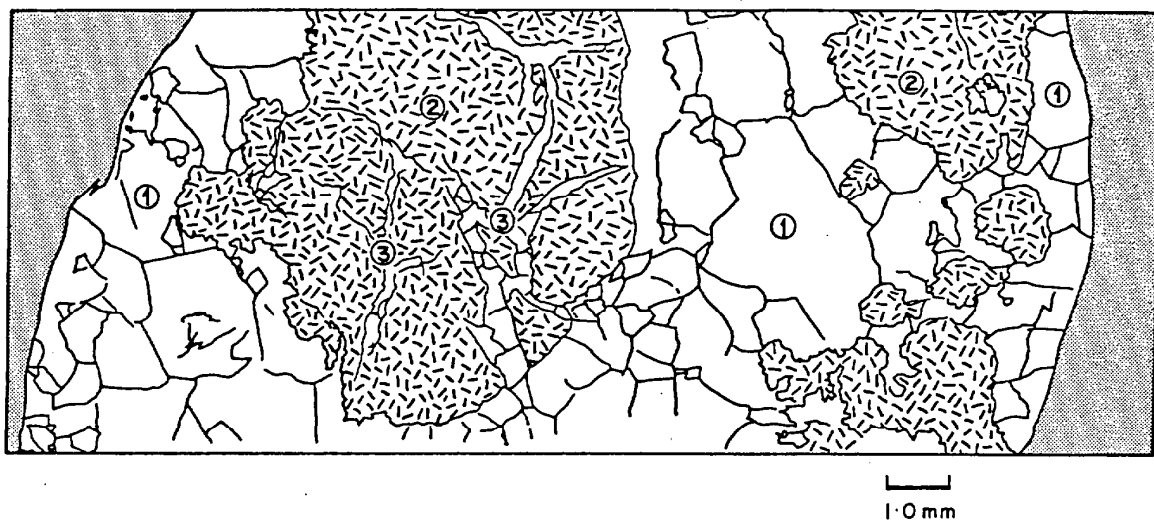


FIGURE 57: PARTLY SILICIFIED SULPHATE EVAPORITE NODULE
THIN SECTION COM768, MARLA -6, 309.95m.

- (1) CELESTITE WITH MINOR BARITE
- (2) DECUSSATE AND FELTED TEXTURE, PARTLY SILICIFIED
- (3) BARITE VEINS.

Paragenesis

The suggested paragenesis involves replacement of the decussate anhydrite lathes by coarsely crystalline celestite, barite and silica. The early stages of silicification have pseudomorphed the original anhydrite texture.

STROMATOLITIC ALGAL BINDSTONE AND OOID GRAINSTONE

Description

This hand specimen contains well developed centimetre scale domed stromatolites with areas of ooid grainstone infill between the algal 'heads'. The rock is medium grey (N5).

In thin section, the stromatolitic lamination is defined by subtle variations in crystalsize and the relative abundance of detrital quartz and feldspar and thin laminae of ?carbonaceous material within a very finely crystalline calcite.

The ooid grainstone consists of a moderately open framework of ooids, coated aggregate grains and rare ?detrital quartz and feldspar clasts in a calcite cement. The ooids average just under 1.0 mm diameter and have been recrystallized, resulting in the loss of radial fabric. The multilayered concentric walls are still obvious in both plane polarized light and under crossed nicols. The ooids appear to have had an original micritic nucleus, although feldspar grains also appear in the core of isolated examples. Several of the ooids were broken prior to cementation. The aggregate grains contain up to 8 ooids within an outer coat similar to the outermost layer of individual ooids. The detrital quartz grains show evidence of syntaxial overgrowth with optically continuous quartz extending up to one third of the grain diameter.

The calcite cement consists of a first generation of fringing bladed to blocky crystals arranged radially to the ooid. Where the ooids are sufficiently close, the cement is contiguous between them. The final cavity fill is very coarsely crystalline calcite, commonly with a single crystal occupying the cavity.

Interpretation

A shallow marine origin is inferred. This is consistent with the environment of the stromatolites and the possible active marine phreatic cementation.

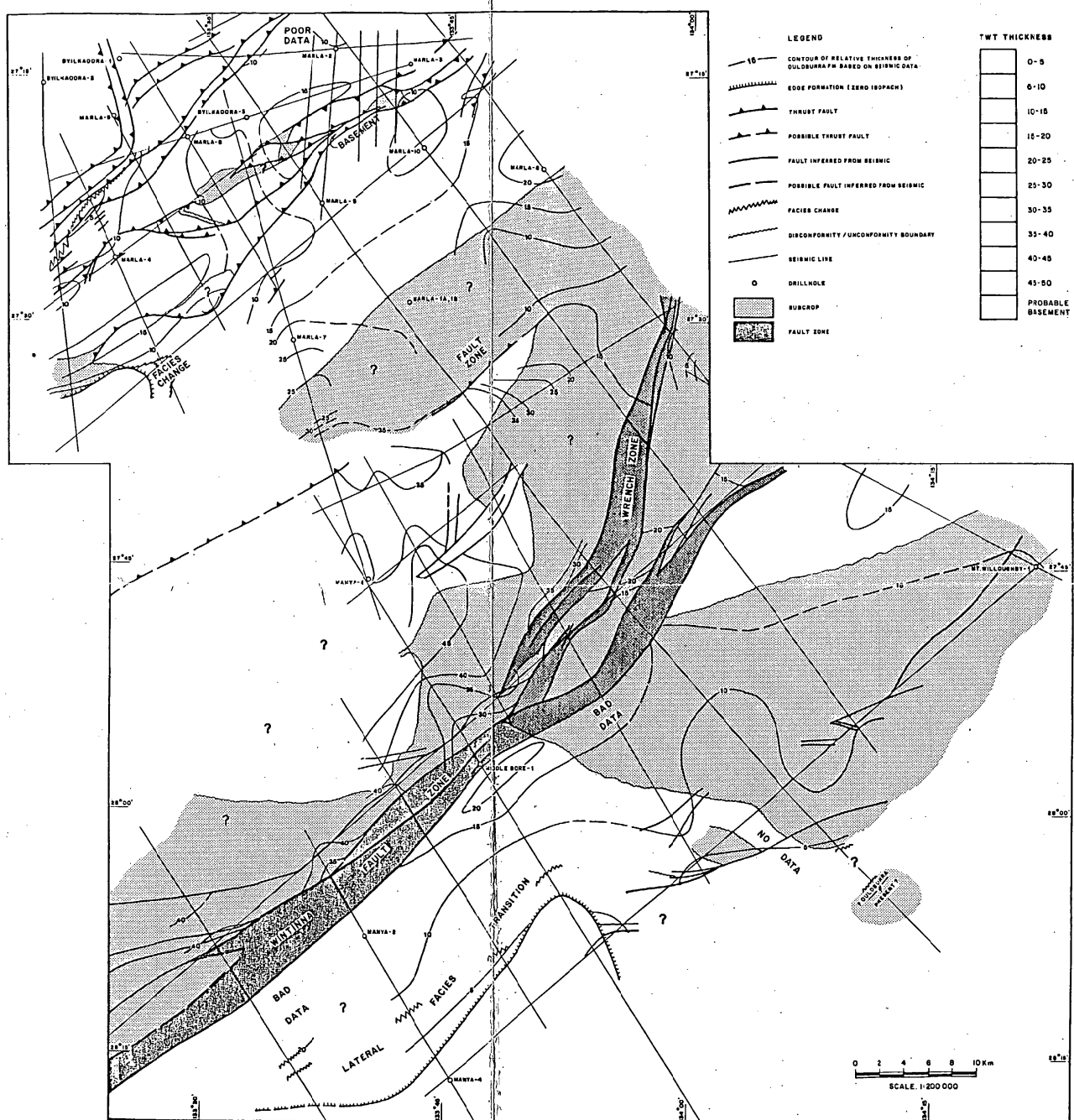


FIGURE 12: ISOPACHS OF RELATIVE THICKNESS OF THE OULDBURRA FORMATION AND ITS POSSIBLE SEISMIC-STRATIGRAPHIC CORRELATES. Contours are calculated from corrected two-way time in milliseconds to top Ouldburra Formation and top Relief Sandstone.